Terms and Conditions of Use of Digitised Theses from Trinity College Library Dublin

Copyright statement

All material supplied by Trinity College Library is protected by copyright (under the Copyright and Related Rights Act, 2000 as amended) and other relevant Intellectual Property Rights. By accessing and using a Digitised Thesis from Trinity College Library you acknowledge that all Intellectual Property Rights in any Works supplied are the sole and exclusive property of the copyright and/or other IPR holder. Specific copyright holders may not be explicitly identified. Use of materials from other sources within a thesis should not be construed as a claim over them.

A non-exclusive, non-transferable licence is hereby granted to those using or reproducing, in whole or in part, the material for valid purposes, providing the copyright owners are acknowledged using the normal conventions. Where specific permission to use material is required, this is identified and such permission must be sought from the copyright holder or agency cited.

Liability statement

By using a Digitised Thesis, I accept that Trinity College Dublin bears no legal responsibility for the accuracy, legality or comprehensiveness of materials contained within the thesis, and that Trinity College Dublin accepts no liability for indirect, consequential, or incidental, damages or losses arising from use of the thesis for whatever reason. Information located in a thesis may be subject to specific use constraints, details of which may not be explicitly described. It is the responsibility of potential and actual users to be aware of such constraints and to abide by them. By making use of material from a digitised thesis, you accept these copyright and disclaimer provisions. Where it is brought to the attention of Trinity College Library that there may be a breach of copyright or other restraint, it is the policy to withdraw or take down access to a thesis while the issue is being resolved.

Access Agreement

By using a Digitised Thesis from Trinity College Library you are bound by the following Terms & Conditions. Please read them carefully.

I have read and I understand the following statement: All material supplied via a Digitised Thesis from Trinity College Library is protected by copyright and other intellectual property rights, and duplication or sale of all or part of any of a thesis is not permitted, except that material may be duplicated by you for your research use or for educational purposes in electronic or print form providing the copyright owners are acknowledged using the normal conventions. You must obtain permission for any other use. Electronic or print copies may not be offered, whether for sale or otherwise to anyone. This copy has been supplied on the understanding that it is copyright material and that no quotation from the thesis may be published without proper acknowledgement.

Investigation of herbicide-based compounds as novel anti-malarial agents

A thesis submitted for the degree of Doctor of Philosophy

by

Enda Dempsey

Department of Microbiology
Moyne Institute of Preventive Medicine
Trinity College
University of Dublin

October 2009

DECLARATION

This is to certify that the experimentation recorded herein represents my own work, unless otherwise stated, and has not been submitted for higher degree at this or any other university. The thesis may be lent or copied at the discretion of the librarian, Trinity College.

Enda Dempsey,
October, 2009.

Summary

Plasmodium falciparum causes the most severe form of malaria in humans. Currently, no effective vaccine exists and the emergence of widespread drug resistance in the parasite has further increased the necessity for novel therapeutics to be discovered.

Microtubules are cytoskeletal polymers which consist mainly of repeating α/β-tubulin heterodimers and play crucial roles in almost all eukaryotic cells. These polymers have the ability to rapidly elongate and shorten. Inhibition of this dynamic behaviour has been successfully exploited in the past to generate potent fungicides, herbicides, anti-parasitics and anti-cancer therapeutics. For *Plasmodium*, two groups of chemically distinct herbicides, the dinitroanilines and the phosphorothioamidates, were previously identified as being potentially useful antimalarial agents. To improve the activity of these herbicides for *Plasmodium*, a library of amiprophosmethyl-related compounds were generated by collaborators in the Royal College of Surgeons in Ireland. The major objective of this project was to investigate the cellular and molecular interactions of these compounds with the *Plasmodium* tubulin.

Previously, recombinant *P. falciparum* α- and β-tubulins had been produced in our laboratory which were capable of co-assembly with mammalian tubulin but not with each other. An attempt was made to discover an improved system which could produce sufficient quantities of assembly-competent tubulin for ligand-binding studies. Several different approaches were examined with different levels of success. It was possible to refold denatured tubulin using eukaryotic chaperones so that they were able to polymerise, but, the final yields were prohibitively low for subsequent ligand-binding studies. Nonetheless, a tryptophan-fluorescence based assay was developed using fusions of *Escherichia coli* maltose-binding protein (MBP) with α- and β-tubulins which was successful in determining ligand-binding data for several known tubulin inhibitors. The dissociation constant (K_d) for APM was found in this way to be 44.14 +/- 7.15 μM using an MBP-αI-tubulin/MBP-β-tubulin mixture.

APM and its derivatives were examined for their ability to inhibit the growth of live cultures of parasites during the intra-erythrocytic cycle. Overall, while most of these compounds were found to be therapeutically irrelevant due to the high concentrations needed for activity, a few were potentially promising. In particular,

switching the positions of the nitro and methyl moieties with each other and replacing the N-propyl group with the more hydrophobic cyclopentane, generated a compound with a 50% inhibitory concentration as low as 1.6 μM. A detailed analysis was conducted on this library of compounds using a modified version of the fluorescence quenching assay and molecular modelling of the compounds. This systematic approach revealed interesting features and details that appeared to predict the activity of these compounds in the cell culture assay. Typically, a high lipophilicity and the presence of sulphur atom were important. However, an electron withdrawing group on the para position of the benzene ring was also suggested to be favourable. Furthermore, the potentially carcinogenic nitro moiety could be replaced by a tri-fluoro group without significantly compromising the activity of these compounds compared to APM.

Three putative binding sites have been proposed for the dinitroanilines on tubulin from different organisms using mainly homology molecular models. However, there was a lack of experimental evidence using purified tubulin to support any of these proposed sites. To address this issue, six independent alterations were made at various residues on the *Plasmodium* αI-tubulin and both APM and oryzalin, a dinitroaniline, were assessed for their ability to bind to these proteins using the fluorescence quenching based assay. Two different alterations for APM and oryzalin were found to partially reduce their binding affinity to tubulin. However, this change in affinity was not as major as expected therefore at least two of these sites were thought not to be applicable in *Plasmodium*.

In summary, the findings presented here provide valuable insights into the molecular and cellular interactions of two promising classes of compounds for *Plasmodium* tubulin. This information has also aided in the improved design of a library of phosphorothioamidate derivatives which may form the basis for promising future anti-malarial agents.

Dedicated to
the folks

ACKNOWLEDGEMENTS

I would sincerely like to thank to Dr. Gus "G-Man" Bell for his exceptional patience and supervision over my years here in the Moyne. Your encouragement and guidance have been invaluable to me in finally completing this thesis!!! I also felt incredible lucky since you took three risks with me; you employed me as a masters student, a PhD and lastly a Post-Doc. Some people just love to gamble!!!

I would also like to thank my collaborators Dr. James Barlow and Mrs. (soon to be Dr.) Christine Mara who were hugely productive in generating novel compounds over the course of this project. The days are numbered for *Plasmodium* thanks to these guys!!!

I would especially like to thank Dr. Brian "Herb" Fennell. You were instrumental in getting me through this project, although if we didn't go the pub every Friday for a full year, it might have gone a bit smoother! You are a true friend or just an incredible fiend for the sauce! You also have an incredible knack for causing controversy both on and off the pitch. You are undeniably a champion at the fantasy football (Winner Alright!) but your last outing will be the one best remembered and not just by me. All I'll say is, Blakey wants his money!!! Cheers boss for the laughs.

A big thanks goes out to the Bell lab members both past and present who all have their own unique but endearing personalities. Julie may be a "short" kickboxing supremo who doesn't like nonsense but when you're in need, she is always there. Cheers Jules! Eddie, what an incredible bird! When it comes to talking about "fun" pastimes, she has absolutely no inhibitions, seriously, none at all!!! Sima, eye of newt. Zenab, master delegator. Gerry, I can't believe you left us. You were our music wardern. As a result, I feel ill when I hear Snow Patrol, Arctic Monkeys or U2 on the radio! Alejandro Marin- Menendez a.k.a Tu Madre. A genuinely sound head who was at times unfairly under-appreciated. However, what was appreciated is his ability to run rings around the Herb even with a dodgy knee (although Im sure that will be hotly debated)!! And since Ireland isn't in the world cup, Go on the Spaniards!!!! Finian Thomas Doyle, a.k.a Fatlad. Built like a reinforced s***house brick but moves slower than a sloth wading through glue. Yet still claims he is the fastest man on grass. Just a pity he has been blighted by injury for the past 2 years especially with mention of the "Great Race". Seriously, I would like to specially

thank the two boys for helping me get the thesis submitted on time, I was a little bit stressed back then. I always believed that a supervisor hires people that tend to have some similar traits to themselves. In this case, maybe you should be worried Gus!!!

Thanks to all the TJF'ers of the East Bunker lab, both past and present. We will win best decorated lab one year!! Mag, you were a bad influence but great craic. You and the Mario Kart cost me a year of my life but it wasn't a waste. I can at least say I was never beaten by the Herb though! Ed...oops I mean Keano, if you ever get lonely in Oz, just apparate your way over here! And just for you Keano, what does the "Confringo" spell do???

Sevgili kahve bayan, bütün eğlenceli anılar için teşekkür ederim! Gerçekten ben sevmiyorum tüm insanların laneti olmalı, fakat onlar bunu çevirmek olabilir!

A big thanks to all the members of the prep-room staff. In particular, thanks to Blakey for the financial support he gave me throughout my project ahahaaha!! I also really appreciated the advice and guidance my committee gave me through the years. Thanks also to all the members of the Moyne, both past and present. A special thanks to all the undergrads that passed through the Moyne, I didn't love you all, but I tried to love as many of you as possible!!!!

Finally, I would like to end the acknowledgements with a sincere thanks to the folks who actually made all of this possible in the first place. They always supported and encouraged throughout the whole experience and that's why I have dedicated my thesis to you. Cheers guys!

TABLE OF CONTENTS

List of Figures

List of Tables

Abbreviations

A.....absorbance

AA.....amino acid

A_{ex}.....Absorbance at excitation wavelength

A_{em}.....Absorbance at emission wavelength

APM.....Amiprophos-methyl

APAD.....3-acetyl pyridine adenine dinucleotide

APS..... ammonium persulfate

bp.....base pair(s)

BSA.....bovine serum albumin

BB.....bovine brain tubulin

C.....Total concentration of ligand

cDNA..... complementary deoxyribonucleic acid

cLogP.....Computed partition coefficient

dH_2O..... deionised water

dpm..... disintegrations per minute

DMSO..... dimethylsulphoxide

DTNB.....5, 5'-dithio-bis(2-nitrobenzoic acid)

DTT.....dithiothreitol

DV.....digestive vacuole

EDTA.....ethylenediaminetetraacetic acid

EGTA.....etheleneglycolbis(aminoethyl)-
tetra-acetic acid

EIR.....entomological inoculation rate

F.....Fluorescence

F_{corr}.....Corrected fluorescence

F_{max}.....Maximum fluorescence

F_{obs}.....Observed fluorescence

IC_{50}.....median inhibitory concentration

kbp.....kilobase pair

kDa.....Kilodaltons

K_d.....Disassociation constant

LDH.....lactate dehydrogenase

L_f.....Free ligand equilibrium concentration

MAP's.....microtubule associated proteins

MBP.....maltose binding protein

MCS.....multiple cloning site

min.....minute(s)

MOE.....Molecular Operating Environment

MT.....microtubule

NBT.....nitroblue tetrazolium

PAGE.....polyacrylamide gel electrophoresis

PBS.....phosphate buffered saline

PCR..... polymerase chain reaction

PV.....parasitophorous vacuole

PES.....phenazine ethosulphate

pLDH.....parasite lactate dehydrogenase

PMSF..... phenylmethylsulphonyl fluoride

PVDF.....polyvinylidene fluoride

rpm.....revolutions per minute

RBC.....red blood cell

RRL.....rabbit reticulocyte lysate

SDS.....sodium dodecyl sulphate

SDS-PAGE.....sodium dodecyl sulphate-polyacrylamide gel electrophoresis

SEM..... standard error of the mean

TAE.....tris-acetate-EDTA

TCA.....trichloroacetic acid

TE.....tris-EDTA

TEMED.....N, N, N', N'-tetramethyl-ethylenediamine

Tris.....tris(hydroxymethyl)aminomethane

UV.....ultraviolet

X.....Fraction of binding sites occupied by a ligand

Y.....Molar concentration of ligand-binding

Chapter 1

General Introduction

1.1 MALARIA AND THE MALARIA PARASITE

Malaria is the most significant vector-borne human disease today due to its high morbidity and mortality rates. The WHO estimates that at least ~50% of the world's population is currently at risk from infection, albeit to different degrees, and there are on average 267 million cases annually (WHO 2008). The majority of these infections occur in sub-Saharan Africa although the disease is prevalent in most tropical environments (see Fig. 1.1). Pioneering work by Alphonse Levaran and Ronald Ross during the end of the 19th century discovered that malaria was caused by a parasite which is transmitted to humans by mosquito bites. From 1958-69, the WHO directed the Malaria Eradication Programme which was implemented globally, except in tropical Africa, to eradicate malaria. The strategy primarily focused on controlling mosquito populations by destroying their natural habitats and extensive use of insecticides. Malaria was completely eradicated in North America and across Europe (Carter *et al.,* 2002) but there were severe ecological repercussions particularly due to the excessive use of the insecticide dichlorodiphenyltrichloroethane (DDT), which due to bioaccumulation becomes toxic both to wildlife and humans. To date the disease is most prevalent and severe in sub-Saharan Africa, where 86% of all infections occur (WHO 2008). The extreme poverty that these countries suffer from serves only to exacerbate the problem. A recent report published by Teklehaimanot *et al* argued that the economic burden of malaria alone had cost Nigeria's GDP to be impeded as much as 3.8% annually and can lead to a "causality effect", whereby poverty and malaria are inextricably linked (Teklehaimanot *et al* 2007). In recent years, global warming has raised fears over a resurgence of this disease and possible spread back into new territories but this has caused controversy among scientists due to the complicated nature of disease transmission and the reliance on computer models to make the predictions (Patz *et al.,* 2006 and Reiter P. 2008). On one hand, mosquitoes are predicted to thrive in a wetter, warmer climate. Furthermore, an escalating number of natural disasters will increase the strain on the healthcare systems reducing the overall population resistance to disease in general thereby aiding the spread of malaria. On the other hand, it has been argued that although global warming will negatively impact on human populations, the predictions are based on simplistic and unreliable models

which are not accurate enough. Nonetheless, it is clear that the disease is a major health issue that needs to be solved.

1.2 DEVELOPMENTAL CYCLE OF *P. FALCIPARUM*

Plasmodium is a member of the phylum Apicomplexa and there are 5 species of the parasite known to cause malaria in humans; *P. falciparum*, *P. vivax*, *P. malariae*, *P. ovale* and *P. knowlesi*. They use a complex, bi-phasic life-cycle which requires both a human and mosquito host to complete (see Fig. 1.2). Approximately 50 species of mosquitoes, all from the *Anopheles* genus, are able transmit malaria to humans, most notably *A. gambiae*. The life cycle begins when a female *Anopheles* uptakes the sexual gametocytes for *Plasmodium* when biting an infected victim during a blood meal. The life cycle inside the mosquito has several distinct phases and is succinctly reviewed by Vlachou *et al.*, (2006) so will not be discussed in detail here; but importantly it permits genetic recombination. The sporozoites are released into the salivary gland cavities during the final stage of this reproductive cycle. The mosquito's second blood meal deposits, on average, less than 25 sporozoites into the human host (Beier *et al.*, 1991). These sporozoites form only 3% of the total population in the mosquito and may represent a conserved mechanism to maximise transmission from one host or the small number may be due to a logistical barrier preventing more parasites from escaping. After infection, these sporozoites travel towards the liver and invade the hepatocytes through a complicated pathway (see Prudencio M. and Mota M., 2007, for a recent review). Specialised liver macrophages called Kupffer cells phagocytosee foreign particles including the parasites and destroy them. However, the sporozoites have developed strategies that bypass this immune defence system so they can safely cross these cells. Once free, the parasites burrow through several hepatocytes before beginning multiple rounds of asexual replication producing thousands of erythrocytic-infective merozoites (Frevert U. 2004). However, it is interesting to note that both *P. vivax* and *P. ovale* can form hypnozoites which remain dormant in the liver cells and can cause relapses of malaria months or years later after reactivation. These merozoites burst from the hepatocytes and re-enter the bloodstream to invade erythrocytes (red blood cells: RBC). Merozoites form the smallest cells in the parasite life-cycle and are covered in a thick

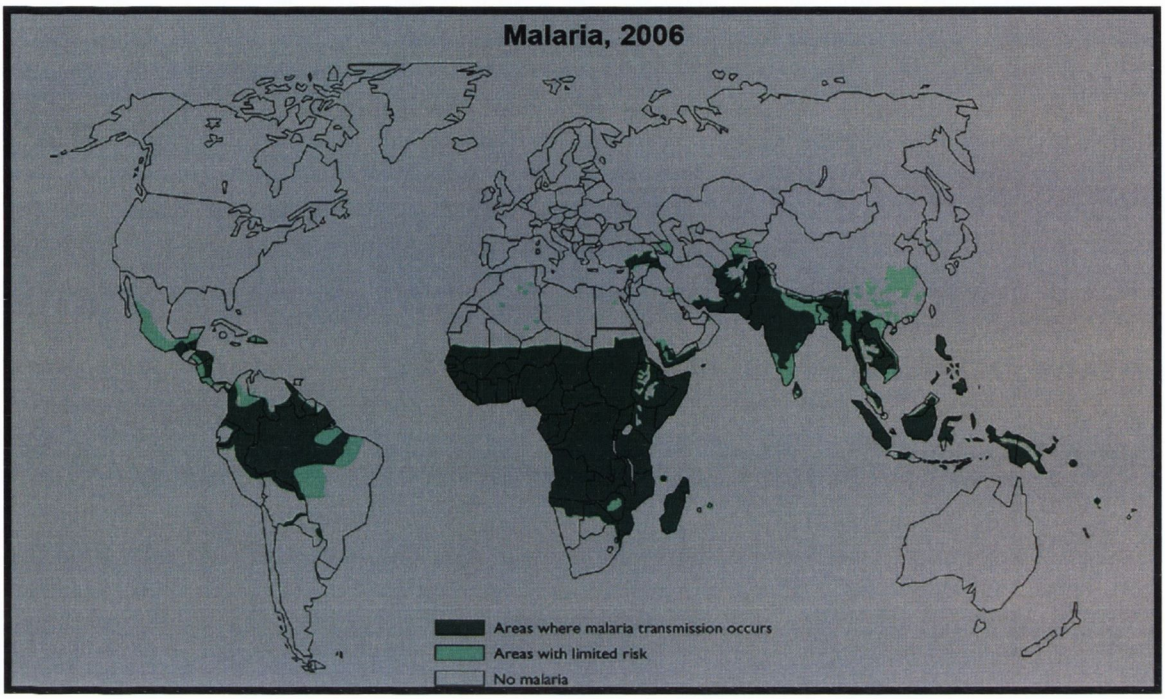

Fig. 1.1 Global distribution of malaria risk areas in 2006. The map is shaded representing area of high (**dark green**), moderate (**light green**) and no risk (not shaded). The map was obtained from http://www.who.int/malaria/malariaendemiccountries.html.

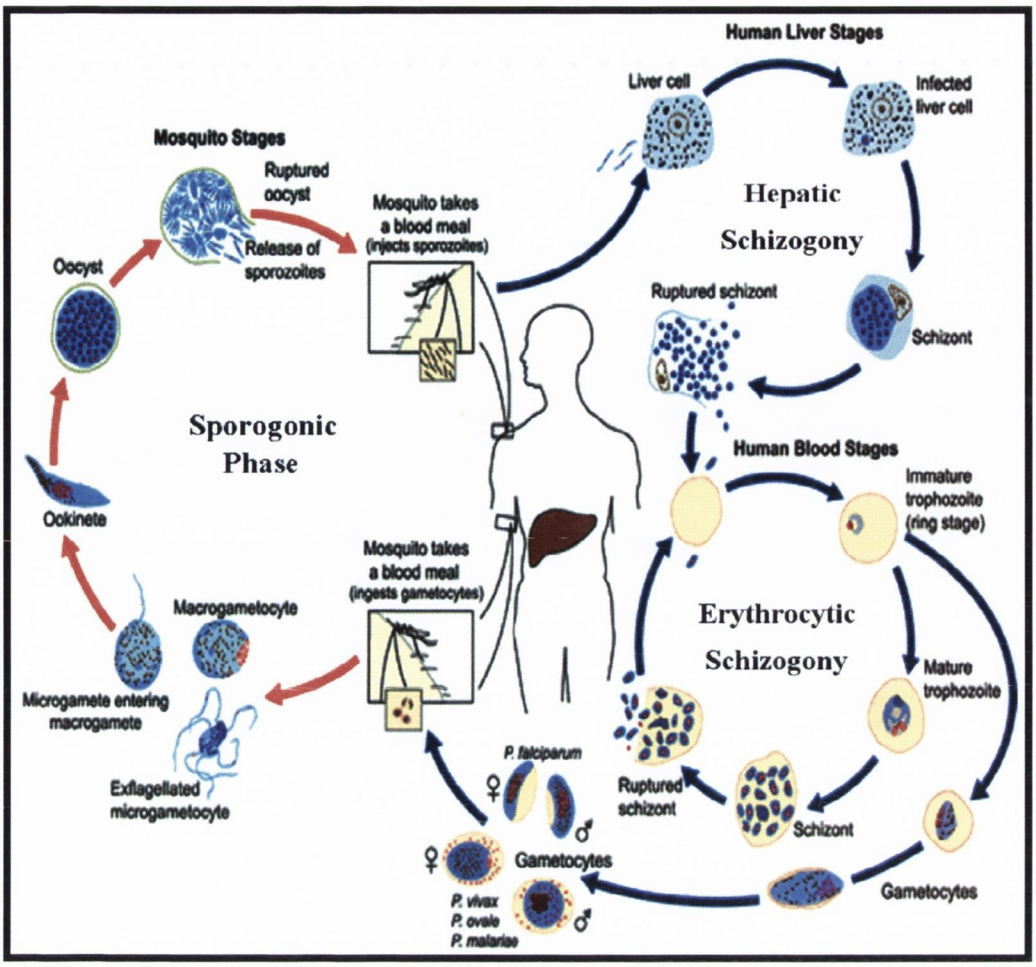

Fig. 1.2 Schematic overview of the *P. falciparum* bi-phasic lifecycle. Adapted from http://www.dpd.cdc.gov/dpdx/HTML/ImageLibrary/Malaria_il.html. See text for details.

bristly coat which is used to adhere to erythrocytes. Once firmly attached, the parasite induces the construction of a vesicle inside the erythrocyte called a parasitophorous vacuole (PV). An actin-myosin motor propels the merozoite into this cavity whereby it subsequently secretes an array of proteins which induce the enlargement of the PV (Bannister *et al.,* 2000). This marks the beginning of the intra-erythrocytic cycle which is typified by multiple rounds of asexual replication. For *P. falciparum*, this cycle spans 44-48 h and is the main source of the clinical manifestations of the malaria disease. Both fever and anaemia result from the erythrocytic invasion and eventual destruction. There are four distinct intra-erythrocytic parasite stages that can be identified from a blood smear by light microscopy which ultimately end with the release of merozoites; rings (0-16 h), early trophozoites (16-28 h), late trophozoites (28-36 h) and schizonts (36-48 h). The initial ring stage is characterised by remodelling of the parasite and RBC structure. Parasites begin digesting the interior of the RBC, including haemoglobin. Furthermore, the RBC membrane sometimes displays the *P. falciparum* erythrocyte membrane protein (PfEMP1). This protein causes infected erythrocytes to bind with uninfected erythrocytes in a process termed rosetting and also permits adherence to vascular endothelial cells. Rosetting acts a cloaking device preventing an immune response towards the parasitized cells and leads to severe parasite infections particularly by causing blot clots. The early and late trophozoite stages are differentiated from the rings based on size and shape. The parasite metabolism also reaches its maximum in terms of growth and activity in the trophozoite stage. Therefore, this stage is often highly sensitive to chemotherapeutics, particularly anti-folate inhibitors. The schizont phase undergoes multiple rounds of nuclear division producing up to 32 merozoites. The PV and the erythrocytic membrane are degraded and the merozoites escape to invade more RBC's. A secondary pathway can be initiated by merozoites which finally produces both macro- (female) and micro- gametocytes. These gametocytes travel from peripheral capillaries just beneath the surface of the skin and infect feeding mosquitoes to restart the process.

1.3 CURRENT MEASURES FOR CONTROLLING THE SPREAD OF THE MALARIA

Due to the global spread of the malarial parasite effective control measures have had limited success. Nonetheless, several strategies have been adopted or are in development which, combined, should reduce further the burden of this disease.

1.3.1 Controlling the transmission rates of the *Plasmodium* parasites

Transmission of malaria in an endemic region is referred to as being stable or unstable depending upon whether the infection rates are relatively constant from year to year or if there are peaks and troughs (Reiter P. 2008). The number of infective bites a person receives on average during the year, the entomological inoculation rate (EIR), in a region with stable transmission is >5 (but often >100) versus <5 for an unstable transmission (WHO recommended treatment 2006). In areas of stable transmission, adult inhabitants frequently have partial immunity but still have low parasite densities in the bloodstream. These infections are often asymptomatic so these people act as a constant reservoir to infect feeding mosquitoes. People with an under-developed or impaired immunity such as young children or pregnant women are disproportionately affected and often comprise the majority of casualties from this disease (White N. 2008). Unstable transmission rates of the parasites often prevent any resistance to the disease from developing so that new infections are almost always symptomatic irregardless of age or immune status (White N. 2008). This can cause sudden devastating epidemics, such as the Sri Lankan outbreak in 1934/35 that killed approximately 100,000 people after several relatively disease-free years led to a low community immunity (Reiter *et al.*, 2004). Furthermore, a comparison between two communities – Linzolo, Congo and Pikine, Senegal – which have stable and unstable transmission rates respectively, showed that Linzolo had only 1.3 times more cases of malaria despite the transmission rates being ~1000 fold greater than in Pikene, highlighting the difficulty in controlling this disease (Trape *et al.*, 2002). A standard control method which is still recommended by the WHO is insecticide impregnated bed-nets. However, their effectiveness was questioned due to the loss of acquired immunity from frequent infection which can lead to increased rates of severe malaria

and that the reduction in transmission rates is insignificant (Molineaux L. 1997, WHO 2006 and Trape *et al.*, 2002). Therefore, vector control strategies where there are stable transmission rates are unlikely to be successful due to the fact that even low mosquito numbers can maintain a viable population of the parasite (see Fig. 1.3). As a result, development of a vaccine or new chemotherapeutics is essential for controlling this disease.

1.3.2 Development of potential malarial vaccines

In recent years, a malaria vaccine has become a realistic goal. GlaxoSmithKline currently lead the way with the RTS,S/AS02A malaria vaccine which is currently in phase III clinical trials after successfully reducing the prevalence of *P. falciparum* infection by approximately a third in Mozambican children aged 1–4 years for up to 45 months (Sacaral *et al.*, 2009). The vaccine is based on using a surface protein from the pre-erythrocytic stage of *P. falciparum* (Guinovart *et al.*, 2009 and Sacaral *et al.*, 2009). However, it could be many years before it becomes widely available, assuming that it passes all the clinical trial studies and even still, its will only reduce rather than cure malaria.

1.3.3 Transgenic mosquitoes

Research is currently underway for designing transgenic mosquitoes that are resistant to the malaria parasite. Mosquitoes have some immunity to infection themselves and in the field carry less than five oocysts (Ito *et al.*, 2002). Early work using a rat model identified a specific ligand that is found in the midgut and salivary glands of the mosquito. This ligand is an essential receptor for the parasites. Mosquitoes were transfected with a plasmid over-expressing a 12 amino acid peptide that is used by the parasite to bind to the aforementioned ligand. This resulted in a significant decrease in parasite transmission to other naïve rats. Although this new strategy sounds promising, it is still in its infancy and there are many obstacles to overcome before it could become a realistic malaria control method (Ito *et al.*, 2002).

1.3.4 Anti-malarial chemotherapeutics

The last line of defence against malaria is chemotherapeutic drugs, which are currently the best method for dealing with this disease. There are several clinically relevant drug targets that are in use today (Table 1.1). However, another 21 new medicines from pre-clinical to stage III trials are in the research pipeline, of which some are novel agents (Olliaro and Wells, 2009). Artemisinins in combination with other drugs such as mefloquine and lumefantrine are considered the drugs of choice due to their ability to clear parasites quickly from the patient with only mild side-effects. However, these drugs tend to be expensive and other treatments such as chloroquine and pyrimethamine-sulphadoxine are frequently used in their place. The majority of the available treatments are effective against the parasite's intra-erythrocytic cycle, which is most likely due to the high metabolism rates caused by rapid asexual reproduction. This is advantageous as most treatments demonstrate cross-activity for all the *Plasmodium* species. Unfortunately, *P. vivax* and *P. ovale* have the ability to form dormant hypnozoites in the hepatocyte cells which can cause recrudescence in patients unless they are removed. Primaquine is considered the only effective treatment to remove them but it often causes severe haemolysis to patients who are deficient in the glucose-6-phosphate dehydrogenase enzyme (Lalloo *et al.*, 2006). As a result, this drug is not commonly used and patients with *P. vivax* or *P. ovale* infections often experience recrudescent infections.

Parasite drug resistance, particularly to chloroquine, has being a growing problem for decades and has being blamed for an average two-fold increase in morbidity and mortality across African nations (Trape *et al.*, 2002). In recent years, the WHO has launched a policy of recommending combinational therapy, which is the use of two drugs with different modes of actions to limit the spread of resistance, which is more important than ever now since the emergence of artemisinin resistance (WHO treatment guidelines 2006). The ability of parasites to develop and spread resistance is a multi-factorial and complex process. A key effect is the transmission of parasites once they have been exposed to anti-malarial compounds. Stressing the parasites in general (e.g. semi-efficacious drug treatment or immune response), anaemia and long infection periods all encourage the production of gametocytes which result in greater transmission rates. Drug regimes can be partially active for numerous reasons e.g. poor adherence to the medication due to side-effects or loss of

Target location	Pathway/mechanism	Target molecule	Examples of therapies	
			Existing therapies	New compounds
Cytosol	Folate metabolism	Dihydrofolate reductase	Pyrimethamine, proguanil	Chlorproguanil
		Dihydropteroate synthase	Sulphadoxine, dapsone	
	Glycolysis	Thymidylate synthase		5-fluoroorotate
		Lactate dehydrogenase		Gossypol derivatives
		Peptide deformylase		Actinonin
	Protein synthesis	Heat-shock protein 90		Geldanamycin
	Glutathione metabolism	Glutathione reductase		Enzyme inhibitors
	Signal transduction	Protein kinases		Oxindole derivatives
	Unknown	Ca^{2+}-ATPase	Artemisinins	
Parasite membrane	Phospholipid synthesis	Choline transporter		G25
	Membrane transport	Unique channels	Quinolines	Dinucleoside dimers
		Hexose transporter		Hexose derivatives
Food vacuole	Haem polymerization	Haemozoin	Chloroquine	New quinolines
	Haemoglobin hydrolysis	Plasmepsins		Protease inhibitors
		Falcipains		Protease inhibitors
	Free-radical generation	Unknown	Artemisinins	New peroxides
Mitochondrion	Electron transport	Cytochrome *c* oxidoreductase	Atovaquone	
Apicoplast	Protein synthesis	Apicoplast ribosome	Tetracyclines, clindamycin	
	DNA synthesis	DNA gyrase	Quinolones	
	Transcription	RNA polymerase	Rifampin	
	Type II fatty acid bio-synthesis	FabH		Thiolactomycin
		FabI/PfENR		Triclosan
	Isoprenoid synthesis	DOXP reductoisomerase		Fosmidomycin
	Protein farnesylation	Farnesyl transferase		Peptidomimetics
Extracellular	Erythrocyte invasion	Subtilisin serine proteases		Protease inhibitors

DOXP, 1-deoxy-D-zylulose 5-phosphate; PfENR, *Plasmodium falciparum* enoyl-ACP reductase.

Table 1.1 Overview of the targets of anti-malarial drugs that are clinically relevant. (This figure was modified from Fidock *et al.*, 2004.)

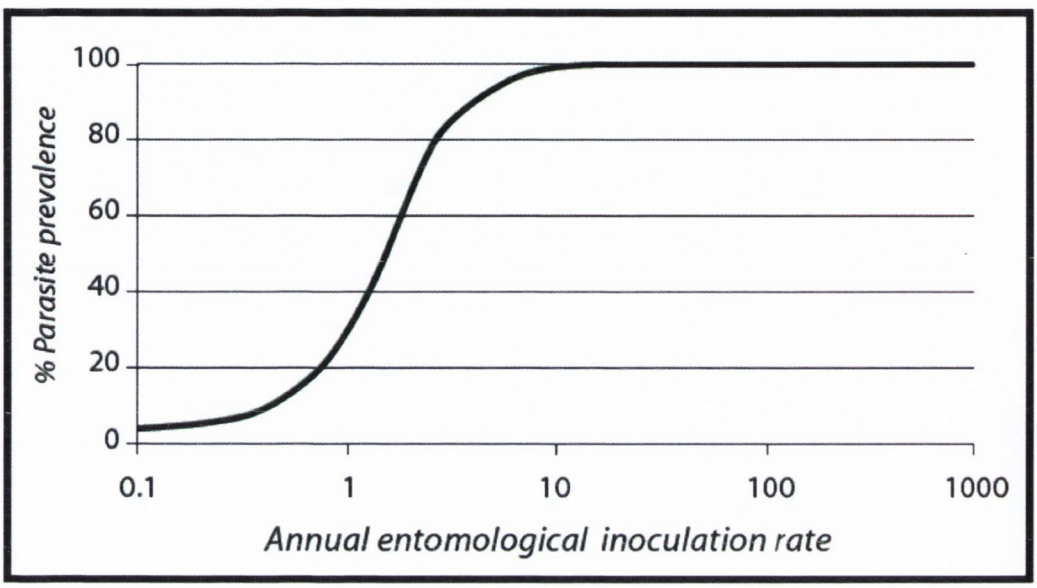

Fig. 1.3 Relationship between the number of infective mosquito bites and parasite prevalence in a population. A small number of infective bites can lead to a dramatic increase in parasite numbers within a population making it difficult to eradicate. (Graph reprinted from WHO 2006 recommended treatment.)

symptoms due to parasitemia reduction, non-optimal drug concentrations due to re-infection near the end of treatment or varying pharmacokinetics (e.g. drug uptake can vary from person to person due to diet and health). Partial immunity can be further problematic as it keeps parasite numbers in check, so that the patient is asymptomatic but still infective. The overall result is sustained infections and greater haemolysis pushing for greater production of gametocytes which are increasingly likely to carry resistance (White N. 2008). Also, chloroquine-resistant strains were demonstrated to produce 2.5 times more gametocytes than their sensitive counterparts (Buckling *et al.*, 1997). Halting the spread of resistance is further compounded by increased rates of transmission due to the elimination of the sensitive strains (Walliker *et al.*, 2005). However, parasite drug resistance frequently incurs a fitness cost which can see the re-emergence of a sensitive strain. This was observed in Malawi whereby chloroquine resistance was up to 80% but 10 years after its use was discontinued is almost 0% (Laufer *et al.*, 2004). The fitness cost may also be overcome by one or more compensatory mutation(s) which would then firmly embed the new changes in the parasite's genes. By understanding the spread of parasite resistance, it may be possible to prevent or control it in the future with novel drugs.

1.4 TUBULIN STRUCTURE, FUNCTION AND REGULATION

1.4.1 General structure of tubulin and microtubules

Microtubules (MT) are hollow filamentous polymers, found in almost all eukaryotic cells, which are comprised of repeating α- and β-tubulin heterodimers (see Fig. 1.4). These structures have an external diameter of ~25 nm but can grow as long as a few μm. They have many critical functions within the cell including separating the chromosomes during mitosis/meiosis, intracellular transport of vesicle and organelles, motility and maintaining the cell shape. Arguably the most important property of MT's is their ability to elongate and shorten rapidly depending on a number of factors; most typical are intrinsic polymer instability, local conditions, the presence of microtubule associated proteins (MAP's) and post-translational modifications of tubulin. Homologues that mimic the functions of MT's such as FtsZ have been found in bacterial systems. These proteins are highly divergent at the amino level but the regions responsible for GTP binding and hydrolysis are

conserved. Furthermore, they maintain an overall 3-D structural similarity suggesting that they evolved from a common source.

In vivo folding of both α- and β-tubulin is an ATP- and a GTP-dependent process which requires a large multi-subunit complex called the eukaryotic cytosolic chaperonin containing t-complex polypeptide 1 (CCT). CCT can bind fully denatured α- or β-tubulin and partially fold them. The intermediate structures are captured by other co-factors; B and E for α-tubulin and A and D for β-tubulin. Only Eα- and Dβ-complexes can interact together with co-factor C. The heterodimeric tubulin is then released upon hydrolysis of the β-tubulin GTP. The co-factors A and B appear to act as a reservoir for semi-folded tubulins. Depletion of one monomer by excess amounts of a co-factor rapidly triggers the other monomer to be degraded, thereby maintaining a tubulin concentration balance within the cell (Lewis et al., 1997).

The major tubulins are α and β but γ, δ, ε, ζ and η tubulins have also been identified, although they do not polymerise in the same way (McKean *et al.*, 2001). α- and β-tubulin are similar in size, ~50 kDa and have a similar overall structure despite only sharing an approximate 43% identity at the amino acid level (Bell A., 1998). The majority of the variation is due to the acidic C-terminus which can even vary in length by several amino acids. The crystal structure of zinc-induced and taxol stabilised bovine brain tubulin sheets has been resolved at 3.5 Å (Lowe *et al.*, 2001). Each monomer contains three distinct domains. The N-terminal nucleotide binding domain (residues 1-206) is formed with 6 parallel β-strands and alternating helices that create a GTP-binding pocket. This site in α-tubulin traps one molecule of GTP when the α/β-dimer is incorporated into a polymer and is also known as the non-exchangeable site (N-site). In contrast, the GTP nucleotide in β-tubulin is freely hydrolysable and this region is called the exchangeable site (E-site). The intermediate domain (residues 207-384) has 5 α-helices and one mixed β-sheet. The nucleotide catalytic site resides in this region and it is able to convert GTP to GDP in the β-tubulin subunit when it is part of a polymer. The final region is the carboxy-terminal domain and this uses two anti-parallel helices to cross over the aforementioned domains. Despite the high resolution achieved with this crystal structure neither of the N-, C-terminal tails nor the N-terminal loop in α-tubulin (residues 35-60) were resolved.

MT's are comprised of repeating α- and β-tubulin heterodimers which bind in a head-to-tail fashion, and usually 13 slightly staggered protofilaments linked together

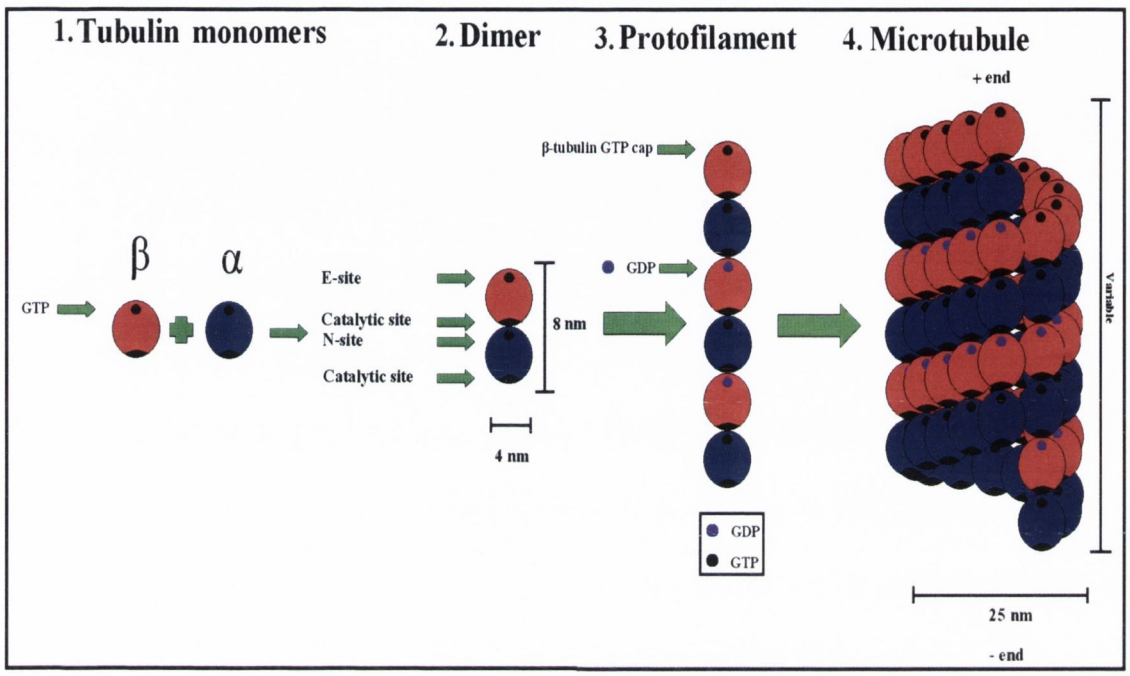

Fig. 1.4 Schematic diagram of microtubule formation and structure. 1. α- and β-tubulin monomers, both with one molecule of GTP. These molecules are not usually found isolated in the cell but are included for completeness. **2.** α/β-tubulin dimers. The exchangeable (E-site) site, non-exchangeable (N-site), and catalytic sites are shown. **3.** The protofilament is an intermediate oligomer that formed from the longitudinal stacking of tubulin dimers. For β-tubulins in the centre of the protofilament, GTP is hydrolysed into GDP by the catalytic action of the α-tubulin **4.** The microtubule is formed from the protofilaments which laterally align and eventually close over. Microtubules have both a + end which is highly dynamic and a – end which is less dynamic. The approximate sizes of some structure are indicated. (Adapted from Fennell, 2005.)

in parallel to form the polymer (Amos *et al.*, 2005). A B-lattice structure was found in MT's whereby the major lateral contacts are made between homologous subunits (i.e. α-α and β-β). The primary lateral contacts between adjacent protofilaments occur through the M loop (residues 279-287) and the loop between S7 and H9, interacting with loop H1-S2 and helix H3. In α-tubulin only, the M loop is further stabilised by the S9-10 loop. A seam, lateral contact between heterologous subunits, exists in the typical 13 protofilament MT and is predicted to result from the closure of the polymer. Its functions include binding of specific MAP's and controlling MT stability.

1.4.2 Microtubule dynamics

MT's have an intrinsic instability, in that they can rapidly elongate or shorten. The stochastic switch between a growing MT and one that is shortening is called "catastrophe" and the reverse is called "rescue". This occurs by either dynamic instability, whereby random switching between growth and shrinking phases occurs, or treadmilling, which is the preference for dimers to be added to the one end of the polymer while being removed from the other. MT ends have distinct polarity, with the minus end being less kinetically active or dynamic than the plus end. The difference is due to the terminal subunit with the α- and β-tubulins crowning the minus and plus end respectively. The nucleotide state of α-tubulin never changes; it is always bound with a GTP molecule. Furthermore, α-tubulin has a stabilised M loop, as previously mentioned, so confers greater lateral contacts than β-tubulin. In contrast, the plus end terminates with a GTP-bound β-tubulin subunit having a GTP cap which has an exposed E-site. The α-tubulin of this subunit rests on another β-tubulin and can hydrolyse its GTP to GDP-P_i. Recent evidence argues that the GTP cap is required to be at least 5 layers deep to compensate for the frequent but brief "growth-phase shortening" phenomenon and not one layer as previously suggested (Schek *et al.*, 2007 and Caplow *et al.*, 1996). However, the hydrolysis of the β-tubulin GTP within the polymer may not be complete as once thought. An antibody specific for GTP-bound tubulin in MT recognised the GTP-cap as expected but also regions in the middle of the polymer. It was suggested that these GTP-islands act as a "speedbump" that encourage rescue in the event of catastrophe (Dimitrov *et al.*, 2008). The GTP cap is crucial in maintaining stability to the inner labile core of the

MT and once it is lost, protofilaments curl up, breaking the lateral bonds and encouraging rapid disassembly (Nogales *et al.,* 2006, Nogales *et al.,* 2003 and Ravelli *et al.,* 2004). This is due to the tendency of GDP-dimers to bend and even form rings with each other as opposed to GTP-dimers which have a straight structure. Therefore, forcing the GDP-dimers to adopt this straight configuration within the polymers, stores up potential conformational energy which can be used for various tasks. Recent data has demonstrated that single dimers and not oligomers are added or lost from MT's in general which is contrary to other published studies (Schek *et al.,* 2007 and Kerssemakers *et al.,* 2006). Schek *et al.,* argued that poor resolution from previous techniques, particularly light microscopy, could only detect large mass changes. However, they used optical tweezers which can track individual tubulin subunits and determined that addition of oligomers occurred <1% of the time (Schek *et al.,* 2007).

1.4.3 Functions of microtubules in the cell

Microtubules can perform many diverse functions due to their flexible architecture. The most common are in cell division, maintaining the cytoskeleton and forming flagella/cilia. However, the structure and stability of the MT's vary significantly.

Mitotic spindles are highly dynamic microtubules that facilitate the separation of chromosomes during the cell cycle. Low intracellular tubulin concentrations are a kinetically limiting factor which requires the nucleation of MT's. Nucleation occurs from the mitotic organising centre (MTOC) which are centrosomes in animals, or spindle pole bodies in fungi, and existing spindles (Wiese *et al.,* 2006 and Zhu *et al.,* 2009). However, γ-tubulin is always required for this event. There are two γ-tubulin complexes, the γ-tubulin small complex (γTuSC) and the γ-tubulin ring complex (γTuRC). γTuRC is a much larger protein complex than γTuSC but they can both carry out the same functions (Raynaud-Messina *et al.,* 2007). Two theories exist to explain the nucleation mechanism; the template model and the protofilament model. The template model suggests that the α-tubulin rests on the γ-tubulin complex forming lateral contacts, whereas, the protofilament model suggests the γ-tubulin complex is partially embedded in the MT and forms both lateral and longitudinal associations with both tubulins (Raynaud-Messina *et al.,* 2007). Furthermore, the

other 4 tubulin isotypes, δ, ε, ζ, and η have been localised in the MTOC and may be important for its construction (McKean *et al.*, 2001).

In contrast to mitotic spindles, cytoskeletal microtubules form a relatively stable and rigid framework within the cell. Their primary functions are to resist compression forces and act as tracks along which organelles or proteins can move. Molecular motors including Dam1 and the kinesin family act as part of the intracellular transport system, although they use different mechanisms. The Dam1 protein complex is an integral component in the *Saccharomyces cerevisiae* kinetochore which is critical in cell division and it forms a ring around the plus end of MT's *in vivo*. This complex is able to reliably move along the polymer without an additional energy source (Gestaut *et al.*, 2008). Two mechanisms in particular have been proposed to explain this phenomenon (Gestaut *et al.*, 2008 and Hill T. 1985 and Koshland *et al.*, 1988). The conformational wave theory works by the protofilaments curling at the ends and physically pushing the Dam1 complex, which acts as a clamp, forward (Koshland *et al.*, 1988). Gestuat *et al.*, have challenged this mechanism and proposed an alternative strategy, biased diffusion that was based on the work of Hill (Gestaut *et al.*, 2008 and Hill T. 1985). The Dam1 complex can function as a sleeve or a small oligomer that tracks along polymer by random diffusion but once it meets a disassembling microtubule tip, it will travel with it because that is more energetically favourable than disassociating (Gestaut *et al.*, 2008 and Hill T. 1985). The kinesin proteins represent a directed method for intracellular transport. These proteins have two heads that are connected by a neck region. Movement is achieved by one head stepping in front, tightly gripping the microtubule lattice, which then allows the trailing head to swivel around and gain the lead at a cost of 1 ATP molecule (Thomas *et al.*, 2002). However, kinesins can also rapidly but randomly diffuse along the polymer without expending energy once both heads release their tight grip (Cooper et al., 2009).

The central core of all eukaryotic cilia and flagella consist of the highly conserved molecular machine called the axoneme. The axoneme is composed of more than 250 proteins but the characteristic structure is the nine peripheral doublet microtubules and the central pair of singlet microtubules (termed A- and B-tubules respectively). The structures are linked together by the dynein motors and flexible nexin molecules making up the radial spokes. Dynein undergoes a conformational change after hydrolysing ATP. This causes a sliding motion between the A- and B-

tubules corresponding to the wave-like movement associated with the flagella and cilia (Downing *et al.*, 2007).

1.4.4 Intracellular regulation of microtubule function

As expected, regulation of the tubulin assembly and disassembly in the cell is tightly controlled. It is influenced by numerous factors, not least its own dynamic instability, but only some of the more important post-translational effects will be mentioned.

MAP's are proteins that transiently attach to MT's but are not essential for polymerisation, although *in vivo* they are vital for regulating their stability. They can bind tubulin dimers, microtubule walls and/or tips (Akhmanova *et al.*, 2008) and frequently have repetitive motifs which allow them to interact across several domains at once (Amos 2005). Two antagonistic regulatory MAP's are katanin and tau (Qiang *et al.*, 2006). Katanin is a heterodimeric protein which is found in high concentrations in the axons of neuronal cells. It destabilises MT's but particularly when they are attached to the centrosomes. This is achieved by forming a temporary hexadimer complex that splits the contact between αβ-tubulin in the walls of MT and eventually severs the polymer. The nascent ends of the polymers have no GTP-cap to stabilise them and rapidly disassemble (Amos *et al.*, 2005 and Nogales E. 2000). Tau is also concentrated in the neuronal cells but it stabilises MT's by inserting into a hydrophobic pocket located on β-tubulin. A similar domain is found in α-tubulin but this is naturally stabilised by the folding of the L-loop. In fact, there is evidence to suggest that the tau binding site overlaps with that of Taxol (Amos *et al.*, 2005). Tau also provides resistance to katanin on the long MT's found in the axon, possibly by physical hindrance. This is important as neurons require a constant population of both long and short MT's (Qiang *et al.*, 2006). This demonstrates one of the many intricate regulatory systems that occur among MAP's and microtubules.

Post-translation modifications (PTM) are mechanisms used by cells to rapidly increase diversity among the MT's. Most of the changes are enzymatically based and are reversible. There are at least 7 types of modifications; acetylation/deacetylation, tyrosination/detyrosination, generation of Δ2-tubulin, polyglutamylation, polyglycylation, palmitoylation and phosphorylation. Their effects range from addition/removal of a single amino acid such as the C-terminal tyrosine to extensive

changes such as polyglycylation which can add on an extra 34 residues. All of the PTM's discovered to date affect the C-terminus of the tubulins with the exception of acetylation (Westermann *et al.*, 2003). Many functions of PTM's have yet to be elucidated but they are known to be important in attracting microtubule associated proteins (MAP) to microtubules. Furthermore, they may affect the stability/structure of MT's, although this could be an indirect effect of recruiting certain MAP's (Hammond *et al.*, 2008).

Isotypes of α- and β-tubulin serve as another means of differentiation and control within the cell. Aside from the very "simple" organisms such as protists, cells or tissues (in the case of higher eukaryotes) have several isotypes which are expressed at different times and amounts (Luduena R. F., 1998). This is particularly evident with higher eukaryotes such as *Arabidopsis* that has at least 9 β-tubulin isotypes, but their expression is localised to certain areas, i.e. TUB1 and 5 are found mostly in the roots leaves respectively (Luduena R. F., 1998). Tubulin isotypes can be functionally interchangeable but in *Plasmodium berghei*, both α-tubulin isotypes are essential (Luduena R. F., 1998 and Kooij *et al.*, 2005). Furthermore, different tubulin isotypes are capable of co-assembly. The reason for this is that a cell undergoing a transition state, whereby a new tubulin isotype dominates expression, can still function with both isotypes present, as in the case of *Physarum spp.* (McKean *et al.*, 2001). The majority of differences between isotypes are at the C-terminal tails which is not surprising considering this is where most of the PTM's occur.

Environmental and intracellular factors, particularly temperature and the tubulin critical concentration, play a critical role in tubulin dynamics. Temperature exerts its effects on tubulin by changing the assembly kinetics as the process is enthalpically driven (Correia *et al.*, 1983). This is most evident with the Antarctic fish, which spend their life in perennially cold climates at ~ -1.8°C. The minimum critical concentration for tubulin assembly (C_c) is 0.74 mg/ml at -1.8°C but at 37°C it is 16 times lower (0.046 mg/ml) as a result of increased polymerisation rates (Williams *et al.*, 1984). The tubulin C_c *in vitro* is an important factor that influences assembly, although the actual concentration values quoted are likely to be inaccurate for *in vivo* polymerisation. In the cell, there are numerous structures and MAP's which can affect this value, including γ tubulin which is an integral component in the microtubule organising centre (MTOC) (Wiese *et al.*, 2006). Small metal ions, particularly Ca^{2+} and Mg^{2+}, also contribute to the MT stability and have antagonistic

effect *in vitro*. Ca^{2+} ions have one high affinity site on the C-terminus of both α- and β-tubulin. Ca^{2+} has been demonstrated to promote tubulin disassembly *in vitro* either as a free ion or in a protein complex, e.g. with calmodulin, by increasing the rate of GTP hydrolysis at the cap of a growing MT (O'Brien *et al.*, 1997 and Lacey E., 1988). Conversely, Mg^{2+} ions are essential for MT polymerisation and high concentrations significantly enhance the assembly rate. There are two well known high-affinity Mg^{2+} binding sites on tubulin; both of them are located at the GTP binding domains, but, other low affinity sites are thought to exist. Mg^{2+} exerts is effects on the proteins by promoting the C-terminal tail interaction with the body of the protein. Therefore, these ions provide another system for controlling tubulin dynamics (Bhattacharya *et al.*, 1994). Also, moderate GTP concentrations (1-5 mM) and pH (~6.9) favour *in vitro* tubulin assembly. However, concentrations of GTP that are either too low (<1 mM) or too high (>5 mM) inhibit tubulin assembly, further highlighting the finely tuned nature of this process (Jameson *et al.*, 1980). Extremes of pH can induce many polymorphic tubulin structures such as open sheets and rings although these effects may not be biologically relevant (Oxberry *et al.*, 2000).

1.5 MICROTUBULE INHIBITORS

Tubulin inhibitors have been used for decades to treat a range of illnesses such as anthelmintic infections and cancer. Although these diseases have a very different pathology, a common factor to both is rapid cell division and they are therefore very sensitive to changes in the MT assembly balance. Tubulin poisons can be broadly categorised into polymerisation stabilisers or polymerisation destabilisers. Three classical tubulin binding sites have been discovered to date; the colchicine binding site, the vinca-domain and the taxol binding site. However, several novel sites have also been proposed which may also prove to be pharmacologically relevant.

1.5.1 Classical inhibitors: Colchicine

Colchicine is a naturally occurring alkaloid that was originally isolated from the meadow saffron (*Colchicum autumnale*). It's therapeutic uses are limited due to high toxicity to humans. However, it has been successfully employed for an array of auto-inflammatory diseases and gout (Bhattacharyya *et al.*, 2008) It is comprised of 3

rings, a trimethoxy benzene ring (A), a septagon ring with an acetamido group (B) and a methoxy tropone ring (C) (see Fig. 1.5). However, analogues with rings A and C only without the B ring could still interact with tubulin dimer. The B ring substituent, the acetamido group, is important for modulating binding kinetics by forming additional contact to the tubulin molecule (Chakrabarti *et al.*, 1996). Colchicine preferentially binds soluble tubulin dimers but these dimers may still join elongating MT's. It has one high affinity binding site buried in the intermediate domain of β-tubulin, beside the GTP-binding site of α-tubulin (49 Ravelli *et al.*, 2004). The binding mechanism is biphasic. The initial interaction is rapid but reversible. The second step is much slower but creates a tight complex that is considered "pseudo-irreversible" due to the very slow disassociation rate. The second step forces the tubulin dimer to adopt a conformational change (Garland D., 1978). The importance of this structural modification was later elucidated when the crystal structure of tubulin with colchicine was solved. Tubulin-colchicine complexes have a bent shape which cannot straighten up even when they join the tips of growing MT's. As a result, the M-loop is prevented from forming lateral contacts with other subunits, destabilising the entire polymer. However, at low concentrations, colchicine just halts the growth of MT's but at higher concentrations, the loss of lateral contacts is so great that the polymer completely depolymerises (Ravelli *et al.*, 2004). The induction of a curved tubulin configuration naturally occurs within the cell upon association with known MAP's which are designed to destabilise MT's (Steinmetz *et al.*, 2000 and Ogawa *et al.*, 2004). This is particularly true for the kinesin 13 MAP which was observed by an atomic model to mediate curvature of an intra-dimer tubulin structure (Tan *et al.*, 2008). Therefore, it is interesting to speculate that the colchicine ligand just hijacked this established mechanism rather than using a novel approach to poison MT dynamics.

There are several other chemically unrelated agents that also bind at or near to the colchicine site. Curacin is another natural product synthesized by the cyanobacterium *Lyngbya majuscula*. This compound binds both faster and tighter to tubulin than colchicine making it an attractive lead compound for further development of anticancer agents (Verdier-Pinard *et al.*, 1999). Other compounds have already demonstrated their clinical effectiveness and are being developed further as anti-cancer agents. Combretastatin, for example, effectively inhibits tumour vasculature by disrupting interphase microtubules (Risinger *et al.*, 2009 and Morris *et al.*, 2008).

1.5.2 Classical inhibitors: Vinblastine

Vinblastine and vincristine are the classic "vinca-alkaloids" produced by the periwinkle plant (*Catharanthus roseus*) that are identical in structure except for a single substitution of a formyl for a methyl group (Fig. 1.6). This single change makes a dramatic impact on the effectiveness of the compounds on particular cancer types. As a result, many semi-synthetic derivatives have since been generated, each with different therapeutic profiles (Risinger *et al.*, 2009). The structure of vinblastine is very complex but it essentially consists of two linked multi-ringed moieties called catharanthine and vindoline. Despite the fact that these compounds have been used for decades the tubulin crystal structure with vinblastine has only recently been solved to 4.1 Å. Only one binding site was elucidated, although other groups did report there may be two, particularly at high concentrations of the ligand (Bhattacharyya *et al.*, 1976, Lee *et al.*, 1975, Gigant *et al.*, 2005). Vinblastine binds so deeply in a hydrophobic wedge between two adjacent αβ-dimers that as much 80% of its total surface area resides within the complex. The ligand interacts equally with one α- and one β- tubulin subunit from either dimer producing a curved conformation inhibiting MT dynamics in a similar fashion to that of colchicine (Gigant *et al.*, 2005). Small conformational changes are made to occur in tubulin which accounts for the rapid and reversible binding equilibrium ($t_{1/2}$ ~15 min) (Lacey E., 1988 and Gigant *et al.*, 2005).

However, the "vinca" domain also accommodates a second, overlapping binding site that is generally used by small highly toxic peptides, e.g. dolastatin 10, that are commonly synthesized by various marine organisms (Molinski *et al.*, 2009). Dolastatin 10 was the first molecule to be associated with this expanded domain because it could non-competitively inhibit radio-labelled vinblastine in a tubulin binding assay (Bai et al., 1990). More recently, another atomic structure with bovine brain tubulin was crystallised with phomopsin A (a dolastatin 10 analogue). This structure confirmed that there are two overlapping binding sites, the aforementioned vinblastine site and a partially novel peptide site (Cormier *et al.*, 2008). Despite dolastatin 10 and phomopsin both having nano-molar activity against cancer cells lines, they are not currently being developed further due to either poor activity *in vivo* or unacceptable toxicity. Nonetheless, several other marine organisms have been found to produce unique and promising peptides. For example, eribulin mesylate, a

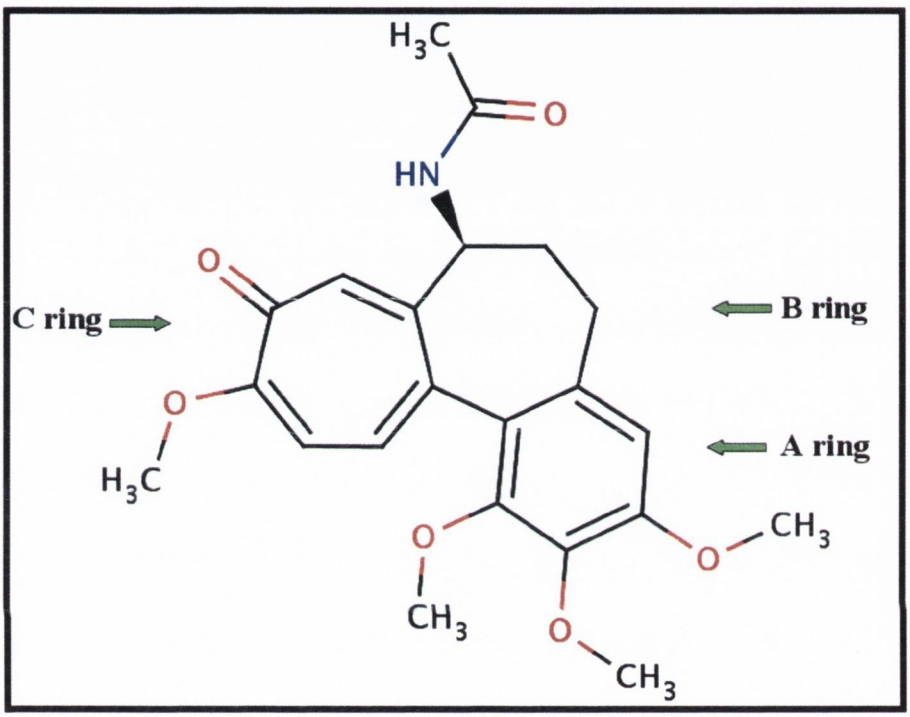

Fig. 1.5 The structure of colchicine. The three rings, A, B and C, are indicated.

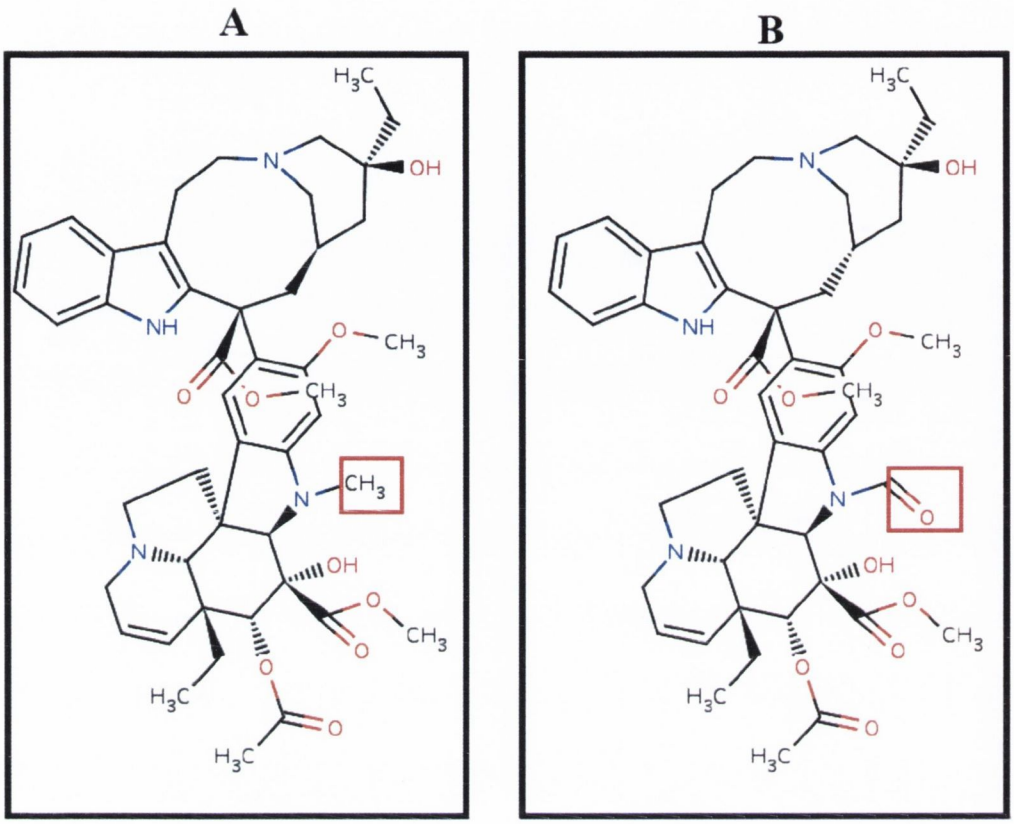

Fig. 1.6 Structures of vinblastine (A) and vincristine (B). The exchange of the methyl group on vinblastine for an oxygen atom on vincristine is highlighted (by a red box.)

truncated version of halichondrin B, is currently undergoing phase III clinical trials for breast cancer treatment (Molinski *et al.*, 2009).

1.5.3 Classical inhibitors: Taxol

Taxol is another natural compound, biosynthesized by the Pacific yew tree (*Taxus brevifola*), that is used as a potent therapeutic for ovarian and breast cancers. Despite being widely successful, the drug has severe dosage limitations due to high toxicity and is prone to resistance via drug efflux pumps (Morris *et al.*, 2008). The structure of taxol is complicated but it is essentially based on a diterpene skeleton (Fig. 1.7). This compound is known to promote microtubule assembly that is resistant to both cold and drug-induced depolymerisation. The taxol binding site is a hydrophobic pocket located in the intermediate domain of the β-tubulin subunit on the lumenal side of the microtubule lattice (Lowe *et al.*, 2001). However, a recent computational modelling study has also proposed the existence of an intermediate binding site within the microtubule nano-pores which aids the drug's diffusion through the polymer until it reaches its final destination. This model would explain the paradox that different human tubulin isotypes have significantly different taxol sensitivities but relatively similar binding sites (Freedman *et al.*, 2009). The presence of the drug initiates the M-loop of one β-monomer to migrate towards the H1-S2 loop of an adjacent β-monomer and bond via van der Waals, electrostatic and ionic forces. Therefore, significant lateral contacts are formed. The conformational curve caused by GTP hydrolysis is also counteracted, possibly by the tubulin becoming more flexible, so the overall MT stability is increased (Elie-Caille *et al.*, 2007, Xiao *et al.*, 2006 and Mitra *et al.*, 2008). Taxol is thought to adopt a T-shaped or butterfly-like conformation in this binding site that resembles the B9-10 loop that in α-tubulin confers extra stability (Synder *et al.*, 2000 and Yang *et al.*, 2009). Clinically relevant doses of taxol suppress microtubule dynamics within a cell rather than causing mass hyper-polymerisation. However, an interesting study reported that taxol could form tubulin-like crystals, when used in excess in a aqueous solution, that could sequester soluble dimers. They suggested that this may be a novel mode of cytotoxicity (Foss *et al.*, 2008).

Recently, other compounds with taxol-like effects have been discovered. Laulimalide and peloruside A are thought to bind in the same site that is close to but

distinct from that of taxol. In fact, both compounds were able to function synergistically with taxol in promoting tubulin assembly. Other taxol-like agents such epothilones and discodermolides which bind at or near the taxol site may also prove to be successful therapeutics in the future (Hamel *et al.*, 2006 and Risinger *et al.*, 2009).

1.5.4 Other Inhibitors: Benzimidazoles

Benzimidazoles are a class of small, broad-spectrum anthelminthic and antiprotozoal drugs that are used in both humans and animals. Albendazole is one of the best known benzimidazole compounds (see Fig. 1.8). A few have been employed as fungicides. They efficiently depolymerise tubulin and it was also thought that these ligands bind in the colchicine site. However, it was recently demonstrated that benomyl, a benzimidazole, and colchicine could bind to tubulin simultaneously. Moreover, this interaction even strengthened their relative affinities for the protein by inducing conformational changes (Clément *et al.*, 2008). Another study generated recombinant β-tubulin and demonstrated that *in vitro* binding is reduced by the mutation Glu198Gly (Holloman *et al.*, 1998). The exact binding site of benzimidazoles has yet to be elucidated but data garnered from resistant protozoa species led to the generation of a molecular model that described a putative cleft in the heart of the β-tubulin protein. The site is located at the interface between the N-terminal and intermediate domain, near the exchangeable nucleotide binding pocket (Robinson *et al.*, 2004). This model predicts a snug fit for the benzimidazole compound, albendazole sulphoxide, potentially allowing for the formation of several hydrogen bonding and hydrophobic interactions. Furthermore, upon entry of the benzimidazole ligand, several conformational changes occur within the tubulin molecule. First, the pocket becomes sealed, further stabilising the tubulin-ligand interaction. Second, the tubulin is forced to adopt a curved shape, as previously described, which is ineffective at forming proper MT's thus explaining the drug's mechanism of action. Although this model satisfies the known molecular data surrounding these compounds, the binding pocket is thought to be inaccessible when the tubulin is dimerised. The authors argued that it may be possible for the drugs to bind monomeric tubulin (Robinson *et al.*, 2004). This is feasible, yet unlikely, as β-tubulin was demonstrated to have an affinity for a range of benzimidazoles but monomeric tubulins are not known to exist in cells except perhaps during their initial

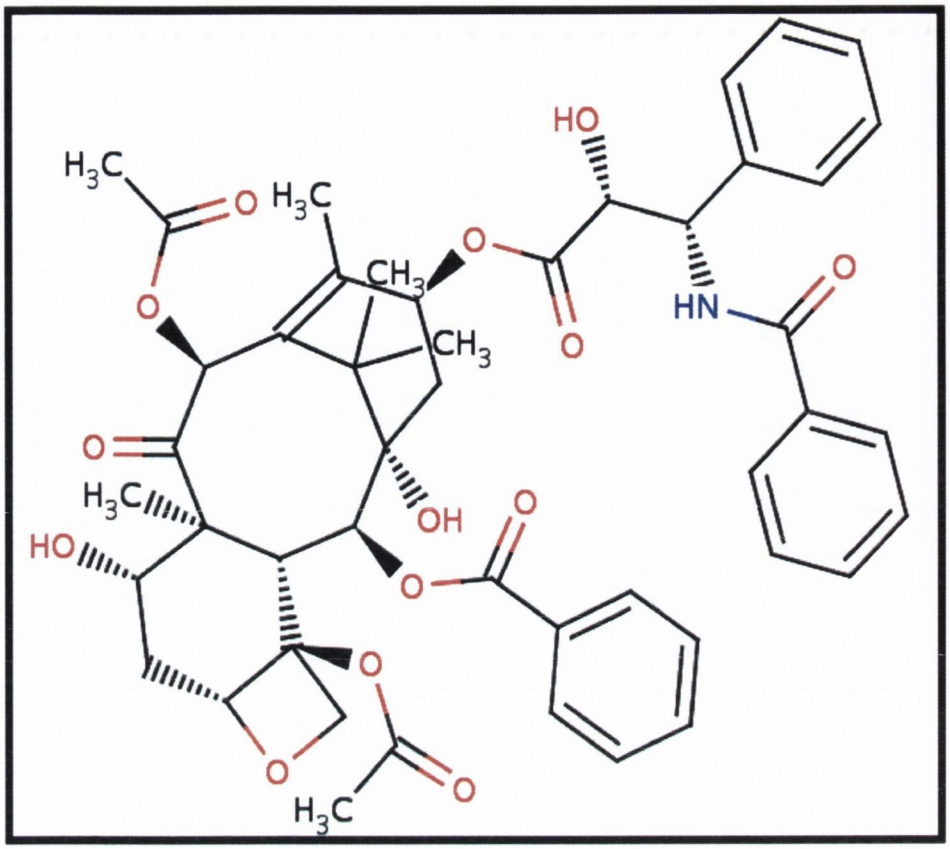

Fig. 1.7 Structure of taxol.

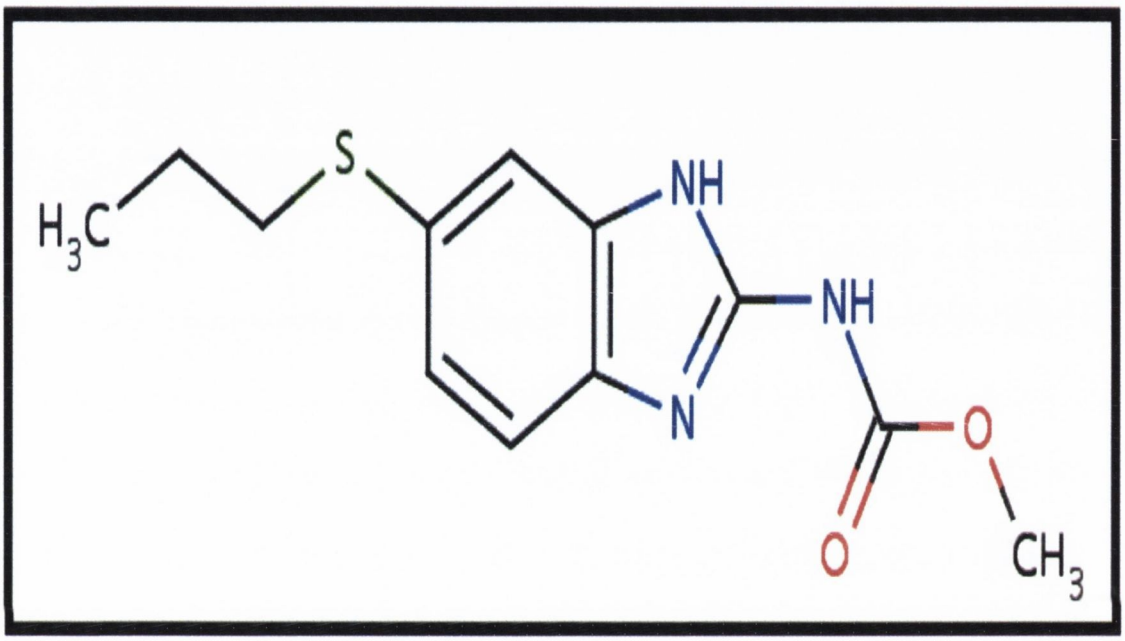

Fig. 1.8 Structure of albendazole. This compound is a representative of the benzimidazoles.

synthesis (McDonald *et al.*, 2004). Alternatively, GTP hydrolysis may cause some residues to expose the cleft, particularly Arg 156 and Leu 265 (Robinson *et al.*, 2004).

1.5.5 The herbicide inhibitors: Dinitroanilines and Phosphorothioamidates

Two mechanistically-related but chemically distinct classes of herbicide compounds, the dinitroanilines and the phosphorothioamidates, are also mitotic inhibitors. The best known dinitroanilines are trifluralin, chloralin and oryzalin, while for phosphorothioamidates mainly amiprophos-methyl (APM) has been extensively studied (see Fig. 1.9). In contrast to the classical tubulin ligands, the dinitroanilines and phosphorothioamidates exhibit a selective toxicity for many plants and certain parasitic protozoa over mammalian cells (Dow *et al.*, 2002, Murthy *et al.*, 1994, Fennell *et al.*, 2006 and Werbovetz *et al.*, 2003). These herbicides are highly potent plant poisons that bind to tubulin inducing depolymerisation (Hughdahl *et al.*, 1993). Murthy *et al.*, argued that these compounds are likely to share the same binding site on tubulin as the affinity of radiolabelled oryzalin for tubulin was competitively inhibited by APM (Murthy *et al.*, 1994). Supporting this finding, a molecular modelling study contrasted the electrostatic potential between the two herbicide classes and discovered that they had unexpectedly similar profiles (Ellis *et al.*, 1994). However, definite proof will require the discovery of the herbicide binding site(s) on tubulin.

Both herbicide class are typically small in size (on average <300 Da) and have relatively simple structures in comparison to the other tubulin ligands. The most active compounds in these groups usually have one central benzene ring with varying numbers of electronegative groups attached (e.g. nitro moieties) (Ellis *et al.*, 1994). However, aqueous solubility for both compound classes is a significant issue. Trifluralin is particularly hydrophobic and can readily adsorb to glass and plastic surfaces, thereby hindering accurate biochemical studies. APM is the most aqueous-soluble in this group with a maximum solubility around 230 μM, which is still poor relative to other MT inhibitors like vinblastine (Morejohn *et al.*, 1991).

These compounds also display a remarkable range of toxicities for related organisms that can depend on subtle structural changes. The most striking example of this phenomenon occurs between trifluralin and chloralin (see Fig. 1.9 C and D). These compounds are identical structurally except that the chloralin has a chloride

group at the R5 substituent while trifluralin has a dipropylamine [$HN(C_3H_7)_2$] group. This difference translates into chloralin being 100-fold more active than trifluralin against cultured *Leishmania major* (Callahan *et al.,* 1996). Strangely, in *L. infantum*, the difference is not as dramatic, with chloralin being only ~20 times more active (Armson *et al.,* 1999). In *P. falciparum*, the two chemicals have similar potencies (Bell A., 1998).

Despite the limitations regarding solubility, oryzalin was used as a lead compound for developing more active anti-protozoal agents. A novel chemical, GB-II-5 was synthesised that has activity 10-fold greater than oryzalin, although similar affinity was observed for mammalian tubulin (Werbovetz *et al.,* 2003). Furthermore, this group was able to replace the potentially carcinogenic nitro moieties with cyano groups while still retaining activity (George *et al.,* 2007). However, previous studies demonstrated that oryzalin had a very low *in vivo* activity in a rat model due to high rates of metabolism (Dow *et al.,* 2002). Therefore, development of new drugs based on this compound could be problematic at a later stage. Nonetheless, these herbicide inhibitors hold much potential for future therapeutics.

1.6 THE PUTATIVE DINITROANILINE AND PHOSPHOROTHIOAMIDATE BINDING SITE(S)

Despite the increasing interest these compounds have received in recent years, their binding site(s) on tubulin is/are still unknown. However, there are hints as to the location of the dinitroaniline site based on mutations in resistant organisms and tubulin molecular modelling studies. *Eleusine inidica*, goosegrass, is a weed common in cotton fields that was first found to have trifluralin resistance back in the early 1970's. Two mutations in the α-tubulin, Thr239Ile and Met268Thr, were found to be associated with a 50% inhibitory concentration up to 200-fold greater than the sensitive strain (Vaughn *et al.,* 1986 and Anthony *et al.,* 1999). A different mutation, Tyr24His, was found to be important for conferring a moderate 2-fold resistance in *Chlamydomonas reinhardtii* to APM. However, this latter mutation also increases the susceptibility to taxol 2-fold, thereby suggesting that this change induces an increase in tubulin stability to counterbalance the destabilising presence of the phosphorothioamidate (James *et al.,* 1993). More significantly, homology modelling using the crystal structure of bovine brain or pig tubulin as a template assisted three

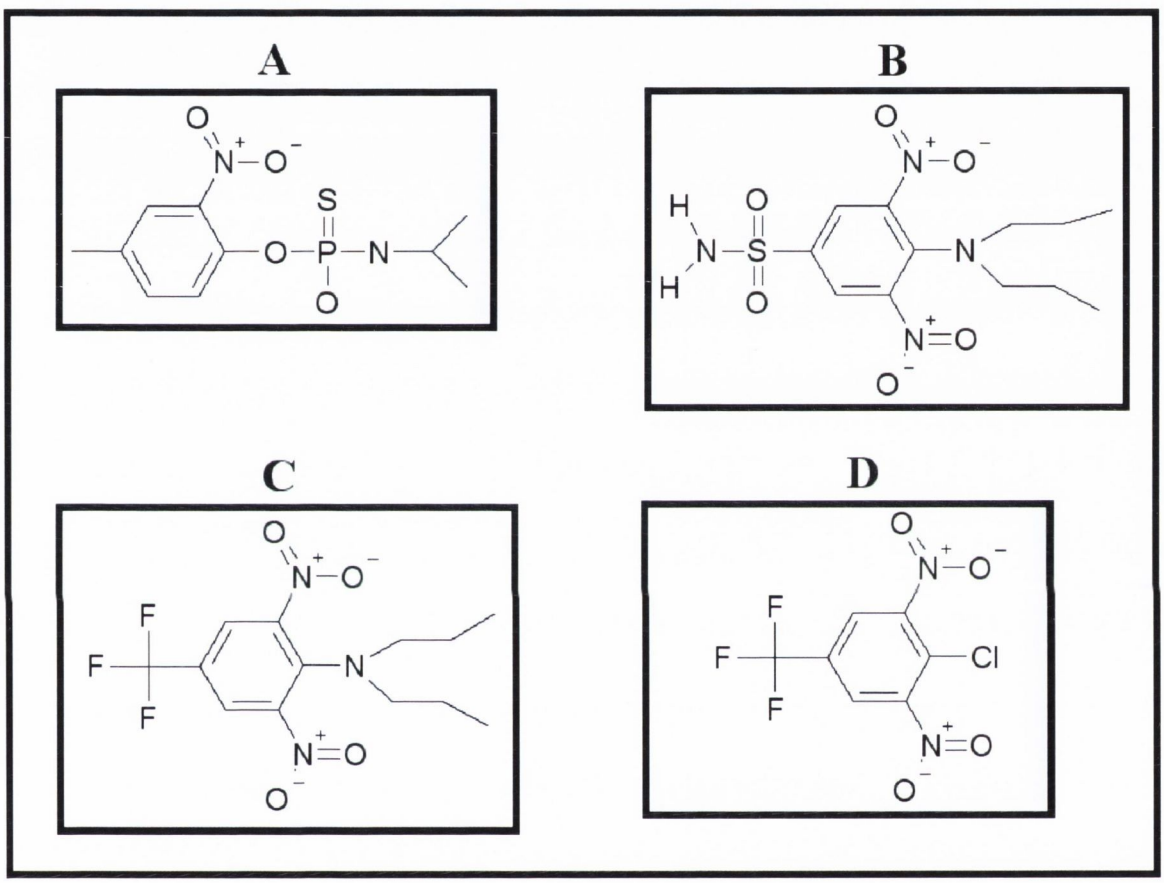

Fig. 1.9 Schematic structures of the phosphorothioamidate, APM (A) and the dinitroanilines, oryzalin (B), trifluralin (C) and chloralin (D).

unrelated groups, Blume *et al.*, (*Eleusine indica*), Délye *et al.*, (*Setaria viridis* L. Beauv.) and Morrissette *et al.*, (*Toxoplasma gondii*) to speculate that the location of the dinitroaniline site exists primarily on α-tubulin (Blume *et al.*, 2003, Délye *et al.*, 2004 and Morrissette *et al.*, 2004).

1.6. The Blume binding site

The Blume model is based on *Eleusine indica* using the original pig tubulin crystal structure that was resolved at 3.7 Å (Nogales *et al.*, 1998). It predicts that the binding site is located at the dimer-dimer interface with a cavity being formed by the following residues: Asp251, Thr253, Val252, Arg243, Leu136, Phe138, Val4 and His8. Other amino acids are also involved: Gln133, Gln 256 and Arg2 are thought to interact with the hydrocarbon chains of the dinitroanilines (see Fig. 1.10). Although the resistance-conferring residue, Thr239Ile, is not part of their binding pocket, the authors suggest that this substitution induces conformational changes in the tubulin molecule making the site inaccessible to the ligand and also causes a "redistribution of electrostatic potential" (Blume *et al.*, 2003).

1.6.2 The Délye binding site

The Délye model was based on *S. viridis* using the refined tubulin crystal structure (1JFF) which is from bovine brain (not pig brain as incorrectly stated in the paper) (Délye *et al.*, 2004). This crystal structure did not resolve the entire tubulin molecule, notably the amino acids between Met-36 to His-61, unlike the unrefined pig brain crystal structure (1TUB). Therefore, Délye *et al.*, (2004) used the 1TUB structure to only rule out the region for the dinitroaniline binding site. The binding site proposed by this group had two essential residues, Asp251 and Thr253 but other residues were important for modulating this interaction; Val16, Phe24, Leu136, Thr239, Val252 and Met268 (see Fig. 1.11). Some of the amino acids are different in *Plasmodium* though, particularly Thr 253 which is Asn in *S. viridis*.

However, some of these of resistant plants examined by this group displayed super-sensitivity to unrelated tubulin inhibitors. Therefore, it may be the case that the region identified by Délye *et al.*, (2004) is affecting the tubulins by increasing their stability so they are less likely to depolymerise in the presence of a destabilising

compound. This was previously shown to happen before by James *et al.,* (1993), whereby a replacement of Tyr24His in *Chlamydomonas reinhardtii* α-tubulin increased the resistance of the organism to unrelated destabilising compounds but also caused super-sensitivity to taxol.

1.6.3 The Morrissette binding site

An alternative model which has attracted considerably more attention is the Morrissette site. This model was based on *T. gondii* using the refined bovine brain tubulin crystal structure (Löwe *et al.,* 2001). Morrissette *et al.* (2004) initially predicted this site existed under the N loop of α-tubulin and is composed of the following residues: Arg2, Glu3, Val4, Try21, Phe24, His28, Ser42, Asp47, Arg64, Cys65, Thr239, Arg243 and Phe244. This was later expanded to include Ile5, Ser6, Cys20, Met36, Asp39, Lys40, Ala41, Pro63, Leu136, Ile235, Ser236, Ala240, Ser241 and Asp245 by Mitra A. and Sept D. (2006) (see Fig 1.12). One issue with this model is that large parts of the N-loop and surrounding residues (amino acids 34-64) on the α-tubulin were not resolved in the bovine crystal structure (Löwe *et al.,* 2001). Therefore, Morrissette *et al.,* used the analogous region in β-tubulin as a template (Morrissette *et al.,* 2004). Despite this problem, oryzalin was used as a template molecule to dock into this putative site. Oryzalin was predicted to limit the flexibility of the N-loop on the α-tubulin molecule which impacts on its interaction with the M-loop from the adjacent protofilament. As a result, lateral contacts are disrupted, thereby destabilising the MT (Morrissette *et al.,* 2004 and Mitra *et al.,* 2006). A number of mutations in *T. gondii* have been generated to date that have increased resistance to oryzalin, although not all have mapped to the Morrissette site (Morrissette *et al.,* 2004, Ma *et al.,* 2007 and Ma *et al.,* 2008). Although several mutations, notably Thr239Ile or Arg243Ser, cause ~100 fold increase in resistance, many of these changes are deleterious to the parasite. In some cases secondary mutations occur spontaneously once the drug pressure is removed from the parasites. Taken together, it is not known whether this resistance is caused by the mutations increasing the stability of tubulin or reducing binding of the ligand (Morrissette *et al.,* 2004, Ma *et al.,* 2007 and Ma *et al.,* 2008).

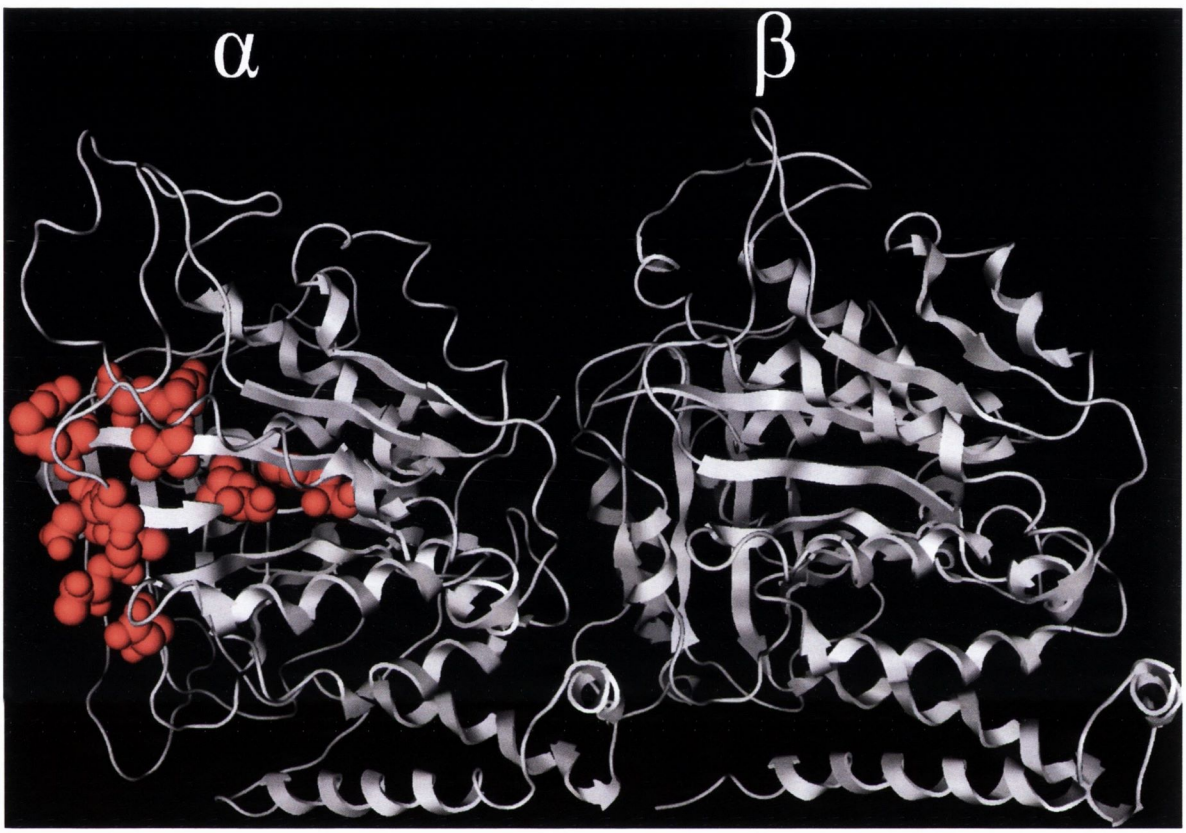

Fig. 1.10 Homology model of *P. falciparum* α/β-tubulin dimer with the residues forming the Blume site highlighted. This model was based on the crystal structure of bovine brain tubulin, 3E22.

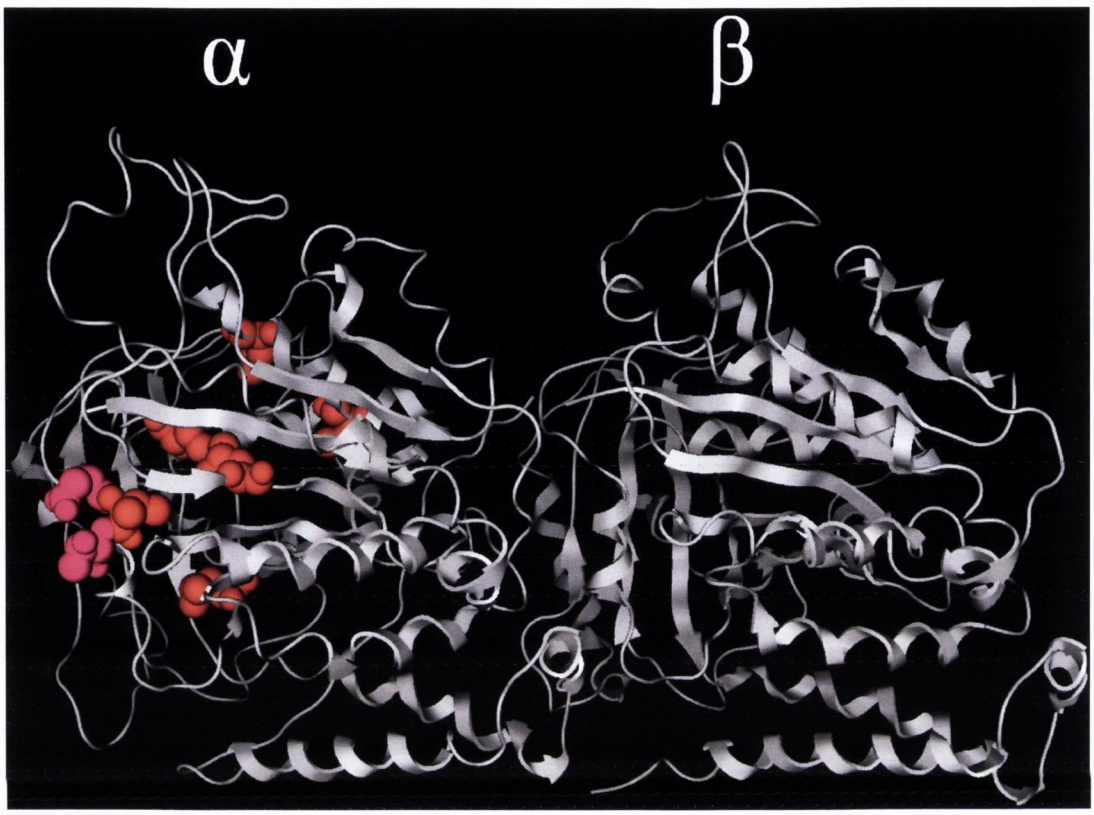

Fig. 1.11 Homology model of *P. falciparum* α/β-tubulin dimer with the Délye site highlighted. The Délye site is highlighted in **red** but the two most important amino acids, Asp 251 and Thr 253 are coloured **purple**. This model was based on the crystal structure of bovine brain tubulin, 3E22.

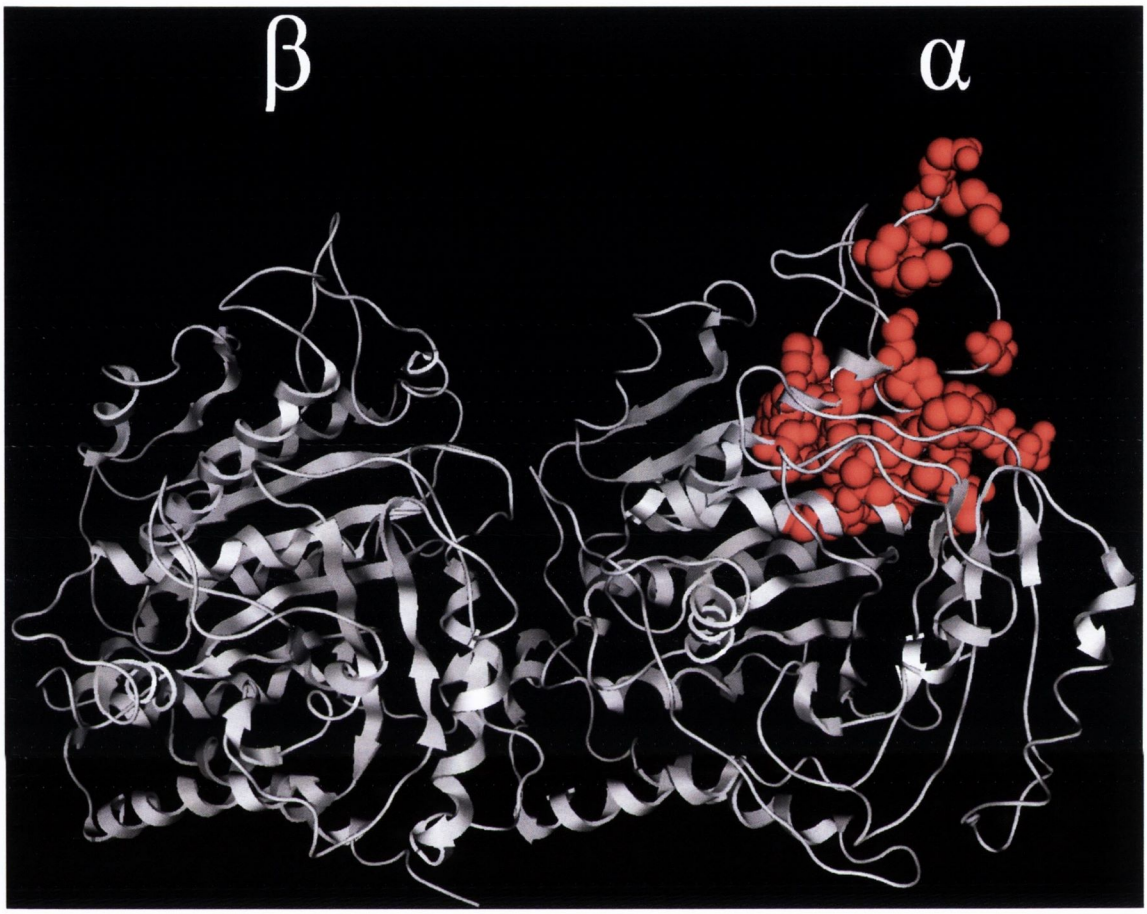

Fig. 1.12 Homology model of the *P. falciparum* α/β-tubulin dimer with the Morrissette site highlighted. This model was based on the crystal structure of bovine brain tubulin, 3E22.

1.7 MICROTUBULES IN *PLASMODIUM*

In *Plasmodium falciparum* there are two α-tubulin isotypes (αI- and αII-tubulin) and one β-tubulin (Holloway *et al.*, 1989, Holloway *et al.*, 1990 and Delves *et al.*, 1989). The α-tubulin isotypes are 94% identical at the amino acid level to each other and are ~40% identical to β-tubulin. In general, the tubulin subunits often exceed 65% identity for all organisms, with the C-terminal tail being the most varied region (Bell A., 1998). Comparing the human and parasite tubulins (either α- or β-tubulin) demonstrated that the overall the similarities are in excess of 92% (although the actual amino acid identities are lower, ~85%). Therefore, generating selective compounds that are active against parasites but not humans is expected to be difficult but not impossible.

1.7.1 Tubulin isotypes in *P. falciparum*

αI-tubulin was thought to be the only isotype expressed in asexual stages of *Plasmodium* and it was believed that αII-tubulin was used for specific functions within the axoneme of the male gametocyte. However, this was proven incorrect in both *P. berghei* and *P. falciparum.* αII-tubulin is in fact expressed in most if not all stages of the parasite life cycle, albeit to different degrees, and is essential for viability (Kooji *et al.*, 2005 and Fennell *et al.*, 2008). The most significant difference between the isotypes is the C-terminal tyrosine that exists on αI-tubulin. Tyrosinated tubulin is associated with more dynamic tubulins while detyrosinated tubulin is usually relatively stable. There is some evidence to suggest that αI-tubulin may function in dynamic roles within the cell, e.g. mitotic spindle, whereby αII-tubulin may be important for maintaining stable MT's such as those in the axoneme of male gametocytes (Fennell *et al.*, 2008). At least one post-translational modification, glutamylation, occurs within *P. falciparum* tubulin. The role for this glutamylated tubulin may be related to centriole maturation and stability (Fennell *et al.*, 2008).

1.7.2 Functional classes of microtubules in *Plasmodium*

In *Plasmodium*, three functional classes of MT's are well known; spindle microtubules, flagellar microtubules and subpellicular microtubules (SPM) (Bell,

1998). Three distinct microtubule-organising centres (MTOC) are used to nucleate these structures; the apical polar ring (APR), spindle pole plaques and centrioles (see Fig. 1.13). All of these structures play different but vital roles within the cell as reviewed by Tilney *et al.*, (Tilney *et al.*, 1996).

The subpellicular microtubules originate at the apical polar ring of the parasite and span about two thirds its body length. They are highly stable, spirally arranged structures that confer both shape and polarity to the cell (Morrissette *et al.*, 2002). The plus ends of the SPM's are attached laterally to the APC but are not capped. The length and number of the SPM's vary depending upon the life cycle stage and species of the parasite. In *P. falciparum* merozoites, only two or three of these structures are present and they are often collectively called the *falciparum* merozoite-associated assemblage of subpellicular microtubules (f-MAST) (Bannister *et al.*, 2000). However, in ookinetes, ~60 SPM's are known to exist (Morrissette *et al.*, 2002). Although these structures are very stable, addition of high concentrations of trifluralin were shown to depolymerise them and attenuate the ability of merozoites to invade the erythrocytes, demonstrating their importance (Fowler *et al.*, 1998). However, once the merozoite has entered the red blood cell, the SPM and apical complex are no longer needed and are dismantled (Bannister *et al.*, 2000).

Asexual replication by *Plasmodium* is termed schizogony and it can produce up to 32 daughter cells (Bannister *et al.*, 2000). The spindle pole plaques are used to nucleate the microtubular hemi-spindles from opposing sides of the cell. These hemi-spindles eventually combine to form complete spindles. In *P. berghei*, three sets of spindles are observed; those connecting the kinetochore to the spindle pole body, pole to pole MT (astral microtubules) and pole spindles that terminate in the central region of the cell (Morrissette *et al.*, 2002). Nuclear division is not tightly controlled so different mitotic spindle structures are often observed, which is in contrast to mitosis in many other eukaryotes (Read *et al.*, 1993). These spindle structures are the frequent target for microtubule inhibitors due to their importance and highly dynamic nature. Furthermore, many of the depolymerising agents preferentially bind to soluble tubulin rather than preformed polymers as mentioned earlier.

The axonemal/flagellar microtubules are crucial for the motile male gametes. The centrioles are used to nucleate the flagella, of which two are commonly located on the anterior end of the cell (Morrissette *et al.*, 2002). The axonemes at the base of the flagella also form the standard "9+2" arrangement (Tilney *et al.*, 1996).

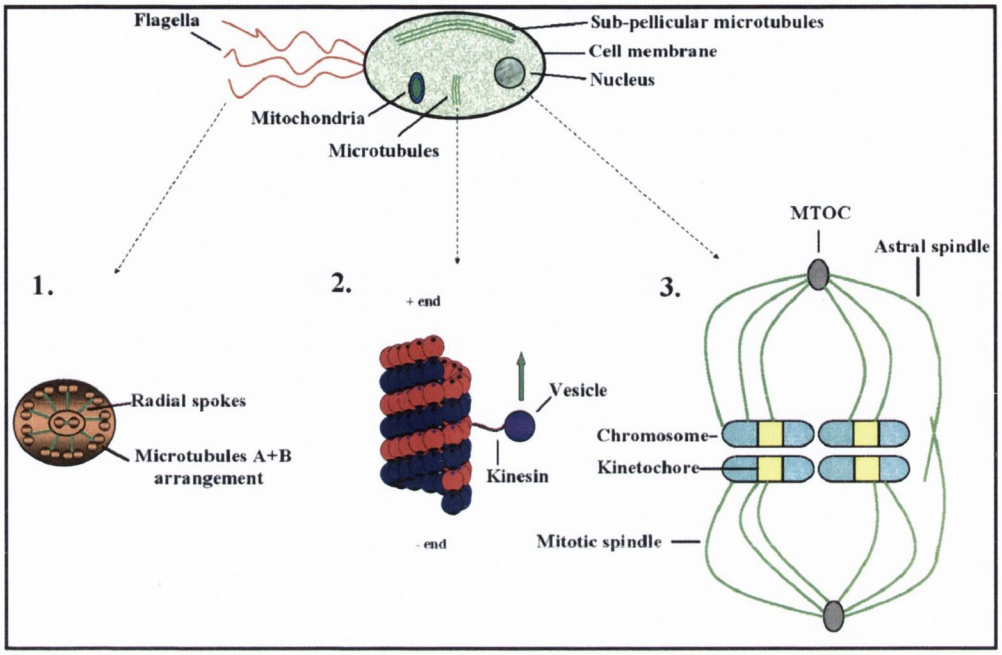

Fig. 1.13 Schematic diagram of the main functional classes of microtubules in the *Plasmodium* cell. 1: The axonemal/flagellar microtubules have the characteristic "9+2" arrangement connected by the radial spokes. **2:** Intra-cellular microtubules are found within the cytosol. Kinesin, a MAP, is demonstrated attached to a microtubule and a vesicle. The direction of transport is indicated. Sub-pellicular microtubules are essentially the same in structure as intra-cellular MT's except that they are more stable. **3:** Microtubule organising centres (MTOC) are the point at which microtubule nucleation occurs. Two types of spindles are produced, the astral spindle (pole-to-pole) and the mitotic spindle (bind to the kinetochore). (The diagram was adapted from Fennell, 2005.)

1.7.3 Isolation of *P. falciparum* microtubules

Purification of microtubules from their native cells is usually a standardised procedure revolving around cycles of assembly/disassembly of the polymer. This permits the isolation of the protein because microtubules are readily sedimented by centrifugation whereby the dimers are very soluble and require much higher speeds to sediment them. Tubulin mixtures of about ~80% purity are obtained with the contaminants primarily consisting of MAP's (Bell A., 1998). Affinity or phosphocellulose chromatography is often employed to remove these accessory proteins, generating a very pure final product. However, the major drawback of the method is the prerequisite of initial high tubulin concentrations, enough to match the critical concentration so that the first round of polymerisation can occur. In bovine brains, tubulin accounts for ~20% of all the protein in the cell. However, in *Plasmodium*, the amounts are much lower (<1%) (Fennell *et al.*, 2008) and this makes direct purification from the parasites very difficult. A common problem that occurs when trying to generate tubulin in a foreign organism, typically *Escherichia coli*, is the formation of insoluble proteins called inclusion bodies. To resolublise the protein, it must first be completely denatured (e.g. with urea) and then refolded either chemically or biologically. This method has been used successfully using a variety of organisms (MacDonald *et al.*, 2004, Bon-Sung *et al.*, 2009, Myung-Hyun *et al.*, 2008, Linder *et al.*, 1998, Bon-Sung *et al.*, 2009, Shah *et al.*, 2001, Wampande *et al.*, 2007, Oxberry *et al.*, 2000, Oxberry *et al.*, 2001, Lubega *et al.*, 1993 and Yaffe *et al.*, 1988). However, Guha *et al.*, (1997) completely denatured goat brain tubulin and found that an intermediate state is eventually reached which cannot be bypassed spontaneously. This may suggest that subtle inter-species differences exist in relation to the folding mechanism for tubulins and that this technique may not be applicable for all organisms. To date, only two studies have attempted to generate recombinant *Plasmodium falciparum* tubulin. The first study utilised a unique feature of *Bacillus brevis* to secrete large amounts of protein into the extra-cellular medium. Despite the initial success of synthesising milligram amounts of protein per litre of culture, further isolation of the tubulin proved impossible (Bell *et al.*, 1995). The second study managed to produce significant amounts of both αI- and β- tubulin (~50 mg/l) tagged with the maltose binding protein (MBP) that was capable of binding the mitotic inhibitor, trifluralin. However, these tubulin fusion proteins were incapable of

polymerisation with each other, although αI-tubulin could co-assemble with bovine brain tubulin demonstrating that it was folded correctly (Fennell *et al.*, 2006 and Fennell, 2005).

1.8 *PLASMODIUM* TUBULIN AS AN ANTIMALARIAL DRUG TARGET

The inhibition of microtubule dynamics by small ligands has been extensively used for the treatment of a wide range of medical conditions for the past half-century, most notably in cancer chemotherapy but also as antihelminthics, anti-fungals and anti-inflammatories (Risinger *et al.*, 2009 and Lacey, 1988). This success has generated a huge interest in these proteins and has resulted in a dearth of information being elucidated regarding their structure and function. However, there has been little research regarding tubulin as a potential antimalarial target. A successful drug target must fulfill several criteria; **1)** Essentiality, **2)** Selectivity, **3)** Tractability and **4)** Assayability. Therefore, this section will outline the potential advantages of using microtubules as a drug target and will summarise its key inhibitors with regard to *Plasmodium*.

1.8.1 Is tubulin essential in *Plasmodium*?

Microtubules are found in virtually all eukaryotic cells but their sensitivity to the classic inhibitors (colchicine, vinblastine or taxol) can vary greatly depending if the microtubules are stable or active. At clinically relevant concentrations, these inhibitors suppress the dynamic nature of microtubules, i.e. reducing the speed at which they polymerise or depolymerise leading to cell death (Okouneva *et al.*, 2003 and Kelling *et al.*, 2003). Therefore, the dynamic mitotic spindle in dividing cells tends to be exquisitely sensitive to these inhibitors while more stable MT structures are resistant. This difference is the basis for MT inhibition in cancer chemotherapy (Risinger *et al.*, 2009). The inhibitory effects of some well known antimitotic compounds are listed in table 1.2.

The *Plasmodium* parasite undergoes numerous rounds of rapid cell division during its life-cycle in the human host, particularly in the erythrocytic schizogony phase (see section 1.2). This makes tubulin an ideal candidate for novel drug development. Therefore, it is not surprising that a significant effort has been made

Compound	IC_{50} (*P. falciparum*, μM)	Ref.	IC_{50} (mammalian cell, μM)	Ref.
Colchicine	10	Dieckmann-Schuppert *et al.*, 1990	0.053	Bell A., 1998
Albendazole	30	Dieckmann-Schuppert *et al.*, 1989	0.31	Bell A., 1998
Vinblastine	0.031	Fennell *et al.*, 2003	0.0006	Bell A., 1998
Dolastatin 10	0.0001	Fennell *et al.*, 2003	0.00012	Fennell *et al.*, 2003
Taxol	0.004	Fennell *et al.*, 2003	0.002	Bell A., 1998
cis-Tubulozole	3	Dieckmann-Schuppert *et al.*, 1989	<1.8	Geuens *et al.*, 1985
Trifluralin	2.9	Fennell *et al.*, 2006	>64	Fennell *et al.*, 2006
Oryzalin	6.1	Fennell *et al.*, 2006	>64	Fennell *et al.*, 2006
APM	3.5	Fennell *et al.*, 2006	>64	Fennell *et al.*, 2006

Table 1.2 IC_{50} of known mitotic inhibitors for *P. falciparum* and mammalian cells.

over the years to determine if known MT ligands would also be effective against the parasite

1.8.1.1 Colchicine

Colchicine is highly toxic to mammalian cells but *Plasmodium* is relatively insensitive to its effects. The minimum inhibitory concentration necessary to reduce cell growth by 50% (IC_{50}) is between 10 and 13 μM in blood cultured parasites but only ~50 nM in human cells (Bhattacharyya *et al.*, 2007, Schrével *et al.*, 1994 and Bell A 1998). It is unclear whether this difference is due to the colchicine binding site not existing on the *Plasmodium* tubulin or if the drug cannot penetrate into the cytosol of the parasite due to the presence of several membranes (i.e. erythrocyte plasma membrane, parasitophorous vacuole membrane and the parasite plasma membrane). Therefore, it would be interesting to determine the exact nature of the parasite resistance and if binding is possible, then this site could function as a potential target for ligand development.

1.8.1.2 Vinblastine

The lowest recorded IC_{50} for vinblastine against the cultured *Plasmodium falciparum* cells is <31 nM with the trophozoite stage being most susceptible (Fennell *et al.*, 2003). This is unsurprising because the schizont stage is characterised by rapid nuclear division. Recent work has established that vinblastine rapidly accumulates in the parasitized cells to ~110 times the external concentration within 15-20 min. Furthermore, the majority of this inhibitor formed a stable complex with tubulin that could not be removed by repeated washing steps (Naughton *et al.*, 2008). However, vinblastine is also a very potent mammalian inhibitor (IC_{50} 600 pM) and therefore development as an anti-malarial drug is not feasible (Bell A., 1998). Dolastatin-10 and -15, which both bind near the vinca domain, were very effective against cultured parasites (IC_{50} 100 pM and 200 nM respectively) but unfortunately they displayed similar activity towards several mammalian cell lines (Fennell *et al.*, 2003)

1.8.1.3 Taxol

The IC_{50} for taxol against cultured parasites is ~71 nM but the full effect on asynchronous parasites is only evident after a 72 h incubation time (Schrével *et al.*, 1994). Dieckmann-Schuppert *et al.*, determined a ~15 fold higher IC_{50} because they used only a 48 h incubation time (Dieckmann-Scuppert *et al.*, 1990). This unusual result is likely caused by the delayed death of the parasites and generates a plateau effect when measuring the drug IC_{50} (Goodman *et al.*, 2007 and Fennell *et al.*, 2003). It has been noted previously that some parasite drugs, e.g. clindamycin, are 3-4 orders of magnitude more effective after 96 h incubation time rather than a typical 48 h (Goodman *et al.*, 2007). In this case, the parasites were capable of completing one cycle of replication but failed to progress through schizogony even after invading new erythrocytes (Goodman *et al.*, 2007). Alternatively, a sub-population of the parasites may not be in the appropriate age range for optimal inhibition. Therefore, the drug exposure time would be too short to determine an accurate IC_{50} (Fennell *et al.*, 2003). Nonetheless, taxol is as effective if not more so against mammalian cells, thereby precluding any further development as an anti-malarial drug.

1.8.1.4 Dinitroanilines and phosphorothioamidates

Unlike the classical tubulin ligands, the dinitroaniline and phosphorothioamidate herbicides display selective activity towards the *Plasmodium* parasites which could be exploited as a novel therapeutic approach. These compounds have only moderate IC_{50} against these cultured cells, though: trifluralin 2.9 μM, oryzalin 6.1 μM and APM 3.5 μM (Fennell *et al.*, 2006). Trifluralin uptake into erythrocytes with and without parasites was monitored by radiolabelling the compound. The hydrophobic nature of the compound permitted the ligand to accumulate up to ~300 times the external concentration with an apparent maximum being reached in ~10 min. However, no saturation point could be achieved and the vast proportion of trifluralin could be removed by washing the parasitized cells indicating that the compound was binding mostly non-specifically. It was suggested that trifluralin was becoming stuck in the membranes of the cells and most of it was not reaching its cellular target (Naughton *et al.*, 2008). This effect was witnessed previously whereby seeds with high lipid content were resistant to the compound

(Parka *et al.*, 1977). Furthermore, a secondary mechanism for inhibition by oryzalin has been suggested, with the possible involvement of Ca^{2+}. It is proposed that release of Ca^{2+} ions in the *Oryza sativa* cells is induced by the presence of oryzalin and this increases the destabilising effect of the compound (Gianí *et al.*, 2002). Werbovetz *et al.*, suggested that the increased Ca^{2+} levels correspond with the inhibition of mammalian cells (Werbovetz *et al.*, 2003). To date, more potent derivatives of oryzalin have been synthesized that still retain their selective activity towards *Leishmania* over mammalian cell lines indicating that this group of inhibitors has a real potential for future anti-protozoan development (George *et al.*, 2007).

Overall, there is overwhelming evidence to support the fact that inhibition of tubulin dynamics is lethal to the parasite.

1.8.2 Is *Plasmodium* tubulin different enough to be selective?

Tubulin is a highly conserved protein. In fact, *Plasmodium* α- and β-tubulin is 84% and 88% identical to human tubulin at the amino acid level. (See Figs. 1.14 and 1.15). Furthermore, the classical tubulin inhibitors are less or equally potent to cells from either organism (see section 1.8.1.1 – 3). As a result, it is unlikely that these drugs could ever be used as antimalarials. However, some ligands, such as the phosphorothioamidates and dinitroanilines, have been demonstrated to show selectivity to the *Plasmodium* tubulin (Fennell *et al.*, 2006). These compounds appear to preferentially interact with tubulin from plants, protozoa and fungi but not mammalian cells, indicating a unique binding site exists in these proteins (Dow *et al.*, 2002, Murthy *et al.*, 1994, Fennell *et al.*, 2006 and Werbovetz *et al.*, 2003). This binding site is likely born from amino acid differences that either indirectly cause a conformational change to parasite tubulin, generating novel folds or are directly involved in the herbicide's interaction with the protein. In the former case, this could create numerous cryptic regions on the tubulin molecule that could only be indentified upon elucidation of its crystal structure. In the latter case, it may be possible to suggest potentially interesting regions which are significantly different from human tubulin by comparing the amino acid sequences of these proteins.

Other significant differences do exist between human and parasite tubulin. In higher eukaryotes (e.g. mammals), α-tubulin migrates slower than β-tubulin on a denaturing gel. However, for lower eukaryotes (e.g. protozoa, plants and fungi), the

opposite is true and the tubulin migration is "inverted" with β-tubulin migrating slower than α-tubulin (see table 5.1). The exact mechanism for this unusual feature has yet to be elucidated although it is likely due to differential binding of SDS to tubulin as this has been observed before in other proteins (Rath *et al.*, 2009 and Matagne *et al.*, 1991). To date, it is not known if one or many amino acids are responsible.

Despite their similarity, significant differences do exist between *Plasmodium* and human tubulin. This is exemplified by the differential binding of the herbicides compounds to the parasite tubulin and the inversion phenomenon. As a result, it is likely that a therapeutic window exists which can be exploited for the generation of novel antimalarials.

1.8.3 How tractable is *Plasmodium* tubulin?

The inherently dynamic nature of microtubules is exquisitely sensitive to perturbation by small molecules such as vinblastine (Okouneva *et al.*, 2003). This drug is capable of killing parasite cells at low nano-molar concentrations (28 nM) despite having a significantly higher K_d (500 nM) for tubulin itself (Bell A., 1998 and Avila J., 1990). It has been suggested that is due to the sub-stoichiometric binding of the ligand to the end of the MT's, i.e. vinblastine binds to tubulin dimers which once attached to the MT affect subsequent dimers from associating (Correia *et al.*, 2001 and Bhattacharyya *et al.*, 2008). Therefore, a low percentage of the tubulin-ligand complex can be effective at suppressing MT dynamics to an extent which is lethal to the cell.

Although both taxol and vinblastine are relatively large (~900 Da), complicated compounds, numerous smaller inhibitors have been discovered to date. The herbicide class of compounds are particularly small (~300 Da) and are amenable to chemical modifications. In fact, a plethora of compounds have been synthesized based on the oryzalin skeleton which has identified inhibitors of nano-molar potency (George *et al.*, 2006 and George *et al.*, 2007). Since these inhibitors are selective for *Plasmodium*, they are likely to be useful for future development.

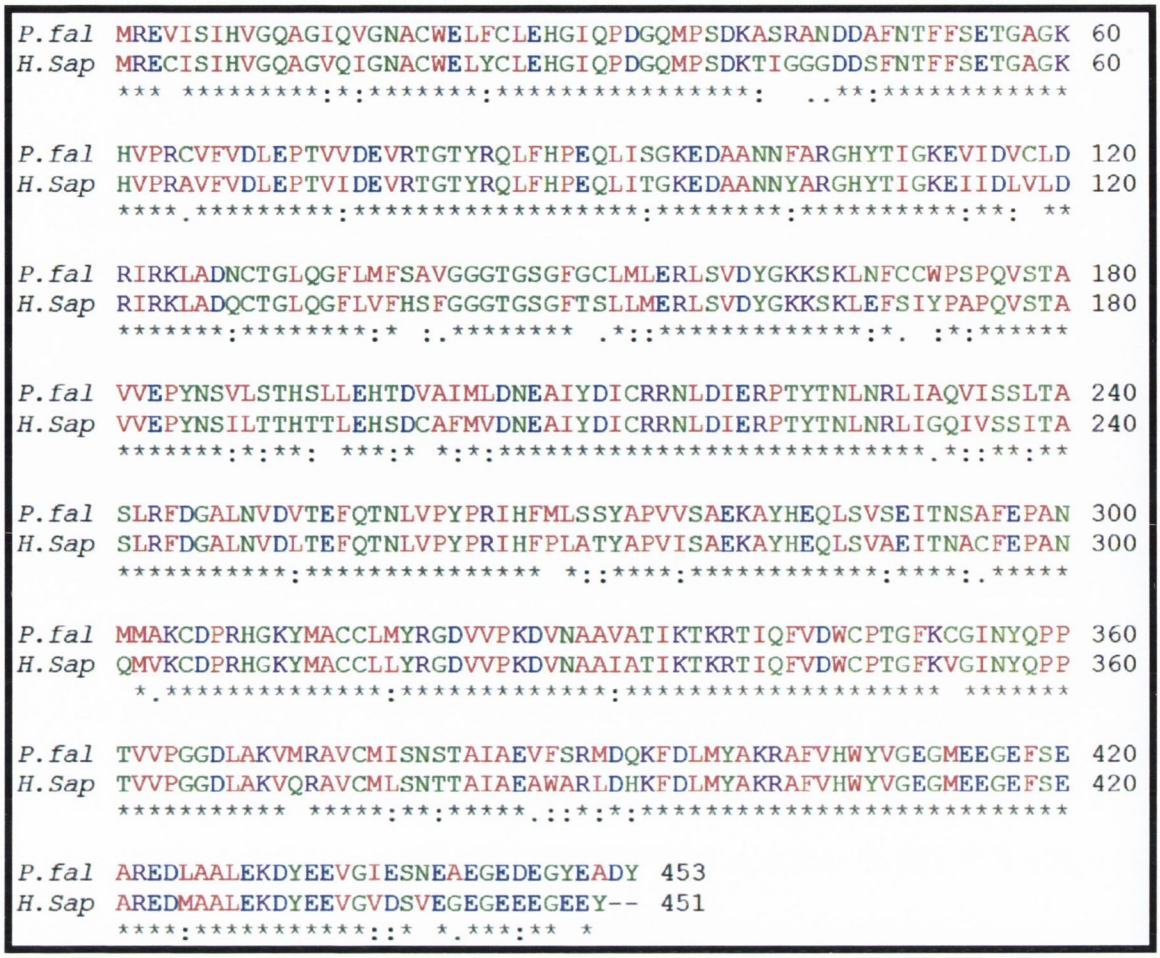

AVFPMILW	RED	Small (small+ hydrophobic (incl.aromatic -Y))
DE	BLUE	Acidic
RHK	MAGENTA	Basic
STYHCNGQ	GREEN	Hydroxyl + Amine + Basic - Q

Fig. 1.14 Alignment of the α-tubulin amino acid sequence from *P. falciparum* and *H. sapiens*. The table shows an AA map that describes the colour coding scheme (reproduced from www.ebi.ac.uk/Tools/es/cgi-bin/tcoffee). "*" means conserved sequence. ":" means conserved according to the type of change i.e. an acidic AA for a different acidic AA. "." means semi-conserved. Semi-conserved means that most of the AA's are similar in type or identical but at least one is completely different.

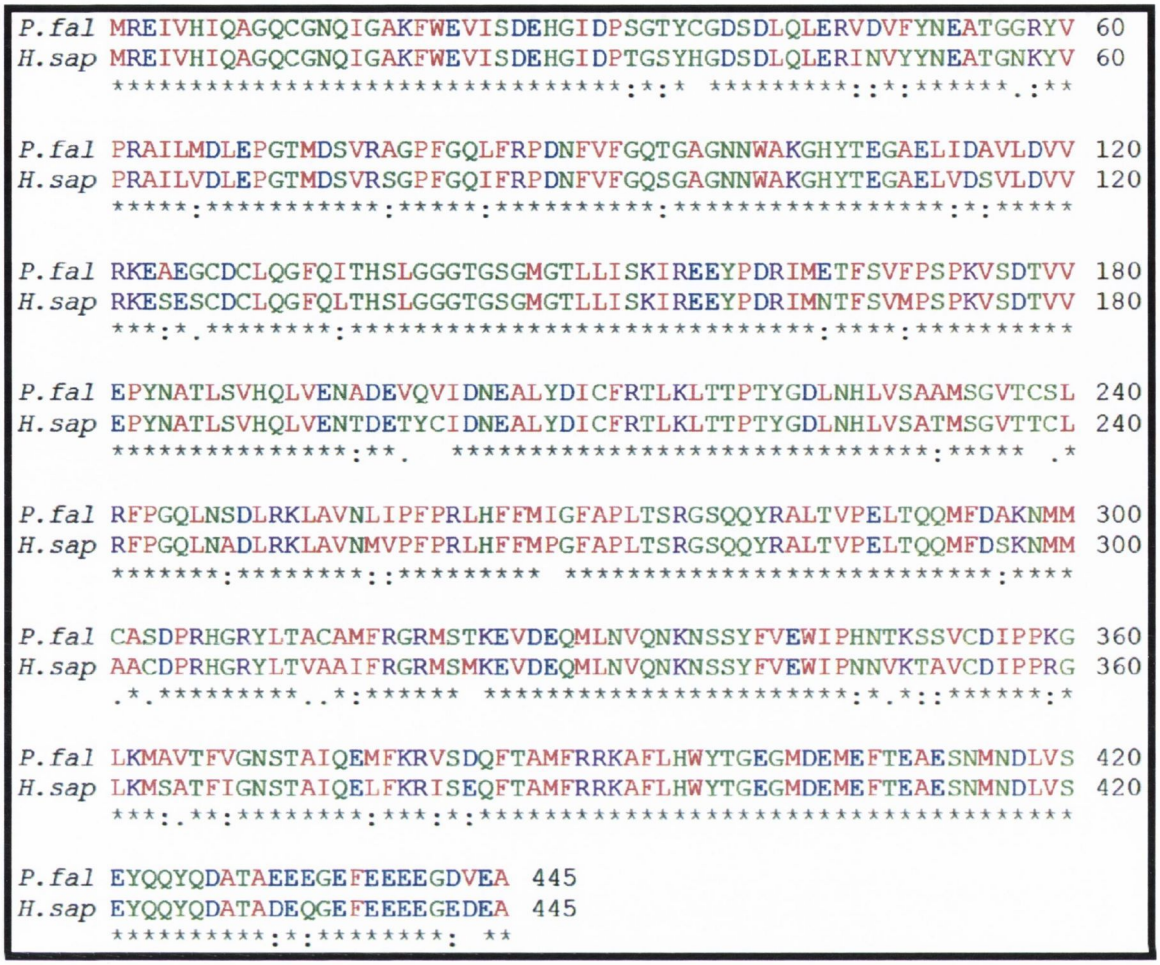

AVFPMILW	RED	Small (small+ hydrophobic (incl.aromatic -Y))
DE	BLUE	Acidic
RHK	MAGENTA	Basic
STYHCNGQ	GREEN	Hydroxyl + Amine + Basic - Q

Fig. 1.15 Alignment of the amino acid sequence of β-tubulin from *P. falciparum* and *H. sapiens*. The table shows an AA map that describes the colour coding scheme (reproduced from www.ebi.ac.uk/Tools/es/cgi-bin/tcoffee). "*" means conserved sequence. ":" means conserved according to the type of change i.e. an acidic AA for a different acidic AA. "." means semi-conserved. Semi-conserved means that most of the AA's are similar in type or identical but at least one is completely different.

1.8.4 How simple are tubulin-ligand interactions to assay?

MT's have several characteristics which have been previously used to develop assays to detect small ligand interactions. These characteristics are: **1)** the ability to polymerise/depolymerise, **2)** GTPase activity, **3)** presence of sulphydryl residues and **4)** presence of tryptophan residues.

Perhaps the most striking feature about tubulin is the ability of its dimers to form MT's. These MT's can rapidly elongate and shorten under the optimal conditions. As MT's are formed in solution, the sample becomes increasing opaque which can easily be measured spectrophotometrically. Addition of tubulin inhibitors to a sufficient concentration tends to either increase or decrease the assembly rate of the polymer. This method can be used to determine I_{50} value (inhibitor concentration required to inhibit rate by 50%) of an inhibitor and has been used for a wide range of unrelated tubulin ligands (Lee *et al.*, 1980, Ray *et al.*, 1996, Kumar, 1981, Werbovetz *et al.*, 2003, Hughdahl *et al.*, 1993 and MacDonald *et al.*, 2004). This assay is particularly useful as some tubulin ligands bind only to soluble dimers (e.g. vinblastine) while others only bind to the polymer (e.g. taxol) (Freedman *et al.*, 2009 and Gigant *et al.*, 2005). Furthermore, it is possible that some ligands may bind to the end of an MT suppressing its growth rate and having the potential to be an effective inhibitor despite having only a relatively weak affinity for molecule itself (see section 1.8.3). This assay can also be adapted to a high-throughput-system by virtue of a fluorescent probe interacting non-covalently with the polymerising tubulin (Barron *et al.*, 2002). Finally, the polymerised tubulin can also be separated from unpolymerised tubulin by centrifugation in the presence of different ligand concentrations. The polymerised tubulin concentration can then estimated to determine the effect of the ligands (Lacey, 1988). This method has the potential to significantly reduce the amount of protein required in the assay if sensitive techniques such as western blotting are employed.

Tubulin polymerisation is coupled to GTP hydrolysis which produces GDP and free inorganic phosphorous (P_i) (Lacey, 1988). Since P_i can be readily detected by non-radioactive dyes, this method can be applied to a 96-well plate format to screen for effective tubulin ligands (Fisher *et al.*, 1994). Typically, soluble tubulin dimers have minimal GTPase activity (Lacey, 1988). However, colchicine and its derivatives are capable of stimulating the tubulin dimer to hydrolyse GTP. This

phenomenon is thought to occur due to the ability of this compound to cause a significant conformational change in the tubulin molecule but may not be suitable for all ligands (Sackett, 1995).

Sulphydryl residues report the interaction of a ligand with tubulin by measuring spectrophotometrically their reactivity with a specific reagent (Gupta *et al.*, 2002). A ligand can either bind to a sulphydryl group or cause a conformational change to the tubulin molecule so that these residues become less reactive. This assay does not require the tubulin to be assembly competent.

The ability of tryptophans to fluoresce when excited can be used to report ligand-tubulin interactions directly. A compound can either bind to a tryptophan residue or cause a conformational change to the tubulin molecule so that they become more stable. This causes the tubulin fluorescence to be quenched and can be used to determine drug binding constants (Panda et al., 2000 and Werbovetz *et al.*, 1999). This assay also does not require the tubulin to be assembly competent.

Overall, there are numerous methods to screen potential drug candidates using purified tubulin.

1.8.5 Conclusion

In summary, tubulin is an essential protein for the *Plasmodium* parasite. Even small perturbations in its activity are damaging to the cell. Despite the fact that the protein is highly conserved among all eukaryotes, significant differences do exist between the human and parasite tubulin. In fact, a group of herbicide compounds have been discovered which are small and selective to *Plasmodium*. Finally, the unique properties of the tubulin molecule allow the development of numerous ligand binding assays. Therefore, *Plasmodium* tubulin has the potential to be an effective drug target.

1.9 PROJECT OBJECTIVES

Since tubulin would make a good drug target, the work conducted in this thesis was undertaken to determine if novel herbicide compounds could be potentially used as anti-malarial chemotherapy. This project had three main aims;

1) to generate recombinant tubulin that is suitable for ligand-binding studies

2) to evaluate a series of novel phosphorothioamidate-related compounds and their effects at both the cellular and molecular level

3) to investigate the molecular basis of herbicide binding and the unusual electrophoretic migration of *P. falciparum* tubulins

Chapter 2

Materials and Methods

2.1 CHEMICALS, REAGENTS AND INHIBITORS

Chemicals and reagents used in this project were purchased from Sigma-Aldrich (Dublin, Ireland) unless otherwise stated. All general chemicals were of analytical grade. The grade of water used was filtered, deionised (dH_2O) and was dispensed from a Milli-Q Synthesis A10 (Millipore, Billerica, Massachusettes, USA). All reagents used during electrophoresis were of electrophoresis grade. All chemicals used for cell culture were of cell culture grade.

2.2 CULTURE OF AND EXPERIMENTS WITH *P. FALCIPARUM*

2.2.1 Routine culture of *P. falciparum*

The *P. falciparum* strain 3D7 (obtained from M. Grainger, National Institute for Medical Research, London, UK) was maintained in continuous culture using human erythrocytes (obtained whole blood from the National Blood Centre, Dublin) and Albumax II ® (Gibco, Auckland, New Zealand) at a haematocrit of 5% (v/v), according to the method of Trager and Jensen (Trager and Jensen, 1976). Erythrocytes were prepared weekly by combining 10 parts whole blood with 1 part PIGPA solution (50 mM sodium pyruvate, 50 mM inosine, 100 mM glucose, 500 mM disodium hydrogen phosphate, 5 mM adenine, 0.72% (w/v) sodium chloride pH 7.2) and incubating the mixture at 37°C with occasional agitation. The blood was then washed in cold, sterile phosphate buffered saline (OXOID Ltd., Basingstoke, Hampshire, UK) (twice) and in complete medium as before (once) to remove the buffy coat, using a Sorvall RT6000D bench top centrifuge (Du Pont Ltd., Stevenage, Herts, UK) at 1500 rpm (488 x g), 4°C for 10 min. Erythrocytes were resuspended to a 50% haematocrit in complete medium (RPMI 1640 medium, supplemented with 25 mM HEPES (4-(2-hydroxyethyl)-1-piperazineethanesulphonic acid), 0.002% (v/v) gentamicin, 0.18% (w/v) sodium bicarbonate, 50 µg/ml hypoxanthine and 5% (w/v) Albumax®, pH 7.0) and stored at 4°C. A sample of washed erythrocytes was incubated at 37°C to check for contamination. This was done by preparing smears that were dried, fixed in methanol, stained with a 1:10 dilution of Giemsa-stain (Fluka Chemie AG, Buchs, Switzerland) and in Giemsa buffer (1% (w/v) $Na_2HPO_4.2H_2O$, 1% (w/v) KH_2PO_4) and destained in Giemsa buffer. The smears were examined

microscopically using 1000X magnification under oil immersion. The parasites were routinely cultured in petri dishes with complete medium at 37°C in a candle jar. Parasitaemia was measured by microscopic counts of Giemsa-stained smears. Routine cultures were diluted with fresh erythrocytes at least twice a week and the medium was replaced depending upon the parasitaemia.

2.2.2 Measurement of inhibition of parasite proliferation using the parasite lactate dehydrogenase (pLDH) method

Inhibition of *P. falciparum* growth was measured spectrophotometrically based on the parasite lactate dehydrogenase assay (pLDH) developed by Makler *et al.* (1993). This enzyme converts lactate to pyruvate, reducing 3-acetyl pyridine adenine dinucleotide (APAD), which is used as a co-factor, in the process. Human erythrocyte LDH can also use APAD but to a lesser extent. In a typical assay, asynchronous parasite cultures of 0.8% parasitaemia, 2% haematocrit were grown in complete medium containing titrations of inhibitors diluted in dimethylsulphoxide (DMSO) in 96-well flat-bottom culture plates (Sarstedt Ltd., Drimnagh, Co. Wexford) for 48 – 72 h. DMSO alone was added to cultures to the same concentration as a control. After 48 and 72 h, 10-µl samples of parasitized erythrocytes were removed and their pLDH activities were determined by mixing the samples with 50 µl of Malstat ® (0.1 M Tris-HCl pH 9.0, 0.2 M lithium lactate, 0.2% (v/v) Triton X-100 and 1 mM APAD), which provides APAD and L-lactate as substrates. pLDH released by the parasites results in the production of pyruvate and reduced APAD. Ten µl of nitro blue tetrazolium (NBT) : PES phenazine ethosulfate (PES) (ratio 1:1 of NBT (2 mg/ml) and PES (0.1 mg/ml)), were added to each sample, forming a blue formazan product in the presence of reduced APAD that was detected using a Titerek Multiskan® Plus spectrophotometer (Eflab, Finland) at 650 nm. The resulting absorbance was proportional to pLDH activity, which correlates to the percentage parasite growth/survival (Makler *et al*, 1993). Uninfected erythrocytes were used as a control to determine the background level of LDH activity in human erythrocytes. Parasites cultured in the absence of inhibitors were used as controls for measurement of uninhibited pLDH activity. All inhibition assays were repeated at least two times in duplicate. Dose-response curves for each compound were created from the

averages of absorbance readings and the median inhibitory concentrations (IC_{50}) were determined graphically.

2.3 CLONING, EXPRESSION AND MANIPULATION OF *P. FALCIPARUM* αI- AND β-TUBULIN GENES

Several plasmids and numerous primers were used throughout the course of this study. The plasmids with the respective tubulins are listed in Table 2.1. The primers used are listed in Table 2.2.

2.3.1 Isolation and purification of DNA

Plasmids were isolated using a Wizard® *Plus* SV Minipreps DNA Purification System kit (Promega, supplied by Medical Supply Co., Dublin, Ireland). Briefly, the kit used a glass fibre membrane to affinity purify the DNA from fresh overnight cultures (5 – 50 ml), which were subsequently washed and eluted with DNAase free dH_2O. A similar kit, Wizard® SV Gel and PCR Clean-Up System (Promega), was used to remove impurities (e.g. old buffers) from previously isolated DNA or in particular DNA fragments. Briefly, separation of different DNA fragments was done by cutting the band of interest directly from a freshly run agarose gel as outlined in section 2.3.2. The agar sample with the DNA was subsequently melted and cleaned up as described in the manufacturer's protocol.

2.3.2 Visualisation of DNA by agarose gel electrophoresis

DNA preparations (DNA base pair markers X (Boehringer Mannheim, Mannheim, Germany), PCR products, purified plasmids, restriction enzyme-treated plasmids and PCR fragments) were examined by mixing 5 – 10 µl of sample with 1–2 µl of loading buffer (0.25% (w/v) bromophenol blue, 0.25% (w/v) xylene cyanol FF, 30% (v/v) glycerol, 10 mM EDTA) and running through a 0.5% –1% (w/v) agarose gel prepared in TAE buffer (40 mM Tris-HCl pH 8.3, 2 mM EDTA, 1 mM acetic acid). Samples were resolved by electrophoresis at 100 V in the direction of the cathode until desired migration was achieved (based on visual inspection). The running buffer for the electrophoresis was TAE buffer. Gels were stained in ethidium

Plasmid	Promoter	Expression strain	Tag	αI-tubulin	αII-tubulin	β-tubulin	Reference
pMAL-c2X	P_{tac}	TB1	MBP-tag	Yes	No	Yes	Fennell *et al.*, 2006
pMAL-c2G	P_{tac}	TB1	MBP-tag	Yes	No	Yes	This study
pET-11a	T7	BL21(DE3)	N.A.	Yes	Yes	Yes	Fennell, 2005
pET-16b	T7	BL21(DE3)	His_{12}-tag	Yes	No	Yes	Fennell, 2005
pET-Duet	T7	BL21(DE3)	N.A.	Yes	Yes	Yes	This study

Table 2.1 List of all the plasmids and tubulin genes used in this study. αII-tubulin was not routinely used: this was due to αI-tubulin being the dominant isotype during the asexual erythrocytic cycle (Fennell *et al.*, 2008).

Plasmid	Purpose	Primers	Template used for PCR
		Foward (Above) and Reverse (Below)	
pMAL-c2G	Insert αI-tubulin	5'-GCGCTACGTAATGAGAGAAGTAATAAGTATC-3'	pMAL-c2X-αI
		5'-CCCAAGCTTTTAATAATCTGCTTCATATCC-3'	
	Insert β-tubulin	5'-GATCTAACGTAATGAAGAGAAATTGTTCATATTC-3'	pMAL-c2X-β
		5'-CTAGTCTAGATTAGGCTTCTACGTCTCCTTC-3'	
	Insert stop codon to generate MBP Δ MCS	5'-GTGCGGCACACTACGTATAATTCGGATCCTCTAGAG-3'	pMAL-c2G
		5'-CTCTAGAGGATCCGAATTATACGTAGTGTGCCGCAC-3'	
pMAL-c2G-αI	Alteration: Val4Cys	5'-CGGCACACTACGTAATGAGAGAATGCATAAGTATCCATGTAGGACAAGC-3	pMAL-c2G-αI
		5'-GCTTGTCCTACATGGATACTTATGCATTCTCTCATTACGTAGTGTGCCG-3'	
	Alteration: Phe24His	5'-GGAAATGCTTGCTGGGAATTGCATTGCCTAGAGCATGGAATAC-3'	pMAL-c2G-αI
		5'-GTATTCCATGCTCTAGGCAATGCAATTCCCAGCAAGCATTTCC-3'	
	Alteration: Cys65Ala	5'-GGGCAGGAAAACATGTACCACGTGCTGTTTTTGTCGATTTAG-3'	pMAL-c2G-αI
		5'-CTAAATCGACAAAAACAGCACGTGGTACATGTTTTCCTGCCC-3'	
	Alteration: Leu136Phe	5'-CTGTACCGGTTTACAAGGATTTTTCATGTTCAGCGCAG-3'	pMAL-c2G-αI
		5'-CTGCGCTGAACATGAAAAATCCTTGTAAACCGGTACAG-3'	
	Alteration: Thr239Ile	5'-GATTGATTGCTCAAGTTATTTCTTCCTTAATAGCATCTTTAAGATTTGATG-3'	pMAL-c2G-αI
		5'-CATCAAATCTTAAAGATGCTATTAAGGAAGAAATAACTTGAGCAATCAATC-3'	
	Alteration: Arg243Ser	5'-TCTTCCTTAACAGCATCTTTAAGCTTTGATGGTGCTTTAAATGTTGA-3'	pMAL-c2G-αI
		5'-TCAACATTTAAAGCACCATCAAAGCTTAAAGATGCTGTTAAGGAAGA-3'	
pET-Duet	Insert β-tubulin	5'-CGCGACGTCATGAGAGAAATTGTTCATATTCAAGC-3'	pMAL-c2G-β
		5'- CGCCTCGAGTTAGGCTTCTACGTCTCCTTC-3'	
pET-Duet-β	Insert αI-tubulin	5'-CGCTCATGAGAGAAGTAATAAGTATCCATG-3'	pMAL-c2G-αI
		5'-CCCGGATCCTTAATAATCTGCTTCATATCC-3'	
pET-Duet-β	Insert αII-tubulin	5'- CGC TC ATG ATG AGA GAA GTC ATT AGT ATT C 3'	pET-11a-αII
		5'- CCC GGA TCC TCA TTC ATA TCC CTC ATC TTC TCC 3'	
pET-11a-αI	Insert stop codon to remove C-terminus	5'-AGAGGTAGGAATTGAATCCTAATGAAGCAGAAGGAGAAG-3'	pET-11a-αI
		5'-CTTCTCCTTCTGCTTCATTAGGATTCAATTCCTACCTCT-3'	
	Alteration: Asn168Glu	5'-TTATGGAAAGAAATCCAAACTGGAATTTTGCTGTTGGCCATCACCTC-3'	pET-11a-αI
		5'-GAGGTGATGGCCAACAGCAAAATTCCAGTTTGGATTTCTTTCCATAA-3'	
pET-11a-β	Insert stop codon to remove C-terminus	5'-CAACAATATCAAGATGCTACAGCAGAATAGGAAGGAGAATTTGA-3'	pET-11a-β
		5'-TCAAATTCTCCTTCCTATTCTGCTGTAGCATCTTGATATTGTTG-3'	

Table 2.2 List of all the primers and their purpose used in this study. The template used for the PCR is also included.

bromide (1 μg/ml) for 15 – 30 min, rinsed in dH_2O and the DNA was visualized and photographed by exposing the gel to ultraviolet (UV) light using an Alpha Imager 2200 gel imaging system (Alpha Innotech Corporation, San Leandro, California, USA).

2.3.3 Generation of the pMAL-c2G construct with *P. falciparum* αI- and β-tubulin genes

The *P. falciparum* 3D7 αI- and β-tubulin genes were previously cloned into the expression vector pMAL-c2x by Dr. Brian Fennell (Fennell *et al.*, 2006). The tubulin genes were re-amplified using this construct to include a 5' *Snab*I (New England Biolabs, Hertfordshire, UK) and a 3' *Hind*III (New England Biolabs) restriction site for αI-tubulin or a *Xba*I (New England Biolabs) restriction site for β-tubulin so that they could be inserted into pMAL-c2g (New England Biolabs). The plasmids differ by the endoprotease site they incorporate just after the maltose binding protein (MBP) tag. pMAL-c2x adds a factor Xa site and pMAL-c2g adds a genenase I site. Briefly, a "Hotstart" PCR was done using 0.5 μM of the αI-tubulin forward (5'-GCGCTACGTAATGAGAGAAGTAATAAGTATC-3') and reverse (5'-CCCAAGCTTTTAATAATCTGCTTCATATCC-3') or 0.5 μM of the β-tubulin forward (5'-GATCTAACGTAATGAAGAGAAATTGTTCATATTC-3') and reverse (5'-CTAGTCTAGATTAGGCTTCTACGTCTCCTTC-3') primers , ~ 100 ng pMAL-c2x-αI- or pMAL-c2x–β-tubulin, 2 mM dNTP (Roche), 0.5 mM $MgCl_2$ (Promega), 1 unit P*fu* Turbo DNA polymerase (Stratagene, La Jolla, California, USA) and *Pfu* turbo buffer (Stratagene) in a 50-μl reaction volume with a Techne TC-300 (Techne, Burlington, NJ, USA) thermocycler. The programme used for the PCR was: denaturation at 95°C for 3 min; followed by 28 cycles of 95°C for 30 s, annealing at 55°C for 1 min and extentsion at 72°C for 3 min; with a final extension at 72°C for 7 min. The tubulin PCR products were subsequently isolated from the parental DNA as detailed in section 2.3.1 and digested with appropriated restriction enzymes before insertion into the pMAL-c2g vector. Briefly, 50-μl reactions were set up in eppendorf tubes using a DNA concentration between 0.5 and 2 μg, 10 units of *Snab*I and *Hind*III or *Xba*I, buffer L (Roche), 50 mM NaCl (pH 7.5) and 5 μg bovine serum albumin (BSA) for 6 h at 37°C. The digested DNA were then isolated as described in section 2.3.1. The plasmid and gene fragments (ratio of 1:3) were then ligated together using

1 unit of T4 DNA ligase (Roche) and ligase buffer in a 20-µl reaction volume at 4°C overnight. Competent *E. coli* XL-1 Blue cells, prepared as described in section 2.3.5 were transformed with the ligate by heat-shock method (as in section 2.3.6) and plated out to L-agar (5% w/v yeast extract, 10% w/v tryptone, 5% NaCl w/v, 1% w/v agar) supplemented with 100 µg/ml ampicillin (Roche) and incubated overnight at 37°C. The resultant transformants were screened for the construct of interest (pMAL-c2g-αI- or pMAL-c2g-β-tubulin) as described in section 2.3.8. Confirmed recombinants were transformed into TB1 (New England Biolabs) cells as described in section 2.3.6.

2.3.4 Generation of the pET-Duet-αI/β and pET-Duet-αII/β constructs

The pET-Duet plasmid (Novagen) has two multiple cloning sites (MCS) that permit the expression of two proteins independently of each other in the same organism. The overall strategy for this cloning experiment is detailed in Fig. 3.10. The β-tubulin gene was inserted first into the vector and was re-amplified using the pMAL-c2g-β vector from section 2.3.3 as a template. The β-tubulin forward primer added an *Aat*II restriction site (5'-CGCGACGTCATGAGAGAAATTGTTCATATTCAAGC-3') and the reverse primer added a *Xho*I site (5'- CGCCTCGAGTTAGGCTTCTACGTCTCCTTC-3') using the same conditions as in section 2.3.3 except that the annealing temperature was 56°C. The tubulin PCR product was subsequently isolated from the parental DNA as detailed in section 2.3.1 and the appropriate restriction enzymes were used for digesting the DNA. Briefly, 50-µl reactions were set up in eppendorf tubes using a DNA amount between 0.5 and 2 µg, 10 units of *Aat*II and *Xho*I buffer 4 (NEB), and 5 µg BSA for 12 h at 37°C. The ligation and subsequent screening of the pET-Duet-β-tubulin clone is outlined in section 2.3.4. The αI- and αII-tubulin genes were re-amplified using either the pMAL-c2g-αI vector or the pET-11a-αII vection as a template (see section 2.3.3). The αI- and αII-tubulin forward primers added a *Rca*I restriction and the reverse primers added a *Bam*HI restriction site. The αI-tubulin primers forward and reverse were; 5'-CGCTCATGAGAGAAGTAATAAGTATCCATG-3' and 5'-CCCGGATCCTTAATAATCTGCTTCATATCC-3'. The αII-tubulin primers forward and reverse were; 5'-CGC TC ATG ATG AGA GAA GTC ATT AGT ATT C-3' and 5'-CCC GGA TCC TCA TTC ATA TCC CTC ATC TTC TCC-3'. The

same conditions were used as detailed in section 2.3.3 except that the annealing temperature was 53°C. The tubulin PCR product was subsequently isolated from the parental DNA as detailed in section 2.3.1 and the appropriate restriction enzymes were used for digesting the DNA. Briefly, 50–µl reactions were set up in eppendorf tubes using αI- or αII-tubulin at a concentration between 0.5 – 2 µg, 10 units of *Rca*I and *Bam*HI, buffer B (Roche), and 5 µg BSA for 12 h at 37°C. pET-Duet-β-tubulin was digested in a similar manner; 50–µl reactions were set up in eppendorf tubes with 10 units of *Nco*I and *Bam*HI, buffer 3 (NEB) and 5 µg BSA for 12 h at 37°C. The αI- or αII-tubulin and pet-Duet-β-tubulin fragments were prepared for ligation and screening as described in section 2.3.3. Confirmed recombinants were transformed into BL-21 (DE3) (Novagen) cells as described in section 2.3.6.

2.3.5 Preparation of competent *E. coli* cells

A single colony from the desired strain of *E. coli* (XL-1 Blue (Stratagene), BL21 (DE3) (Novagen) or TB1 (New England Biolabs)) was used to inoculate 20 ml of L-broth and grown overnight with agitation at 200 rpm at 37°C. 5 ml overnight cultures were used to inoculate 400 ml of fresh L-broth in a 2–l baffled flask and the bacteria were then grown at 37°C with agitation at 200 rpm until they had an absorbance reading at 600 nm (A_{600}) of ~0.4. Cells were decanted into two 250 ml Sorvall GSA containers and were chilled on ice for 20 min. Cells were sedimented by centrifugation at 4000 rpm (2600 x g) for 10 min at 4°C in a Sorvall RC-50 centrifuge (Du Pont Ltd. Stevenage, Herts, UK). The supernatant was decanted and the pellet was gently resuspended in 100 ml of ice-cold $CaCl_2$ (100 mM) and incubated on ice for 1 h. Cells were resuspended in 20 ml of ice-cold $CaCl_2$ solution, divided among pre-chilled sterile eppendorf tubes (200 – 500 µl volumes), snap frozen in liquid nitrogen and stored in a – 70°C freezer.

2.3.6 Transformation of competent *E. coli* strains

Competent *E. coli* cells were transformed using the heat-shock method as described by Maniatis *et al* (1982). XL-1 Blue cells were always used for the initial plasmid transformation and subsequent cloning experiments (e.g. screening of transformants) due to its high levels of competency and that these cells were not able to express either the "pMAL" or "pET" vector's which is advantageous if the

recombinant protein(s) is toxic to the cell. The "pMAL" plasmids were always transformed into the *E. coli* TB1 strain while the "pET" plasmids always used the BL21 (DE3) strain only. The competent cells were thawed on ice for 30 min and were mixed with 1–30 µl of ligation mixture or expression plasmid in a sterile eppendorf. Samples were incubated on ice for 30 min, heat-shocked in a 43°C water bath for 2 min and were transferred to ice for 2 min. One ml of pre-warmed L-broth was added to the samples, which were then incubated in a 37°C water bath for 1 h. After incubation, 100–µl volumes of each sample were plated in duplicate on L-agar/ampicillin and incubated overnight at 37°C. The remaining cells were sedimented by centrifugation at 14,000 rpm (18,000 x g) for 1 min at room temperature and most of the supernatant was removed except for ~100 µl. The pellet was then resuspended in the excess L-broth and plated on duplicate L-agar plates as previously described. Controls for the transformation experiment included undigested and digested vector (with appropriate restriction enzymes), PCR fragments and untreated competent cells.

2.3.7 Screening of the transformants

Putative transformants were grown at 37°C for 12 – 16 h and then individual colonies were transferred onto a gridded L-agar plate with a suitable antibiotic for rapid identification in the future. DNA sequencing was conducted by GATC (Konstanz, Germany) on clones that were confirmed to have the gene of interest.

2.3.7.1 Screening by small-scale plasmid isolation

Putative transformants and controls were grown overnight at 37°C, with agitation at 200 rpm, in 5 ml of L-broth with suitable antibiotic added in a test tube. The cultures were then transferred to an eppendorf tube and sedimented by centrifugation at 14,000 rpm (18,000 x g) for 1 min (all centrifugation steps were conducted at room temperature). The supernatants were discarded and the pellets were resuspended in 100 µl of a glucose solution (10 mM Tris-HCl pH 8.0, 50 mM glucose, 1 mM EDTA). Two hundred µl of freshly prepared lysis solution (200 mM NaOH, 1% w/v SDS) were added and the tubes were mixed by inverting them 4 times and then incubated on ice for 5 min. Three hundred µl of potassium acetate solution

(4 M potassium acetate, 2 M acetic acid) were added, mixed and incubated on ice for 5 min. The tubes were centrifuged for 5 min at 14,000 rpm (18,000 x g) and the supernatants were transferred to fresh tubes. One ml of absolute ethanol was added and the tubes were mixed by inversion and left on ice for 5 min. The DNA was sedimented by centrifugation at 14,000 rpm (18,000 x g) for 10 min. The supernatants were discarded and the pellets washed in 500 µl of 70% v/v ethanol. The tubes were inverted and placed in a 37°C incubator for 1 h to remove residual ethanol. The pellets were resuspended in 50 µl dH_2O containing 0.01 µg RNase A and 10 – 20 µl were loaded onto an agarose gel and treated as described in section 2.3.2. Following the ethidium bromide staining procedure, putative recombinants were identified by a slower migration through the gel than the vector alone.

2.3.7.2 Rapid colony screening

Colonies were emulsified in 16 µl lysis buffer (0.67% (v/v) SDS, 130 mM NaOH, 10x loading buffer (see section 2.3.2 for reagents) in eppendorf tubes before adding 3 µl of a potassium acetate acetic acid solution (3 M potassium acetate, 1.8 M acetic acid). Tubes were centrifuged for 4 min at 14,000 rpm (18,000 x g) to sediment cellular debris. Ten–fifteen µl of the resultant supernatant were loaded directly onto an agarose gel and treated as detailed in section 2.3.2. Following the ethidium bromide staining procedure, putative recombinants were identified by a slower migration through the gel than the vector alone.

2.3.7.3 Screening by restriction endonuclease digestion

To confirm that the putative recombinants contained the insert of interest, restriction enzymes were used to linearise the original vector and the putative recombinant plasmids. The putative recombinants were used to inoculate 5 ml of L-broth supplemented with appropriate antibiotic and grown overnight at 37°C with agitation at 200 rpm. The plasmids were isolated as described in section 2.3.1. Restriction enzyme digestion was conducted using appropriate enzymes as outlined in section 2.3.3. The linearised putative recombinant plasmids and plasmid alone were compared by size on an agarose gel as detailed in section 2.3.2. This permitted the comparison of known size for the plasmids.

2.3.7.4 Screening by PCR

PCR amplification for the gene of interest was conducted using the putative recombinant plasmids to determine the presence of the insert. The putative recombinant plasmids were isolated as detailed in section 2.3.7.3. These putative recombinants were used as a template in a PCR reaction as outlined in 2.3.3.

2.3.8 Generation of altered tubulins by site directed mutagenesis

Inverse PCR was used to introduce point mutations directly into the tubulin genes. Briefly, bi-directional, overlapping primers with nucleotide changes specific to the target sequence were designed so that the entire plasmid would be amplified during the reaction (see Fig 2.1). All of the plasmid templates were generated as described in section 2.3.1

2.3.8.1 Generation of pMAL-c2G-αI-tubulin alterations

The pMAL-c2g-αI-tubulin vector was used as a template to generate specific mutations in the αI-tubulin gene which led to an amino change when translated (Val4Cys, Phe24His, Cys65Ala, Leu136Phe, Thr239Ile and Arg243Ser). One of the following primer sets was used to generate the mutants; **VAL4CYS** (G10T, T11G and A12C) forward 5'-CGGCACACTACGTAATGAGAGAATGCATAAGTATCCATGTAGGACAAGC -3' and reverse 5'-GCTTGTCCTACATGGATACTTATGCATTCTCTCATTACGTAGTGTGCCG -3', **PHE24HIS** (T70C and T71A) forward 5'-GGAAATGCTTGCTGGGAATTGCATTGCCTAGAGCATGGAATAC -3' and reverse 5'- GTATTCCATGCTCTAGGCAATGCAATTCCCAGCAAGCATTTCC -3', **CYS65ALA** (T93C and G94C) forward 5'-GGGCAGGAAAACATGTACCACGTGCTGTTTTTGTCGATTTAG -3' and reverse 5'- CTAAATCGACAAAAACAGCACGTGGTACATGTTTTCCTGCCC -3', **LEU136PHE** (A408C) forward 5'-CTGTACCGGTTTACAAGGATTTTTCATGTTCAGCGCAG -3' and reverse 5'-CTGCGCTGAACATGAAAAATCCTTGTAAACCGGTACAG -3', **THR239ILE**

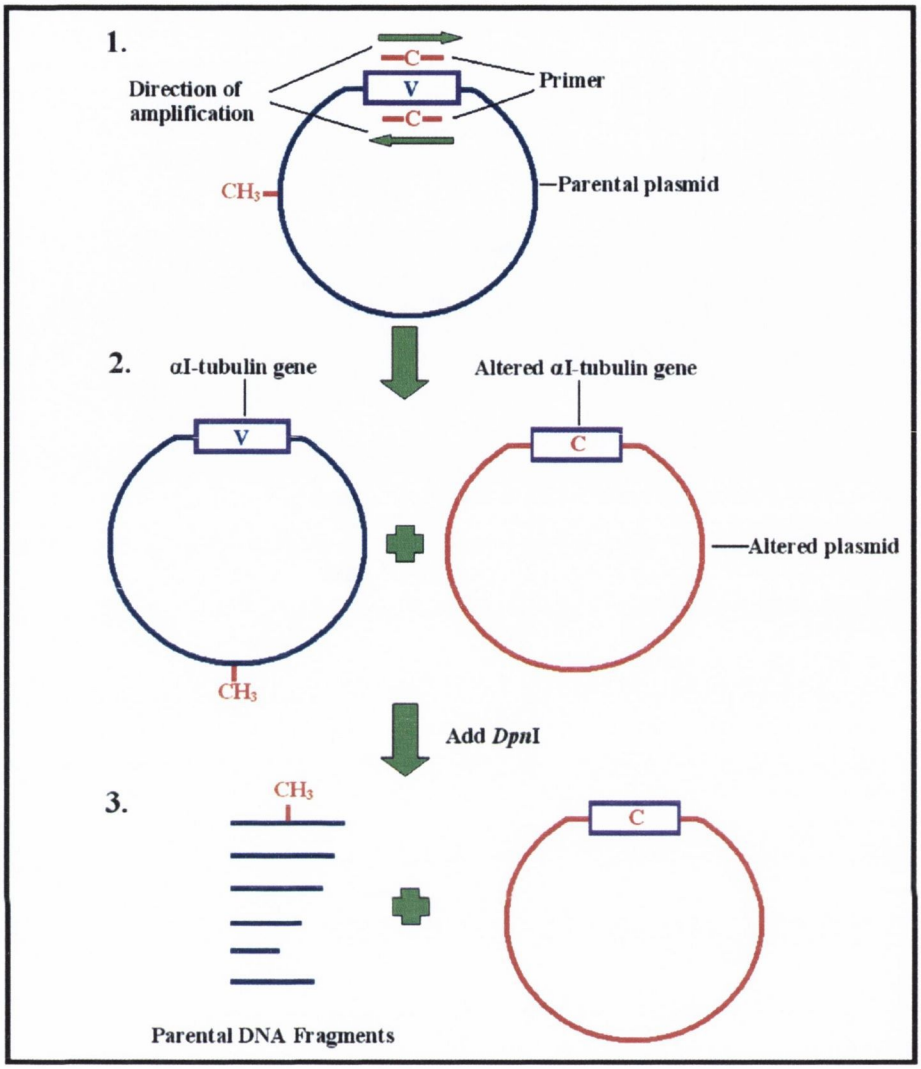

Fig. 2.1 Schematic outline for generating specific alterations in the αI-tubulin gene. 1. Primers were designed so that they overlap each other with specific nucleotide change in the centre. This nucleotide change causes a specific amino acid change when the gene is expressed. The example shown has a valine being swapped for a cysteine. **2.** The amplification occurs in opposite directions, so the entire plasmid is copied. The newly transcribed plasmid is not methylated unlike the parent (represented by $-CH_3$). **3.** Addition of the restriction enzyme, *Dpn*I digests only methylated DNA. Therefore, the newly transcribed plasmid is not digested while the parental plasmid is. (The parental plasmid has numerous methylation sites, only one is shown for demonstration purposes.)

(C717T) forward 5'-GATTGATTGCTCAAGTTATTTCTTCCTTAATAGCATCTTTAAGATTTGATG -3' and reverse 5'-CATCAAATCTTAAAGATGCTATTAAGGAAGAAATAACTTGAGCAATCAATC -3', **ARG243SER** (A729C) forward 5'-TCTTCCTTAACAGCATCTTTAAGCTTTGATGGTGCTTTAAATGTTGA -3' and reverse 5'-TCAACATTTAAAGCACCATCAAAGCTTAAAGATGCTGTTAAGGAAGA -3'. The PCR was conducted using a 50–µl reaction volume with the primers added first and diluted to the correct concentration (0.5 µM). This mixture was heated for 10 min at 95°C to ensure the primers were completely denatured. A "Hotstart" PCR was set up using ~ 100 ng pMAL-c2g-αI, 2 mM dNTP, 0.5 mM $MgCl_2$, 1 unit *Pfu*, *Pfu* turbo buffer with a Techne TC-300 thermocycler. The programme used for the PCR was: denaturation at 95°C for 3 min; followed by 28 cycles of 95°C for 30 s, annealing at 55°C for 1 min and extension at 72°C for 9 min; with a final extension at 72°C for 10 min. The PCR product was treated with 1 unit *Dpn*I (Roche) for 3 h at 37°C and then cleaned up as described in section 2.3.1. The plasmids were transformed into XL-1 blue cells as described in section 2.3.6 and screened as described in section 2.3.7. Confirmed recombinants were transformed into *E. coli* TB1 cells as described in section 2.3.6.

2.3.8.2 Generation of pMAL-c2G MBP Δ MCS alteration

MBP translated from the pMAL-c2g vector contains 73 extra amino acids compared to the MBP attached to the tubulin fusions due to translation through the MCS. Therefore, a stop codon was inserted into the pMAL-c2g vector in the appropriate position, **V390Stop** (G1171T), so that pMAL-c2g MBP Δ MCS produces MBP which was identical to the MBP on the fusion tubulins. A PCR amplification was set up as described in section 2.3.8.1 with the following exceptions; 0.5 µM MBP forward (5'-gtgcggcacactacgtataattcggatcctctagag-3') and reverse (5'-ctctagaggatccgaattatacgtagtgtgccgcac-3') primers and ~100 ng pMAL-c2g were used. The annealing temperature used was 58°C.

2.3.8.3 Generation of pET11a-αI- and -β-tubulin alterations

pET-11a-αI-tubulin and pET-11-β-tubulin constructs were previously generated by Dr. Brian Fennell (Fennell, B. J., PhD Thesis 2005). Specific nucleotide changes were introduced into the tubulin genes: pET-11a-αI-tubulin; **N168E** (A502G and T504A) (forward 5'-TTATGGAAAGAAATCCAAACTGGAATTTTGCTGTTGGCCATCACCTC -3' and reverse 5'-GAGGTGATGGCCAACAGCAAAATTCCAGTTTGGATTTCTTTCCATAA -3') and **I437Stop** (insertion T1318) (forward 5'-AGAGGTAGGAATTGAATCCTAATGAAGCAGAAGGAGAAG -3' and reverse 5'- CTTCTCCTTCTGCTTCATTAGGATTCAATTCCTACCTCT -3') and pET-11a-β-tubulin; **E431Stop** (T1293) (forward 5'-CAACAATATCAAGATGCTACAGCAGAATAGGAAGGAGAATTTGA -3' and reverse 5'- TCAAATTCTCCTTCCTATTCTGCTGTAGCATCTTGATATTGTTG -3') by inverse PCR as described in section 2.3.8.1. These were generated by Miss Deirdre O'Flynn under my supervision.

2.3.9 Recovery of DNA by ethanol precipitation

DNA was concentrated by adding $1/10^{th}$ the sample volume of 5 M sodium acetate (pH 5.2) and 2 volumes of absolute ethanol (ice-cold). The sample was stored at -70°C for 1 h and centrifuged at 14,000 rpm (18,000 x g) for 10 min. The supernatant was removed and the pellet was washed with 2 volumes of ice cold 70% (w/v) ethanol. The sample was centrifuged at 14,000 rpm (18,000 x g) for 5 min. This wash step was repeated twice. The supernatant was discarded and the DNA pellet was air dried in a 37°C incubator for ~1 h. The pellet was then resuspended in an appropriate volume of dH_2O.

2.4 PROTEIN QUANTIFICATION AND ANALYSIS

2.4.1 Quantification of protein concentration by the Bradford assay

Protein quantification was determined using the colourimetric assay from Bradford (1976), which is based on the binding of a dye, Coomassie Brilliant Blue G250, to the protein of interest. Protein amounts in experimental samples were determined with reference to a bovine serum albumin (BSA) standard curve. A standard stock of 0.5 mg/ml BSA was diluted from a maximum of 15–1 µg/ml in a final volume of 100 µl in PBS. Samples for quantification were also diluted in PBS to a final volume of 100 µl. One ml of Bradford reagent (0.01% (w/v) Coomassie Brilliant Blue G-250, 0.25% (w/v) ethanol and 10% (v/v) orthophosphoric acid) was added to all samples, followed by vigorous vortexing to ensure a homogenous mixture. Samples were incubated at room temperature for 20 min and absorbances were determined at 595 nm using a Shimadzu UV-1601 PC spectrophotometer (Shimadzu Scientific Instruments Inc., Columbia, MD, USA).

2.4.2 SDS-polyacrylamide gel electrophoresis (SDS-PAGE)

Protein samples were electrophoretically separated by SDS-PAGE according to the method of Laemmli (1970). The separating gel consisted of 0.375M Tris-HCl (pH 8.8), 0.1% (v/v) SDS, 0.06% (v/v) ammonium persulphate (APS) and 0.05% (v/v) N, N, N', N'-tetramethyl-ethylenediamine (TEMED). Five %, 7.5% and 10% gels had 15%, 22.5% and 30% respectively of acrylamide/bisacrylamide solution (30% w/v, 37.5:1) (Protogel, National Diagnostics, Hull, UK) added. Stacking gels consisted of 0.125 M Tris-HCl (pH 6.8), 13.33% acrylamide/bisacrylamide (30% w/v, 37.5:1), 0.1% (v/v) SDS, 0.1% (v/v) APS and 0.1% (v/v) TEMED. Mini-gel glass plates were clamped together, the separating gel was poured to ~1.5 cm from the top of the plates and the solution was then covered using water-saturated iso-butanol for 15-30 min. After polymerisation, the gel was washed with water to remove the iso-butanol and dried using Whatman paper. The stacking gel was then poured over the set separating gel and a comb was inserted carefully to avoid adding air-bubbles. The gel was allowed to polymerise for another 15-30 min. Protein samples were mixed in an equal volume of 2x reducing SDS sample loading buffer (0.125 M Tris-HCl (pH 6.8), 2.3% (v/v) SDS, 10% (w/v) glycerol, 10% (v/v) 2-mercaptoethanol and 0.009%

bromophenol blue (w/v) as a tracking dye) and boiled at ~100°C for 10 min. A combination of proteins of known molecular weight (New England Biolabs or Invitrogen) was loaded onto each gel as reference standards (Fig. 2.2). The protein samples (0.2 – 30 µl) were resolved at 147 V using an EC105 power supply pack (E-C Apparatus Corp., Holbrook, New York, USA) until the tracking dye reached the bottom. Running buffer consisted of 0.3% (w/v) Tris-HCl, 1.44% (w/v) glycine and 0.1% (w/v) SDS.

2.4.3 Electrophoresis of the tubulin fusions by native PAGE

Protein samples were electrophoretically separated by native PAGE using the same technique as outlined in section 2.4.2 except that SDS and in some cases (see results section) 2-mercaptoethanol were omitted. Protein samples were mixed in an equal volume of 2x non-reducing loading buffer (0.125 M Tris-HCl (pH 6.8), 100 mM EDTA, 10% (w/v) glycerol, a few grains of bromophenol blue and xylene cyanol as tracking dyes) and the gel was run in non-reducing running buffer (30 mM Tris-HCl pH 8.3, 0.19 M glycine).

2.4.4 Visualisation of protein samples on polyacrylamide gels

SDS-PAGE gels were stained with 20 – 25 ml of Coomassie blue reagent (0.15% (w/v) Coomassie Brilliant Blue R250 (Phiobio, Fisons Scientific Equipment, Loughborough, UK), 45% (v/v) methanol (BDH), 10% (v/v) glacial acetic acid (BDH)) for 1-4 h. The gels were destained in 20% (v/v) methanol and 7.5% (v/v) glacial acetic acid until the background was clear. The gels were photographed with the Alphaimager 2200 (Alpha Innotech Corp.) and stored in cellophane (Bio-Rad Laboratories, Hercules, CA, USA).

2.4.5 Protein precipitation with trichloroacetic acid (TCA)

Certain dilute proteins samples were concentrated by TCA precipitation prior to loading onto SDS-PAGE gels. Protein samples were mixed with 25% ice-cold TCA (1:1 ratio), incubated on ice for 5 min and then centrifuged at room temperature at 14,000 rpm (18,000 x g) 5 min. The supernatant was discarded and the pellet was resuspended an appropriate volume (1-20 µl) of 1x reducing SDS sample loading buffer (62.5 mM Tris-HCl pH 6.8, 1.15% (v/v) SDS, 5% (v/v) glycerol, 5% (v/v) 2-

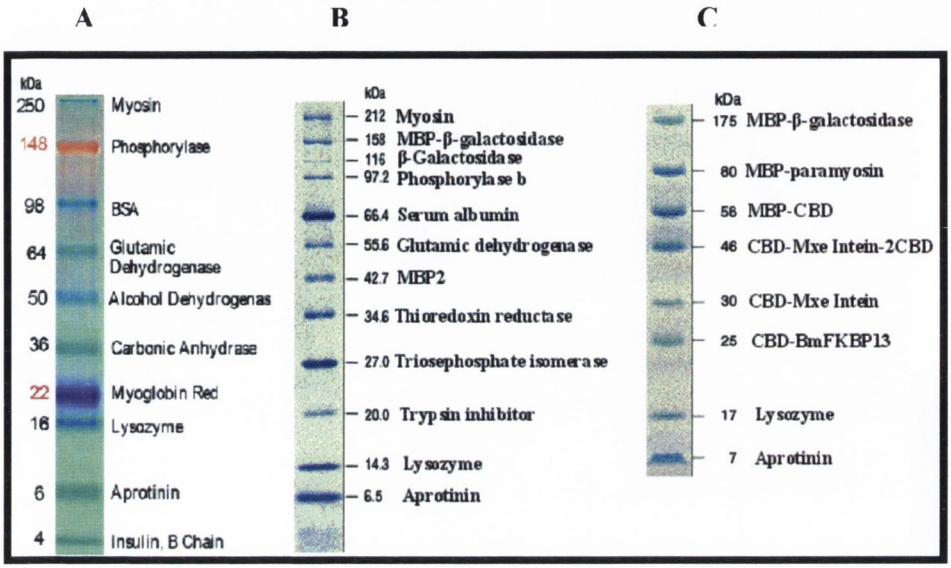

Fig. 2.2 Standard molecular weight markers that were resolved on the polyacrylamide gels. A. See-blue 2 (Invitrogen). **B.** Broad range marker (Roche). **C.** Pre-stained broad range marker (Roche). **kDa**, molecular weight in kilodaltons.

mercaptoethanol and 0.005% (v/v) bromophenol blue as a tracking dye). Occasionally the loading buffer turned yellow and required the addition of a few crystals of Tris to restore the pH of the solution. The samples were then boiled for 10 min and loaded onto SDS-polyacrylamide gels.

2.4.6 Western immunoblotting

Protein samples resolved on SDS-PAGE gels (as described in section 2.4.2) were further analysed by antibody staining. Polyvinylidiene difluoride (PVDF) membrane (Roche Diagnostics GmbH, Mannheim, Germany) was used to capture proteins transferred from unstained SDS-polyacrylamide gels. Briefly, the PVDF membrane was soaked in methanol for 10 s before being soaked in transfer buffer (1.44% (w/v) glycine, 0.3% (w/v) Tris-HCl pH 8.3%, 20% (v/v) methanol). The gel and PVDF membrane were compressed together to form a sandwich, backed either side by blotting paper, in the blotting tank filled with ~1 l of transfer buffer. The transfer was conducted at 4°C, with an ice-block and magnetic stirrer present to minimise the heat generated, for 90 min using 100 V. After the transfer, the blot was blocked in 5 – 10% skimmed milk in Towbin's buffer (10 mM Tris-HCl pH 7.4, 0.9% (w/v) NaCl) for at least 1 h with shaking at room temperature. The membrane was incubated with the primary antibody to a final concentration 1:2000 in 3% (w/v) skimmed milk in Towbin's buffer for 1 h. The blot was washed in Towbin's buffer with 0.05% (v/v) Tween 20 for 1 h. Goat-anti-rabbit-immunoglobulin–peroxidase (GARIg-PO), diluted to a final concentration of 1:4000 in 3% (w/v) skimmed milk, was used as the secondary antibody to probe the blot for 1 h. The blot was treated with chemiluminescence western blotting substrate (Roche) according to manufacturer's instructions in a darkroom before exposing it to X-OMAT UV film (Kodak, Dublin) for an appropriate time. The film was developed manually by a standard procedure; 30 s in developer (Kodak), 30 s in dH_2O and 30 s in fixative (Kodak) or automatically by using a Kodak X-OMAT 1000 Processor (Rochester, New York, U.S.A). The film was air-dried and the photo was taken using an Alphaimager 2200 (Alpha Innotech Corp.).

2.4.7 Estimation of relative protein amounts on a SDS-polyacrylamide gel by densitometry

SDS-polyacrylamide gels that coomassie stained as outlined in section 2.4.4 were scanned and analysed by the specific densitometry program, Quantity One® (Bio-Rad Laboratories, Inc., California, U.S.A.). The relative amount of protein in each lane was compared to a control sample loaded on the same gel.

2.5 GENERATION, PURIFICATION AND REFOLDING OF RECOMBINANT TUBULINS

2.5.1 Expression of tubulins from the pMAL-c2x-tubulin and pMAL-c2g-tubulin constructs

L-agar plates supplemented with ampicillin (100 µg/ml) were streaked out with the *E. coli* TB1 expression strain containing the construct of interest and left overnight at 37°C. A single colony was used to inoculate 5 ml of L-broth supplemented with ampicillin (100 µg/µl) and was left overnight in an orbital shaker (Gallenkamp Ltd., Stockton-on-tees, England) at 37°C with 200 rpm agitation. An appropriate volume of L-broth in a baffled flask (20 ml – 500 ml), supplemented with ampicillin (100 µg/µl), was inoculated with a $1/200^{th}$ volume of the overnight sample. The culture was grown in an incubator at 37°C, with an agitation of 200 rpm until an absorbance between 0.5 – 0.7 was reached. Recombinant gene expression was induced by adding 0.35 mM isopropyl β-D-1-thiogalactopyranoside (IPTG) to the culture and incubating it for a further 3 h. Cells were harvested by centrifuging them using a SLA-1500 rotor in a Sorvall RC50 Plus centrifuge at 8,000 rpm (7670 x g) for 10 min at 4°C. The supernatant was discarded and the pellets were frozen at -20°C.

2.5.2 Expression of the pET-11a-tubulin, pET-16b-tubulin and pET-Duet-tubulin constructs

L-agar plates supplemented with ampicillin (100 µg/ml) were streaked out with the *E. coli* BL21 (DE3) expression strain containing the construct of interest and left overnight at 37°C. A single colony was used to inoculate 20 ml of L-broth supplemented with ampicillin (100 µg/µl) and was incubated in an orbital shaker at

37°C with 200 rpm agitation until an absorbance of~ 0.375 was achieved. The culture was then left at 4°C overnight. A 1/200th appropriate volume of culture was taken to be used as an inoculum. The inoculum was centrifuged at 14,000 rpm (18,000 x g) for 1 min at room temperature and resuspended to its original volume in fresh L-broth. The remaining expression steps were conducted as described in section 2.5.1.

2.5.3 Affinity purification using an amylose column

The pellets were resuspended in 20 ml of ice-cold amylose column buffer (20 mM Tris-HCl pH 7.4, 200 mM NaCl, 1 mM EDTA; filter-sterilised) with 1-2 complete mini protease inhibitor cocktail tablets (Roche). Cells were lysed by 2-3 passages through a pre-cooled French® Pressure cell press (Slm-Aminco/Spectronic Instruments Inc., Rochester, NY, U.S.A) at a pressure of 1500 psi. The extract was centrifuged in a polypropylene tube using a pre-cooled SS-34 rotor at 4°C, 17,000 rpm (35,000 x g) for 1 h. Small particulate matter was further removed by passing the supernatant through a 0.2 µM filter (Millipore). All of the amylose column steps were conducted at 4°C in a cold room. The amylose column was prepared by pouring ~ 5-10 ml amylose resin into a 2 x 10 cm column (Bio-Rad) and equilibrated by running ≥ 10 column volumes of amylose column buffer through it using a peristaltic pump, Pump P-1 (Pharmacia Biotech, New Jersey, U.S.A) at 2 ml/min (the pump was used at 2 ml/min for all steps except where otherwise stated). The supernatant was then diluted with 5 volumes of amylose column buffer and loaded onto the column at 1 ml/min. The column was washed with ≥ 15 column volumes of amylose column buffer. The bound protein was released using ~50 ml elution buffer (10 mM maltose in amylose column buffer, filter sterilised). The eluted proteins were concentrated using an Amicon centrifuge filter (Millipore), with a molecular weight cut-off of 50 kDa, by centrifuging it at 3000 rpm in a Sorvall RT 6000 D to ~ 1/50th of its original volume.

2.5.4 Affinity purification using a HiTrap Mono Q® column

A 5–ml cationic-exchange colum, HiTrap Mono Q® (Amersham Pharmacia, Pollards Wood, Bucks, UK), was pre-equilibriated by washing it with ≥ 10 column volumes of high–salt buffer (20 mM Tris-HCl pH 8.0, 1 M NaCl, filter sterile) and ≥ 10 column volumes of low–salt buffer (20 mM Tris-HCl pH 8.0, filter sterile) using a

peristaltic pump at 2 ml/min. Concentrated, amylose–purified protein (see section 2.5.3) was diluted 10–fold in low–salt buffer and loaded onto the column at 1 ml/min. The column was washed with ≥ 10 column volumes of low salt buffer and then a range of increasingly concentrated salt buffers in this order; 100 mM, 200 mM, 300 mM, 400 mM, 600 mM and 1M NaCl. The 600 mM salt buffer eluted the tubulin so this fraction was concentrated using an Amicon centrifuge filter (Millipore), with a molecular weight cut-off of 50 kDa, by centrifuging it at 3000 rpm Sorvall RT 6000 D to ~ $1/50^{th}$ its original volume. Buffer exchange was formed on the sample by both dilution and re-concentration using an Amicon centrifuge filter as described above or by dialysis. Dialysis was conducted as described in section 2.5.5. The freshly buffered sample was divided into pre-chilled eppendorf tubes and snap–frozen in liquid N_2 before being stored at -70°C.

2.5.5 Buffer exchange using dialysis

Dialysis tubing (Sigma-Aldrich) with a molecular weight cut–off of ≤ 36 kDa was soaked in boiling dH_2O for 10 min. Crocodile clips were used to seal both ends of the tubing once the purified protein sample (≤ 30 ml) was pipetted in. The dialysis sample was transferred to an ice-cold 5–l solution of 20 mM Tris-HCl, pH 7.4, with constant stirring and left overnight at 4°C.

2.5.6 Determination of recombinant protein solubility

In order to determine the solubility of the recombinant proteins produced by the pET–Duet αI/β-tubulin construct, 400 ml of cells obtained as described in section 2.5.2 were resuspended in 10 ml cold MME buffer (0.1 M 2-(N-morpholino)ethanesulfonic acid (MES) pH 6.9, 1 mM $MgCl_2$ and 1 mM EGTA) with one complete mini protease inhibitor cocktail tablet (Roche) added. The cells were lysed by 2-3 passages through a pre-cooled French pressure cell at a pressure of 1500 psi. The lysate was spun in a polypropylene tube using a pre-cooled SS-34 rotor at 4°C, 17,000 rpm (35,000 x g) for 1 h. Small particulate matter was further removed by syringing the supernatant through a 0.2 μM filter (Millipore). The supernatant was transferred to a cold falcon tube and the insoluble fraction was resuspended in 10 ml cold MME buffer. The sample was spun at 18,000 RPM for 10 min 4°C. This wash step was done twice. The insoluble fraction was finally resuspended with 10 ml cold

MME buffer so as to be in equally diluted as the supernatant. The samples were then prepared for resolution on a SDS 10%–PAGE as described in section 2.4.2.

2.5.7 Isolation of tubulin-containing inclusion bodies

Tubulin-containing inclusion bodies were isolated by a method adapted from Jang *et al* (2008). Briefly, *E. coli* cells containing either the pET-11a-tubulin or pET-16b-tubulin vector were induced to produce the tubulin protein as detailed in section 2.5.2. The frozen pellet was resuspended in ~ 20 ml Tris buffer (20 mM Tris-HCl pH 8.0) with 2 "mini complete" inhibitor cocktail tablets added. The resuspended cells were lysed with two passages at 4°C through the French pressure cell. The lysate was clarified by centrifuging it at 17,000 rpm (35,000 x g) at 4°C for 1 h using a SS-34 rotor. The supernatant was discarded and the pellet was washed using 40 ml of isolation buffer (20 mM Tris-HCl pH 8.0, 300 mM NaCl and 2% (v/v) Triton X-100) followed by centrifugation at 10,000 rpm (11,950 x g) at 4°C for 10 min. This wash step was repeated twice. The pellet, which was almost exclusively tubulin, was either refrozen at -20°C or used immediately.

2.5.8 Solubilisation and renaturation of insoluble tubulin

Two separate strategies were used to denature and renature insoluble tubulin that had been isolated in section 2.5.7; a biological approach using a rabbit reticulocyte lysate mixture to provide molecular chaperones and a chemical approach using a urea gradient. The biological method used native-like tubulin produced from the pET-11a-tubulin vectors while the chemical method used hexahistidine–tagged tubulin produced from the pET-16b-tubulin vectors.

2.5.8.1 Solubilisation and renaturation of insoluble tubulin using rabbit reticulocyte lysate

This experiment was assisted by Miss Sara Leddy as part of her 4th year research project. The tubulin inclusion bodies isolated in section 2.5.7 were solubilised in 40 ml of concentrated urea buffer (0.02 M Tris-HCl pH 7.5, 10 mM 2-mercaptoethanol, 7.5 M urea) based on the technique described by Shah *et al* (2001) (Shah *et al.* 2001). Tubulins were concentrated to 35 µg/µl by centrifugation with a 30–kDa Amicon filter (Millipore) at 3,000 rpm, 4°C and stored at -75°C until further

use Sorvall RT 6000 D. A refolding mixture of 100 µl crude rabbit reticulocyte lysate (Pel-Freez Biologicals, Rogers, AR, U.S.A) and 11 µl of refolding buffer (0.4 M 2-(N-morpholino)ethanesulfonic acid (MES) pH 6.8, 0.1 M KCl, 5 mM GTP, 0.5 M trimethylamine oxide (TMAO)) was prepared on ice. Approximately 1.7 µl (~60 µg) of αI-tubulin and ~4.25 µl (~148 µg) of β-tubulin were added to the refolding mixture with rapid mixing. The solution was incubated at 30°C for 1 h. The sample was then snap frozen using liquid nitrogen for later use.

2.5.8.2 Solubilisation and renaturation of insoluble tubulin by metal–affinity chromatography

Each tubulin protein was refolded in a separate but identical experiment using this procedure. The tubulin–rich pellets isolated in section 2.5.7 were solubilised in 40 ml of concentrated guanidine hydrochloride buffer (20 mM Tris-HCl pH 8.0, 6 M guanidine hydrochloride, 300 mM NaCl, 5 mM imidazole and 1 mM 2-mercaptoethanol). The solubilised tubulin was incubated at room temperature with gentle stirring for 30 min. The solution was centrifuged at 14,150 rpm (23,700 x g), 4°C for 10 min. The supernatant was recovered and filtered through a 0.45 µM syringe filter. The supernatant containing either His_{12}-αI- or His_{12}-β-tubulin was loaded onto a Ni^{2+}–charged column (Amersham Pharmacia) pre-equilibrated with 3 column volumes of binding buffer (6 M guanidine hydrochloride, 20 mM Tris-HCl pH 8.0, 300 mM NaCl, 5 mM imidazole and 1mM 2-mercaptoethanol) at 1 ml/min using a peristaltic pump. The column was washed with 10 column volumes of binding buffer and then 10 column volumes of washing buffer (20 mM Tris-HCl pH 8.0, 6 M urea, 300 mM NaCl, 20 mM imidazole and 1 mM 2-mercaptoethanol) at 2 ml/min. The bound protein was then renatured on the column by using a gradient of 6 M to 0 M urea over a period of 100 min with a flow rate of 1 ml/min, starting with wash buffer and ending with refolding buffer (20 mM Tris-HCl pH 8.0, 300 mM NaCl, 20 mM imidazole and 1mM 2-mercaptoethanol) using an Akta FPLC (GE Healthcare Biosciences, Uppsala, Sweden). After the gradient was completed, the column was washed with 5 column volumes of refolding buffer and eluted using 10 column volumes of a concentrated imidazole buffer (20 mM Tris-HCl pH 8.0, 300 mM NaCl, 0.5 M Imidazole and 1 mM 2-mercaptoethanol). The dilute tubulin sample was concentrated to ~5 ml using a 30–kDa Amicon centrifuge filter (Millipore) by

centrifuging it at 3,000 rpm, 4°C. The sample was then dialysed as detailed in section 2.5.5.

2.5.9 Partial removal of the MBP tag from the fusion tubulins by an endonuclease

The MBP fusion tubulin proteins were produced using either the pMAL-c2X vector which incorporated a factor Xa (New England Biolabs) endoprotease site (I(E or D)GR) or the pMAL-c2G vector which incorporated a genenase I (New England Biolabs) endoprotease site (PGAAHY). A range of slightly varied conditions were used to improve the cleavage efficiency of these enzymes.

2.5.9.1 Attempted cleavage of the fusion tubulins with factor Xa

Purified tubulin (as described in section 2.5.3 and 2.5.4) was digested with factor Xa using a range of conditions to optimise the cleavage reaction. Approximately 100 µg of tubulin (MBP-αI, MBP-β or a mixture of MBP-αI/β) was digested with 2 units of factor Xa from 0 – 24 h at 4°C and 37°C in the cleavage buffer (50 mM Tris-HCl pH 8.0, 100 mM NaCl, 5 mM $CaCl_2$; filter sterilised).

2.5.9.2 Attempted cleavage of the MBP-fusion-tubulin while attached to an amylose column

Previous attempts to cut the MBP-tag from the MBP fusion proteins using factor Xa proved difficult as there appeared to be non-specific breakdown due to the enzyme cutting at an unknown site somewhere on the tubulin protein (personal communication with Dr. Brian Fennell). To minimise the protein breakdown, factor Xa was added to MBP-β-tubulin while it was still on the amylose column. Briefly, 200 ml of culture producing MBP-β-tubulin was lysed as outlined in section 2.5.3 and was loaded onto a 2–ml amylose column and extensively washed. The buffer covering the amylose resin was removed except for ~1 cm. Sixty µl (120 units) of factor Xa were mixed with 1.8 ml of factor Xa cleavage buffer and slowly added on top of the amylose resin. The solution was allowed to seep into the resin by releasing fluid from the base of the column. The column was stored at 4°C for 20 h. The column was refilled with ~5 ml of amylose column buffer and washed with a further 25 column volumes but only the first 10 ml were collected which should contain the

cleaved samples and factor Xa only. The remaining protein was eluted with 50 ml of 10 mM maltose solution. This fraction should contain uncut protein and MBP and was collected for analysis. The column was regenerated as described in section 2.5.3. The diluted samples were concentrated by centrifugation at 3,000 rpm, 4°C with an Amicon centrifuge filter and were prepared for analysis by SDS-PAGE (section 2.4.2).

2.5.9.3 Attempted cleavage of the MBP-αI-tubulin while attached to an amylose column

An attempt was made to remove the MBP tag from MBP-αI-tubulin using the same method as described in section 2.5.9.2 with a few exceptions. Fifteen µl of genenase I (1 µg/µl) was diluted into ~2 ml of genenase I cleavage buffer and loaded onto the column instead of factor Xa. The experiment was conducted at room temperature for 24 h. Ten fractions of 20 µl were captured in pre-chilled eppendorf tubes and were analysed on a SDS-PAGE as described elsewhere (section 2.4.2).

2.5.9.4 Removal of the MBP tag from the fusion proteins using genenase I

Purified tubulin (as described in section 2.5.3 and 2.5.4) was digested with genenase I using a range of conditions to optimise the cleavage reaction; 10–100 µg of tubulin fusion protein, 0.05 µg – 10 µg genenase I, 0 h – 168 h incubation time, 0.005% - 0.1% (w/v) SDS, 1% - 10% (v/v) 2-mercaptoethanol, 1 mM phenylmethylsulphonyl fluoride (PMSF), 1 mM GTP at 4°C, 22°C or 37°C. A standard reaction was set up using 50 µg fusion tubulin, 1 µg genenase, 0.005% (w/v) SDS, 1% (w/v) 2-mercaptoethanol, 1 mM PMSF in a total volume of 50 µl. The reaction was usually conducted at either 4°C for a maximum of 168 h or 22°C for a maximum of 24 h. Samples were prepared for analysis by SDS-PAGE (section 2.4.2).

2.5.9.5 Removal of the MBP tag from the fusion proteins using enterokinase

Purified tubulin (as described in section 2.5.3 and 2.5.4) was digested with enterokinase (NEB) over a range of conditions; 4°C, 22°C and 37°C for 0–24 h using half, double or recommended protease concentrations in the standard cleavage buffer (20 mM Tris-HCl pH 7.4, 50 mM NaCl, 2 mM $CaCl._2$). Samples were prepared for analysis by SDS-PAGE (section 2.4.2).

2.6 FUNCTIONAL ANALYSIS OF RECOMBINANT TUBULINS

2.6.1 Assessment of dimerisation of the recombinant tubulins

The recombinant tubulins monomers were mixed together in equal molarity to promote dimerisation. Tubulin monomers and MBP were used as negative controls. Bovine brain tubulin was used a positive control. All samples had GTP added (1 mM final concentration) and were incubated on ice for 30 min before use.

2.6.2 Glutaraldehyde crosslinking of the tubulin fusions

A 1% solution of glutaraldehyde was prepared to determine if the recombinant αI- and β-tubulins could dimerise. Bovine brain tubulin (Cytoskeleton Inc., Denver, CO, USA) was used a positive control while MBP served as negative control. The samples were prepared for dimerisation as described in section 2.6.1 with the exception that some samples had 2-mercaptoethanol (1% (v/v) final concentration) added during the dimerisation step to prevent non-specific cross-linking through cysteine residues. A 25–µl reaction solution was set up using 1 µl of the protein sample (5 µg/µl), 4 µl GTP (6 mM), 2.5 µl glutaraldehyde (1% (v/v)) and 17.5 µl GPEM buffer (5% (v/v) glycerol, 80 mM Piperazine-1,4-bis(2-ethanesulfonic acid) pH 7.4, 1 mM EGTA and 1 mM $MgCl_2$). The reactions progressed for 0–2 h with samples being terminated at different time intervals by addition of 2.5 µl Tris-HCl (1 M, pH 7.4) and subsequently boiled for 10 min. Samples that were taken at 0 h had Tris-HCl added before the glutaraldehyde to prevent any non-specific reactions. The samples were analysed by 5% or 7.5% polyacrylamide SDS-PAGE as outlined in section 2.4.2.

2.6.3 SEDIMENTATION ASSAYS FOR TUBULIN POLYMERISATION

2.6.3.1 Tubulin sedimentation assay for purified recombinant protein

Recombinant tubulin were assessed for their ability to polymerise and sediment under particular conditions when centrifuged (see Fig. 3.17). Briefly, samples were prepared for dimerisation as described in section 2.6.1. A 50–µl sample

made up with GPEM buffer was prepared with either recombinant tubulin or bovine brain tubulin (10 μM final protein concentration) and GTP (2.5 mM final concentration). Two-point five μl of Taxol (9 mM) dissolved in DMSO were added to each of the samples before centrifugation at 18,000 rpm (38,828 x g), 4°C for 1 h using a pre-cooled SS-34 rotor with Sorvall 408 adapter cones. The supernatant was transferred to a new eppendorf tube which was incubated at 37°C for 1 h. The pellet was washed with 100 μl cold GPEM buffer and centrifuged at 18,000 rpm (38,828 x g) for 10 min to remove residual soluble protein. The pellet was resuspended in the same volume from which it was sedimented using GPEM buffer and an equal volume of 2X SDS sample loading buffer was added (see section 2.4.5). The supernatant was centrifuged at 18,000 rpm (38,828 x g), 37°C for 1 h using a SS-34 rotor. The supernatant was removed and an equal volume of 2X loading buffer was added (see section 2.4.5). The pellet was washed with 500 μl warm GPEM buffer as described above. The pellet was resuspended in the same volume from which it was sedimented using GPEM buffer and an equal volume of 2X SDS sample loading buffer was added (see section 2.4.5). All of the samples were boiled at ~100°C for 10 min after the addition of the reducing buffer.

2.6.3.2 Sedimentation assay for tubulin refolded with rabbit reticulocyte lysate

One ml of the refolded tubulin (as described in section 2.5.8.1) was added to one ml of GPEM buffer. The solution was concentrated to ~500 μl by centrifugation at 3,000 rpm using an Amicon centrifugal filter (30-kDa molecular weight cut–off). The sample was spun at 400,000 x g, for 15 min at 4°C in a Beckman ultracentrifuge using a TL 100 rotor to remove aggregated protein. The supernatant was incubated at 37°C for 60 min in the presence of taxol (20 μM final concentration). The pellet was resuspended 30 μl PBS. The supernatant was centrifuged at 37°C for 15 min at 20,000 x g using a pre-warmed SS-34 rotor. The pellet was washed in warm GPEM buffer to prevent any residual soluble protein clinging to sides of the eppendorf tube. A second centrifugation was conducted using the same conditions as described. The supernatant was discarded and the pellet was resuspended in cold polymerisation buffer with vinblastine (final concentration 100 μM) for one hour while on ice. The sample was then centrifuged at 4°C for 15 min at 20,000 x g using a SS-34 rotor. The supernatant was removed and the pellet was washed using cold GPEM buffer. The

pellet was centrifuged as before to remove any residual protein. Samples taken during the procedure were mixed with 2X loading buffer and boiled for 10 min.

2.7 ANALYSIS OF THE ELECTROPHORETIC BEHAVIOUR OF TUBULINS IN *P. FALCIPARUM*

Bryan and Wilson originally labelled the two tubulin subunits, α and β, based on their mobility through a urea-polyacrylamide gel, with the slower migrating protein being designated α (Bryan and Wilson, 1971). However, it has been observed in many species that the migration of the tubulin subunits flip, a phenomenon called "α/β inversion".

2.7.1 Investigation of the "α/β inversion" of *Plasmodium falciparum* tubulins

Full length wild type and altered tubulins were generated as described in section 2.5.2. Equal amounts of whole cell extract were loaded onto a SDS-polyacrylamide gel and electrophoresis was conducted as described in section 2.4.2.

2.7.2 Comparisons of tubulin sequences by alignment studies

Multiple amino acid sequence alignments, from a broad range of eukaryotic organisms, were conducted for α- and β-tubulin using an online program, T-coffee (http://www.ebi.ac.uk/Tools/t-coffee/). Sequences were only used if the α- and β-tubulins had been clearly identified by an appropriate technique (e.g. western blotting). The amino acid sequences were obtained from the PubMed database (www.ncbi.nlm.nih.gov/sites/entrez) and their accession numbers are shown in Table 2.3. The alignments were colour coordinated to represent the types of amino acids.

2.8 INVESTIGATION OF THE PHOSPHOROTHIOAMIDATE BINDING SITE ON *P. FALCIPARUM* TUBULINS

The binding site of phosphorothioamidates to tubulin has to date not been elucidated. However, several putative sites have been suggested to exist on the tubulins of other organisms which may or may not be relevant to the *Plasmodium* species.

2.8.1 Molecular modelling of *P. falciparum* tubulins

The crystal structure of bovine brain tubulin (1TUB) served as a template for the generation of a homology model for the *Plasmodium* tubulins. An older and less well defined model of bovine brain tubulin, 1TUB, was chosen over a newer model, 1JFF because it was more complete (e.g. the N-loop amino acids, 35-60, are present on the α-tubulin). The homology modelling program, Molecular Operating Environment (MOE 2008.10 release of Chemical Computing Group Inc., Quebec, Canada) was used to generate a 3-D structure of the *Plasmodium* αI- and β-tubulin. The default settings were used.

2.8.1.1 Generation of molecular models for the dinitroanilines and phosphorothioamidates

2-D structures of all the compounds used were drawn in Chemsketch (ACDLabs, http://www.acdlabs.com/download/chemsketch). These structures were imported to MOE, where they were the partial charges were assigned by Gasteiger forcefield and energy minimised using the MMFF94x forcefield. The solvation model used was the reaction field with a dielectric constant of 1 for the interior and 80 for the exterior. A stochastic conformational search was conducted whereby all rotatable bonds were reordered to generate the lowest energy conformation for the molecules.

2.8.1.2 Alignment of the dinitroaniline and phosphorothioamidate molecular models

The energy minimised models generated in MOE were superimposed on each other using a "flexible alignment" function in MOE. The models randomly rotated to achieve the best fit that satisfied a number of criteria; H-bond donor, H-bond acceptor, aromaticity, polar hydrogens, LogP(octanol/water), molar refractivity, partial charge, volume and exposure. The most similar alignments were used for analysis. The other alignments were also examined, however, the differences between similar alignments were minor and did not affect the analysis.

Organism	Tubulin Subunit	Gene Name	Accession Number
Plasmodium falciparum	αI	PFI0180w	XM_001351875
	αII	PFD1050w	XM_001351490
	β	PF10_0084	XM_001347333
Bos taurus	α	Tub4a	NM_001078158
	β	β-2A	BC105401
Homo Sapiens	α	TUBA1A	NM_006009
	β	TUBB2B	NM_178012
Drosophila melanogaster	α	α-1	M14643
	β	β-1	M20419
Ovis aries	α	TUBA4A	FJ958352
	β	N/A	N/A
Strongylocentrotus droebachiensis	α	TUBA1	AF465681
	β	N/A	N/A
Sus scrofa	α	α-1	DQ225365
	β	β-1	NM_001113696
Chlamydomonas reinhardtii	α	α-1	M11447
	β	β-2	M25919
Daucus carota	α	TBA	AY007250
	β	β-2	U63927
Oryza sativa	α	α-1	Z11931
	β	β	L33263
Zea mays	α	α-1	U05258
	β	β-1	X52878
Tetrahymena thermophila	α	ATU1	M86723
	β	BTU1	L01415
Naegleria gruberi	α	α-1	X12561
	β	β	X81050
Trypanosoma brucei rhodesiense	α	α-1	XM_001218933
	β	β	K02836
Toxoplasma gondii	α	α	M20024
	β	β	TGGT1_065490

Table 2.3 Tubulin sequences used in alignment studies. All sequences can be found using PubMed/Nucleotide except *T. gondii* β-tubulin which is hosted on ToxoDB.

2.8.2 Tubulin sequence alignments

Amino acid sequences were aligned using an online program, ClustalW 2 (http://www.ebi.ac.uk/Tools/emboss/align). The sequences were obtained from the PubMed database (www.ncbi.nlm.nih.gov/sites/entrez).

2.8.3 Development of tubulin ligand binding assays

To generate ligand binding data for the recombinant tubulins, two assays were developed. Bovine brain tubulin (cytoskeleton) was used as a positive control to assess the validity of these assays. All compounds used in these experiments were previously dissolved in DMSO to a concentration of 10 mM or 20 mM.

2.8.3.1 Sulphydryl based tubulin-ligand binding assay

A sulphydryl assay, adapted from Roychowdhury *et al.* (2000), was developed to investigate tubulin ligand interactions. The tubulin proteins were prepared for dimerisation as described in section 2.6.1. One – six μM (final concentration) of tubulin or MBP was dissolved in MME buffer. Three-point eight μl of a tubulin ligand (e.g. taxol) with a final concentration ranging from 0–200 μM were added to the sample and incubated at 37°C for 30 min. The sample was transferred to a quartz cuvette in a temperature controlled Shimadzu UV-1601 PC spectrophotometer (Shimadzu Scientific Instruments Inc., Maryland, U.S.A) which was set at 37°C. The reaction was started by the addition of 9.5 μl of 4 mM 5,5'-dithiobis(2-nitrobenzoate) (DTNB) (final reaction volume 380 μl). The sample was read every second for 1 h at 412 nm.

2.8.3.2 Fluorescence quenching–based tubulin-ligand assay

A fluorescence quenching–based assay was adapted from Gupta *et al.* (2002) to determine the binding equilibrium of tubulin ligands. Tubulin samples, MBP or tryptophan were prepared as described in section 2.6.1. The final concentration for the tryptophan samples was either 2.4 μM or 3.6 μM. The final concentration for the tubulin and MBP samples was either 0.15 μM or 0.3 μM. Five μl of a tubulin ligand (with a concentration from 0 – 20 mM) was added to the sample (final volume 500 μl) and the mixture was incubated at 37°C for either 5 or 30 min. The sample was

transferred to a thoroughly cleaned luminescence cuvette (Perkin Elmer) and was read using a spectrofluorimeter (PerkinElmer LS-50B, Waltham, MA, USA). The excitation and emission wavelengths were 280 nm and 300–400 nm respectively and both had a 4-nm slit size. The absorbance of the sample was measured using a spectrophotometer (Shimadzu Scientific Instruments Inc.). The sample was scanned every 0.5 nm from 280 nm – 400 nm. The non-specific quenching of the tryptophans due to different ligand concentrations were corrected by using control samples (MBP and N-acetyl-tryptophanamide) and determining the inner filter effects according to the Lakowicz equation, $F_{corr} = F_{obs}\text{antilog}[(A_{ex} + A_{em})/2]$ (where F_{corr} is corrected fluorescence, F_{obs} is observed fluorescence, A_{ex} is absorbance at the excitation wavelength and A_{em} is absorbance at the emission wavelength) (Lakowicz, 1999). The dissociation constant (K_d) was determined using the following equation; $F_{max}/(F_0-F) = 1+K_d/L_f$ (Acharya *et al.*, 2008). L_f represents the free ligand equilibrium concentration in the reaction mixture and was determined by $L_f = C - X\ [Y]$. C represents the total concentration of ligand in the sample and Y is the molar concentration of ligand-binding sites. One high affinity binding site was assumed for all the calculations. The fraction of binding sites (X) occupied by a ligand were determined using the equation $X = (F_o-F)/F_{max}$, where F_o is the corrected fluorescence intensity of tubulin in the absence of a ligand, F is the tubulin fluoresence in the presence of a ligand and F_{max} was calculated by plotting $1/(F_o-F)$ vs. 1/[ligand] and extrapolating 1/[ligand] to zero.

2.9 ADDITIONAL ANALYSES OF THE SYNTHETIC PHOSPHOROTHIOAMIDATE AND RELATED COMPOUNDS

Sixty-eight mostly novel compounds related to amiprophosmethyl (APM) were generated by Mrs. Christine Mara in the Dept. of Medicinal Chemistry, Royal College of Surgeons in Ireland (RCSI). All of these compounds were initially dissolved in DMSO (10 mM – 20 mM) as they displayed only partial aqueous solubility. Measurement of the inhibition of the parasite growth by these compounds is described in section 2.2.2.

2.9.1 Solubility determination of the synthetic compounds

A spectrophotometric assay was developed to determine if a compound was still in solution by recording the turbidity of the sample using an infrared spectrum (700 nm – 900 nm). None of compounds could absorb strongly this at wavelength. Therefore, only insoluble compounds physically reflected the light by forming a cloudy suspension in the solution. A standard assay was prepared by using an eppendorf tube with 5 µl of a compound (0 – 20 mM) and 495 µl of MME buffer. This solution was incubated at 37°C for 5 min and transferred to either a quartz or luminescence cuvette. The sample was scanned every 1 nm over a range of 700 – 900 nm.

2.9.2 Predicted hydrophilicity (clogP) of the compounds

The cLogP is an estimate of the likely octanol/water partition co-efficient and was predicted using the formula, Log $P_{oct/wat}$ = Log($[Solute]_{octanol}$/$[Solute]_{deionised\ water}$). Chemsketch (ACDLabs, http://www.acdlabs.com/download/chemsketch) was used to draw the structures and to generate the cLogP values.

Chapter 3

Improved Recombinant Expression, Purification and Functional Analysis of *P. falciparum* Tubulins and Development of a Ligand-Tubulin Binding Assay

3.1 INTRODUCTION

Plasmodium tubulin represents a possible novel target for the development of antimalarial compounds. To date the majority of work with microtubule inhibitors was done using cultured parasites, in particular, determining their minimum concentrations needed to inhibit the parasite growth by 50% (IC_{50}) and also examining the effects of these ligands on the architecture of the microtubule containing structures (Bell A., 1998, Dieckmann-Schuppert *et al.,* 1990, Fennell *et al.,* 2003, and Fennell *et al.,* 2006). Only a limited amount of information exists for *Plasmodium* tubulin with respect to *in vitro* biochemical studies, a situation in stark contrast to that for mammalian organisms. The main reason for this discrepancy is the ease with which tubulin can be purified from mammalian cells in comparison with *Plasmodium* parasites. The procedure for purifying tubulin from microtubule-rich sources, such as bovine brain, was first achieved over four decades ago by Weisenberg *et al.*, 1968 (Weisenberg *et al.,* 1968). This was accomplished by the unique ability of tubulin to be sedimented when differentially centrifuged at 40,000 x g depending upon the conditions used (Kumar 1981). At 4°C and in the presence of Ca^{2+} ions *in vitro*, tubulin exists primarily as soluble dimers that remain in the supernatant after centrifugation. Conversely, it can rapidly assembly into polymers at 37°C in the presence of GTP and Mg^{2+} ions, in which case it can be readily sedimented. Repeating this cycle of assembly and disassembly permits the isolation of tubulin. This technique has also been successfully employed using several species of the protozoan parasite, *Leishmania,* such as *L. mexicana amazonesis*, *L. donovani* and *L. tarentolae* (Werbovetz *et al.,* 2003, Werbovetz *et al.,* 1999 and Yakovich *et al.,* 2006). In these parasites, tubulin can represent >10% of the total cellular protein content (Bell A., 1998). However, in the case of tubulin-poor organisms such as *P. falciparum*, this cycling method is not conducive to tubulin isolation due to the prerequisite of a "critical concentration" for tubulin polymerisation. Furthermore, over-expression of tubulin genes in the parasites is unlikely to be successful due to the fact that this protein is highly regulated and would probably be toxic to the organism if its concentration were not controlled.

Expression of recombinant tubulin offers the potential to generate large quantities of the protein but also permits the option of including an affinity tag (e.g. His-tag or MBP-tag) to assist the isolation procedure. Furthermore, recombinant

tubulin can be readily altered genetically, which can be exceedingly difficult using native tubulin. Since eukaryotic organisms use a specific chaperone system (i.e. CCT) to correctly fold tubulin, they would logically be the first choice for a surrogate organism for generating functional tubulin (Lewis *et al.*, 1997). However, the presence of endogenous tubulin could inextricably contaminate the recombinant protein. Furthermore, over-expression of tubulin in *Saccharomyces cerevisiae* was not successful as it was lethal or was not accumulated in the cell (Burke *et al.*, 1989).

Therefore, bacterial cells have been used to generate recombinant tubulin. *Bacillus brevis* was employed before to secrete recombinant *P. falciparum* β-tubulin but it was unfortunately impossible to purify the recombinant protein (Bell *et al.*, 1995). Commonly, tubulin is expressed in the cytosol of *E. coli* but a common issue with over-expressing foreign eukaryotic genes in a bacterium is mis-folding of the protein and the subsequent generation of insoluble aggregates called inclusion bodies. These inclusion bodies are composed almost solely of non-functional tubulin. Previously, some groups have been able to successfully denature these inclusion bodies (typically with urea) and refold them using either a biological approach, i.e. employing the eukaryotic chaperones in rabbit reticulocytes to specifically renature the protein (Yaffe *et al.*, 1988 and Shah *et al.*, 2001) or a chemical approach, i.e. removing the denaturant so that spontaneous refolding of the protein can occur (Koo *et al.*, 2009, Lubega *et al.*, 1993, Wampande *et al.*, 2007 and Oxberry *et al.*, 2000). It has been possible to generate soluble tubulin which retains at least partial functionality by attaching a MBP-affinity tag (Fennell *et al.*, 2006, Giles *et al.*, 2008 and Holloman *et al.*, 1998). The exact mechanism by which MBP is able to enhance the solubility of its partner protein is unclear. However, it has been suggested that it may act as a general molecular chaperone which prevents an aggregation-prone fusion protein from self-associating (Fox *et al.*, 2002). Alternatively, the translation of a hydrophilic partner at the N-terminus may dictate the solubility of the entire fusion protein (MacDonald *et al.*, 2003). *E. coli* does not possess the tubulin folding chaperone system, CCT, but a homologous system, GroEL, can act as a substitute producing a reduced amount of assembly-competent tubulin (Phadtare *et al.*, 1994). Furthermore, MBP-fusion tubulins appear to be at least partially folded correctly as they were able to co-polymerise with bovine brain tubulin and bind known tubulin inhibitors specifically (Fennell *et al.*, 2006, MacDonald *et al.*, 2004 and Holloman *et al.*, 1998). In order to build upon the previous work of Fennell *et al.*, (2006), several

experiments were employed here to better characterise the functionality of the recombinant fusion tubulins. Furthermore, the work of Fennell *et al.,* (2006) on ligand tubulin binding was limited to determining whether or not the dinitroaniline, trifluralin could bind to the protein or not. Considering that a number of reliable and well established tubulin-ligand-binding assays exist, it seemed prudent to advance this early work to cover a larger number of potential tubulin binding compounds. The dinitroanilines and phosphorothioamidates are particularly interesting as they have demonstrated a preferential affinity for parasite tubulin over mammalian tubulin (Fennell *et al.,* 2006, Werbovetz *et al.,* 2003, Bell. A., 1998, Dow *et al.,* 2002, Morrisette *et al.,* 2004, Wu *et al.,* 2006 and George *et al.,* 2007). Therefore, the main aims of the work described in this chapter were to generate, if possible, assembly-competent recombinant tubulin in *E. coli* and to develop a reliable tubulin-ligand-binding assay for the examination of herbicides, their derivatives and other compounds.

3.2. RESULTS

3.2.1 RECOMBINANT PRODUCTION OF *P. FALCIPARUM* αI-TUBULIN, αII-TUBULIN AND β-TUBULIN

3.2.1.1 Expression and attempted MBP tag removal from the tubulin fusions using factor Xa

N-terminal MBP-tagged αI- and β-tubulin were previously generated by over-expressing the recombinant proteins in *E. coli* TB1, a strain that lacks endogenous MBP. These proteins were soluble although they were not demonstrated to co-assemble with each other (Fennell *et al.,* 2006). It was considered possible that the MBP could sterically hinder the tubulins from dimerising and/or subsequently polymerising, so an attempt was made to remove this tag.

The generation of the pMAL-c2X-αI- or –β-tubulin construct had a specific recognition site for factor Xa present between the MBP tag and the tubulin (see Fig. 3.1 A). Therefore, this would allow the separation of the tag from the tubulin after the purification step, generating native-like tubulin. An initial effort to remove the MBP tag from the fusion proteins was previously unsuccessful due to the generation of

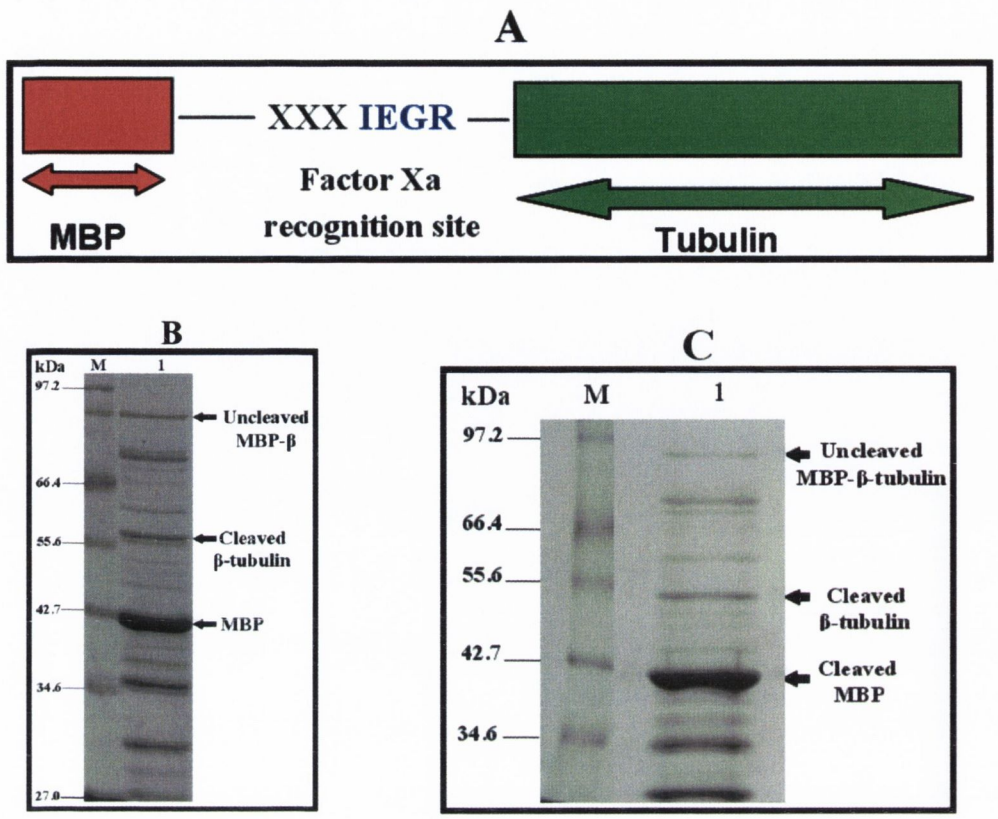

Fig. 3.1. Schematic representation of the factor Xa cleavage site on the pMAL-c2X construct (Panel A) and the resolution of an elution fraction from the in-column cleavage of MBP-β-tubulin with factor Xa while still attached to an amylose column, analysed by Coomassie Blue-stained SDS 10%-PAGE (Panels B and C). **A.** This diagram represents the factor Xa recognition site on the MBP-tubulin fusions (**IEGR**). **B. M**, molecular weight marker (Roche). MBP-β-tubulin was chosen for in-column cleavage with factor Xa to determine the effectiveness of this method. The fusion protein was over-expressed in *E. coli* TB1 cells. These cells were lysed and loaded directly onto the amylose column. The column was thoroughly washed with column buffer and factor Xa was added (as described in section 2.5.9.2). The column was left at 4°C for 24 h, after which the cleaved proteins were washed off with column buffer (Lane **1.**). Uncleaved proteins were later eluted with maltose (data not shown). **C.** To improve the purity of the wash fraction (**B.** Lane **1**), the sample was re-run over a clean amylose column and cleared proteins washed off in the same way (**C.** Lane **1**).

numerous bands of <50 kDa (Fennell *et al.*, 2006). This was despite the fact that there appeared to be only one cleavage site for factor Xa on the tubulin fusions. Therefore, it was possible that this tubulin degradation was caused by a non-specific protease which co-purified with the MBP-fusion tubulins. In order to circumvent this problem and reduce the concentration of contaminating proteins in the final yield of MBP-free tubulin, factor Xa was incubated with MBP-β-tubulin immobilised on an amylose column (as outlined in section 2.5.9.2). Therefore, applying wash buffer to the column should only remove the cleaved tubulin protein and factor Xa. The uncut MBP-tubulin and MBP should remain immobilised on the column.

The experiment was conducted at 4°C for 24 h to minimise breakdown caused by the possible presence of non-specific proteases. Although the recognition site for factor Xa is present on both fusion tubulins, MBP-β-tubulin was used for a trial to determine if this method could be used to generate pure tag-free tubulin. The wash fraction contained numerous proteins of varying sizes which were not identified but were likely non-specifically digested tubulin, especially since these bands did not appear in control samples that were stored under the same conditions (data not shown). Bands corresponding to the predicted size of cleaved MBP and β-tubulin were observed (Fig. 3.1 B), indicating that factor Xa probably did cut the fusion tubulins at the specific recognition site highlighted in Fig. 3.1 A. In an attempt to remove some of the contaminating proteins, including MBP and MBP-β-tubulin, this wash fraction was reloaded onto a new amylose column. However, this did not change the sample purity as the contaminating proteins also eluted with the β-tubulin (Fig. 3.1 C). Therefore, it appears that MBP had lost its affinity for the amylose molecule, possibly due to the presence of trace amounts of maltose in the sample or a conformational change in the protein. Ion-exchange chromatography was also used in an attempt to further isolate the cleaved β-tubulin. This was also unsuccessful due to the inability to significantly improve the sample purity (data not shown).

3.2.1.2 Production of αI-tubulin and β-tubulin using pMAL-c2G

It was concluded that factor Xa could not be used to remove the MBP tag from the tubulin fusion proteins as this endoprotease appeared to digest these proteins at more than one site. Nonetheless, it was still perceived that specifically removing the MBP tag from the tubulin fusions was an achievable goal. Therefore, two other

commercially available pMAL vectors which have either enterokinase or genenase I recognition sites present instead of the factor Xa site were investigated. To ensure that these enzymes did not digest the fusion tubulins non-specifically, an initial cleavage experiment was designed.

The MBP-tubulin fusions were produced and isolated using the pMAL-c2X construct (outlined in sections 2.5.1 and 2.5.3). These fusion tubulin proteins were incubated with either enterokinase or genenase I using the recommended conditions as stated by the manufacturer in order to determine if these endo-proteases would non-specifically digest the proteins (outlined in sections 2.5.9.4 and 2.5.9.5).
The tubulin fusion proteins were stable at room temperature (R.T.) for at least 24 h (Fig. 3.2 A). Genenase I did not cleave the tubulin fusions as expected (Fig. 3.2 B). Conversely, enterokinase degraded the fusion tubulins non-specifically at 22°C (Fig. 3.2 C) and at the recommended temperature of 37°C (data not shown for the 37°C incubation). Based on these results, new constructs (pMAL-c2G-αI-tubulin and pMAL-c2G-β-tubulin) were generated which were identical to the original pMAL-c2X constructs except that there was a genenase I recognition site present in the place of the factor Xa site.

The pMAL-c2X constructs containing the tubulin genes were used as templates for the PCR reaction. Both tubulin genes were cloned into the pMAL-c2G vector using the restriction site for *Snab*I so that upon cleavage of the tubulin fusion proteins by genenase I, there would be no additional amino acids (Fig. 3.3).

The tubulin genes were produced by using "hot-start" PCR conditions to minimise amplification errors (described in section 2.3.3) and were subsequently inserted into the pMAL-c2G vector separately after being digested with appropriate restriction enzymes. The clones were first transformed into the competent non-expression *E. coli* strain, XL-1 blue. The pMAL-c2G vector encodes an ampicillin resistance marker for isolation of putative transformants. Insertion of the tubulin gene into the vector was detected by slower migration of the plasmids than the vector alone on an agarose gel, and by PCR (Fig. 3.4). The genes were also sequenced to validate the presence of the clones and to ensure that there were no errors (data not shown).

Tubulin fusion expression was controlled by a P*tac* promoter which was induced by IPTG. The *E. coli* expression strain TB1 was capable of over-expressing the tubulin fusions, producing up to ~50 mg of recombinant protein per l of culture. The apparent molecular weights of MBP-αI-tubulin and MBP-β-tubulin as determined

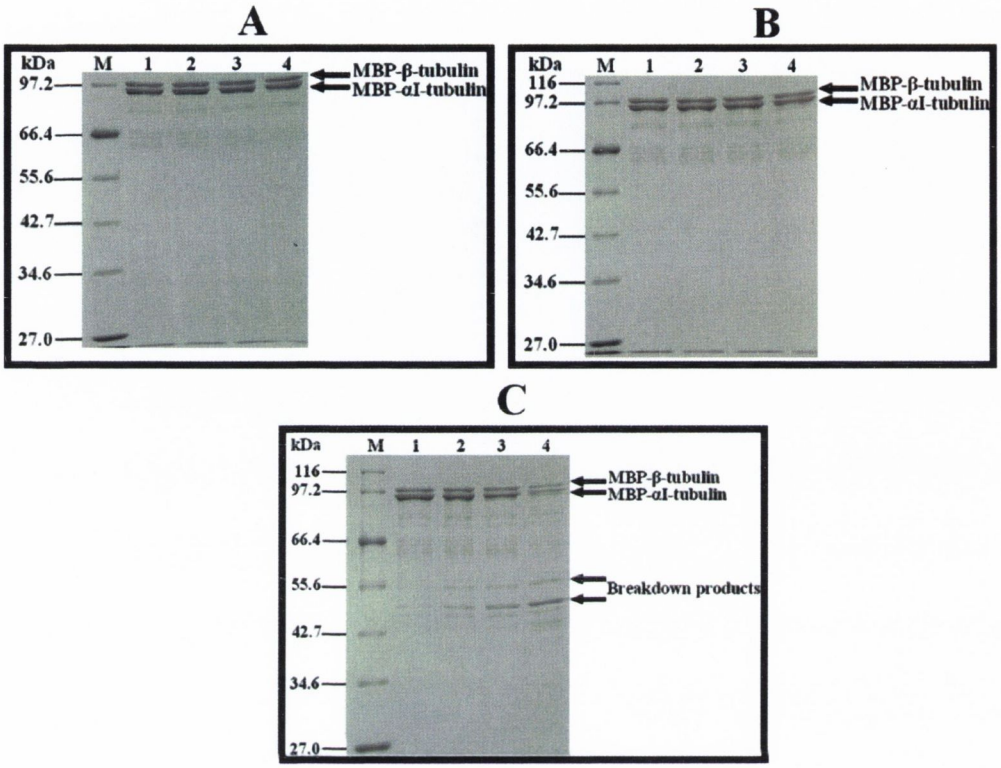

Fig. 3.2. Resolution of MBP-αI- and -β-tubulin in the absence (A) or presence of either genenase I (B) or enterokinase (C) proteases by SDS 10%–PAGE. Samples shown in lanes 1-4 were incubated at 22°C with the recommended concentrations of protease (when present). **M.** Molecular weight marker (Roche). Lane **1)** 0 h, **2)** 3 h, **3)** 6 h and **4)** 24 h. The amylose-purified fusion proteins were stable at 22°C for at least 24 h in the presence or absence of genenase I. However, enterokinase non-specifically degraded the fusion proteins indicating the presence of cryptic cleavage sites.

Fig. 3.3 Schematics of the tubulin fusion protein with genenase I recognition site. Genenase I cleaves between the tyrosine at the end of its cleavage site (**blue residues**) and the methionine (**green residue**) at the beginning of the tubulin leaving no extra residues.

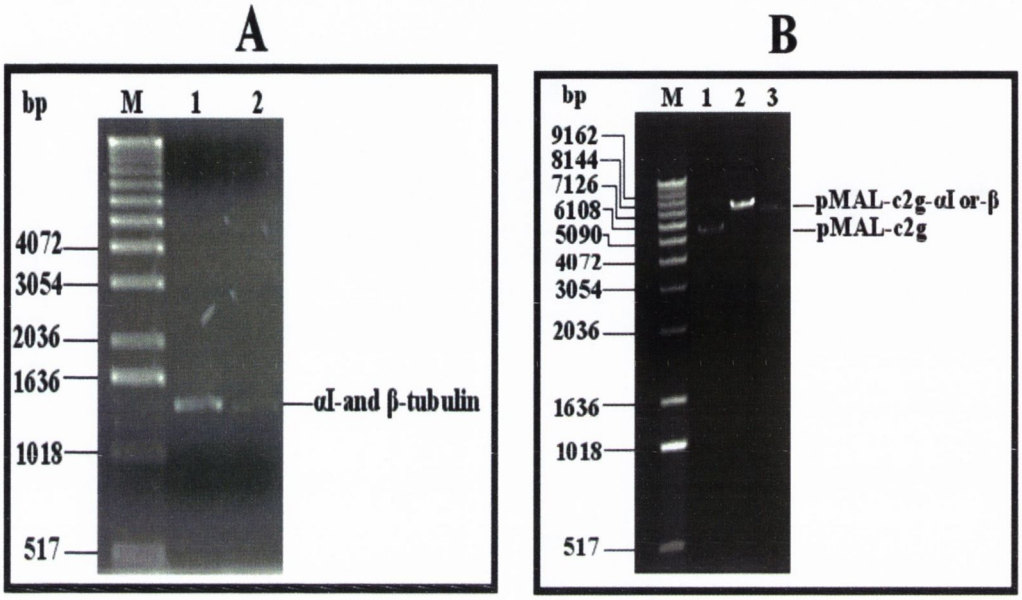

Fig. 3.4. Visualisation of the PCR amplification of the αI- and β-tubulin genes and analysis of the pMAL-c2G-αI clone on a 1% (w/v) agarose gel. M. DNA marker X (Roche) in gels **A** and **B. A:** Lane **1)** PCR amplification of αI-tubulin and **2)** PCR amplification of β-tubulin. The tubulin genes were amplified by PCR in preparation for insertion into the pMAL-c2G plasmid. The αI-tubulin gene is slightly heavier than the β-tubulin gene (1.36 kb and 1.34 kb respectively) and migrated slightly slower through the gel. **B:** Lane **1)** pMAL-c2G linearised with *Snab*I, **2)** pMAL-c2G-αI-tubulin linearised with *Snab*I **3)** pMAL-c2G-β-tubulin linearised with *Snab*I. The size of the linearised plasmids were as expected (pMAL-c2G vector = ~6.64 kb, pMAL-c2G-αI-tubulin = ~8 kb and pMAL-c2G-β-tubulin = ~7.98 kb).

by SDS 10%-PAGE were 95.5 kDa and 99.5 kDa respectively, although the predicted size is smaller for both proteins (92.9 kDa for MBP-αI-tubulin and 92.36 kDa for MBP-β-tubulin) (Fig. 3.5). The apparent molecular weights for αI-tubulin and β-tubulin (~53 kDa and 57 kDa respectively: Fennell *et al.*, 2008) have also been shown to be different from their predicted molecular weight (~50.3 kDa and 49.8 kDa respectively) but this will be discussed in more detail in chapter 5. The tubulin fusion proteins were purified to near homogeneity with one purification step on the amylose column. Ion exchange chromatography was conducted but since it did not significantly increase the purity of the protein samples and decreased overall yields, it was not used routinely (data not shown).

To confirm that factor Xa was responsible for the non-specific degradation of the tubulins, it was incubated with the tubulin fusion proteins produced using the pMAL-c2G plasmid (which did not include a known recognition site for this protease). Both MBP-αI- and MBP-β-tubulin were set up for the cleavage experiment using the optimal digestion conditions for factor Xa as recommended by the manufacturer (outlined in section 2.5.9.1). It was clear from the gel that factor Xa digested the tubulin and that non-specific proteases were not the reason for the tubulin breakdown observed before (Fig. 3.6).

Removal of the MBP tag from the fusion tubulins by genenase I was attempted using a number of different approaches. Cleavage of the MBP tag from the MBP-αI-tubulin by genenase I was attempted using the recommended conditions: ~6 h incubation time at 22°C with 1 μg of enzyme for every 100 μg of protein (data not shown). However, the cleavage reaction was inefficient so double the recommended enzyme concentration (ratio of 1 μg genenase I : 50 μg tubulin fusion protein) and a longer incubation time (24 h) was used. The samples were incubated at R.T. and examined using denaturing polyacrylamide gels (Fig. 3.7). From the gels it became clear that some free tubulin was produced although the reaction was inefficient. Also, more MBP seemed to be produced than free tubulin. It was possible that the extended incubation time caused some of the tubulin which was freed from the MBP tag to be degraded by non-specific proteases.

Since the cleavage reaction was inefficient, the experiment was set up on an amylose column to maximise the amount of cleaved protein (described in section 2.5.9.3). Briefly, lysed *E. coli* cells, which had over-expressed the MBP-α-tubulin fusion protein, were loaded onto a 2 ml amylose column. This column was

thoroughly washed with column buffer to remove any unbound protein. The amylose column was almost completely drained of solution. Two ml of genenase I, diluted into its cleavage buffer, were added to the column and allowed to soak in. The column was incubated for 24 h at 22°C. Four fractions of 500 µl of unbound protein were collected when the column was washed. Analysis by SDS 10%-PAGE determined that some of the tubulin was excised by the enzyme, although the amounts were low (Fig. 3.8 A). Also, there appears to be a disproportionate amount of MBP compared to cleaved αI-tubulin. This may be explained by some of the tubulin degrading non-specifically. This was later confirmed by use of a western blot which highlighted two presumed breakdown products (Fig. 3.8 B). The presence of MBP-αI-tubulin and cleaved αI-tubulin was expected but other unidentified breakdown products appear which are not immediately obvious from looking at the Coomassie stained gel only (Fig. 3.8 A).

This poor cleavage efficiency may be related to partial occlusion of the enzyme recognition site (Holloman *et al.,* 1998). Therefore, a range of low SDS concentrations (0.0005% - 1%) were added to the cleavage solutions to determine if the efficiency could be improved by partially denaturing the protein complex. A low concentration of SDS (0.005%) produced the optimal cleavage conditions. Higher amounts decreased enzyme efficiency, possibly by denaturing the enzyme, and lower amounts were ineffective. The optimum cleavage conditions were different for the two fusion tubulins. Generation of cleaved αI-tubulin reached a maximum when a ratio of 1:50 enzyme to tubulin was incubated at 22°C for 4 h. In contrast, MBP-β-tubulin required a much longer incubation period, ~96 h at 4°C with a ratio of 1:5 enzyme to tubulin (Fig. 3.9). However, a plateau of MBP-tubulin cleavage occurred after which no more free tubulin could be generated. This was not related to the enzyme being inhibited as addition of more enzyme did not improve the situation. Aggregation of tubulin due to the formation of cystine bridges did not appear to be an important factor either as varying the concentration of 2-mercaptoethanol proved ineffective. Therefore, only a limited percentage of the tubulin sample could be cleaved using this enzyme.

Overall, it was not possible efficiently to remove the MBP tag even with SDS and subsequent attempts to further isolate the low amounts of cleaved tubulins by ion-exchange chromatography were not successful, mainly due to poor improvement in purity and a significant loss of protein yield. Since the MBP tag could not be

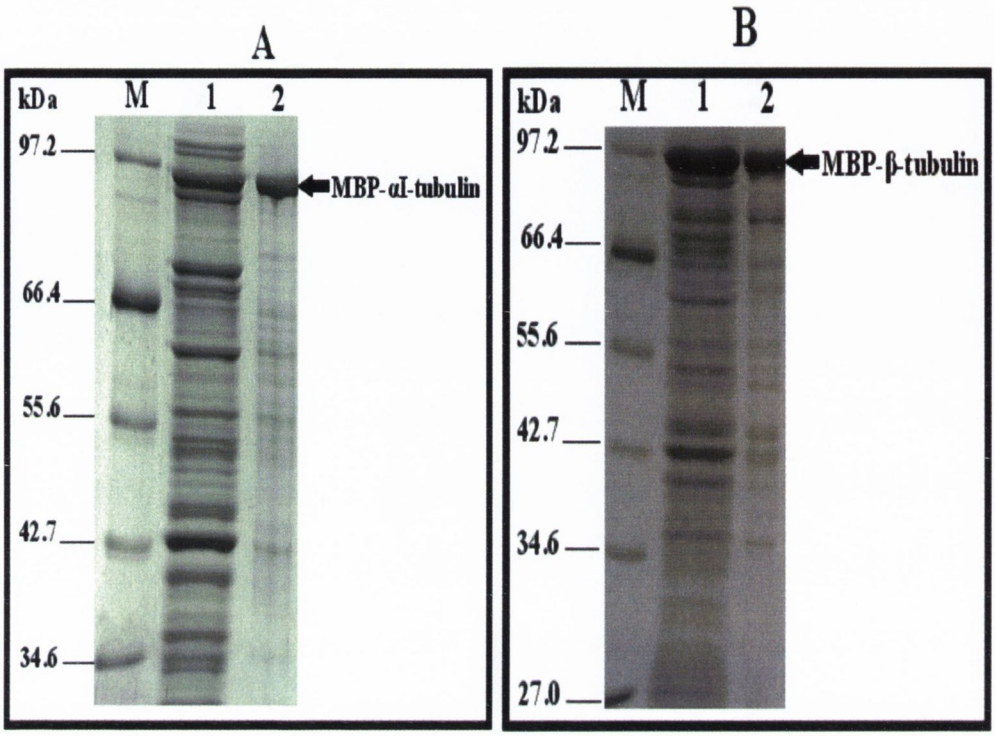

Fig. 3.5. Resolution of the expression and amylose purification of the tubulin fusion proteins MBP-αI- (A) and MBP-β-tubulin (B) using the pMAL-c2G vector by SDS 10%-PAGE. M. Molecular weight marker (Roche). Lane **1)** Extract of *E. coli* expressing the tubulin fusion protein, **2**) MBP-tubulin fusion protein after amylose-affinity purification. ~ 3 μg of purified MBP-αI- and MBP-β-tubulin were resolved on lane 2 of both gel **A** and **B**.

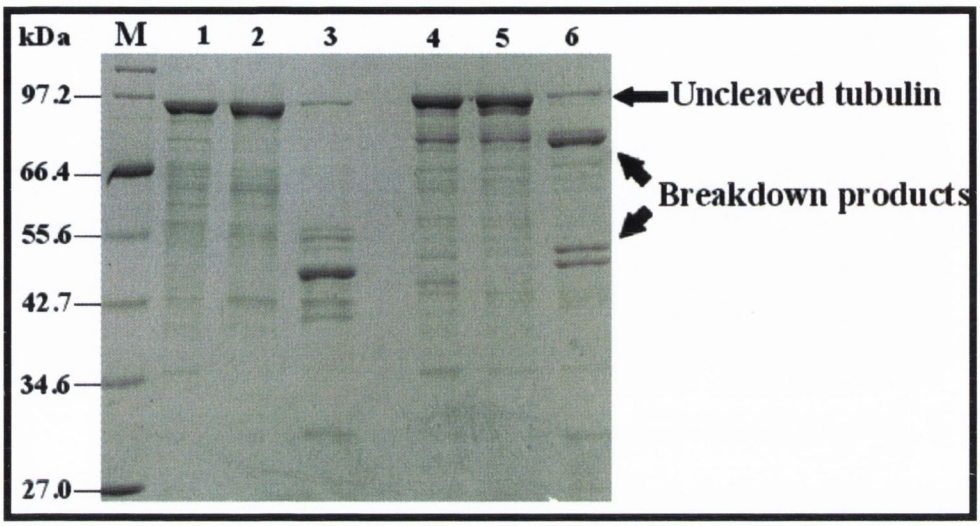

Fig. 3.6. Resolution of undigested and digested fusion tubulin proteins MBP-αI and MBP-β, produced using the pMAL-c2G vector, by SDS 10%-PAGE. MBP-αI- and MBP-β-tubulin were incubated in the absence and presence of factor Xa to determine if this enzyme was able to digest the tubulins at an unknown site. **M.** The molecular weight marker (Roche). **1)** MBP-αI-tubulin 0 h, **2)** MBP-αI-tubulin incubated alone at 37°C for 24 h, **3)** MBP-αI-tubulin incubated at 37°C for 24 h in the presence of factor Xa, **4)** MBP-β-tubulin 0 h, **5)** MBP-β-tubulin incubated alone at 37°C for 24 h and **6)** MBP-β-tubulin incubated at 37°C for 24 h in the presence of factor Xa. Both MBP-αI- and -β-tubulin demonstrated they were stable at 37°C for at least 24 h by comparison to the control sample. However, in the presence of factor Xa, significant digestion of the tubulin fusions was observed indicating that this enzyme can digest the tubulins in spite of the absence of known cleavage sites.

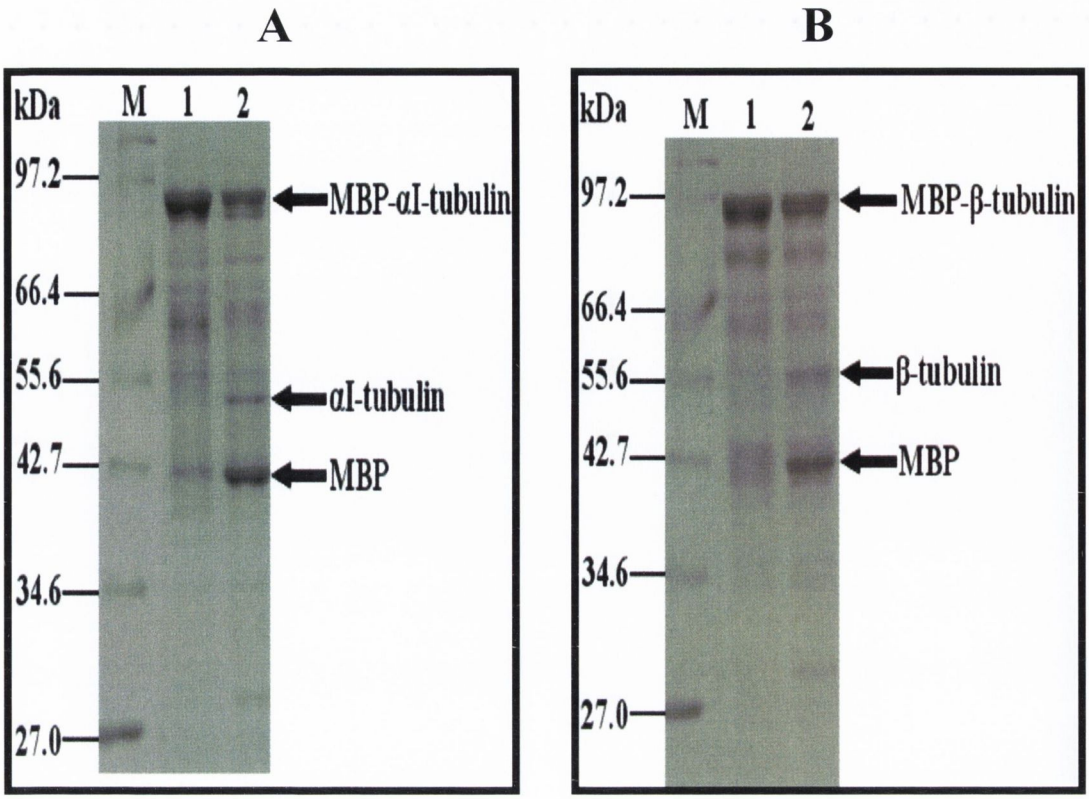

Fig. 3.7. Resolution of MBP-αI-tubulin (A) and MBP-β-tubulin (B) purified as described in section 2.5.3 by SDS 10%-PAGE in the absence and presence of genenase I at 22°C for 24 h. M. Molecular weight marker (Roche). Lane **1)** tubulin fusion sample after 24 h in the absence of genenase I, **2)** tubulin fusion sample after 24 h in the presence of genenase I (0.1 μg). Five micrograms of fusion protein were loaded onto the gel but only a fraction of the tubulin fusion sample appeared to be digested by genenase I.

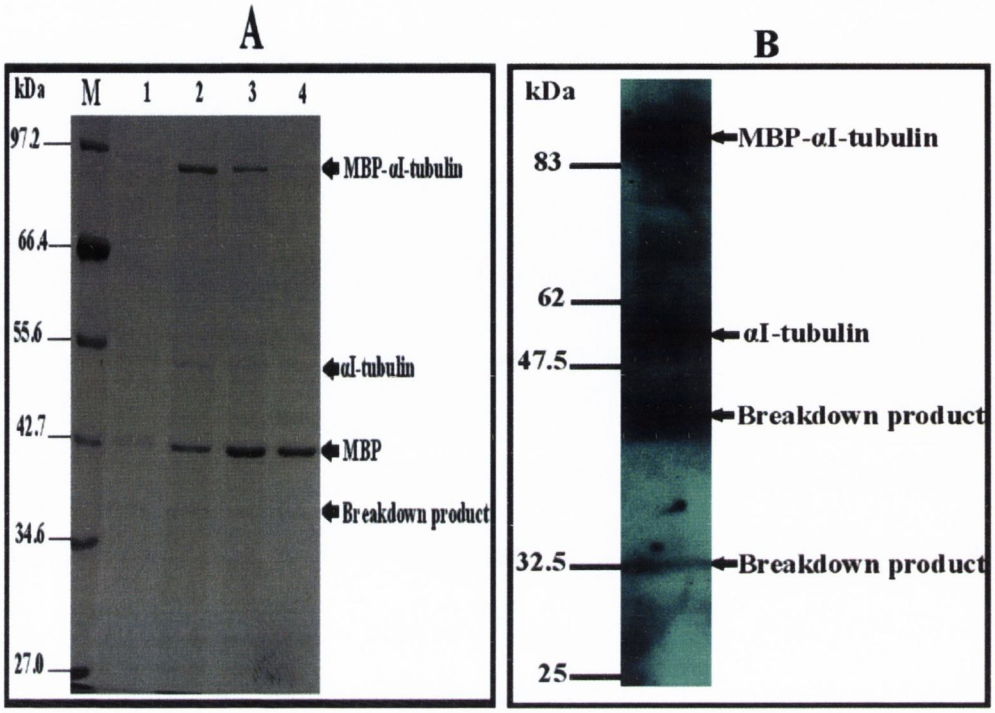

Fig. 3.8. Resolution of MBP-αI-tubulin digested on-column in the presence of genenase I (A) and a western blot of an identical gel highlighting the sample from lane 3 (B). M. Molecular weight marker (Roche). Panel **A:** lanes **1-4**) represent the unbound protein eluted from the column using wash buffer. Each fraction consisted of 500 µl, which represents the total volume of reaction solution (2 ml in total of genenase I in cleavage buffer was initially loaded onto the column). **B.** Western blot using an anti-αI-tubulin antibody against an identical gel to **A** but only lane **2** is shown.

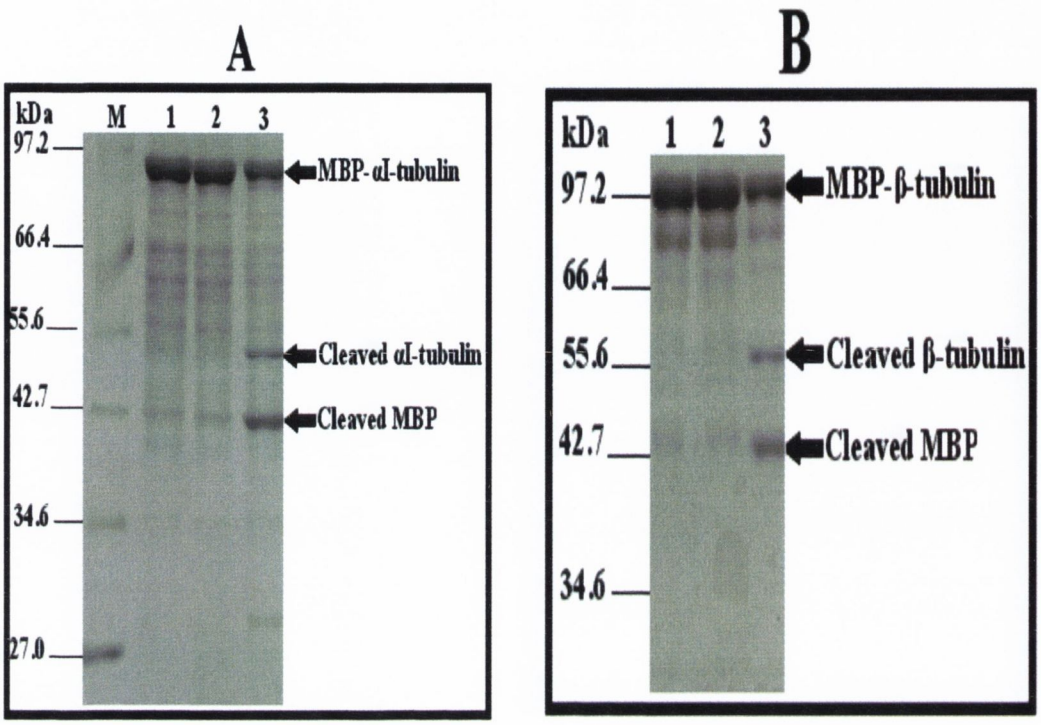

Fig. 3.9 Resolution of MBP-αI-tubulin (A) and MBP-β-tubulin (B) cleaved with genenase I in the presence SDS (0.005% final conc.) by SDS 10%–PAGE. M. Molecular weight marker (Roche). **A.** Lane **1)** MBP-αI-tubulin (~5 μg) 0 h, **2)** MBP-αI-tubulin alone incubated for 4 h at 22°C and **3)** MBP-αI-ubulin with genenase I (0.1 μg) incubated at 22°C for 4 h. **B.** Lane **1)** MBP-β-tubulin (5 μg) 0 h, **2)** MBP-β-tubulin incubated alone at 4°C for 96 h and **3)** MBP-β-tubulin with genenase I (1 μg) incubated at 4°C for 96 h.

removed from the fusion tubulins, the proteins were used in subsequent experiments with the tag still attached

3.2.1.3 Production of αI/β-tubulin and αII/β-tubulin using the pET-Duet vector

The production of tubulin in *E. coli* is frequently problematic due to the formation of insoluble protein. In native cells, tubulin seldom exists as a free monomer so it seemed logical to try to co-express the proteins in the same cell as this may enhance their solubility and functionality if they can dimerise.

The pET–Duet plasmid has two multiple cloning sites (MCS) which permit the insertion of two separate protein-encoding genes on one plasmid. Both genes are controlled by separate T7*lac* promoters which are indirectly activated by the presence of millimolar amounts of IPTG. Addition of fusion tags (an N-terminal His-tag or a C-terminal S-tag) were possible, but were avoided as they may interfere with the function of the final product.

β-tubulin was cloned first into the MCS-2 as this reduced the amount of necessary cloning work, i.e. inserting β-tubulin into pET-Duet each time for both αI-tubulin and then again for αII-tubulin. The cloning strategy is outlined in section 2.3.4 and diagrammatically explained in Fig. 3.10. Due to cloning limitations, the β-tubulin gene was inserted into the pET-Duet vector using both *AatII* and *Xho*I. However, an upstream restriction site, *Nde*I, contains a start codon (ATG), which meant that the β-construct was translated with an extra 14 amino acids. Several attempts were made to remove the ATG start codon from the pET-Duet vector by either restriction digestion or site-directed mutagenesis. However, the plasmid became unstable and degraded into several bands of ~1000bp (data not shown). This prevented removing the *Nde*I site and also preventing sequencing of the pET-Duet-tubulin constructs. αI- and αII-tubulin were subsequently cloned into the pET-Duet-β construct using *Rca*I and *Bam*HI restriction sites. The restriction enzyme *Rca*I generates the same sticky ends as *Nco*I. Therefore, *Rca*I was used to digest the αI- and αII-tubulin (Fig. 3.10). The presence of the tubulin genes in the pET-Duet vector was confirmed using restriction digestion experiments and PCR (Fig. 3.11).

The pET-Duet-αII/β-tubulin construct was also made. PCR amplification and linearised DNA run on an agarose gel were used to determine the presence of both genes (data not shown). Since the majority of work was already done using αI-tubulin

during this project (see section 3.2.1.2), the pET-Duet-αII/β clone was not used further. The pET-Duet-αI/β-tubulin clone was transformed into *E. coli* BL21(DE3) cells as described in section 2.3.6. These cells contain a chromosomal copy of the T7 RNA polymerase which is controlled by the T7*lac* promoter and are also deficient in the *lon* and *ompT* proteases. These cells were induced as described in section 2.5.2. Induction of these cells caused the over-expression of at least one protein as judged by SDS 10%–PAGE (Fig. 3.12 A). This band was thought to represent the tubulins (Fig. 3.12 A). This was subsequently confirmed by use of a western blot which detected both the αI- and β-tubulins (Fig. 3.12 C and D). The apparent molecular weights of both αI- and β-tubulin should be different enough for both proteins to separate clearly on a denaturing polyacrylamide gel. αI-tubulin has an apparent molecular weight of ~53 kDa (Fennell *et al.*, 2008). The apparent molecular weight of β-tubulin produced by this vector (which has 14 additional amino acids than the native protein) is ~ 58.5 kDa (Fig. 3.12).

To determine if the over-expressed tubulins were soluble or insoluble, a culture containing the pET-Duet-αI/β construct was induced using IPTG and the cells were broken with a pre-cooled French Pressure® cell press as described in section 2.5.2 and 2.5.6 respectively. This method separated the proteins into two fractions, soluble and insoluble. The sedimented fraction was resuspended in an equal volume as the soluble fraction (the supernatant) with the same buffer so the relative protein concentrations between the samples would be comparable. Equal volumes of both the soluble and insoluble fractions were loaded onto the denaturing polyacrylamide gels. It became apparent that the tubulins produced using this system was mostly insoluble (Fig. 3.12 B). This indicated that the co-expression of these proteins did not make a significant difference to their solubility.

A western blot using anti-αI-tubulin antibodies (see Fig. 3.12 C) and anti-β-tubulin antibodies (see Fig. 3.12 D) was conducted using the soluble and insoluble fractions that was resolved by the SDS-polyacrylamide gel in Fig. 3.12 B. These western blots confirmed that both αI- and β-tubulin were expressed. Furthermore, significant degradation was observed for both proteins. The majority of αI-tubulin appeared to exist in the soluble fraction. However, for β-tubulin the majority appeared to exist in the insoluble fraction, although some may have been soluble.

Overall, it was possible to co-express both the αI- and β-tubulins in the same cell. The solubility of the proteins varied: αI-tubulin appeared to be relatively soluble

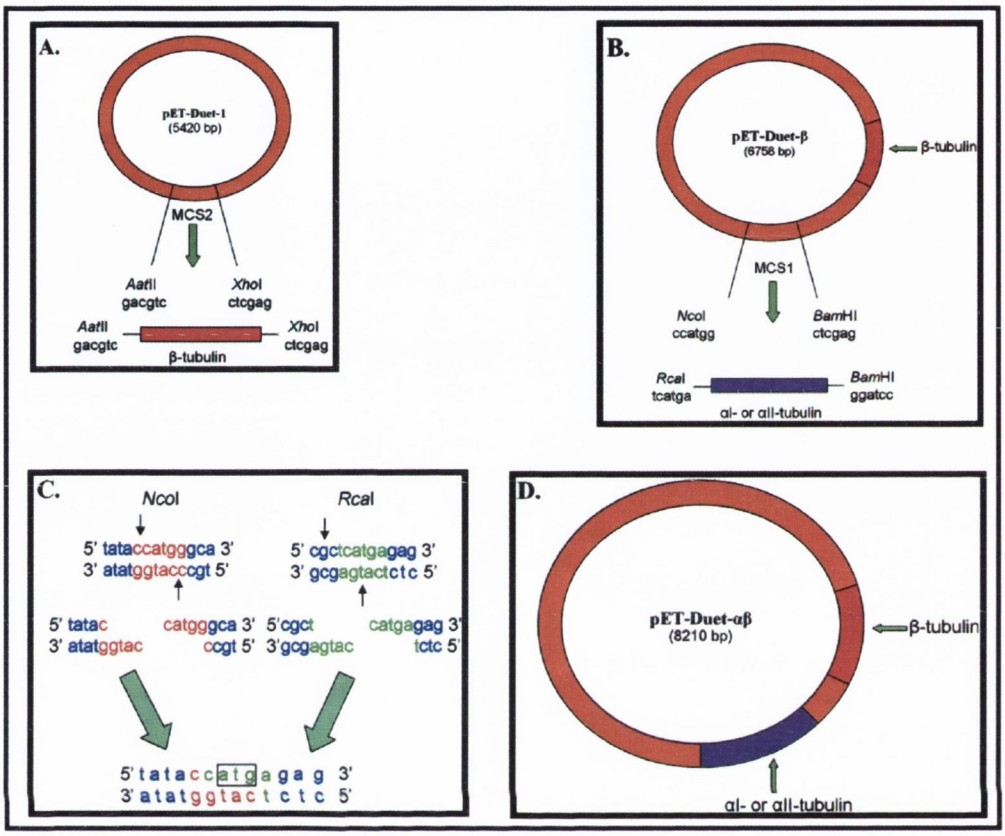

Fig. 3.10. Schematic representation of the cloning process for inserting αI-tubulin, αII-tubulin and β-tubulin genes into the pET-Duet vector. A. β-tubulin was cloned into the pET-Duet vector first using both *Aat*II and *Xho*I restriction sites. **B.** αI-tubulin and αII-tubulin were subsequently cloned into the pET-Duet-β vector using an enzyme generating cohesive ends compatible with the *Nco*I restriction site on the vector, *Rca*I (**C**). This created a hybrid sequence that neither enzyme (*Nco*I or *Rca*I) could recognise, therefore the forward restriction site for both α-tubulins was removed.

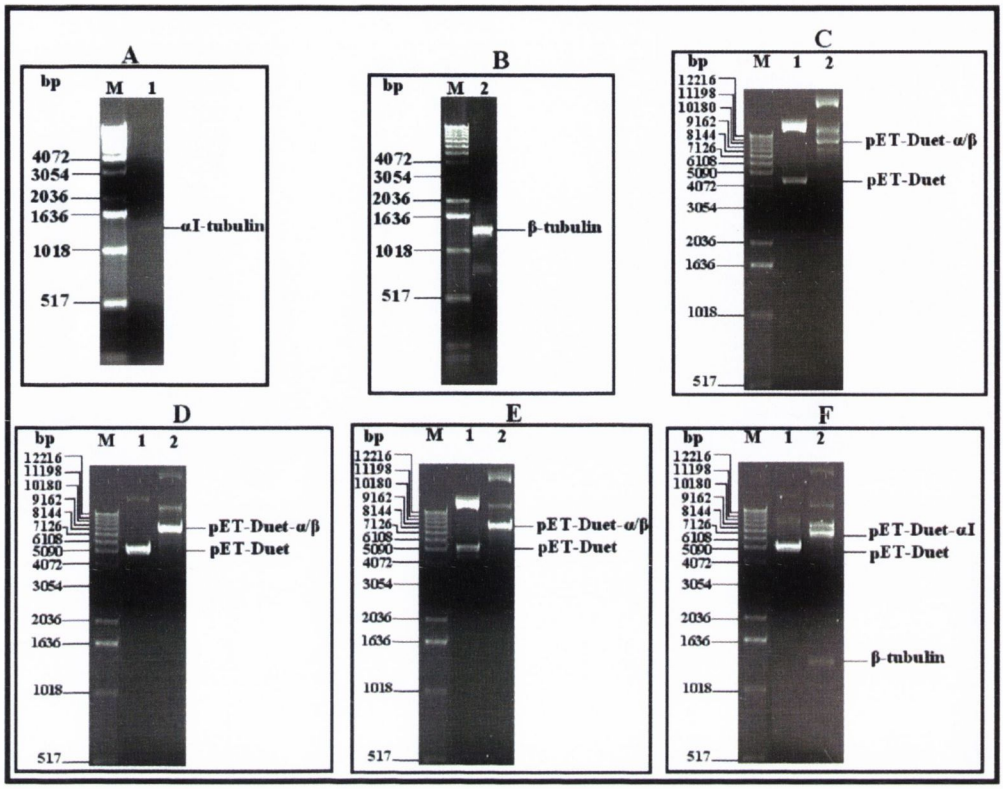

Fig. 3.11. Visualisation of pET-Duet constructs on 1% agarose gels. **M**, DNA marker X (Roche). All sizes are listed in base pairs (bp). **A.** Lane **1)** PCR confirmation of αI-tubulin in the pET-Duet-α/β construct. **B.** Lane **1)** PCR confirmation β-tubulin in the pET-Duet-α/β construct. **C.** Lane **1)** uncut pET-Duet and **2)** uncut pET-Duet-αI/β. Panel **D.** Lane **1)** pET-Duet linearised with *Xho*I (~5420 bp) and **2)** pET-Duet-αI/β (~8210) linearised with *Xho*I. **E.** Lane **1)** pET-Duet partially linearised with *Aat*II and **2)** pET-Duet-αI/β partially linearised with *Aat*II. **F.** Lane **1)** pET-Duet cut with *Xho*I and *Aat*II and **2)** pET-Duet-αI/β cut with *Xho*I and *Aat*II (~6872 bp). The PCR was used to show the presence of the tubulin genes in the pET-Duet-αI/β construct. The restriction digestion experiment demonstrated that both restriction enzymes only cut the pET-Duet vector and the pET-Duet–αI/β vector once but also when used in combination could drop out a fragment that equates to the size of the β-tubulin gene (1338 bp). Five µl of a 50 µl total volume for the PCR product were loaded and ~250 ng of DNA were loaded for the restriction experiments.

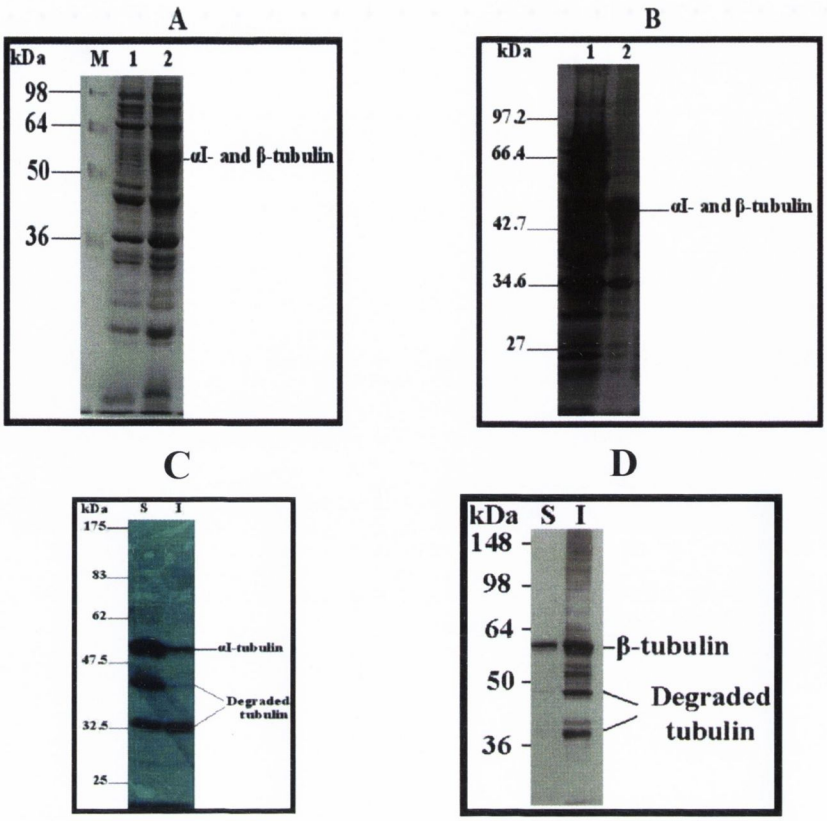

Fig. 3.12. Visualisation of the production and solubility of tubulins from *E. coli* BL21 (DE3) carrying pET-Duet-αI/β by Coomassie Blue stained SDS 10%-PAGE (A and B) and western immunoblots using anti-αI-tubulin (C) and anti-β-tubulin (D) antibodies. **M**. Molecular weight marker (Roche or Invitrogen). **A.** SDS-polyacrylamide gel showing the expression of the αI/β-tubulin proteins using the pET-Duet-αI/β construct. Lane **1)** Uninduced *E. coli* BL21 (DE3) cells carrying pET-Duet-αI/β and **2)** IPTG-induced *E. coli* BL21 (DE3) cells carrying pET-Duet-αI/β. One large band representing an over-expressed protein in lane **2** was observed. This band was thought to be the tubulins. **B.** An induced *E. coli* sample was lysed and centrifuged to separate the proteins into soluble and insoluble fractions. Lane **1)** Soluble protein fraction of and **2)** insoluble fraction. The majority of the over-expressed tubulin appeared to be insoluble. **C.** Western blot using anti-αI-tubulin antibodies of an identical gel to the one shown in panel **B**. Lane **S)** soluble fraction and lane **I)** insoluble fraction. More αI-tubulin was present in the soluble fraction although at least two significant breakdown products were present. **D.** Western blot using anti-β-tubulin antibodies for an identical gel to that shown in panel **B**. Lane **S)** soluble fraction and lane **I)** insoluble fraction. Some β-tubulin was observed in the soluble fraction, although the majority appeared to be insoluble.

but β-tubulin was almost completely insoluble. Therefore, it was considered unlikely that these tubulins would be assembly-competent. However, some subsequent work was done to determine if they could co-polymerise.

3.2.1.4 Refolding untagged tubulin by rabbit reticulocyte lysate

It was previously demonstrated that fully denatured bovine brain tubulin could be correctly refolded and made competent to form normal microtubules by virtue of the chaperone machinery present in rabbit reticulocyte lysate (RRL) (Yaffe *et al.,* 1988 and Shah *et al.,* 2001). Based on this work, it seemed reasonable to assume that these eukaryotic chaperones would also be capable of refolding the *Plasmodium* tubulin produced as inclusion bodies in *E. coli,* considering that the tubulin folding pathway is highly conserved.

These experiments were conducted with the assistance of Miss Sara Leddy. The pET-11a constructs containing αI-, αII-tubulin and β-tubulin were generated previously by Dr. Brian Fennell (Fennell, 2005). The tubulins were highly expressed from cultures grown at 37°C but were completely insoluble (Fig 3.13 A) (outlined in section 2.5.7). The insoluble proteins were relatively pure when compared to the original lysate, which facilitated the use of the inclusion bodies without necessitating further purification (Fig 3.13 B). Recombinant tubulin was refolded as described in section 2.5.8.1

A sedimentation assay was set up to determine if the recombinant tubulins were assembly-competent in the presence and absence of vinblastine (described in section in 2.6.3.2). Due to the low yields of protein, it was necessary to conduct a western blot on the samples from the sedimentation assay. This also confirmed the presence of the tubulins. The β-tubulin antibody was determined not to cross-react with the residual native rabbit tubulin in the RRL.

Samples were taken at various points during the experiment to determine the presence of the tubulin (Fig 3.14). In group **1**, the soluble fraction was heavily smeared masking the presence of other bands. However, it was possible to observe a band running at the expected size for β-tubulin (~57 kDa) in both the soluble and insoluble fractions. This sedimented tubulin was perhaps still mis-folded. In groups **2** and **5**, the majority of tubulin seemed not to polymerise as it remained in the soluble fraction. However, in group **2** only, a faint band was present in the sedimented

fraction possibly representing a small amount of polymerised tubulin (Fig 3.14 group 2 P). In group **3**, this faint band was repeated in the soluble fraction indicating that the tubulin was able to become soluble depending upon the temperature (Fig 3.14 group 3 S). This was not repeated with samples treated with the assembly inhibitor vinblastine (Fig. 3.14 group 4 P and group 5 S) which suggests that the tubulin were, as expected, unable to polymerise when the drug was added. Although this experiment appeared to have worked, the amount of assembly-competent tubulin generated was negligible (<<1 μg). These low amounts are not conducive to most ligand-binding studies. A possible exception might be surface plasmon resonance but even still a greater yield would likely be necessary. Therefore, other strategies to generate recombinant tubulin were investigated.

3.2.1.5 Refolding His_{12}-tagged tubulin while attached to a metal-chelate-affinity chromatography column

To determine if a higher yield of assembly-competent tubulin could be generated by chemical refolding, a method devised by Jang *et al.*, was used (Jang *et al.*, 2008). Briefly, the pET-16b-αI-tubulin and pET-16b-β-tubulin constructs (previously designed by Dr. Brian Fennell; Fennell, 2005) were used to over-express His_{12}-tagged tubulins in the *E. coli* strain BL21 (Fig. 3.15 A). The inclusion bodies were isolated as outlined in section 2.5.7 and washed once with detergent, and consisted of almost pure tubulin (Fig. 3.15 B and C). In separate experiments, the tubulin inclusion bodies were denatured using a urea solution and loaded onto a Ni^{2+}-chelate affinity column where they were exposed to a decreasing gradient of denaturant, guanidine hydrochloride (outlined in section 2.5.8.2). The tubulins eluted from the Ni^{2+}-chelate column were very pure (Fig 3.15 B and C). These proteins were concentrated to a maximum of ~5 μg/μl where they were stored at -70°C for use in subsequent experiments to determine their functionality (see section 3.2.2).

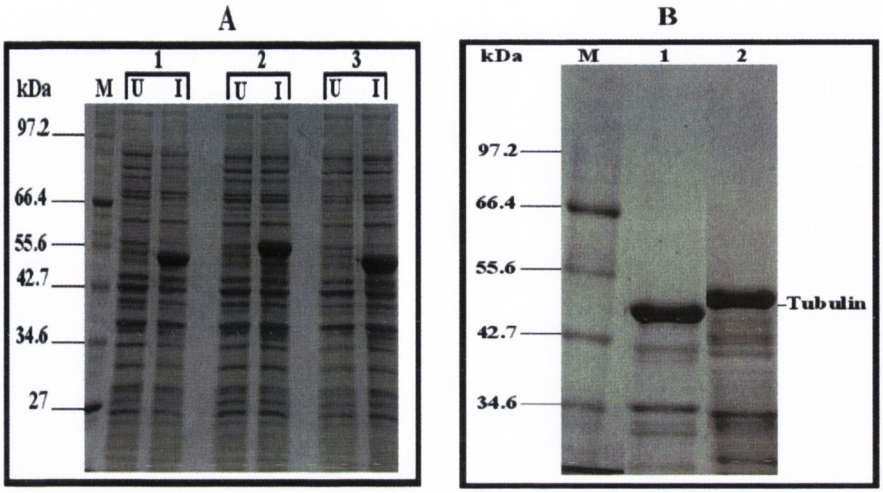

Fig. 3.13. Expression of αI-tubulin, αII-tubulin and β-tubulin using the pET-11a vector and the subsequent isolation of the tubulin-containing inclusion bodies. **M**. Molecular weight marker (Roche). **A.** SDS 10%–PAGE of αI-tubulin, αII-tubulin and β-tubulin from uninduced (**U**) versus induced (**I**) cultures. Lanes **1)** pET-11a-αI-tubulin, **2)** pET-11a-β-tubulin and **3)** pET-11a-αII-tubulin. **B.** SDS 10%–PAGE of the isolated inclusion bodies of αI-tubulin and β-tubulin produced from the pET-11a constructs. Lanes **1)** insoluble αI-tubulin and **2)** insoluble β-tubulin.

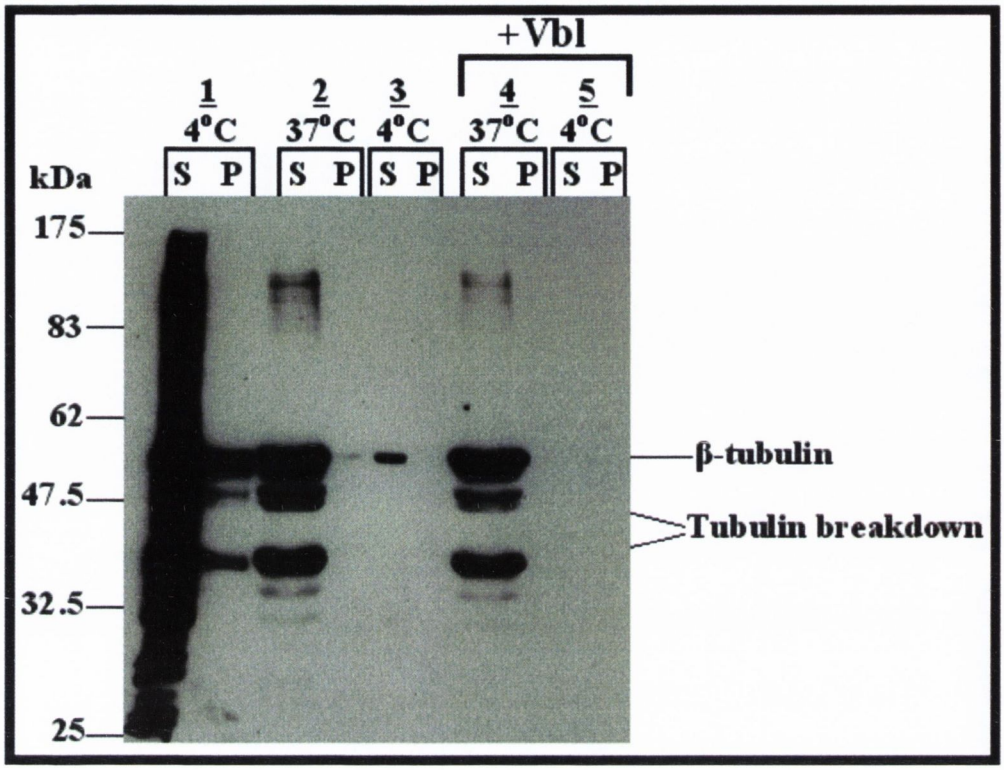

Fig. 3.14. A western blot stained with anti-β-tubulin antibody detecting the probably refolded tubulin from the rabbit reticulocyte sedimentation assay. S, soluble fraction and P, pellet. The different temperatures used are indicated where necessary. + **Vbl**, vinblastine added (50 μM final conc.) Group **1.** These samples were obtained after ultracentrifugation (400,000 x g) of the rabbit reticulocyte lysate at 4°C. Groups **2** and **4.** These samples were obtained after centrifuging (20,000 x g) the soluble fraction (**S**) from group **1** at 37°C in the absence (group **2**) or presence (group **4**) of vinblastine (50 μM). Group **3** and **5**. These samples were obtained after centrifuging (20,000 x g) the 37°C sedimented (**P**) fraction in the absence (group **3**) or presence (group **5**) of vinblastine (50 μM) respectively. All samples were loaded at 5% their original volume except the "pellet" in group 2 which only ~1% was loaded. This was due to lack of sample.

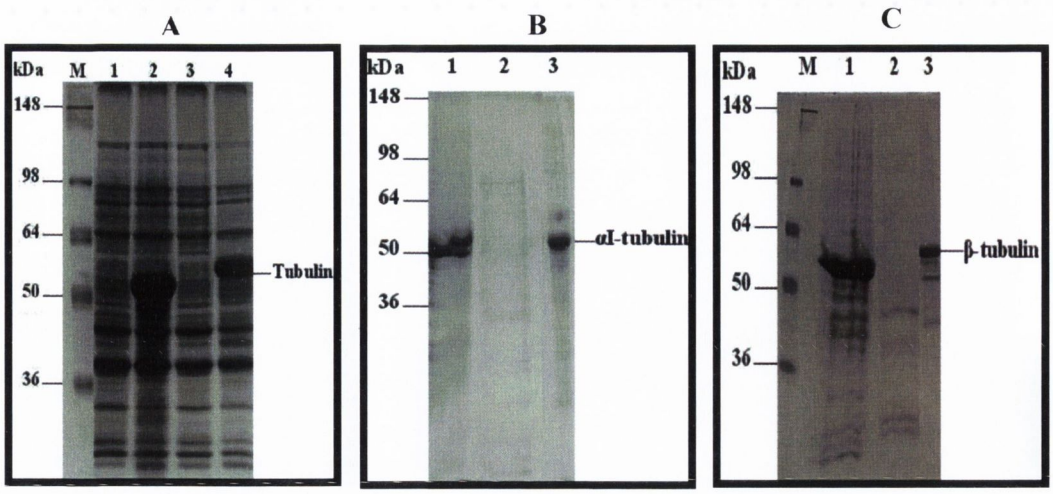

Fig. 3.15. Expression of His_{12}-αI-tubulin and His_{12}-β-tubulin (A) and the refolding of both proteins (B and C) as resolved by SDS 10%–PAGE. M. Molecular weight marker (Invitrogen). For all samples unless otherwise stated, equal volumes were loaded. **A.** Lane **1)** pET-16b-αI uninduced, **2)** pET-16b-αI induced with 2 mM IPTG, **3)** pET-16b-β uninduced and **4)** pET-16b-β induced with 2 mM IPTG. Both of the tubulins were produced in high concentrations (Lanes **2** and **4**). **B.** Lane **1)** A sample of the urea-denatured inclusion body fraction for His_{12}-αI-tubulin that was applied to the Ni^{2+}-chelate column, **2)** unbound protein fraction and **3)** eluted His_6-αI-tubulin (3 μg). **C.** Lane **1)** A sample of the urea denatured inclusion body fraction for His_{12}-β-tubulin that was applied to the Ni^{2+}-chelate-column, **2)** unbound protein fraction and **3)** eluted His_{12}-β-tubulin (3 μg).

3.2.2 FUNCTIONAL ANALYSIS OF RECOMBINANT *P. FALCIPARUM* TUBULINS

3.2.2.1 Examination of recombinant tubulin dimerisation by native PAGE

To determine if the recombinant tubulins could form heterodimers, the proteins were separated under non-denaturing conditions on a polyacrylamide gel (as outlined in section 2.4.3). Mammalian tubulin forms a distinctive ladder-like pattern when separated by this method as a result of the formation of differently sized protein oligomers (Sulimenko *et al.*, 2002). Tubulin monomers were compared with the tubulin mixture that was prepared for dimerisation (described in section 2.6.1). Initial experiments using the MBP-fusion tubulins revealed that the proteins could not enter the separating region of the polyacrylamide gel (data not shown). This was thought to have resulted, at least in part, from the non-specific crosslinking of the cystine residues on both tubulins resulting in the formation of high-molecular-weight aggregates. Therefore, excess 2-mercaptoethanol (10% v/v final concentration) was added and the experiment repeated (Fig. 3.16). The reducing agent had no effect on the separation pattern of bovine brain tubulin. However, it did enhance the resolution of the MBP-tubulin fusions, although no differences between the tubulin monomers and the tubulin mixture were apparent. Since it was possible that the recombinant tubulin dimers were too large to be clearly resolved, 5%-PAGE was used but this did not yield clearer results (data not shown). The presence or absence of GTP did not affect the migration patterns of any of the tubulin samples. Also, no different bands which may correspond to dimerised MBP-αI/β-tubulin were obvious by comparison to the monomer samples. Therefore, it was unclear whether the tubulin fusions were able to form heterodimers so more experiments were conducted to get a definite answer.

3.2.2.2 Examination of recombinant tubulin dimerisation by glutaraldehyde cross-linking

To overcome the problem of resolving the tubulin proteins on a non-denaturing polyacrylamide gel, glutaraldehyde cross-linking was performed. This reagent conveniently generates covalent bonds between closely interacting proteins

via its aldehyde groups reacting primarily with amine residues. Therefore, a denaturing polyacrylamide gel can be employed to resolve the proteins without disrupting this interaction. An excess of Tris-HCl quenches the reagent due to the presence of the amine groups. Recombinant MBP-fusion tubulins, affinity-purified MBP and bovine brain tubulin were prepared for dimerisation as outlined in section 2.6.2.

Optimal cross-linking times were determined empirically by conducting a range of cross-linking experiments with and without 2-mercaptoethanol from 2 min up to 180 min (data not shown). The optimal cross-linking time in the absence of 2-mercaptoethanol was 5 min (data not shown). Although the presence of this reducing agent did not affect the final results, optimal cross-linking required a longer period of time, 30 min (Fig 3.17). The recombinant tubulins, either alone or as a mixture, did not resolve on SDS 7.5%–PAGE when cross-linked. This was evident as the majority of the protein remained at the stacking/separating gel interface. Some of the tubulin was still resolved on the gel indicating that it had not yet reacted with the reagent. However, it was not possible to find an intermediate point where the tubulin was only lightly cross-linked but could still be resolved on the polyacrylamide gel. In contrast, bovine brain tubulin appeared to be successfully cross-linked with two faint bands of approximately 110 and 220 kDa in size being resolved. However, some of the protein was also trapped at the stacking/separating gel interface indicating the formation of higher oligomers. Furthermore, the smearing effect of the bovine tubulin oligomers is a known phenomenon and was a result of the increased resistance of the protein to denaturation by SDS (Turner *et al.,* 1996). Bovine tubulin was similarly affected by the presence of the reducing agent as it took longer for obvious cross-linked bands to appear. MBP was used as a negative control and it did not form any oligomers. SDS 5%-PAGE was conducted using the same samples as in Fig. 3.17, but it was still not possible to resolve the recombinant tubulins (data not shown). The recombinant MBP-fusions once cross-linked were unable to be resolved on the acrylamide gel. Bovine tubulin dimers were detected and MBP was unaffected by the presence of glutaraldehyde as expected, indicating that the experiment was conducted correctly. Therefore, this experiment could not conclusively prove that the tubulins did not form heterodimers as these crosslinked proteins appeared to become insoluble so they could not be resolved on the gel.

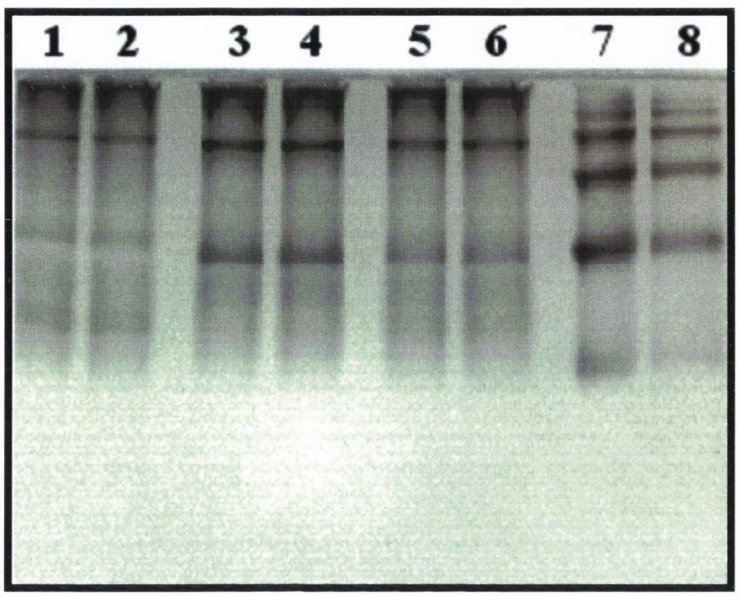

Fig. 3.16. Resolution of the recombinant tubulins and bovine tubulin on a 10%–polyacrylamide gel. Lanes **1** and **2)** MBP-αI-tubulin, **3** and **4)** MBP-β-tubulin, **5** and **6)** MBP-αI/β-tubulin, **7** and **8)** bovine brain tubulin. Samples in lanes **1**, **3**, **5** and **7** had no GTP added while samples in lanes **2**, **4**, **6** and **8** had GTP added (1 mM final concentration).

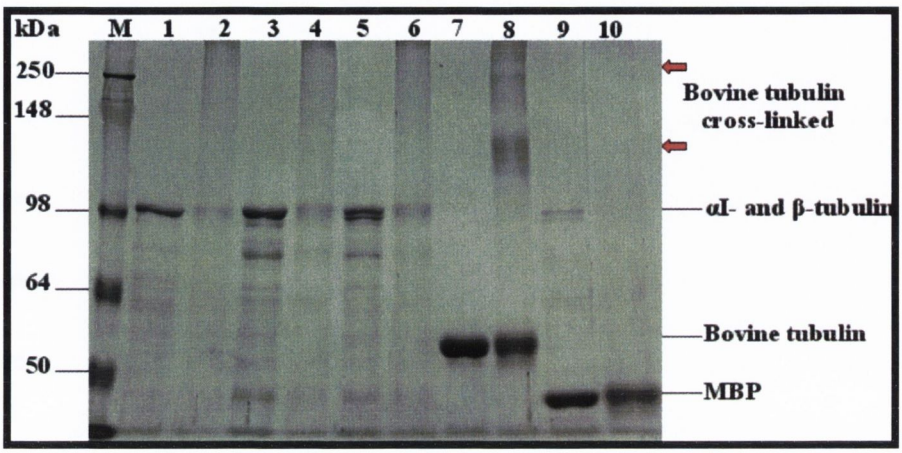

Fig. 3.17. Glutaraldehyde cross-linking of the recombinant MBP-tubulin fusions, bovine brain tubulin and MBP resolved on a SDS 7.5%–PAGE. M. Molecular weight marker (Invitrogen). Lanes **1** and **2)** MBP-αI-tubulin (4 μg each), **3** and **4)** MBP-β-tubulin (4 μg each), **5** and **6)** MBP-αI/β-tubulin (4 μg each), **7** and **8)** bovine brain tubulin (4 μg each) and **9** and **10)** MBP (4 μg each). Lanes **1**, **3**, **5**, **7** and **9** all had Tris-HCl (0.1 M) added before the addition of glutaraldehyde to quench the glutaraldehyde before it could cross-link the proteins. Lanes **2**, **4**, **6**, **8** and **10** had Tris-HCl (0.1 M final concentration) added after 30 min after exposure to the glutaraldehyde. The crosslinked proteins tended to aggregate and did not always resolve on the gel.

3.2.2.3 Tubulin polymerisation as assessed by sedimentation assay

Microtubules are easily separated from the more soluble tubulin dimers by differential centrifugation. Therefore, a sedimentation assay was designed based on a modified procedure of Kumar (Kumar N., 1981). Essentially, this assay used a series of centrifugation steps (~40,000 x g) at different temperatures (4°C or 37°C) that either encouraged or discouraged the formation of microtubules (see Fig. 3.18). Tubulin monomers or dimers remain soluble when centrifuged at ~40,000 x g but are mostly sedimented when they form microtubules (Kumar N., 1981). Therefore, this method was used to determine if the recombinant tubulins could form microtubules. Bovine brain tubulin was used as positive control and the MBP-tubulin monomers with equal amounts of purified MBP were used as negative controls to confirm that these proteins do not sediment when centrifuged. 2-Mercaptoethanol (2% (v/v)) was added to all the samples to eliminate the possibility that non-specific disulphide bond formation was precluding MT formation in the recombinant tubulin samples. The experiment was set up as described in section 2.6.3.1 (see Fig. 3.19). In order to quantify the protein, in each of the lanes, densitometry was employed (as outlined in section 2.4.7) to determine the relative amount (by percentage) of tubulin compared to the initial sample. Some of the sample was lost as the experiment continued mainly due to wash steps. Its also possible that small technical inaccuracies influenced the results in a minor way.

To test whether the proteins were soluble or insoluble at the different cycles, an equal volume from each sample was taken when necessary. The sample concentration would only change for two reasons: 1) division between soluble and insoluble fractions and 2) accidental loss of protein due to the wash steps. All samples were representative of the protein concentration that was present at the point of measurement and were directly comparable. The vast majority of the tubulin in the samples was soluble after the first centrifugation at 4°C, although some protein was sedimented (Fig. 3.19 A, lanes 2 and 3). This may be due to some residual protein clinging to the sides of the eppendorf tubes. Extensive wash steps were avoided due to the ease of accidentally disrupting the sedimented samples. The 4°C-soluble fraction was incubated at 37°C before being centrifuged at 37°C. Approximately three-fifths (60%) of the bovine brain tubulin was sedimented while the remaining two-fifths (38%) was soluble (Fig. 3.19 A, lanes 3 and 5). To determine if a

significant amount of protein was lost during the wash step for the 37°C-sedimented protein fraction, a sample was also taken. An insignificant amount of protein was lost (~0.5%; Fig. 3.19 A, lane 4a). MBP-αI-tubulin was fully soluble at 37°C and no sedimented sample was observed (Fig 3.19 B, lane 4) . However, for MBP-β-tubulin (Fig. 3.19 C, lane 4) and MBP-αI/β-tubulin (Fig. 3.19 D, lane 4), some of the protein sedimented at 37°C, indicating that the protein may have either polymerised or aggregated. The 37°C-sedimented fractions were subsequently resuspended and incubated on ice (30 min) before being centrifuged at 4°C. The bovine brain tubulin was expected to be completely soluble but the majority of the protein was still insoluble (Fig. 3.19 A lanes 6 and 7). The recombinant tubulins were completely insoluble, which suggested that these proteins had aggregated rather than polymerised (Fig. 3.19 C and D lanes 6 and 7). Although the MBP-β-tubulin had a greater concentration (9%) in final sample than the MBP-αI/β-tubulin mixture (0.6%), this was likely due to accidental loss of protein during the wash procedure.

Overall, the fusion tubulin tubulins did not appear capable of forming MT's. In contrast, bovine tubulin was able to assemble and disassemble depending upon the conditions.

3.2.3 TUBULIN-LIGAND-BINDING ASSAYS

APM derivatives were synthesised by a collaborator, Mrs. Christine Mara, in the Medicinal Chemistry Dept. of the Royal College of Surgeons in Ireland, Dublin. In order properly to evaluate these compounds, a tubulin–ligand-binding assay was required. However, since it was not possible to use some of the well-established tubulin polymerisation assays, other possibilities were investigated. The reactive sulphydryl groups and the fluorescent tryptophan amino acids have both being exploited extensively over the years to determine small ligand-protein interactions. Therefore, these assays were developed for use with the MBP-tubulin fusions as previous tubulin-ligand-binding experiments using, for example, radiolabelled trifluralin were successful with these proteins (Holloman *et al.*, 1998, Fennell *et al.*, 2006 and Giles *et al.*, 2008).

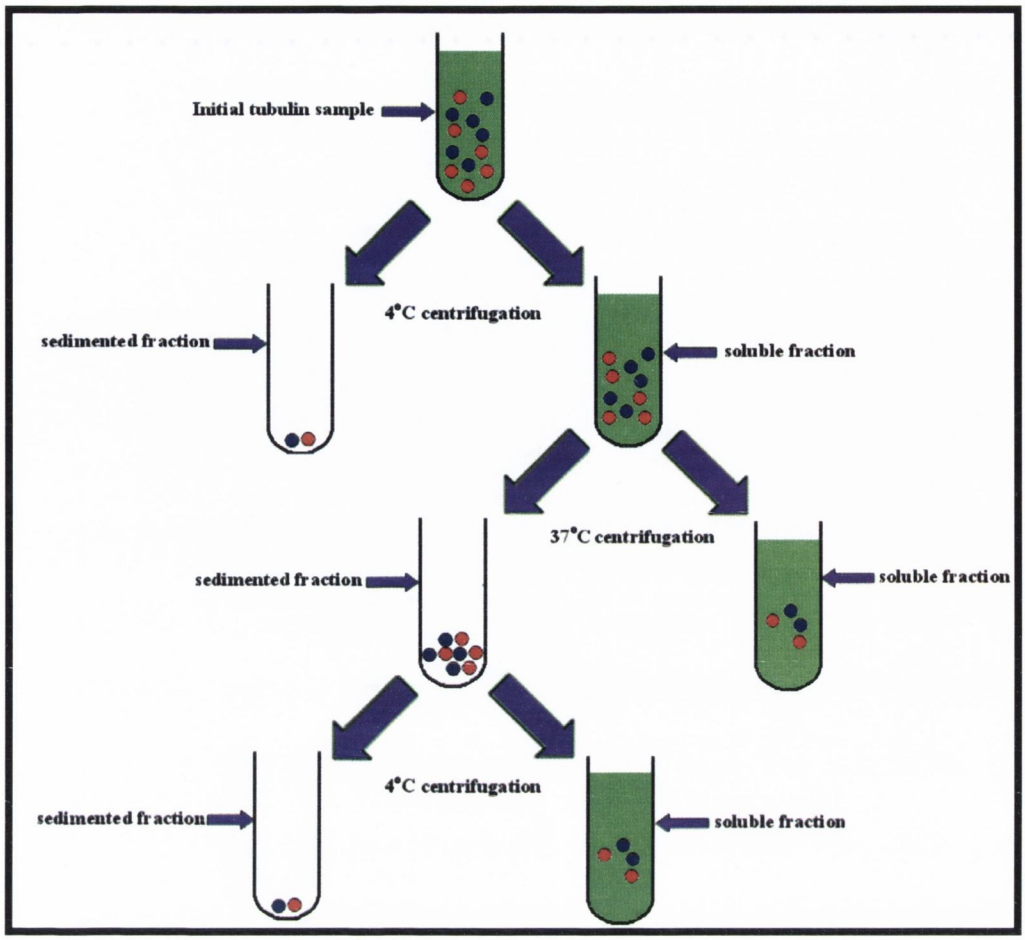

Fig. 3.18. Schematic diagram representing the central centrifugation steps in the sedimentation assay for assembly-competent tubulin. The **red** circles represent MBP-αI-tubulin and the **blue** circles represent MBP-β-tubulin. The initial tubulin sample was centrifuged at 4°C to remove any aggregated protein. The soluble fraction was transferred to a new eppendorf tube where it was subsequently centrifuged at 37°C. The sedimented tubulin sample was resuspended and finally centrifuged at 4°C. Assembly-competent tubulin should be found in the supernatant after the last centrifugation at 4°C.

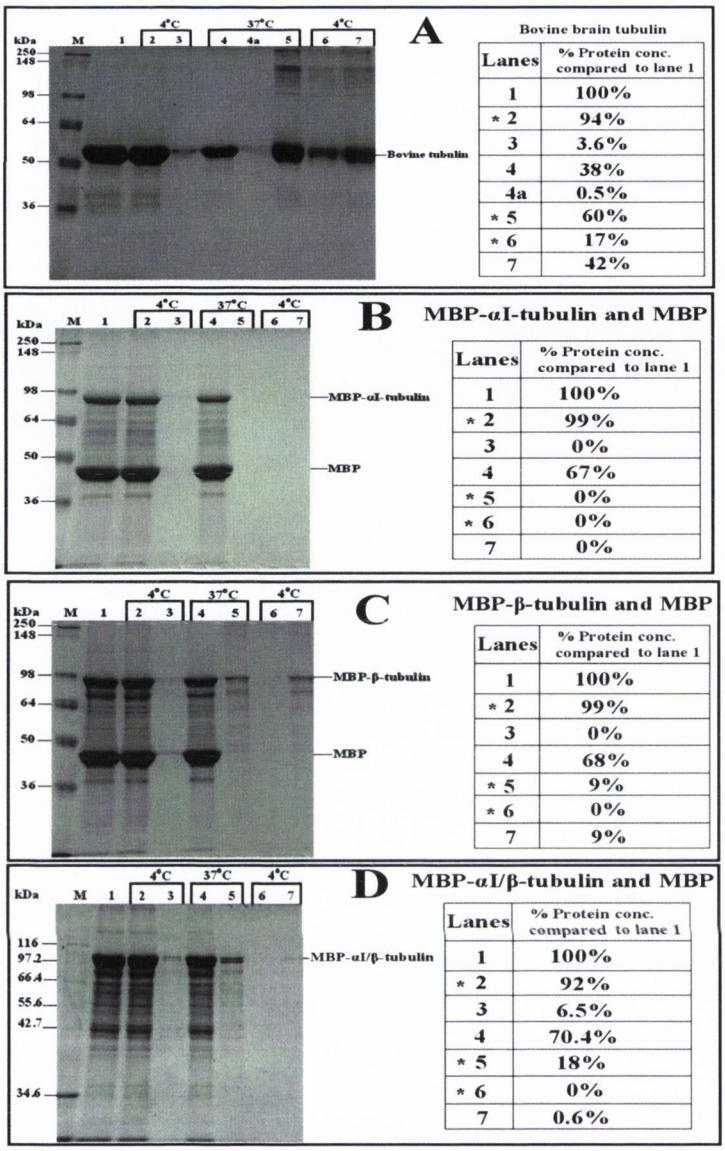

Fig. 3.19. Analysis of the ability of bovine brain tubulin and the recombinant MBP-tubulin fusions to polymerise by the sedimentation assay. M. Molecular weight marker (Roche). **A.** Bovine brain tubulin. **B.** MBP-αI-tubulin. **C.** MBP-β-tubulin. **D.** MBP-αI/β-tubulin. All gels were loaded as follows; lane **1)** Initial tubulin sample (10 μg), **2)** soluble fraction after the 4°C centrifugation, **3)** insoluble fraction after the 4°C centrifugation, **4)** soluble fraction after the 37°C centrifugation, **4a)** wash fraction of sedimented sample at 37°C, **5)** insoluble fraction after the 37°C centrifugation, **6)** soluble fraction after the 4°C centrifugation and **7)** insoluble fraction after the 4°C centrifugation. The results from the densitometry analysis are listed beside the applicable SDS-polyacrylamide gel. * lists the lanes in which the bulk of the assembly-competent tubulin should be found. See Fig. 3.18 for an explanation of the protocol.

3.2.3.1 Measurement of ligand-tubulin interactions using a sulphydryl-reactivity based assay

The sulphydryl residues on tubulin have been used by many different groups in the past to determine the dynamics of ligand-tubulin interactions (Werbovetz *et al.*, 1999, Koo *et al.*, 2009 and Gupta *et al.*, 2002). The assay is based upon the reagent, 5,5'-dithiobis(2-nitrobenzoate) (DTNB), reacting with the free thiol groups (–SH), that exist only on cystine amino acids, to form a bright yellow product, 2-nitro-5-thiobenzoate (TNB), which can be measured spectrophotometrically at 412 nm (Fig. 3.20). Unreacted DTNB is almost colourless so there is very little background noise. MBP itself contains no cystine residues. By constrast, *P. falciparum* αI-tubulin has 15 cystines while β-tubulin has 9.

The 20 cystine residues on bovine brain tubulin are scattered throughout the protein which makes it ideal for reporting small ligand-binding. Two μM bovine tubulin were incubated with single concentrations of known inhibitors to determine whether this assay could detect their interaction with the protein. After 30 min, the effect of the tubulin ligands was compared to the control, DMSO alone. Colchicine (50 μM) and vinblastine (50 μM) produced significant absorbance quenches of ~32% and ~34% respectively (Fig. 3.21). APM (50 μM), however, gave no significant effect (<1%) on the reactivity of DTNB with bovine tubulin, suggesting that there was no interaction between the compound and protein at this concentration, as expected. Following this result, the His_{12}-tagged tubulins were tested for their reactivity with DTNB. The His_{12}-tagged tubulins were completely insensitive to the presence of DTNB, indicating that their sulphydryl groups were not fully reduced (data not shown). The MBP-fusions, both as monomers and as a mixture were then examined using this assay. MBP was used as a negative control and did not react with DTNB. By contrast, the MBP-tubulin fusions demonstrated a dose–dependent response to this reagent (data not shown for the monomers). However, these recombinant tubulins did not appear to be as active in this respect as the bovine tubulin, which is evident from the graphs in Fig. 3.21. An approximate comparison of the sulphydryl reactivity for bovine tubulin (2 μM) with the MBP-tubulin fusion mixture (2 μM) was made by calculating the total absorbance change for both proteins over 60 min. The MBP-fusions were approximately ~35 % as reactive as the bovine tubulin, which possibly suggests that the some of recombinant sulphydryl residues were not reactive. Despite

this result, ligand-interaction studies were attempted using different inhibitors at various concentrations, e.g. APM (200 μM), vinblastine (200 μM) and taxol (20 μM). However, none of these compounds affected the sulphydryl reaction. Therefore, it was not clear if these compounds were not able to bind to the proteins or if their binding was not being reported by the sulphydryl groups.

To determine if high concentrations of APM could bind to bovine tubulin, low amounts of the protein (0.15 μM) were incubated with high concentrations (50 μM and 100 μM) of the ligand. An increase in the DTNB reactivity was observed by when a ratio of 666:1 ligand to tubulin was used (Fig. 3.22). However, this effect disappeared when the APM concentration was lowered. This may indicate a weak interaction between the compound and the protein.

In summary, this was a very useful assay that had no background noise from non-specific reactions of DTNB with the compounds. It was also capable of detecting the interaction of small ligands to bovine brain tubulin. However, despite the DTNB being able to react with the sulphydryl groups on the tubulin fusions, this reaction appeared to be less than that of the bovine brain tubulin. Therefore, it was assumed that not all of the cystine residues were reactive. This was especially true for the His_{12}-tagged tubulins which did not react at all with DTNB. This may explain why the presence of tubulin ligands did not affect the reaction profile of DTNB with the tubulin fusions. As a result, this assay could not be used to determine the binding of ligands to the tubulin fusions.

3.2.3.2 Measurement of ligand-tubulin interactions using a tryptophan fluorescence-based assay

Plasmodium αI- and β-tubulin contain 4 tryptophans each. These residues fluoresce strongly when excited at 280 nm giving a characteristic emission spectrum which peaks around 350 nm. This technique has been widely employed to analyse ligand-tubulin interactions for a number of distantly related organisms including mammals, plants and protozoa (Acharya *et al.*, Joe *et al.*, 2008, Panda *et al.*, 2000, Sackett D., 1995, Lee *et al.*, 1975, Murthy *et al.*, 1994, Hughdahl *et al.*, 1993, Bhattacharya *et al.*, 2002, MacDonald *et al.*, 2004, Prichard *et al.*, 2000, Yakovich *et al.*, 2006, Werbovetz *et al.*, 2003 and Werbovetz *et al.*, 1999). Ligand interactions are detected by a reduction in the intrinsic tubulin fluorescence intensity (quenching).

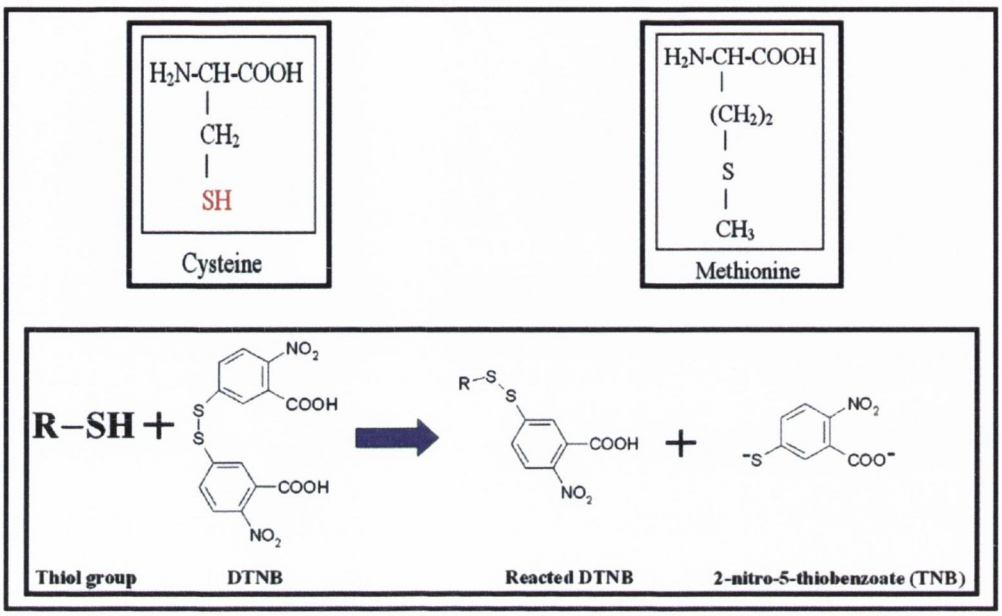

Fig. 3.20. Diagram showing the reaction mechanism of DTNB with a free thiol group on cystine. The free thiol group on the cystine (top left and highlighted in **red**) contrasts with the unreactive sulphur in methionine (top right). Once DTNB reacts with the thiol group it releases TNB^{-2} as a by-product which has the yellow colour. An excess of DTNB is always used in this assay to ensure that the TNB^{-2} does not react with another thiol group as it would no longer produce the yellow hue.

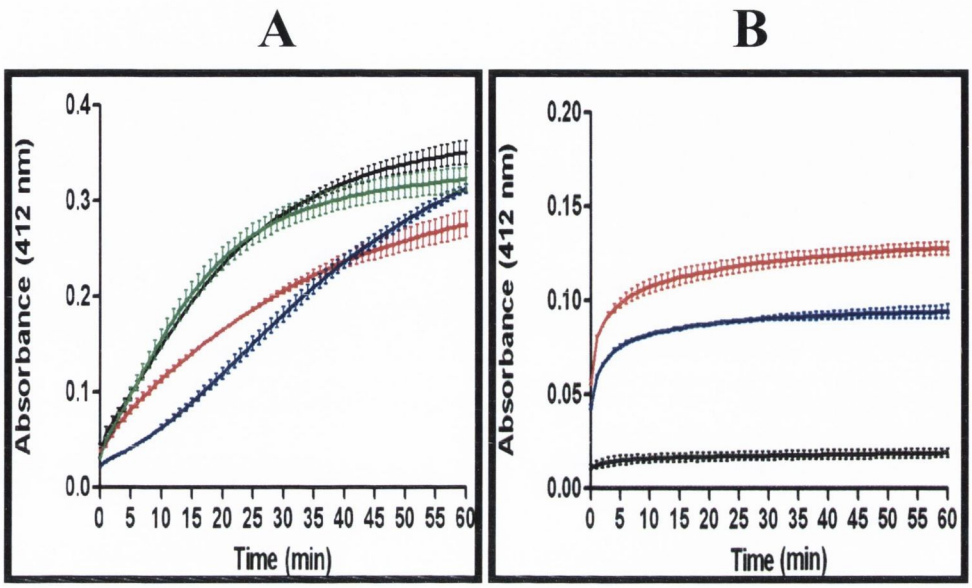

Fig. 3.21. Reactivity of the tubulin sulphydryl residues with DTNB. A. Bovine tubulin (2 μM) in the presence of DMSO (1% (v/v)) as control (**black**), APM (50 μM) (**green**), colchicine (50 μM) (**red**) and vinblastine (50 μM) (**blue**). After 30 min, the percentage reduction of DTNB reactivity with the sulphydryl groups was determined. APM - <1%, colchicine – ~32% and vinblastine – ~34%. This indicated that APM did not bind to bovine tubulin but colchicine and vinblastine did. Panel **B:** MBP (8 μM) (**black**), recombinant MBP-αI/β-tubulin 1 μM (**red**) and 2 μM (**blue**). None of the compounds used on their own was able to react with DTNB (data not shown). All experiments were repeated and the error margins are indicated by the vertical bars on the graph.

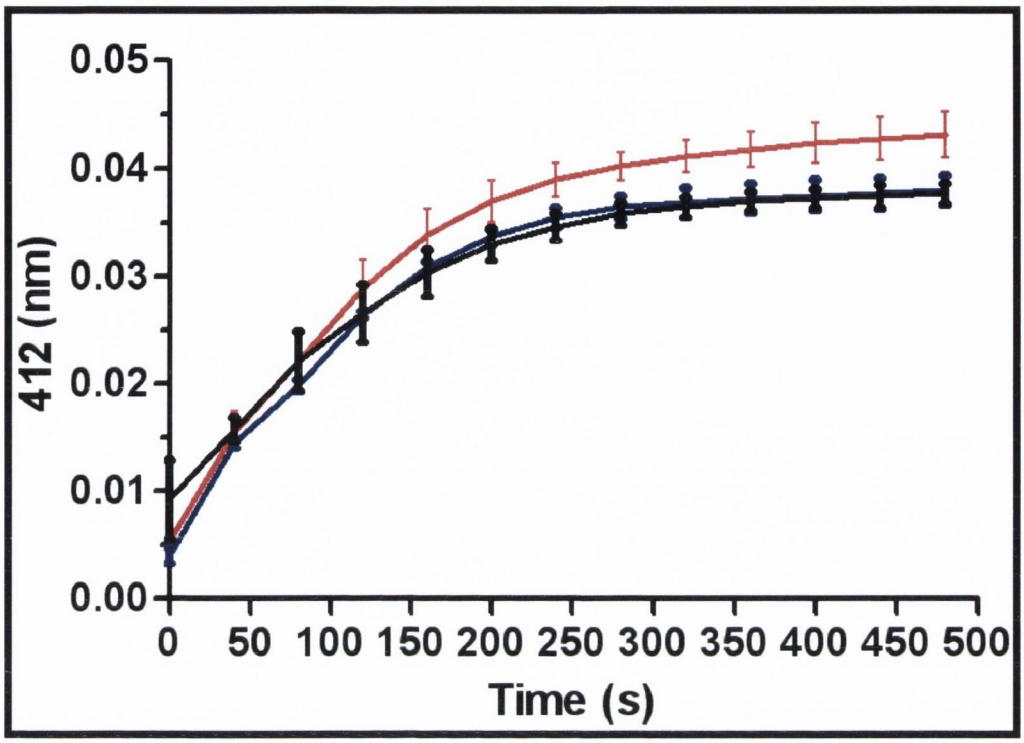

Fig. 3.22 Analysis of the sulphydryl reactivity of bovine brain tubulin with high concentrations of APM. **A**: reactivity of bovine brain tubulin (0.15 μM) in the presence of DMSO (1% (v/v)) as control (**black line**) and two concentrations of APM, 50 μM – ~0.15% quench (**blue line**) and 100 μM – ~11.12% increase (**red line**). All experiments were repeated as and the error margins are indicated by the vertical bars on the graph. APM (100 μM) was demonstrated to affect the sulphydryl activity of bovine brain in a statistically significant fashion, as deduced by a Student t-test with a 95% confidence (P value <0.0001). However, at a lower concentration of APM (50 μM), there was no significant difference (P value = 0.8701). This may indicate that at high concentrations, APM may be able to bind to bovine tubulin.

Quenching was quantified by combining the total fluorescence change from all the points that were gathered over the range of 300 – 400 nm (200 points) and comparing that value to the control (DMSO only). Since a range of points were used to calculate the fluorescence change, fluctuations that occur at single points were minimised. MBP contains 8 tryptophans and fluoresces strongly at 350 nm when excited at 280 nm. Therefore, it was necessary to compensate for the effects of MBP and any non-specific interactions with the tubulin. This was done using a molar-equivalent of free tryptophan in place of the fluorophore(s) to predict the non-specific quenching (Werbovetz *et al.,* 2003 and Yakovich *et al.,* 2006). Therefore, free tryptophan amino acids replaced the 4 residues that exist on either of tubulin and the 8 residues that exist on the MBP molecule (Werbovetz *et al.,* 2003 and Yakovich *et al.,* 2006). Also, a certain proportion of the excitation and emission light are non-specifically absorbed or scattered by the sample, a phenomenon known as "inner filter effects". This phenomenon can be minimised by reducing the concentration of the fluorophore(s) so that the overall sample absorbance is <0.1 (Pain R., 2004). However, this was not always possible so it was necessary to correct for these changes by using a specific equation (see section 2.8.3.2) developed by Lakowicz (1999). These corrections were most evident at high ligand concentrations (Fig. 3.23).

Bovine brain tubulin was also used as a negative control by incubating it with APM for 5 min at 37°C. A longer incubation time did not affect the fluorescence quench. Only at high concentrations (~ 100 μM) was a slight effect observed after the results were corrected for non-specific quenching (Fig. 3.23 B), which was in good agreement with the results from the sulphydryl assay (Fig. 3.22).

The disassociation constants (K_d) for tubulin-ligand interaction were determined using the method as described by Acharya *et al.,* 2008 (Acharya *et al.,* 2008). Briefly, the maximum quench a ligand could achieve by occupying every available binding site on the tubulin was calculated (i.e. the F_{max}). This data was obtained by extrapolating the double reciprocal plot of the change in tubulin fluorescence versus the ligand concentration back to the y-axis (Fig. 3.24 and 3.25). The F_{max} value was compared to the predicted number of currently occupied tubulin-ligand sites at a particular ligand concentration. Vinblastine was known to bind specifically to bovine tubulin at one site per dimer and was used as a positive control for the assay. A 30 min incubation time of bovine brain tubulin with vinblastine at

37°C was required to generate reproducible results. The calculated K_d was 0.91 ± 0.29 μM (Fig. 3.24 and Table 3.1).

The tubulin-fusion proteins were incubated with APM for 5 min at 37°C. The tubulin fusions were measured as monomers (0.3 μM) or as a mixture (0.15 μM each). An equi-molar concentration of tryptophans was present in the samples to minimise error caused by using different tryptophan controls which was the reason for using twice the molar concentration of the monomer compared to the mixture. At least five different ligand concentrations were used for determining the K_d. The K_d for the recombinant tubulins was calculated in the same way as bovine tubulin. APM was able to quench the tubulin fusion mixture significantly over a range of concentrations (Fig. 3.25), which was not possible with bovine tubulin (Fig. 3.24). MBP-β-tubulin had less affinity for APM than MBP-αI-tubulin but the mixture had a greater affinity still. Oryzalin was demonstrated to bind almost 3–fold better to the tubulin-fusion mixture than APM (Table 3.1).

The fluorescence quenching assay was able to generate ligand-binding data for the MBP-tubulin fusions. It was not attempted with the other recombinant tubulins (e.g. His_{12}-tagged) as they did not appear to be functional. Unfortunately, this assay was a low-throughput assay but it was suitable for generating some binding data that will be discussed in subsequent chapters.

3.3 DISCUSSION

Purification of tubulin directly from *P. falciparum* is hindered by the scarcity of the protein in the erythrocytic stage of the parasite life-cycle and the limited amount of starting material available. Therefore, recombinant tubulin was previously generated to achieve sufficient quantities of the protein for biochemical analysis (Fennell *et al.,* 2006). However, this recombinant tubulin was produced with an MBP-tag attached and only limited functional studies were conducted. The aim of the work in this chapter was to generate tubulin that could be used for ligand-protein binding assays.

Recombinant MBP-fusion tubulins were previously generated by using the pMAL-c2X vector in an *E. coli* expression system. Initial attempts to cleave the MBP tag from the recombinant tubulin using a specific endo-protease, factor Xa, were unsuccessful due to the formation of numerous bands <50 kDa. Since the tubulin

Protein Sample	Conc. (μM)	Compound	F_{max} R^2 Value
Bovine Tubulin	0.15	***Vinblastine*** 0.91 μM ± 0.29	0.8797
MBP-αI/β-tubulin	0.15	***Oryzalin*** 15.51 μM ± 3.55	0.9453
	0.15	***APM*** 44.14 μM ± 7.15	0.9712
MBP-αI-tubulin	0.3	***APM*** 87.4 μM ± 19.91	0.8852
MBP-β-tubulin	0.3	***APM*** 162.63 μM ± 24.72	0.9048

Table 3.1. Representation of the K_d generated by the fluorescence quenching assay using the recombinant tubulin and bovine brain tubulin. A significantly lower K_d was generated for the MBP-fusion mixture (0.15 μM) than the monomers (0.3 μM). This may be a result of a one high–affinity binding site when the monomers are mixed together. Oryzalin was also used and it was demonstrated to have a greater affinity for tubulin than APM. Bovine brain tubulin and vinblastine were used as a positive control. F_{max} R^2 value, the accuracy of the best fit line for determining the F_{max} (closer to 1.00 the more accurate the fit).

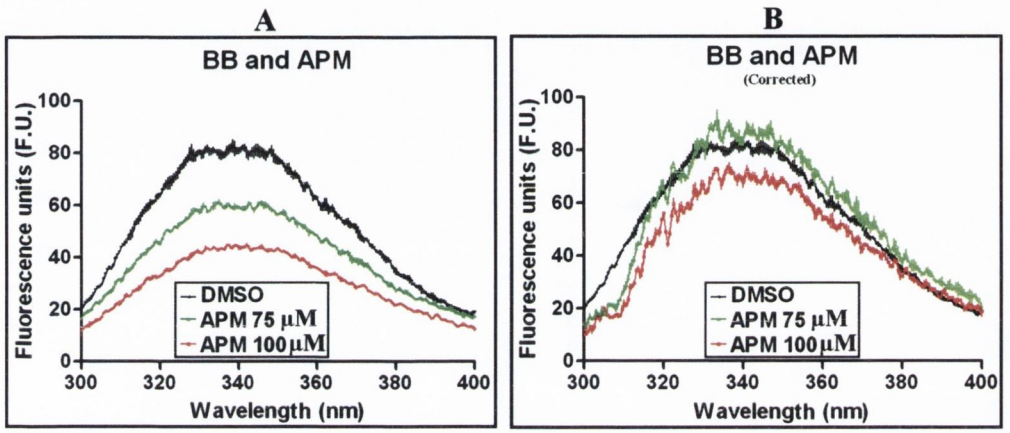

Fig. 3.23 Intrinsic fluorescence of bovine brain (BB) tubulin (0.15 µM) in the presence/absence of APM (75 µM or 100 µM) when excited at 280 nm. A. The bovine brain tubulin fluorescence was significantly reduced in the presence of APM but the majority of this quench was non-specific. This non-specific quench was corrected using tryptophan fluorescence and compensating for the inner filter effects. **B.** The corrected bovine brain tubulin graph showed that 100 µM of APM caused a ~11.72% quench which was statistically significant (P value <0.0001) but the quench at 75 µM APM of ~ 0.26% was not significant (P value = 0.1409).

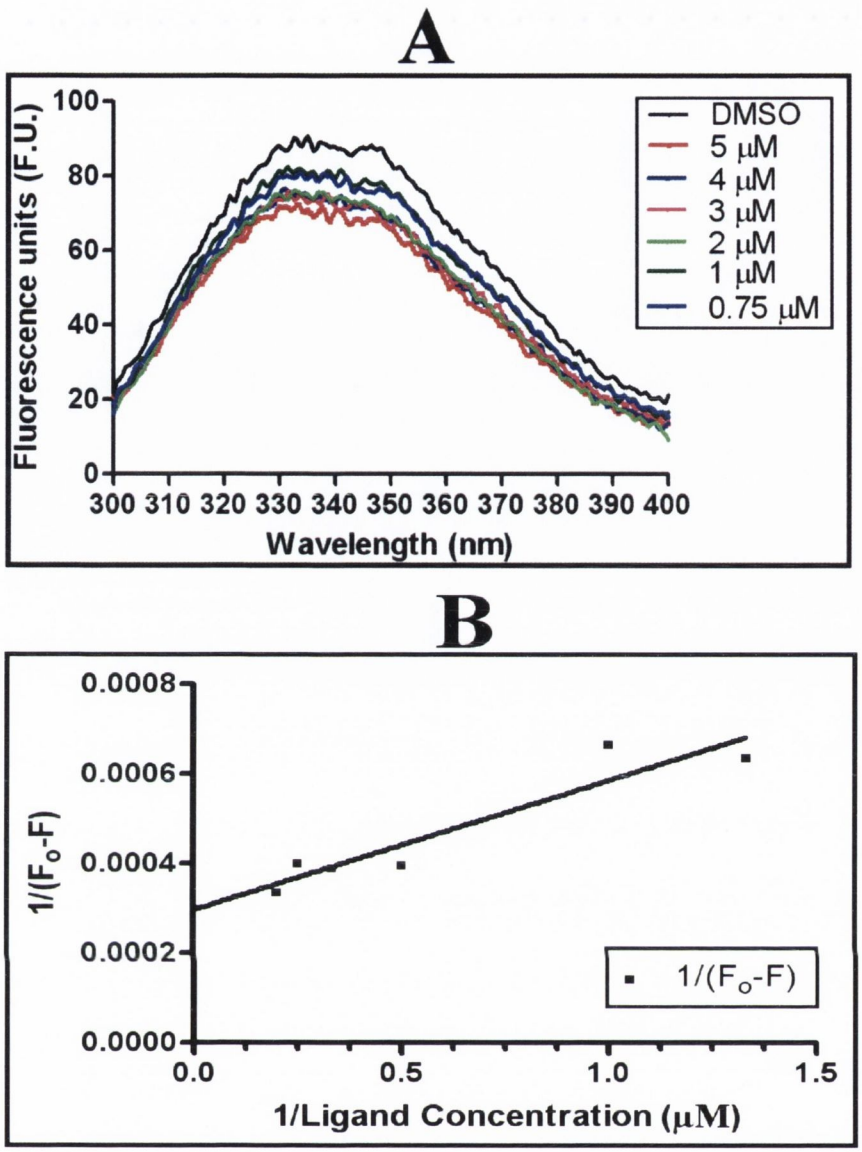

Fig. 3.24. Analysis of bovine brain tubulin intrinsic fluorescence in the presence of different concentrations of vinblastine. A. Bovine brain tubulin (0.15 μM) was incubated with either DMSO (control) or different concentrations of vinblastine for 30 min at 37°C. Three independent samples were used for each concentration. Error bars have been omitted for clarity. **B:** this graph depicts the double reciprocal plot of the fluorescence change and ligand concentration. A best fit line was used to plot the graph (R^2 value = 0.8797). The F_{max} (the point of interception at the y-axis) was used to predict the maximum fluorescence quench achievable. $\mathbf{F_o}$ represents the observed fluorescence in the absence of a ligand (after correction). **F** represents the observed fluorescence in the presence of a ligand (after correction).

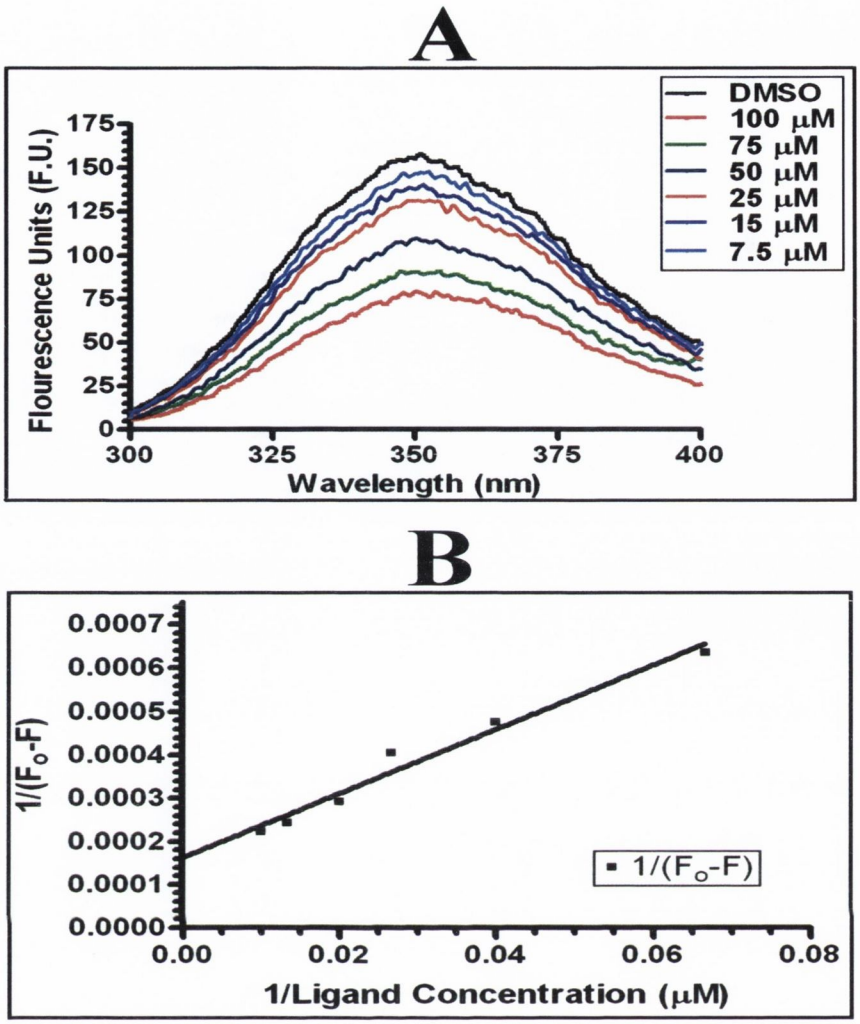

Fig. 3.25. Analysis of the intrinsic fluorescence of MBP-αI/β-tubulin mixture in the presence of different concentrations of APM. **A.** The MBP-αI/β-tubulin mixture (0.15 μM) was incubated with either DMSO (control) or different concentrations of APM for 5 min at 37°C. Three independent samples were used for each concentration. For reasons of clarity, the errors bars have been omitted and the uncorrected fluorescence was graphed. **B.** The double reciprocal plot of the corrected fluorescence change and ligand concentration. A best fit line was used to plot the graph (R^2 value = 0.9712). The F_{max} (the point of interception at the Y-axis) was used to predict the maximum fluorescence quench achievable. $\mathbf{F_0}$ represents the observed fluorescence in the absence of a ligand (after correction). **F** represents the observed fluorescence in the presence of a ligand (after correction).

fusions were stable under the same conditions in the absence of the enzyme, it was likely that factor Xa was responsible for non-specifically cutting the chimeric protein despite the absence of any obvious recognition sites. However, since some cleaved tubulin was generated, it was worthwhile determining if it were possible to isolate this tubulin. Cleaving the fusion tubulins while they were attached to the amylose column had the advantage of removing the largest sources of contamination, uncleaved tubulin and cleaved MBP. Furthermore, since the tubulin samples did not require maltose to elute them, the samples could be re-run over the amylose column further to remove residual contamination. However, significant breakdown was observed after MBP-β-tubulin was incubated with factor Xa. Also, cleaved MBP and uncleaved MBP-β-tubulin were also eluted from the column. Re-running the samples over the amylose column did not remove this contamination. It is possible that the MBP-amylose bond weakened over time releasing the uncleaved proteins. In conclusion, factor Xa is not a suitable enzyme for cleaving the MBP-tag from *P. falciparum* tubulin.

Although factor Xa could not be used, two alternative enzymes, genenase I and enterokinase, whose cleavage sites have already been encoded into the pMAL vector, were commercially available. The MBP-tubulin fusions which had a specific cleavage site for factor Xa only were incubated with these enzymes using the recommended conditions to determine if they were suitable for future cleavage experiments. Enterokinase was determined to degrade the tubulin fusions and was ruled out. However, genenase I did not digest either of the fusion tubulins. Therefore, both αI-tubulin and β-tubulin were cloned into the pMAL-c2G vector which encoded a genenase I recognition site. These clones were designed so that genenase I would cleave the MBP tag from the tubulins with no additional amino acids. Both tubulins were expressed and purified to near homogeneity as before. Factor Xa was incubated with these MBP-fusion tubulins and it was shown to degrade the proteins non-specifically. Initially, genenase I was very inefficient at cleaving the MBP-tag from the tubulin-fusions, with an eventual plateau of free tubulin being reached that could not be increased despite using excess enzyme, extended incubation times and various temperatures. The reason for this plateau was not known, although one possibility was that the enzyme became inhibited or denatured over time which reduced its efficiency. Therefore, an experiment was designed so that increasing amounts of enzyme were added to a tubulin fusion sample at a set period of time.

However, this did not increase the overall yield of free tubulin. A second possibility was that the genenase I recognition site was partially buried between the tubulin and MBP proteins. Therefore, it was investigated whether the tubulin fusions could be slightly denatured to increase the efficiency of genenase I. A range of SDS concentrations were added during standard cleavage experiments to determine if it had any effect. More than 0.01% (w/v) of SDS reduced the activity of genenase I, presumably by denaturing the enzyme. However, an optimum concentration of SDS was discovered that increased the efficiency of the enzyme compared to that obtained in samples without SDS. Therefore, the genenase I recognition site appears to be occluded in the chimeric protein, reducing the activity of the enzyme. This occlusion could be due to the fact that the enzyme cleavage site is at the very start of the tubulin instead of being in a more exposed position. The reason the site was chosen was to minimise additional amino acids being left attached to the tubulin once the MBP tag was cut off. This further explains why increasing concentrations of genenase I did not also increase the production of free tubulin. Interestingly, the optimal cleavage conditions for the two tubulin fusions were significantly different. This is likely due to conformational differences between the MBP-tubulin fusions affecting the exposure of the genenase I recognition site. Isolation of this free tubulin was attempted using ion–exchange chromatography but it was not possible to remove the uncleaved tubulin (data not shown). Therefore, this strategy was not suitable for large scale production of untagged tubulin.

P. falciparum tubulin over–produced in *E. coli* was generally completely insoluble, with the exception of the MBP-fusions. One possible reason for tendency of the tubulin consistently to aggregate in *E. coli* cells was the fact that the protein was expressed in isolation preventing it from forming a natural heterodimer. This was demonstrated to be an essential factor for improving the solubility and functionality of other dimeric proteins (Li *et al.,* 1997). This approach is not novel for tubulin, though, as Linder *et al.,* (1998) generated a bicistronic vector to express *Reticulomyxa filosa* tubulin (Linder *et al.,* 1998). They reported an increase in tubulin solubility and protection from non-specific degradation, but the tubulin could not polymerise. Nonetheless, this strategy merited investigation as the *Plasmodium* α- and β-tubulin were only 86% and 51% identical to *Reticulomyxa* tubulins at the amino acid level respectively (data not shown). Although this vector permitted the use of fusion tags (His_{12}-tag or S-tag), these were avoided in favour of generating native-like tubulin

that, if assembly-competent, would have been purified by the standard assembly/disassembly technique. The pET-Duet-αI/β-tubulin and pET-Duet-αII/β-tubulin constructs were successfully generated. However, due to cloning restrictions, translation of the β-tubulin protein began prematurely so that 14 extra amino acids were added to its N-terminus. Site–directed mutagenesis was used to remove an upstream ATG start codon and generated an "altered" plasmid which coded for native αI- and β-tubulin. Unfortunately, this plasmid became unstable and could not be sequenced so it was not possible to verify if this ATG was removed. Therefore, expression of the pET-Duet-αI/β-tubulin construct which included the upstream ATG and the potentially "altered plasmid" were used for expression of the recombinant proteins. One large band was observed after Coomassie blue staining of an SDS poly-acrylamide gel. It was not clear whether this band included both αI-tubulin and β-tubulin so a western blot was used to confirm that both of these proteins were expressed. A solubility test determined that proteins were mostly insoluble although it was possible to detect the presence of both tubulins in the soluble fraction by a western blot. This may however just represent residual insoluble protein. The samples were kept consistently cold to minimise the possibility of unwanted polymerisation, in case this was a factor. Furthermore, the proteins appeared to be degraded non-specifically in at least two different sites. Overall, this method does not appear to improve the solubility of the tubulins. However, it may still be worthwhile in the future to use the same vector with a His_{12}-tag attached to one of the proteins which would permit an easy method for purification but also allow for the detection of tubulin dimerisation.

Refolding aggregated tubulin has been achieved independently by several groups over the years using two general approaches, biological renaturation and chemical renaturation. Aggregated tubulin can be forced to become soluble, typically by dissolving it in concentrated urea. The biological refolding approach for tubulin uses the native chaperone machinery present in eukaryotic cells, notably rabbit reticulocytes, to correctly and specifically to renature the tubulins. Rabbit reticulocytes are particularly useful as they contain all the components of the tubulin chaperone system (CCT) but virtually no tubulin (Shah *et al.*, 2001). However, this technique is known to produce only low yields of refolded tubulin (microgram amounts) compared to the initial sample (milligrams). Despite this limitation, assembly–competent tubulin could perhaps be used to nucleate tubulin directly from

the parasite, increasing the amount of the original protein sample. Also, surface plasmon resonance techniques, require only microgram concentrations of protein to coat a chip which can be re-used several times for different ligand interaction studies. Therefore, microgram yields like those obtained by Shah *et al.,* (2001) would not be a significant barrier. Untagged tubulin was produced as insoluble inclusion bodies. Several rounds of mild detergent washes generated almost completely pure tubulin. The tubulin was completely solubilised in urea but only limited quantities could be added to the rabbit reticulocyte lysate (RRL) as high urea concentrations would denature the chaperone proteins. More β-tubulin was added into the refolding sample than αI-tubulin due to the reduced efficiency of β-tubulin refolding (Shah *et al.,* 2001). Unfortunately, it was not possible to obtain the same quantities of RRL (100 ml) as Shah *et al.,* (2001) due to the high cost associated with this product and a scaled–down version of the same experiment was conducted instead using less RRL (1 ml). A sedimentation assay was used to determine whether the tubulin was assembly–competent. The initial fraction at 4°C was primarily soluble although there was significant smearing on the gel. The cause could not be determined exactly. It is possible that an excess of sample was used by accident. At 37°C, nearly all of tubulin was present in the soluble fraction indicating that it did not polymerise. This may be the result of non-optimal assembly conditions, particularly due to the presence of urea (<0.4 M) which was introduced to the RRL with the denatured tubulins. Alternatively, the tubulins may still be still mis-folded and are only soluble due to the presence of urea. However, a very faint band was visible in the pellet fraction which could represent polymerised tubulin. This was further verified by the presence of a weak but obvious band in the 4°C soluble fraction indicating that the refolded tubulin was sensitive to temperature shifts. Although it appears that this method can generate functional tubulin, it is unlikely to be used further due to its technical difficulty and very low yields.

Chemical refolding is dependent upon the tubulins' spontaneously refolding themselves into the correct conformation. Several groups have argued that tubulin requires specific machinery in order for it to be correctly folded (Guha *et al.,* 1997, Llorca *et al.,* 2000 and Lewis *et al.,* 1997), which contradicts other reports that have demonstrated tubulin which can bind known tubulin inhibitors or form MT's (Koo *et al.,* 2009, Lubega *et al.,* 1993, Oxberry *et al.,* 2001, Jang *et al.,* 2008, Koo *et al.,* 2009 and Wampande *et al.,* 2007). Therefore, this technique remains controversial but one

striking difference between the opposing groups is the source of tubulin that is used in these studies. Generally, protozoal, fungal or plant tubulin were successfully refolded in contrast to the mammalian brain tubulin which could not be renatured. However, significant differences between these proteins may explain the disparity of results with regard to producing refolded tubulin.

Previous attempts in our lab using a chemical refolding strategy based upon the work of Lubega *et al.,* (1993) were unsuccessful primarily due to mis-folding of the protein (Dr. Brian Fennell; Fennell, 2005). However, a new on-column procedure developed by Jang *et al.,* (2008) has since claimed to generate assembly–competent tubulin (Jang *et al.,* 2008). This method primarily differed from that of Lubega *et al.,* (1993) as it would theoretically prevent partially folded tubulins from interacting and aggregating. The tubulins generated from this system were determined to be almost completely pure and soluble in the absence of urea. However, concentrating the tubulins past > 6 μg/μl caused them immediately to precipitate out of solution. These tubulins were incapable of polymerising, unlike those of Jang *et al.,* (2008) (Jang *et al.,* 2008). Protein refolding is a difficult procedure that often requires optimisation by empirical investigation for a specific protein. Therefore, it is possible that further optimisation of this procedure could lead to success with *Plasmodium* tubulin.

Although it was known that the MBP-αI- and β-tubulin fusions were unable to polymerise with each other as judged by the turbidimetric assay, it was unknown if they could dimerise (Dr. Brian Fennell; Fennell, 2005). Evidence that MBP-αI-tubulin could co-polymerise in a dose–dependent manner with bovine brain tubulin suggested that this protein was correctly folded and capable of forming dimers and polymers (Fennell *et al.,* 2006). Therefore, non-denaturing 5% and 10% polyacrylamide gels were used to resolve the tubulins. MBP and bovine brain were used as controls. It was not possible to resolve the tubulin fusions by native PAGE in the absence of 2-mercaptoethanol. This reagent cleaves disulphide bonds, which can form over time, especially in tubulins which generally have numerous cystine residues (20 exist on bovine brain tubulin and 24 on MBP-αI/β-tubulin). The presence of 2-mercaptoethanol should not interfere with dimer formation as fully reduced tubulin is still capable of forming normal MT's (Britto *et al.,* 2005). The bovine tubulin formed a ladder of bands on the native PAGE, which represented dimers and oligomers of the protein, in agreement with previous work (Sulimenko *et al.,* 2002). MBP migrated as

one band only as expected. The tubulin-fusion mixture did not appear to form additional bands in comparison to the monomers alone, although two distinct bands were resolved. To clarify the results a western blot was conducted but the results were unclear due to excessive smearing on the blots (data not shown). Therefore, dimers may be formed, but they could not be distinguished. The His_{12}-tagged, refolded tubulins were also examined using this method, but it was not possible to resolve these proteins on the gel indicating that perhaps they had permanently aggregated.

In order to avoid further use of non-denaturing gels, a covalent crosslinking strategy was employed so that a denaturing polyacrylamide gel could be used to resolve the proteins, producing a sharper image. Glutaraldehyde is capable of non-specifically covalently cross-linking proteins that are in close proximity to each together by acting as a link between amine groups of different proteins. Optimal conditions for this experiment needed to be determined empirically by incubating the glutaraldehyde and tubulins for different lengths of time. The proteins were resolved on SDS-polyacrylamide gels of different concentrations (5% and 7.5% polyacrylamide) to encourage the proteins to resolve on the gels. The 7.5% polyacrylamide gels were able to clearly resolve proteins of ~250 kDa (myosin molecular weight marker). The fusion proteins should form dimers of around ~200 kDa and it should be possible to resolve them on these gels. Bovine brain tubulin was able to form obvious dimers on the gel. However, despite using a range of incubation times, the MBP-fusion tubulins immediately aggregated once they were cross-linked. This aggregation appeared to occur immediately as there was no intermediate stage at which some cross-linked tubulin could resolve. His_{12}-tagged refolded tubulins were also examined using this technique but it was not possible to resolve them clearly either (data not shown).

To characterise whether the tubulin fusions could assemble, a temperature-regulated sedimentation assay was used. Essentially, the tubulins are sedimented by centrifugation at either 4°C or 37°C. This permits the isolation of assembly-competent tubulin from soluble tubulin (sedimented at 37°C but not at 4°C). Residual protein (not sedimented due to temperature) that adhered to the polymerised tubulin or the eppendorf tube was washed away leaving only the sedimented tubulin. Previous attempts in our lab to sediment the MBP-αI/β- tubulins were unsuccessful (Fennell, 2005). However, oxidation of the cystine residues inhibits tubulin polymerisation

(Britto *et al.*, 2005). Therefore, an excess of 2-mercaptoethanol, a reducing reagent, was added to all the samples before the assay was conducted. Bovine brain tubulin was used as a control for this assay and despite being sensitive to temperature changes, a significant proportion of the protein was sedimented after the 37°C centrifugation (60%) but the majority of this sample remained insoluble (42%) after the final 4°C centrifugation. This result was surprising as almost all of the tubulin was expected to be soluble at this point with just some residual insoluble amounts. Chaudhuri *et al.*, (2001) suggested that at least one intra-chain disulphide bond exists in both the α- and β-tubulin subunits and it is essential for MT assembly and stability (Chaudhuri *et al.*, 2001). This would explain why some of the tubulin did not polymerise, hence remained in the soluble fraction after the 37°C centrifugation and also the possible formation of bovine aggregates that were insoluble at 4°C. However, this disulphide bond was not recorded in the bovine tubulin crystal structure, nor did Britto *et al.*, (2002) concur with these results (Nogales *et al.*, 1998 and Britto *et al.*, 2005). Alternatively, aged tubulin is known to lose the ability to polymerise and forms aggregates. This phenomenon is both temperature (optimum is 37°C) and time (≥1 h) dependent (Roychowdhury *et al.*, 2000). Tubulin aging is not caused by disulphide bond formation or cystine oxidation (Britto *et al.*, 2005 and Correia *et al.*, 1993). The centrifugation steps and incubations on ice or in a 37°C water bath were kept deliberately short in order to minimise this effect. However, the incubations needed to be sufficiently long for tubulin to either polymerise or depolymerise and then it was necessary to sediment the sample. As a result, it was not possible completely to dissolve the bovine brain tubulin after the 37°C step. To compensate for the protein difference in the MBP-α/β-tubulin mixture, MBPΔmultiple cloning site (MCS) was added to the monomer samples. The MBPΔMCS was designed so that it was identical to the MBP protein portion that was attached to the MBP-fusion tubulins. Expression of the pMAL vector produces MBP along with the MCS. The tubulin fusions were mostly soluble after the first 4°C centrifugation. It is likely that any sedimented tubulin was just residual soluble protein as the amounts were very low and varied from 0% – 7% (from different experiments) of the total sample added. Although the MBP-αI-tubulin was not sedimented at 37°C, indicating that it could not polymerise, both MBP-β-tubulin and the MBP-α/β-tubulin produced a significant pellet. It has been shown before that the recombinant tubulin proteins can form homo-dimers under assembly–promoting conditions (Koo *et al.*, 2008 and

Oxberry *et al.,* 2001). Therefore, it was not possible to determine if MBP-tubulins were in fact forming polymers or if they had aggregated due to the increased temperature. Both of the tubulins were insoluble at 4°C but this was also the case for bovine tubulin so it was possible that the same phenomenon of tubulin ageing-related aggregation had occurred. It may be worthwhile in the future to examine these sedimented tubulins by electron microscopy to determine if MT structures are in fact formed. It may also be possible to increase the yield of polymerised tubulin by removing the MBP tag. The MBP-tag could allosterically hinder the formation of MT's or it may increase their solubility which would mean that higher centrifugation speeds are required to sediment the tubulin sample.

MBP-tubulin fusions which still have the tag attached have been used previously for ligand interaction studies (Fennell *et al.,* 2006, Giles *et al.,* 2008 and Holloman *et al.,* 1998). Therefore, two well-established assays were focused on to measure the binding of APM, a representative from the phosphorothioamidate family and oryzalin, a representative from the dinitroaniline family.

Reduced sulphydryl residues are highly reactive with the DTNB reagent and have been used to determine conformational changes occurring in tubulin due to ligand interactions or the aging effect (Werbovetz *et al.,* 1999, Koo et al., 2009, Gupta et al., 2002, Chaudhuri *et al.,* Roychowdhury *et al.,* 2000, Britto *et al.,* 2002 and Britto *et al.,* 2005). Therefore, this assay was developed to measure ligand-induced changes to the recombinant tubulins. Bovine tubulin was used as a comparison to the recombinant tubulins, although it does have fewer cystine residues on the heterodimers (20 on bovine tubulin and 24 on the *Plasmodium* tubulin). An immediate reaction between DTNB and tubulin was believed to be a result of a specific group of solvent–exposed "fast-reacting" sulphydryl residues which tend to be very sensitive to this reagent (Roychowdhury *et al.,* 2000). The steady climb to the plateau was thought to be the result of buried "slow-reacting" sulphydryl groups finally reacting (Roychowdhury *et al.,* 2000). Both colchicine and vinblastine significantly decreased the sulphydryl reactivity of bovine tubulin by either binding close to or interacting with cystine residues. Therefore, it is possible to determine small ligand-protein interactions by this method. Although APM has a sulphur atom, it did not react with DTNB even at the highest concentration used (200 μM), which was expected as DTNB only reacts with reduced sulphydryl groups. It was interesting to determine if APM could bind to bovine tubulin as previous reports did suggest that

high concentrations of dinitroanilines (thought to have the same binding site as phosphorothioamidates) could bind to mammalian tubulin (Werbovetz *et al.,* 2003). Therefore, a low concentration of bovine tubulin (0.15 μM) was incubated with high concentrations of APM (50 – 100 μM). At the highest concentration used (100 μM), the APM interaction with tubulin caused a statistically significant increase in sulphydryl reactivity rather than a decrease. It was likely that the binding of the ligand caused a conformational change in the tubulin dimer that exposed buried cystines. This has been shown before with an unrelated tubulin ligand, griseofluvin (Chaudhuri *et al.,* 1996). Furthermore, at lower APM concentrations (50 μM) this effect was reversed indicating a weak binding between tubulin and the ligand. This is in good agreement with previous *in vitro* tubulin binding studies (Werbovetz *et al.,* 2003) and known lack of effect of APM on mammalian cell cultures (Murthy *et al.,* 1994 and Fennell *et al.,* 2006). This assay was used with the His_{12}-tubulin fusions and MBP-tubulin fusions. DTNB did not react with the His_{12}-tagged tubulins. It is possible that the sulphydryl groups became oxidised during the refolding or purification procedure. MBP-tubulin fusions previously lost all their reactivity to DTNB following dialysis (data not shown). However, other groups have successfully employed this technique, so it is possible that another factor is responsible for the unreactive nature of the His_{12}-tubulin fusions (Koo *et al.,* 2009). The MBP-tubulin fusions were capable of generating a dose-dependent response to the reagent DTNB as either monomers (data not shown) or as a mixture (Fig. 3.21 B). However, even at the highest ligand concentration used for either vinblastine or APM (200 μM), no difference in the sulphydryl reactivity was observed indicating that the ligands either did not interact with the tubulins or the sulphydryl residues could not detect the change. The tubulins may have aged which could reduce their ability to react with DTNB (Britto *et al.,* 2002). This might explain also their apparent lack of activity compared to bovine brain tubulin, although, the two cannot be compared as a strict measure. This is especially true since *Plasmodium* tubulin dimers have more cystine residues than bovine tubulin, 24 and 20 respectively. The aging effect may be exacerbated by the prolonged exposure of the recombinant tubulins to 37°C for 3 h during their production in *E. coli.* This aging effect may be minimised if the protein synthesis was reduced to 1 h or less. However, this would obviously have a significant impact on yield, but the optimal time may be worth investigating. Since it was possible that the tubulins became oxidised during the purification, 2-

mercaptoethanol was added to all the buffers. However, this did not make a significant difference indicating that oxidation of the cystines was not a major problem during routine purifications.

Since it was not possible to determine tubulin-ligand-binding via the reactivity of cystine residues, exploitation of tryptophan fluorescence was investigated based on previous accounts (Werbovetz *et al.,* 1999, MacDonald *et al.,* 2004 and Sardar *et al.,* 2007). By using the crystal structure of bovine tubulin, it was possible to view the distribution of the tryptophans on the dimer in the presence of vinblastine (Fig. 3.26). The vinblastine binding site lies between the tubulin dimer-dimer interface and four tryptophans are within 30 . Therefore, it is not surprising that this drug can create a noticeable fluorescence quench. The large excess of ligand to tubulin was used to create a pseudo-first order reaction so the binding equilibrium would be rapidly established. This reduced the need for prolonged tubulin incubations at 37°C which could be detrimental to the protein by promoting the aging effects previously described. Initially, the MBP-fusion tubulins were examined for an optimal incubation time and a steady fluorescence was apparent after ~ 5 min (data not shown). For vinblastine binding experiments, a 30–min incubation time was used as it was previously reported to require ~15 min to reach an equilibrium (at a 2:1 ligand to protein ratio) (Lacey E., 1988). To determine the tubulin-ligand K_d, a series of calculations developed by Acharya *et al.,* (2008) were employed (Acharya *et al.,* 2008). Vinblastine binding to bovine brain tubulin was previously determined using this method so it was repeated here as a positive control. The vinblastine K_d was determined to be 0.91 μM +/- 0.29 μM which is comparable to previously published data (Avila, 1990).

The exact binding site for the herbicide compounds on tubulin is unknown, although at least 3 putative sites have been proposed (see section 1.6). Using a homology model of *Plasmodium* αI/β-tubulin, it was possible to highlight the position of the tryptophans in relation to the Morrissette site (Fig. 3.27). This model predicted that at least 3 tryptophans were within 30 of the potential binding site. Furthermore, one tryptophan actually forms part of this molecular pocket. Therefore, this assay should be useful at determining the herbicide compounds interaction with tubulin. Both of the monomers and the mixture of the tubulin proteins were used in an attempt to demonstrate the binding of APM. This tubulin mixture had a final concentration of 0.15 μM but each of the tubulin monomers had a final concentration

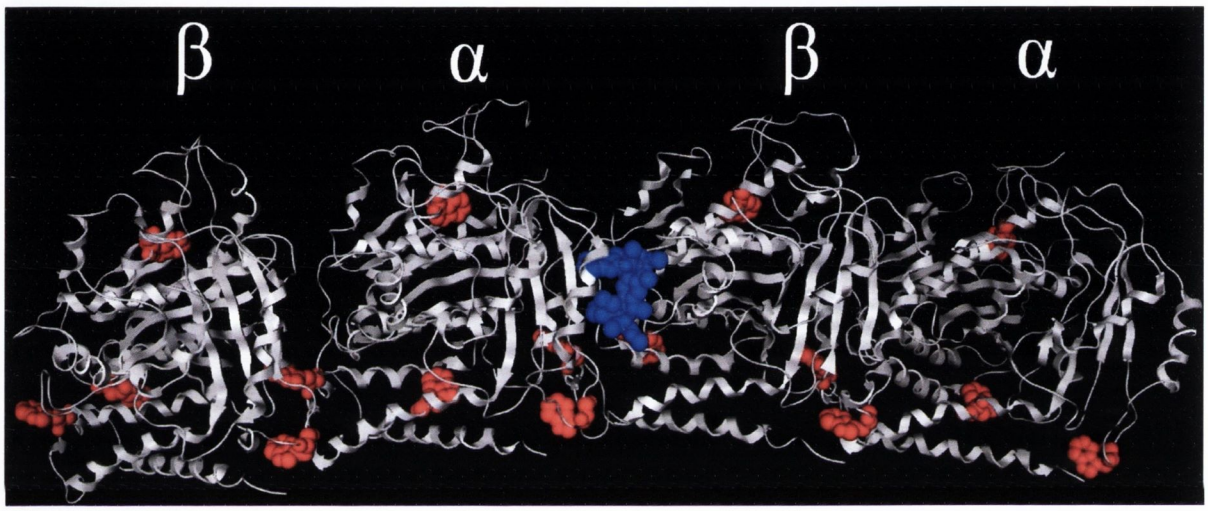

Fig. 3.26 Ribbon diagram of the α/β-tubulin dimer-dimer (1FFX) with vinblastine and tryptophans residues highlighted. Tryptophans residues, **red**. Vinblastine, **blue**. This model demonstrates that vinblastine compound is located <30 from 4 tryptophans.

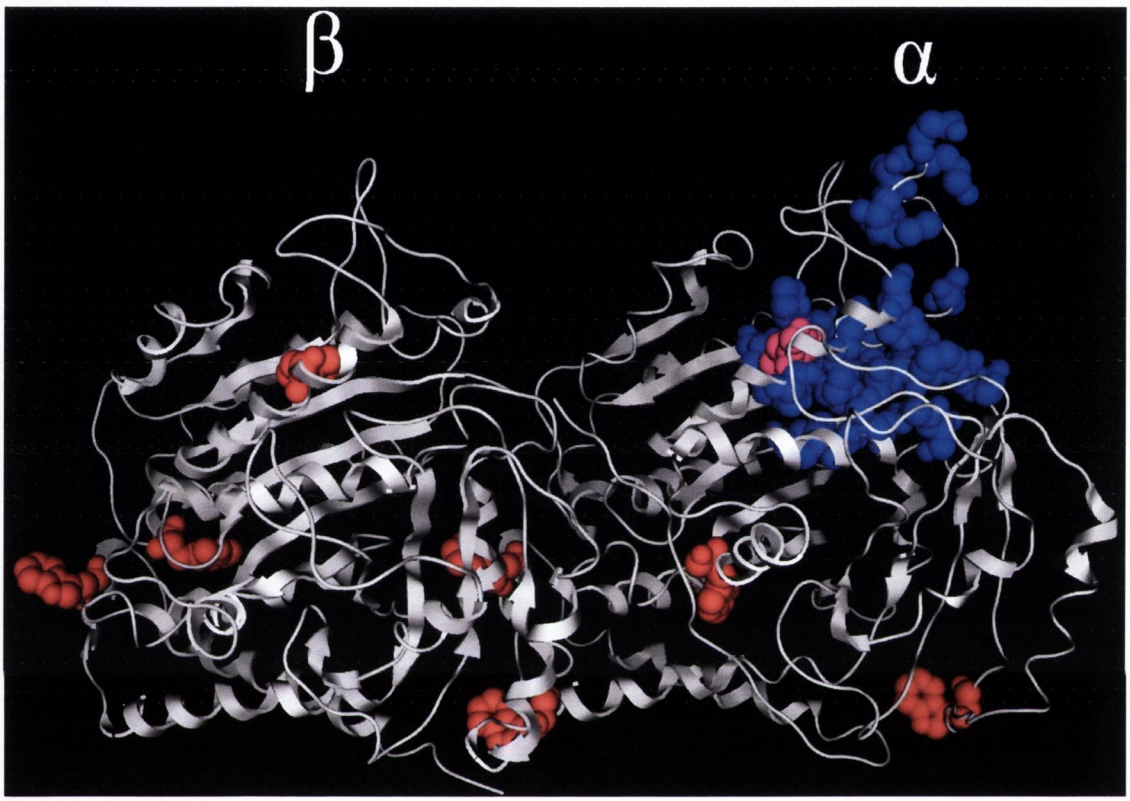

Fig. 3.27 Ribbon diagram of the *Plasmodium* αI/β-tubulin heterodimer with the putative Morrissette site and tryptophans residues highlighted. The tryptophans residues are **red** or **purple** (tryptophan 21 forms part of the putative Morrissette site) and the Morrissette site is **blue**. From the diagram, it was possible to measure that at least 3 tryptophans are within 30 of predicted herbicide binding site.

of 0.3 μM. The reason for this difference was to use equal amounts of protein in each sample so that the tryptophan controls would apply for all the experiments. This was done primarily to minimise the error caused by using different tryptophan controls. This approach meant that there was twice the concentration of MBP-αI-tubulin in the monomer samples as in the mixture, which would affect the tubulin/ligand ratio, particularly if the binding site existed solely on α-tubulin. However, this difference was accounted for during the calculations. Furthermore, since an excess of ligand was used, the tubulin-ligand complex was not critically affected so the data from the monomer and αI/β mixture samples could be compared. It was not possible to detect vinblastine binding to the fusion-tubulins. There are several possible explanations for this result. The vinblastine binding site may be obscured or sterically hindered by the presence of the MBP protein. The binding site may not exist if tubulins do not form dimer-dimer interactions or were incorrectly folded. Finally, it is possible that vinblastine affinity is lost or reduced if the tubulin had aged. This is the case for colchicine, whereby aged tubulin loses up to 30% of its original capacity to bind the compound after 2 h incubation at 37°C (Roychowdhury *et al.*, 2000). The binding data suggested that APM could bind to both monomers, although a ~2 fold stronger affinity was observed for MBP-αI-tubulin (Table 3.1). A tubulin mixture was also used whereby MBP-αI- and -β-tubulin were mixed together and allowed to dimerise. The K_d for APM was almost 2-fold lower than αI-tubulin alone. This may suggest that the tubulin mixture has one high affinity binding site that exists only when both monomers are combined together. Since this was first report of the K_d of APM for tubulin, no comparable data exists. The dinitroanilines are thought to share the same or an overlapping binding site on tubulin as the phosphorothioamidates (discussed in detail in chapter 5) (Murthy *et al.*, 1994, Ellis *et al.*, 1994, Blume *et al.*, 2003 and Mitra and Sept, 2006). Therefore, it was interesting to elucidate the K_d for oryzalin to the recombinant tubulins-fusions also. The K_d measured, 15 ± 3 μM, was similar to the previously reported value for native *Leishmania tarentolae* tubulin, 17 ± 8 μM (Yakowich *et al.*, 2006). This suggests that the MBP-tubulin-fusions are at least partially folded correctly. Oryzalin appeared to bind to tubulin nearly 3-fold better than APM. The compounds have a similar IC_{50} against cultured parasites (6.1 μM and 3.5 μM respectively) (Fennell *et al.*, 2006). This discrepancy may be a result of the better accumulation of APM at its site of action in the live parasites. Trifluralin, a dinitroaniline which is structurally similar to oryzalin and has a IC_{50} of ~1.5 μM, was

demonstrated rapidly to accumulate inside parasitized erythrocytes. However, the majority of this compound became trapped in the cell membrane, which significantly reduced the amount of soluble compound available to interact with the tubulin (Naughton *et al.,* 2008). It is feasible that a similar problem exists with oryzalin despite it being more hydrophilic than trifluralin.

This represents the first time K_d values have been elucidated for interactions between small molecules and *P. falciparum* tubulin and may open the way for generating ligands with increased affinity for the protein. The aim of this work was to generate sufficient quantities of recombinant tubulin suitable for ligand-binding studies. Although several different strategies were attempted to generate functional native-like tubulin, this was not possible and the MBP-fusion tubulin remained the best option for biochemical studies. Despite the presence of the MBP-tag, it was possible to measure the interaction of representative compounds from the phosphorothioamidate and dinitroaniline groups despite the small size of these molecules.

Chapter 4

Antimalarial Activity and Structure-Activity Relationships of Compounds Related to Amiprophos-methyl (APM)

4.1. INTRODUCTION

Tubulin has been highly successful as a drug target particularly for cancer treatment. Inhibition of MT dynamics is a very effective method for controlling fast-dividing cells. *Plasmodium* is equally sensitive to some classical MT inhibitors, such as vinblastine or taxol, as mammalian cells. It is more resistant to colchicine. This lack of favourable selectivity has until now precluded the development of novel antimalarial drugs from tubulin inhibitors.

The dinitroaniline and phosphorothioamidate herbicides are different in the fact that they are more active against "lower" eurkaryotes such as plants, fungi and protozoa than against mammalian cells (Dow *et al.* 2002, Murthy *et al.* 1994, Fennell *et al.* 2006 and Werbovetz *et al.* 2003). This feature has lead to the development of novel herbicide-based compounds that exhibit strong affinities for purified tubulin from trypanosomes and *Leishmania* species, some of which are also highly effective against the cultured parasites (George *et al.*, 2007 and Giles *et al.*, 2008). George *et al.* used oryzalin as a starting compound for modifications but it was demonstrated that their derivatives were ineffective even at the highest possible dosage *in vivo* (George *et al.*, 2007 and Wu *et al.*, 2006). It was later established that their compounds were susceptible to significant metabolism and were completely cleared from the treated animal within several hours (Wu *et al.*, 2006). Nonetheless, these compounds were interesting as they demonstrated that parasite tubulin can be targeted, although it remains to be seen if the problems with *in vivo* metabolism can be overcome.

In view of the selective activity of the dinitroaniline and phosphorothioamidates herbicides on malarial parasites, we considered whether they might form the basis for development of new anti-malarial agents. There were several reasons for choosing APM over the dinitroanilines as a starting compound. The IC_{50} of APM and oryzalin are comparable for cultured parasites (Fennell *et al.*, 2006). However, oryzalin has been linked with secondary effects in plant cells such as changing the morphology of the endoplasmic reticulum and Golgi apparatus. This effect does not occur with other MT inhibitors, most notably APM (Langhans *et al.*, 2009). Furthermore, oryzalin can also open Ca^{2+} channels and possible even affect mRNA translation of tubulin (Giani *et al.*, 2002). These additional targets were thought likely to affect the assessment of novel derivatives, making it difficult to

discern what changes are important and why. The solubility of APM is known to be greater than that of the dinitroanilines which would be an important if an active compound was developed (Murthy *et al.* 1994). Also, the highly lipophilic nature of trifluralin meant that it was largely trapped in the membranes where it is unlikely to be active (Naughton *et al.*, 2008). Six novel derivatives of trifluralin were previously examined in our lab but did not show any improved activity (Naughton J. A., PhD Thesis 2007). Finally, in light of the extensive *in vivo* metabolism associated with the dinitroanilines, it seemed prudent to use APM as a starting point. Therefore, collaborators in the department of Pharmaceutical and Medicinal Chemistry, Royal College of Surgeons in Ireland, Mrs. Christine Mara and Dr. James Barlow, generated 68 mostly novel compounds based on the structure of APM which had never been tested for their antimalarial activity. The purpose of the work described in this chapter was to examine the antimalarial activities of these compounds and try to identify the structural features associated with potent activity so that new, improved compounds could be synthesised in the hope of identifying a novel antimalarial lead compound.

4.2 RESULTS

4.2.1 Growth inhibition of cultured *P. falciparum* by compounds related to APM

Mrs. Christine Mara synthesized 68 compounds, that fall into four broad categories, based on the structure of APM (see Fig. 4.1 or the appendix for the complete list). The purity of these compounds was assessed to be >99% by nuclear magnetic resonance (NMR) spectroscopy (Mrs. Christine Mara, personal communication). All the compounds were initially dissolved in DMSO to a final concentration of 10 mM or 20 mM.

To determine their effects on cultured parasites, a lactate dehydrogenase assay was employed as described earlier (see section 2.2.2). This assay measures the concentration at which 50% of the parasite growth is inhibited (IC_{50}). The highest concentration that was measured by this assay was 128 μM. Here the compounds are grouped together based on their structure, with a decreasing order of activity. The

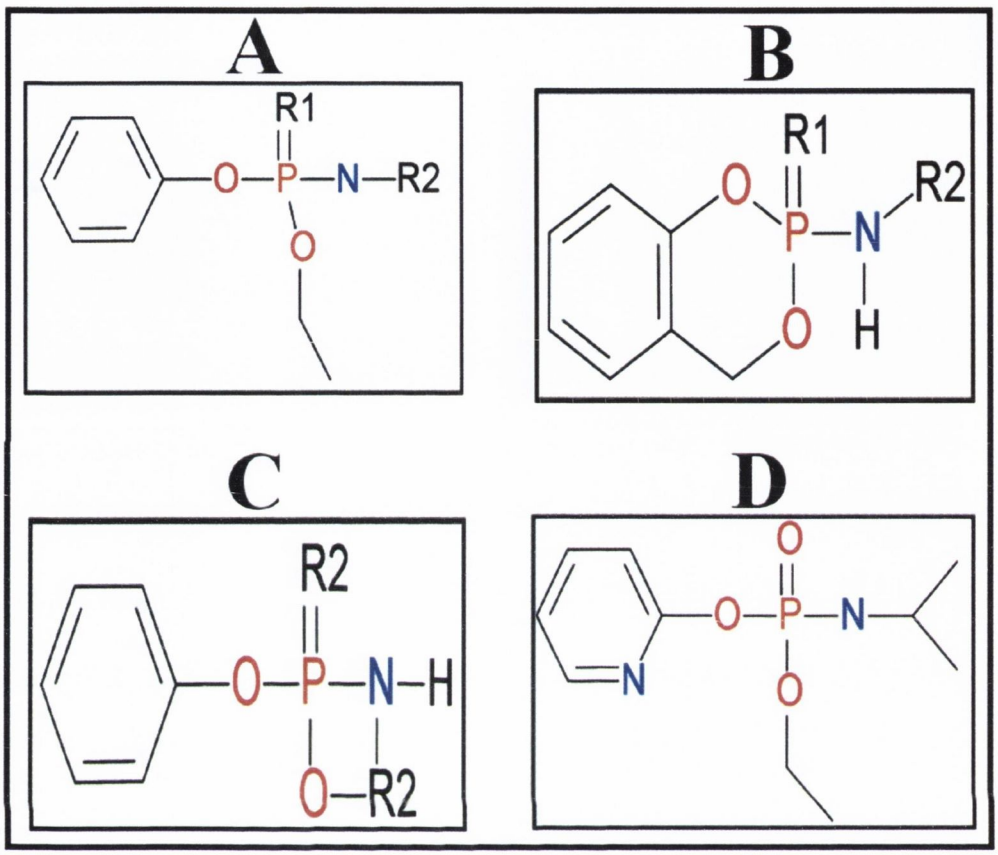

Fig. 4.1. The schematic structures of the compounds that were used for determining the tolerance of the synthesised ligands for changes in different moieties. **A)** APM analogues. **B)** Oxalobenzoates. **C)** Phenoxyoxaza(oxathio)phosphinanes. **D)** Heterocyclic derivatives based on APM. R1 and R2, variable substituents. These are generalised structures. A complete list can be found in the appendix.

graphs of the most active compounds (<10 μM) are shown in Fig. 4.2 and the IC_{50} for all the compounds are displayed in Table 4.1.

The effect of the incubation time for the IC_{50} was in some cases significantly different (e.g. C5 had IC_{50} of >128 μM and 15 μM at 48 h and 72 h respectively). This "plateau" effect can be seen with the APM graph (Fig 4.1 A). This was observed before with other MT inhibitors but it was usually abolished after longer incubation times (Fennell *et al.*, 2006 and Fennell *et al.*, 2003). Another possible explanation for this result is the delayed death phenomenon which is often associated with plastid-targeting drugs. Essentially, parasites are capable of completing one 48 h replication cycle and can still invade new erythrocytes. However, they cannot replicate further possibly due to the disruption of crucial genes or organelles being passed on to the next generation (Goodman *et al.*, 2007). Therefore, it is vital novel inhibitors, particularly drugs which affect the cell cycle, are incubated with the parasites to accurately determine their full potential. Overall, one compound, C70, showed an improvement against the cultured parasites over APM while C71 was comparable. The remaining compounds had a range of activities inferior to APM.

4.2.2 Solubility of the compounds in aqueous solution

It was important first to determine the aqueous solubility of these compounds so that they could be used in subsequent ligand-binding experiments, in particular the fluorescence quenching assay (see section 2.9.1). To minimise the effort required to gather the data on all of the compounds, a simplistic approach was taken to estimate the approximate solubility of these compounds in a particular buffer (MME) with DMSO (1% (v/v) final conc.). Briefly, the compounds were made up at 100 μM concentration and measured spectrophotometrically over a range of excitation spectrums (200 nm – 800 nm) to determine at which wavelength they did not specifically absorb. Although some compounds were coloured, and some absorbed only when DMSO was added, this did not affect the results. The infra-red spectrum (700 nm – 800 nm) was chosen as none of the compounds were able to absorb at this wavelength. This permitted the detection of compounds which were insoluble under the conditions tested as they would precipitate out of solution. In these cases the suspension was able non-specifically to scatter the infra-red light causing an increase in absorbance. DMSO and buffer alone were used as a blank control in the

experiment. Taxol was used as a positive control since it was determined accurately by other methods to have a maximum aqueous solubility of ~12 μM when DMSO (1% (v/v) final conc.) was present (Sharma *et al.*, 2006). Vinblastine and colchicine were also examined as they are known to have much higher aqueous solubilities (up to ~11 mM and ~25 mM respectively according to Sigma-Aldrich). All the samples were examined for their solubility up to 100 μM after they were incubated at 37°C for 5 min. The total absorbance of a compound at a particular concentration was compared to a DMSO control. A compound was considered insoluble if there was a statistically significant difference between spectra for the concentration used and the DMSO control. A solubility range was established by comparing the lowest concentration at which the compound was still insoluble with the highest concentration at which it became soluble. Therefore, the final results represent an approximation of the compound solubility and are not exact values. This was sufficient information for deciding whether a compound was suitable for the tubulin fluorescence assay. More exact information could be extracted using this technique although it was not necessary for these experiments. Trifluralin and taxol were noted to be particularly insoluble (Fig. 4.3). Since the majority of the APM-related compounds appeared to be soluble up to at least 100 μM under these conditions, only the insoluble compounds and the controls are listed in table 4.2.

4.2.3 Binding of APM-related compounds to tubulin

To compare the binding affinities of the compounds to *P. falciparum* tubulin, a relative fluorescence quenching experiment was conducted. One concentration (37.5 μM) of a ligand (APM or related compound) was incubated with MBP-αI/β-tubulin as described earlier (see section 2.8.3.2). The quench generated by the APM derivative was compared to that of APM. The rationale behind this experiment was that this method should be able to rapidly deduce if a compound has better affinity for the tubulin than the parent, rather than conducting more labour-intensive K_d determinations. Eight compounds with a range of activities in the pLDH assay and various structure types were chosen. Compounds that did not have an aqueous solubility of ≥100 μM were avoided as this could affect the results. The results are presented as a relative quench of the fusion-tubulin fluorescence (Fig. 4.4).

A

APM analogues					
Compound	48 h (μM)	72 h (μM)	Compound	48 h (μM)	72 h (μM)
APM	54	2.3	c23	64	57
c70	3.9	1.6	c43	70	59
c71	7.74	4.1	c18	66	64
c72	7.78	7.8	c56	67	64
c69	8.1	8.1	c11	>128	68
c64	32	16	c68	>128	78
c47	42	16	c32	>128	80
c33	64	32	c51	82	84
c65	46	32	c25	100	86
c52	64	32	c53	95	94
c48	46	32	c22	>128	98
c66	55	32	c14	>128	102
c55	90	32	c16	>128	118
c44	41	32	c8	>128	>128
c45	40	32	c9	>128	>128
c54	46	32	c10	>128	>128
c31	64	32	c12	>128	>128
c42	32	32	c13	>128	>128
c63	>128	46	c19	>128	>128
c17	32	49	c20	>128	>128
c15	110	52	c35	>128	>128
c24	49	56	c67	>128	>128

B

Oxalobenzoates		
Compounds	48 h (μM)	72 h (μM)
c30	45	32
c1	55	53
c6	74	84
c27	>128	85
c28	>128	100
c7	>128	108
c4	>128	118
c3	>128	>128

C

Phenoxyoxaza(oxathio)phophanes		
Compounds	48 h (μM)	72 h (μM)
c5	>128	15
c36	19	23
c41	89	49
c39	64	58
c37	>128	58
c50	64	64
c38	>128	102
c40	>128	120
c2	>128	>128
c26	>128	>128
c29	>128	>128
c49	>128	>128

D

Heterocyclic compounds		
Compounds	48 h (μM)	72 h (μM)
c59	33	23
c62	32	32
c58	>128	126
c57	>128	>128
c61	>128	>128

Table 4.1. IC_{50} of all compounds after 48 h and 72 h incubations, generated using the pLDH method. At least two identical duplicate experiments were conducted for all the compounds (n = 2). The four lists represent, in decreasing order of activity at 72 h (except for APM) the APM analogues (**A**), oxalobenzoates (**B**), phenoxyoxaza(oxathio)phosphinanes (**C**) and pyridine-based compounds (**D**).

Compound	Concentration (μM)	p-value insoluble	p-value soluble
APM	≥100	N.A.	0.4553
Oryzalin	≥100	N.A.	0.6278
Trifluralin	10-25	0.0002	0.1382
Taxol	10-25	0.0001	0.3464
Vinblastine	≥100	N.A.	0.3715
Colchcicine	≥100	N.A.	0.8687
C36	10-25	0.0001	0.8481
C42	10-25	0.0012	0.337
C69	25-50	0.0013	0.8158
C70	50-100	0.0001	0.8045
C71	10-25	0.0029	0.5609
C72	25-50	0.0001	0.6446

Table 4.2. Solubility limits of APM-related compounds and several known tubulin inhibitors by the spectrophotometric assay. Only the APM derivatives that appeared to be insoluble at 100 μM are shown; all others were soluble up to ≥ 100 μM. Several tubulin inhibitors are listed as their aqueous solubility is known. P-value for insoluble, the probability that the compound was insoluble at the highest concentration shown (i.e. for trifluralin this was 25 μM) by Student t-test. P-value for soluble, the probability that the compound was soluble at the lowest concentration shown (i.e. for trifluralin this was 10 μM). **N.A.**, not applicable.

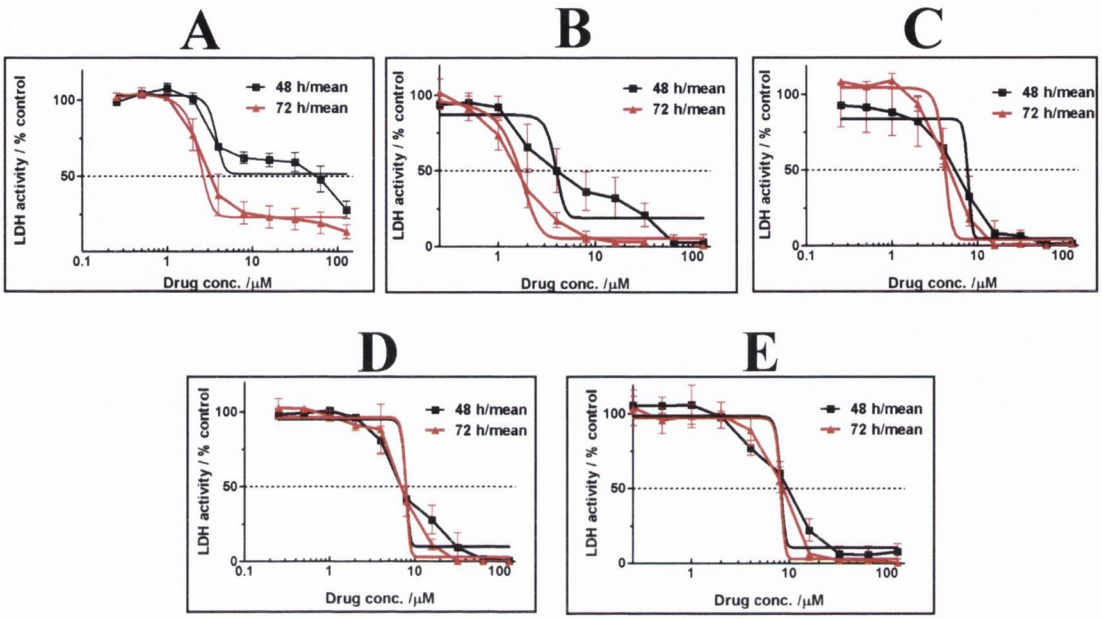

Fig. 4.2. Susceptibilities of asynchronous *P. falciparum* 3D7 cultures to APM and its most potent derivatives (<10 µM) as measured by the pLDH method. A. APM. **B.** C70. **C.** C71. **D.** C72. **E.** C69. Geometric mean values were taken from six to eight determinations after 48 h (**black line**) and 72 h (**red line**) are shown; the initial parasitemias were 0.8%. The 50% mark which determines the IC_{50} is shown as a dotted line. The IC_{50} values were calculated using a 4-parameter fit model. The error bars are represented by the vertical lines. The "plateau" effect is obvious on APM (**A**) which explains the apparent IC_{50} discrepancy between the two incubation times.

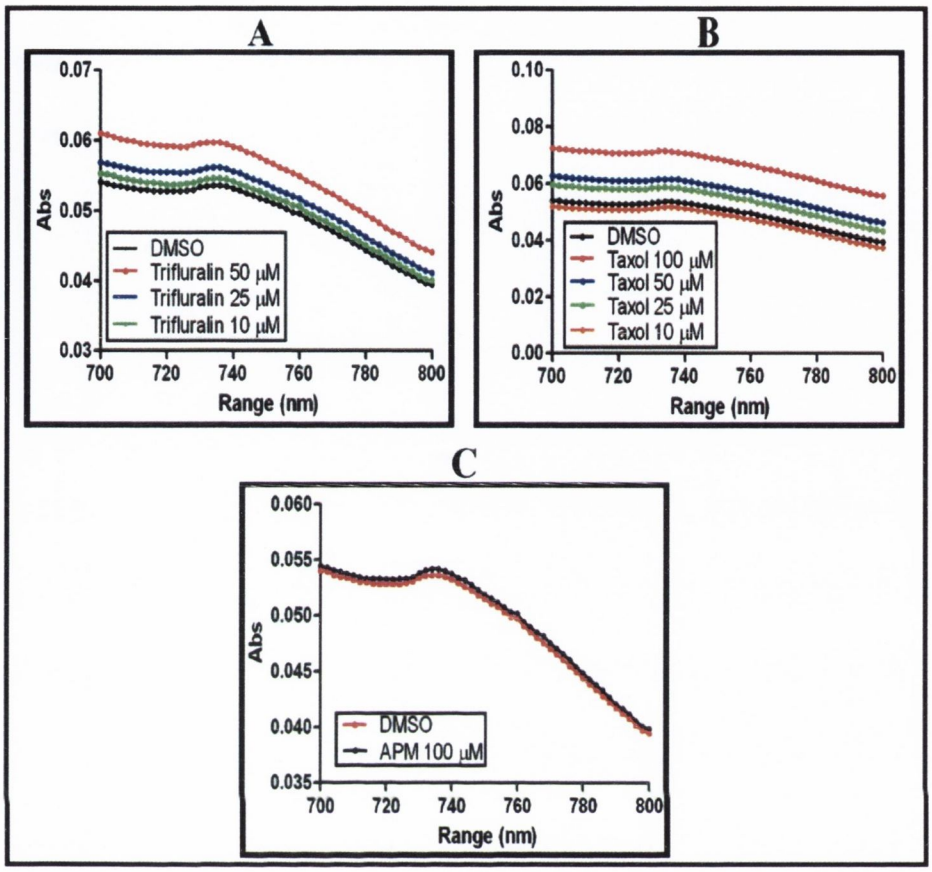

Fig. 4.3. Spectrophotometric assay used to determine the solubility of known tubulin inhibitors. The absorbance of the solution (DMSO alone or compound in DMSO) was recorded over a wavelength of 700 nm – 800 nm. None of the compounds appeared to be able to absorb at this wavelength regardless of whether they were coloured or not. All the experiments were done in triplicate.

A

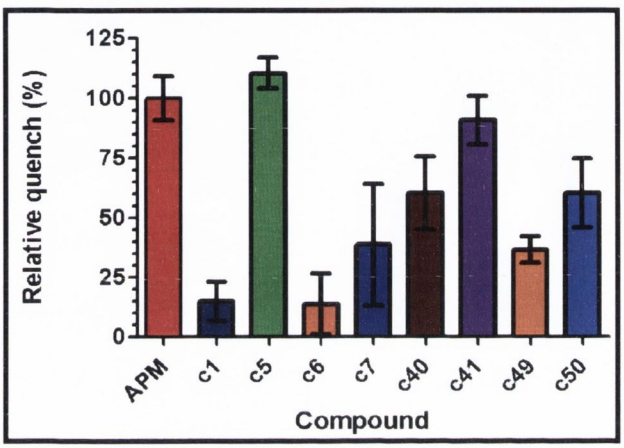

B

Compound	% Quench of APM	IC_{50} (μM)
APM	100	2.3
C5	110.51	15
C41	90.91	49
C1	14.9	53
C6	13.77	84
C7	38.76	108
C40	60.35	120
C2	0	>128
C49	36.55	>128

Fig. 4.4. Relative quenching ability of the APM-related compounds in comparison with APM. The table shows the average quench for each of the compounds compared to APM when it is set at a value of 100%. C5 and C41 were determined (by a Student t-test) not to be significantly different from APM at this concentration (p values of 0.1768 and 0.3131 for C5 and C41 respectively). However, the six other compounds were considered to bind less to the tubulin fusions at this concentration. C2 was set to 0% as the actual value was slightly negative. The thin vertical bars represent the standard deviation for margin of error from three determinations.

Although C5 has a slightly higher quench than APM, it was demonstrated not to be significant at 95% confidence (p value of 0.1768). The same was true for C41 (p value of 0.3131). All of the other compounds tested were determined to bind less well to the tubulin fusions under these conditions. These initial results suggest that the compounds with the best affinity for tubulin (C5 and C41) also had the best activity for live parasites. However, this sample is too small to make a clear correlation between good binding and good activity against whole parasites.

4.2.4 Investigation of the relationship between modelled structures of the compounds and their activities

To investigate the structural basis of the differential activity of the APM-related compounds, molecular models of all the compounds, including APM, trifluralin and oryzalin, were constructed using MOE (see sections 2.8.1.1 and 2.8.1.2). A stochastic randomised search approach was employed whereby the entire molecule was freely rotated until the most energetically favourable conformation was elucidated. From these models, estimates of their lipophilicities were determined by calculating the predicted partition coefficient (cLogP) (see section 2.9.2). This measurement predicts the proportion of a compound that should be found in an aqueous solute (hydrophilic) versus an octanol solute (hydrophobic), with high positives values representing very hydrophobic compounds.

Typically, an increase in the lipophilicity of a compound aids its passage through the cell membrane and improves its potency. To determine if this factor was significant for the APM analogues, a scatter plot using the predicted cLogP values and the IC_{50} values was generated (see Fig. 4.5). There was a low correlation between the data ($R^2 = 0.4936$) so it was difficult to deduce any obvious trends. However, some compounds appeared to be significant outliers. These were APM, C48, C63 and C70. It may be the case that the different affinity these compounds have for tubulin affects their IC_{50} value. Deletion of these four points increased the correlation co-efficient of the graph by 20% ($R^2 = 0.7096$). Although the data was still variable, it suggested that lipophilicity was directly related to activity in the parasite assay. An increase in lipophilicity may be important for two reasons. First, it could be related to uptake of the compound into the parasite. Second it could suggest that the binding site of these

herbicides on tubulin is hydrophobic and therefore, lipophilic compounds are favoured.

To understand the mechanism of action of these compounds, their molecular models were aligned with APM alone or in groups to generate the most similar structure based on a number of factors (see section 2.8.1.2). This was done previously to identify physiochemical properties and the pharmacophore features for other small organic ligands (Prasanna *et al.*, 2004). These structures were then evaluated to explain their IC_{50} and when applicable, the relative fluorescence quenching data.

The initial alignment was to compare APM to oryzalin and trifluralin. These compounds are expected to share the same binding site, so it was expected that APM would have a similar conformation to these dinitroanilines (Ellis *et al.*, 1994 and Murthy *et al.*, 1994). These compounds all adopted a very similar profile, which is in agreement with Ellis *et al.* (1994) (Fig. 4.6 A). Essentially, the oxathiophosphinane group lined up with the alkyl chains of both trifluralin and oryzalin. The three molecules were separated and several regions were highlighted. The hydrophobic, the mildly polar and hydrogen bonding domains were used to demonstrate that the overall structure and charge of APM is very similar to both the dinitroanilines (Fig. 4.6 B). All three compounds had a very hydrophobic head which was a result of the alkyl chains, with a mildly polar body which is formed from the nitro moieties and the benzene ring. The obvious exception is the hydrogen-bonding region which is unique to oryzalin. One difference between APM and the dinitroanilines is the partial exposure of the oxygen atom on the O-methyl group (Fig. 4.6 C and D). The oxygen atom can form hydrogen bonds and has slight negative charge which is not found in trifluralin or oryzalin. It is not known whether this charge difference is important or not.

Although no compound was produced that was the same as APM except that the sulphur has been replaced with an oxygen atom, one compound was very similar, C32. C32 had an ethyl group attached to the oxygen whereas APM had a methyl group. Since the difference was likely to be relatively minor, a model was made aligning the structures to determine what difference exists when the sulphur is replaced with oxygen. The conformations of both molecules were almost identical indicating that the replacement of the sulphur atom was not predicted to cause a conformational change (Fig. 4.7 A). However, the one difference that is immediately obvious was that the exposed oxygen atom was capable of forming hydrogen bonds

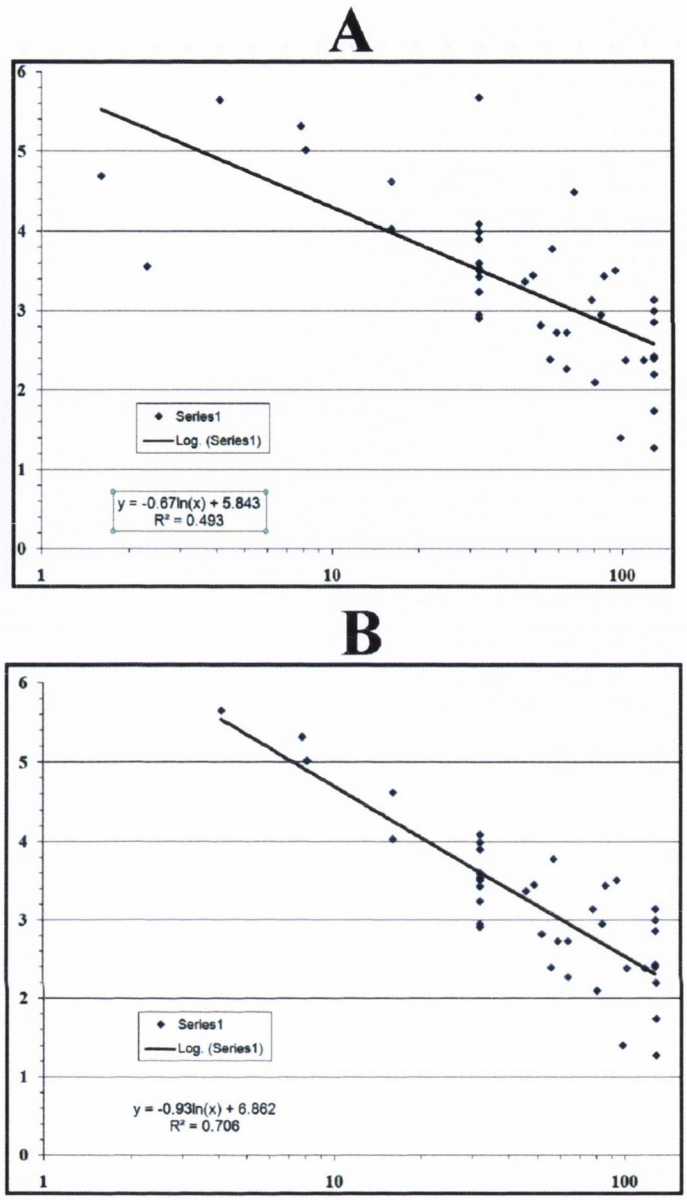

Fig. 4.5 Scatter plot of the predicted cLogP values versus the IC_{50} values for the APM-analogues and APM. A. APM and the APM-analogues were plotted. A best fit line was calculated with a R^2 value of 0.493. **B.** APM, C48, C63 and C70 were removed from the graph and the best fit line was calculated with a R^2 value of 0.7096.

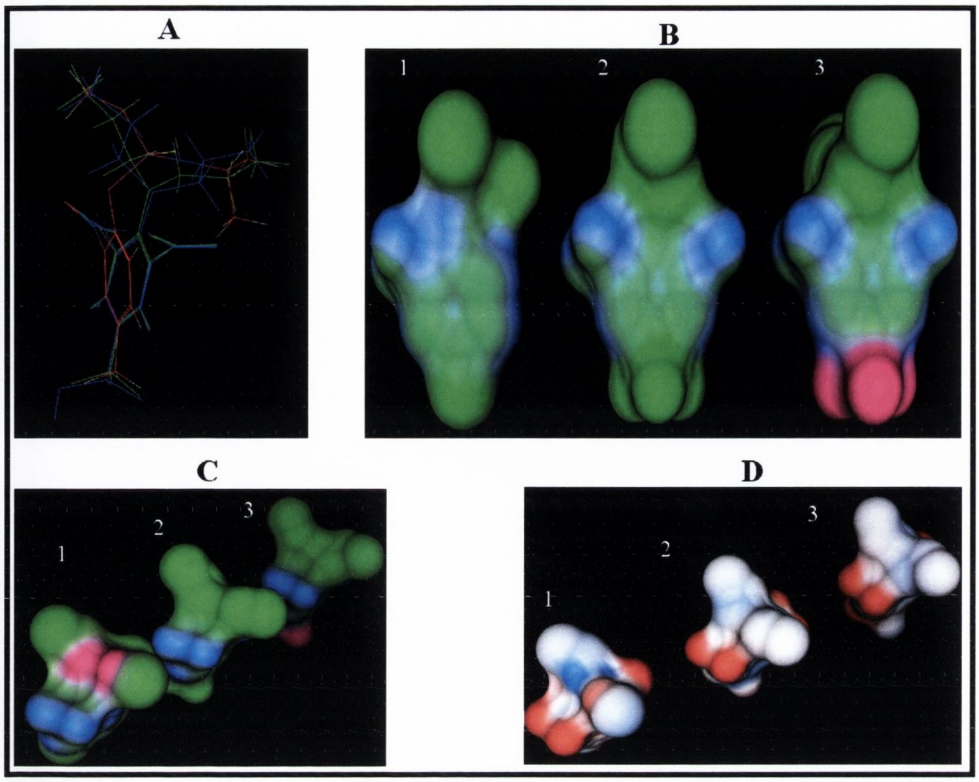

Fig. 4.6. Alignment of APM, oryzalin and trifluralin using a molecular modelling programme (MOE). A. APM (**red**) matched up well with both oryzalin (**blue**) and trifluralin (**green**). However, it was evident that the APM benzene ring was not flush with that of oryzalin and trifluralin. **B.** APM (**1**), trifluralin (**2**) and oryzalin (**3**) were separated and the major hydrophobic (**green**), polar (**blue**) and hydrogen bonding (**purple**) regions were highlighted. From the models presented here, it is evident that the overall shape and charge of APM is very similar to the dinitroanilines with obvious exception of the hydrogen bonding region of oryzalin. **C.** The same picture of **B** was used but rotated to display the head groups of the three compounds (APM is **1**, trifluralin is **2** and oryzalin is **3**). An obvious difference between APM and the dinitroanilines was the exposure of an oxygen atom which was capable of forming hydrogen bonds in the otherwise hydrophobic head-group. **D.** Depiction of the electrostatic charge for APM (**1**), trifluralin (**2**) and oryzalin (**3**). The regions were colour coded to highlight negative charges (**red**), neutral atoms (**white**) and positive charges (**blue**) that were $\geq$ +/- 35 kcal/mol.

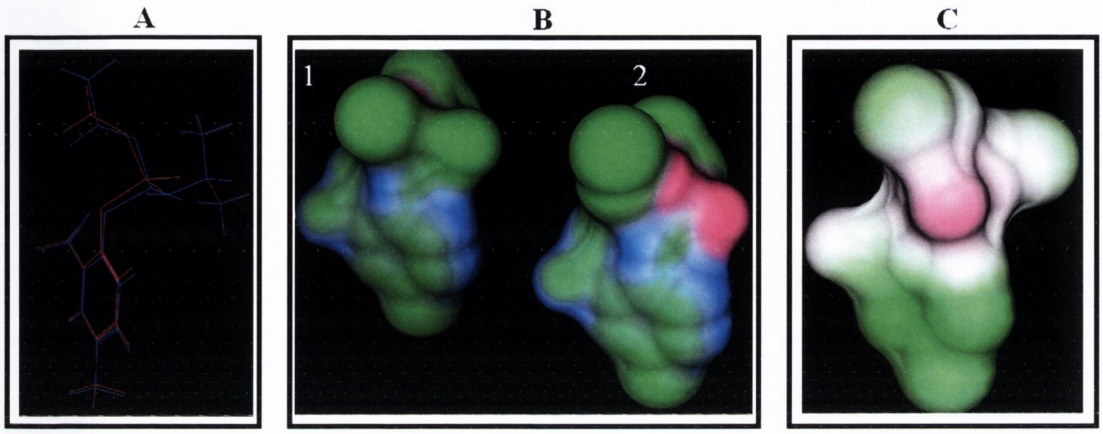

Fig. 4.7. Alignment of the molecular models of APM and C32. A. Stick figures of APM (**red**) and C32 (**blue**). Both compounds were almost identical when aligned. **B.** APM (**1**) and C32 (**2**) were separated and the major hydrophobic (**green**), polar (**blue**) and hydrogen bonding (**purple**) regions were highlighted. The sulphur atom was depicted as being strongly hydrophobic on APM (right) while the oxygen replacement on C32 was more capable of hydrogen bonding. **C.** The major lipophilic (**green**), neutral (**white**) and hydrophilic (**purple**) regions on C32 were highlighted. This demonstrated that oxygen replacement was hydrophilic as opposed to the hydrophobic sulphur atom.

and was more hydrophilic (Fig. 4.7 B and C). Conversely, the sulphur atom was more hydrophobic and could not form hydrogen bonds like the oxygen atom. This was the only significant difference between the molecules, yet APM was a significantly more potent inhibitor of the cultured parasites (IC_{50} of 2.3 μM) than C32 (IC_{50} of 80 μM). Therefore, there are three possible explanations for this result. It was possible that C32 was more susceptible to metabolism by the parasite compared to APM as a result of the oxygen-sulphur change. However, it would be expected that the IC_{50} after 72 h would be higher than IC_{50} after 48 h due to the reduction in concentration of the compound and the recovery of the parasites. This trend was not only observed as a whole for any of the compounds with the sole exception of C17. Therefore, this suggests that metabolism is unlikely to be a significant reason. The sulphur atom makes APM significantly more lipophilic (cLogP of 3.56) than the corresponding oxygen atom on C32 (cLogP 2.2) so the latter compound may have reduced entry into the cell. Finally, the oxygen atom could affect the binding of the ligand to tubulin. This seems reasonable considering the head group in APM and both dinitroanilines is very hydrophobic. This hydrophobicity is further exacerbated by the presence of the sulphur atom.

The IC_{50} of C2 and C5 was very different (>128 μM and 15 μM) despite these compounds being identical except that the nitro and methyl groups are in opposite positions. The alignment of these compounds highlighted that these structures did not fit neatly with APM (Fig 4.8 A), particularly the linker oxygen between the benzene ring and the phosphorous atom. This was predicted to force the molecules to flip their shape so that the nitro group on C2, which resides in the ortho position like APM, finally ended up on the opposite side of the molecule. This meant that the C2 nitro group was positioned where APM had a hydrophobic moiety ($-CH_3$) and vice versa (Fig. 4.8 B). The opposite was true for C5 which had the nitro and methyl groups reversed with regard to C2. This was predicted to affect the relative distribution of both lipophilicity (see Fig. 4.8 C) and electrostatic charge (see Fig. 4.8 D) of C2 compared to APM and C5. For C2, a lipophilic moiety ($-CH_3$) was in the place of a neutral nitro group found on APM and C5 (see Fig. 4.8 C). With regards to the electrostatic charge, C2 had a neutral, even slightly positive group ($-CH_3$) in place of the strongly negatively-charged nitro group on for APM and C5 (see Fig. 4.8 D). Therefore, it seems reasonable to suggest that the movement of the nitro and methyl group are not tolerated for these compounds and that this may be related to a reduced

binding affinity to tubulin rather than metabolism. C2 was predicted to be only slightly more lipophilic (2.85 +/- 0.54) than C5 (2.79 +/- 0.55) so in this case, this was unlikely to be an important factor.

An intriguing feature of these molecules was the exposure of an oxygen atom which was buried in the APM model. The exposure of this atom was the main difference between APM and C32 (see Fig. 4.7. B). For C2 and C5 an oxygen atom, albeit a different oxygen to that found in C32 (see Fig 4.8), is also exposed in the in this hydrophobic head group (Fig 4.8 B). The oxygen atoms for C2, C5 and C32 were capable of forming hydrogen bonds (the **purple** region in Fig. 4.7. B and Fig 4.8 B). However, for C32, this oxygen atom was hydrophilic (Fig. 4.7 C) but for C2 and C5 this oxygen was neutral and even slightly lipophilic (Fig. 4.8 C). Furthermore, the electrostatic map revealed that the slight negative charge associated with this oxygen atom in C2 and C5 was not out of place, as the sulphur beside the oxygen had a large negative charge (Fig. 4.8 D).

The relative quenching assay showed that the sulphur-containing compounds C1 and C6 were weak binders of the recombinant tubulin fusions (see Fig. 4.4). To explain this, APM, C1 and C6 were aligned (see Fig. 4.9). C1 and C6 did not line up well with APM which may reflect reduced flexibility in these compounds in the oxalobenzoates. The overall hydrophobicity and hydrophilicity were ultimately quite similar between all three compounds (data not shown). However, the electrostatic map revealed that the positions of several charged groups, both positive and negative, were not aligned with APM. Therefore, it appeared that the charge rearrangement was responsible for the reduced affinity that these ligands (C1 and C6) displayed for the tubulin.

4.3 DISCUSSION

A wide variety of APM-related compounds were generated, which could be separated into four different families: APM analogues, oxalobenzoates, phenoxyoxaza(oxathio)phosphinanes and heteroaromatic derivatives of APM. This permitted a detailed examination into the different features that affected their activity. This was done by gathering information about the properties of the compounds from their several different experiments and analyses. The effectiveness of the compounds against cultured parasites was compared with their binding to purified tubulin and

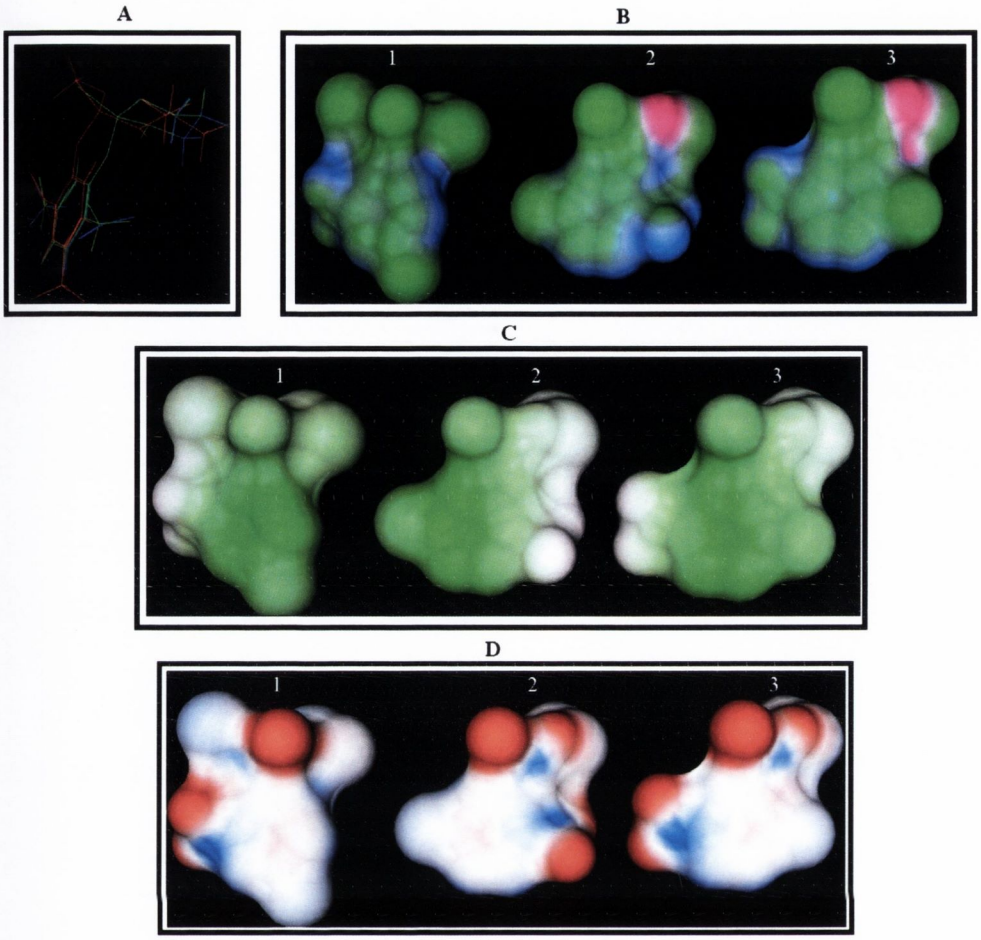

Fig. 4.8. Alignment of the molecular models of APM, C2 and C5. A. Stick figures of APM (red), C2 (blue) and C5 (green). C2 and C5 did not line up well with APM which was likely a result of lack of flexibility in the alkyl chain that connects nitrogen to oxygen. **B.** The major hydrophobic (**green**), mildly polar (**blue**) and hydrogen bonding regions (**purple**) are highlighted for APM (**1**), C2 (**2**) and C5 (**3**). It is evident that the hydrophobic methyl group (on the benzene ring) of C2 resides in the place of the polar nitro groups (on the benzene ring) on both APM and C5 and vice versa. **C.** The major lipophilic (**green**), neutral (**white**) and hydrophilic regions (**purple**) are highlighted for APM (**1**), C2 (**2**) and C5 (**3**). It is evident that the exposed oxygen residue on both C2 and C5 was not hydrophilic unlike in C32 (Fig. 4.7 C). **D.** Depiction of the electrostatic charge for APM (**1**), C2 (**2**) and C5 (**3**). The regions were colour coded to highlight negative charges (**red**), neutral (**white**) and positive charges (**blue**) that were ≥ +/- 35 kcal/mol. The large negatively charged atom in the head group for all 3 compounds was the sulphur atom. In C2 and C5, the less negatively charged atom behind the sulphur was the oxygen.

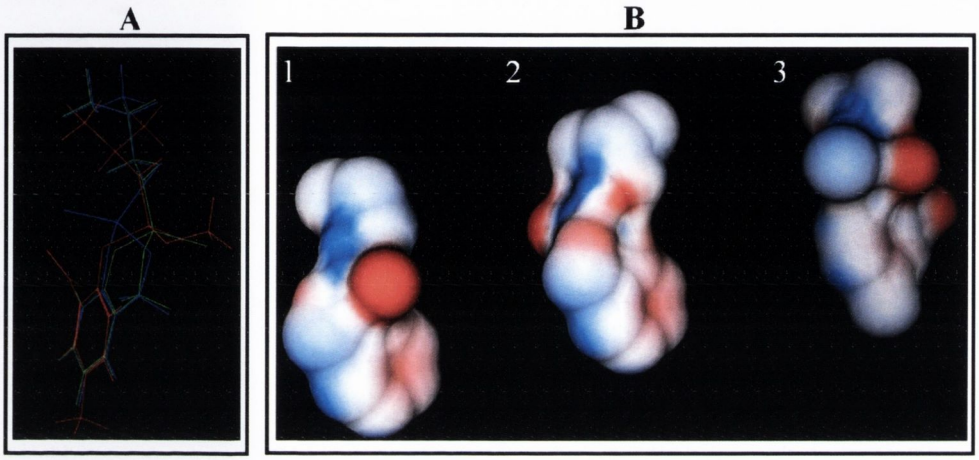

Fig. 4.9. Alignment of the molecular models of APM, C1 and C6. A. Stick figures of APM (red), C1 (blue) and C6 (green). C1 and C6 did not line up well with APM. **B.** Depiction of the electrostatic charge for APM (**3**), C1 (**2**) and C6 (**1**). The regions were colour coded to highlight negative charges (**red**), neutral atoms (**white**) and positive charges (**blue**) that were ≥ +/- 35 kcal/mol. The electrostatic map shows the a displacement of several charged atoms for C2 and C5 in relation to APM.

predicted lipophilicity. This data was backed up by the construction of molecular models which also permitted the interrogation of the critical features of the phosphorothioamidates and related compounds. This led to a prediction of possible pharmacophores (see below).

The pLDH assay provided a huge amount of information regarding the effectiveness of these compounds. However, it was still important to distil this data so that accurate structure-activity relationships could be derived. This was done based on the compound families (see Fig. 4.1) as these compounds were related to each other.

To determine if the lipophilicity of the compounds affected their activity, a scatter plot using the IC_{50} and the predicted cLogP was generated (Fig. 4.5). Using APM and the APM-analogues, there appeared to be a low correlation between these two features (R^2 = 0.4937). However, APM, C48, C63 and C70 were significant outliers and removing them greatly improved the accuracy of the graph (R^2 = 0.7096). This result appeared to suggest that the lipophilicity was a significant factor for activity to cultured parasites. This is not altogether surprising, considering these compounds must traverse three lipid membranes (the erythrocyte plasma membrance, the parasitophorous vacuole and the parasite plasma membrane) before entering the cytosol. However, it is also possible that the binding site on tubulin is also relatively lipophilic. Therefore, a highly lipophilic compound would be able to rapidly permeate into the parasite but also have a strong affinity to tubulin.

The four outliers, APM, C48, C63 and C70, are interesting also. APM and C70 had better activity in relation to their cLogP than the other compounds. However, it seems likely that the reason for this was due to an increased affinity for the tubulin. Conversely, C48 and C63 had a very poor activity in relation to their predicted cLogP. Their high cLogP would suggest that their uptake into the cell should be as good as if not better than C70, therefore, this likely suggests that these compounds had a lower affinity for tubulin. Overall, lipophilicity seems to play an important role for the activity of these compounds for cultured parasites.

The sulphur atom on APM was also substituted for oxygen in many compounds. This was due to the unstable nature of the sulphonated compounds, including APM, which disintegrated when heated past 65°C for prolonged periods of time (C. Mara, personal communication). Furthermore, an O-ethyl chain was attached to nearly all of the APM analogues (C63 was the exception) instead of an O-

methyl, due stability problems (Mara, personal communication). Therefore, it was interesting to determine if this affected the activity of the compounds. Twenty-one compounds out of 70 were synthesized with a sulphur. However, two sets of identical compounds were produced with a sulphur or an oxygen attached; C47 versus C69 and C42 versus C71. In both cases the sulphur compound was at least 3-4-fold more active (after 72 h). This is a very a small sample and it is possible that the results would not hold true in a larger sample size. Furthermore, the predicted lipophilicity for the sulphur compounds is more than 1 log greater than the oxygen analogues. Therefore, it is possible that the effect is due to increased transport into the cell rather than an increased binding affinity for the tubulin.

Nitro groups were previously determined to play an important role in the binding of dinitroaniline compounds such as oryzalin and its derivatives to *Leishmania* tubulin (Chan *et al.*, 1993, Bhattacharya *et al.*, 2002, Bhattacharya *et al.*, 2004 and George *et al.* 2007). These groups have been suggested to confer carcinogenicity, although this is still disputed (Berman J., 1994, Chan *et al.* 1994 and Rawlings *et al.*, 1998). Nonetheless, it would be preferable not to have these groups. A detailed assessment of the nitro-containing compounds was conducted. Several compounds were identified which were identical except for the presence or absence of a specific moiety (i.e. a methyl or group nitro only). For the oxalobenzoate compounds (Fig. 4.1 B), C6 versus C7 and C3 versus C30 were comparable. In this case, C7 had a para nitro substitution and was comparable to C6 which had no substitutions although both compounds had a high IC_{50} (84 μM and 108 μM for C6 and C7 respectively after 72 h). A similar comparison was made between C3 (ortho nitro and para methyl groups) versus C30 (no benzene ring substituents). C30 was at least 4 times more active than C3 (IC_{50} 32 μM and >128 μM respectively after 72 h), at least indicating that the nitro moiety was not essential to generate active oxalobenzoate compounds. Several comparisons were possible for the APM analogues (see Table 4.3). The absence of either the methyl (C20), the nitro (C67) or both groups (C35) from the benzene ring meant that the ligand had undetectable activity in the pLDH assay. However, certain combinations of the methyl and nitro groups were beneficial (ortho nitro and para methyl as in C32) while others were not (C8 and C9). This result concurs with APM which has the same distribution of substituents as C32. However, this result was not repeated for the phenoxyoxaza(oxathio)phosphinanes compounds (see Fig. 4.1 C). In fact, the ortho

A

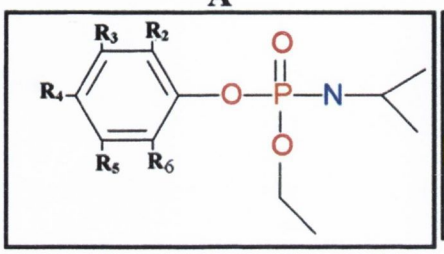

B

Compound	Methyl position	Nitro position	IC_{50} (μM)
C35	N/A	N/A	> 128
C67	Para (R_4)	N/A	> 128
C20	N/A	Ortho (R_2)	> 128
C32	Para (R_4)	Ortho (R_2)	77
C9	Meta (R_5)	Ortho (R_2)	> 128
C8	Ortho (R_6)	Meta (R_5)	> 128

Table 4.3 Comparison of the IC_{50} of the APM analogues with different moieties attached. **A**. Structure of C32 which was used for the comparisons. **B.** Table representing the position of the substituents and the IC_{50} from the pLDH assay. Only C32 gave a detactable IC_{50}. The R group represents the position of the methyl group in relation to the nitro moiety on the benzene ring.

nitro moiety and para methyl moiety compounds were completely inactive (C26 and C29). By contrast, a meta nitro group and a ortho methyl group were relatively potent in these compounds, C5. Notably, a direct swap of these substituents, for example C2 had an ortho nitro group and meta methyl group, caused a complete loss of activity. Overall, the optimal position of the nitro and methyl groups seem to depend on the compound family. However, the nitro groups are still replaceable since other active phosphorothioamidates have been generated that do not have this group (C69 and C71 in particular). This result is in agreement with that of George *et al.* (2007), as this group also synthesized effective dinitroaniline derivatives for trypanosomes with no nitro moieties.

The tri-fluoro groups ($-CF_3$) were synthesized on 24 compounds, predominately on the para position in order to provide an electron-withdrawing alternative to nitro moieties. Three identical compounds were generated that had the tri-fluoro group in different positions, meta on C23, para on C24 and ortho on C25. C23 and C24 had identical IC_{50} (56 μM each) whereby C25 was slightly higher (86 μM). It is not known if the tri-fluoro groups are important for the binding of the APM-related compounds or if they are just useful for increasing the overall lipophilicity of the compounds. Replacement of a para tri-fluoro group on C47 with that of a bromine atom on C64 did not significantly change the IC_{50} (16 μM and 16 μM for C47 and C64 respectively). Both the bromine and the tri-fluoro group are stongly lipophilic and mildly negatively charged. Since these groups are unrelated, it likely that one of these properties is important. In the most active compound, C70, a strong negatively charged nitro group resides at the para positive. A negative group at this position may be important. However, the para benzene group has mild positive charge in other compounds where it is just hydrogenated e.g. C35 or has a methyl group, e.g. APM. Therefore, it is not conclusive whether the tri-fluoro groups are important for lipophilicity or for the negative charge they supply.

One significant problem that arises when working with novel compounds is that their aqueous solubility is unknown. Although it is possible to estimate the solubility *in silico*, it is harder to predict the effect different buffers and solvents, DMSO in particular, will have on the compounds. Therefore, this problem required the development of a quick and reliable assay that was able to measure the solubility of a compound under specific conditions. This assay was validated using tubulin inhibitors which have known solubilities in aqueous solutions. It was possible to

determine that taxol was soluble at a maximum concentration between 10-25 μM (Table 4.2). A more accurate prediction could be made but this was not needed. The same was true for trifluralin which is very hydrophobic. Oryzalin seemed to be soluble past 100 μM, which is contrary to Hughdahl *et al.* 1993 who estimated that the maximum concentration was ~14 μM (Hughdahl *et al.* 1993). However, oryzalin was only used for short time in our assay, 5 min, and may not have immediately precipitated out of solution. This would concur with the findings of Hughdahl *et al.* who stated that oryzalin came out of solution over a long period (3 h), albeit at lower starting concentrations (Hughdahl *et al.* 1993). Although, in the pLDH assay, high concentrations of oryzalin were used for long periods of time (72 h), it is still likely that the majority remained in solution. The reason is that the presence of the cells makes the environment more lipophilic so the compounds can be easily absorbed. This was demonstrated previously by Naughton *et al.*, who showed that trifluralin was rapidly accumulated into the cells and in particular their membranes rather than precipitating out of solution (Naughton *et al.* 2008). Overall, the majority of the APM derivatives appeared to be soluble in the buffer used for the intrinsic fluorescence quenching assay. There were a few exceptions but these compounds were predicted to be very lipophilic. This compromised our ability to determine the tubulin-binding-affinity for these less-soluble compounds.

Of the 68 compounds examined, 64 were >5 fold less active than APM. This result was surprising considering some of the derivatives had relatively minor changes to their structure. This would suggest that the APM binding site on *P. falciparum* must be very specific and intolerant of significant deviation from the parent compound. Therefore, although these compounds have selective activity to the parasite, developing novel chemotherapeutics may yet prove challenging.

In order to evaluate the tubulin-ligand binding interaction, the intrinsic fluorescence quenching assay (see section 2.8.3.2) was employed. Since this assay is very labour intensive when used to determine K_d's, a more rapid strategy was used with a single concentration (37.5 μM) at which moderate APM binding was achieved. This assay was also designed to identify compounds which may have a reasonable or potent binding affinity for tubulin but are ineffective against parasite cultures, suggesting poor penetration into parasite cells or metabolism. The low concentration also minimised the error caused by non-specific effects, although it was still important to take account of this change in the calculations. A sample of APM derivatives were

chosen based on their activity but also the type of structure, e.g. oxalobenzoates and phenoxyoxaza(oxathio)phosphinanes (see Fig. 4.1). No other APM analogues were used, as the K_d for APM was established. C5 and C41 were found to have an equal affinity for tubulin to APM at this concentration by this technique. C5 was also effective in the pLDH assay with a moderate IC_{50} (15 μM). Therefore, it was not surprising that it had a relatively strong affinity for tubulin. It is not exactly clear why APM has a lower IC_{50} (2.3 μM) than C5. C5 might be subject to metabolism by parasite, although this is unlikely as it should be obvious from the pLDH assay that the 48 h incubation is more effective than the 72 h incubation. This difference is more likely to be related to the penetration of the compound into the cell, as APM has a higher cLogP (3.56) than C5 (2.79). The same explanation may hold true for C41 which has a higher IC_{50} (49 μM) and lower cLogP (2.44) than APM again. Therefore, the results of this assay, when combined with the cLogP seemed to be successful at picking out good tubulin-ligands although a larger number of compounds would need to be tested to verify this conclusion.

To characterise further the structures of these ligands, it was necessary to generate molecular models that could be contrasted to APM. It has been previously suggested that the dinitroanilines and phosphorothioamidates bind to the same site on plant tubulin (Murthy *et al.*, 1994). Therefore, it was deemed prudent to compare the structure of APM to the most widely used dinitroanilines, trifluralin and oryzalin. Also, oryzalin was previously determined to have a greater affinity for tubulin than APM (see section 3.2.3.2). The most striking result with these aligned compounds was how very similar they were in shape and charge distribution (Fig. 4.6). The major difference was the partially exposed oxygen atom on the hydrophobic head group of APM compared to the dinitroanilines. Also, on the benzene ring of the dinitroanilines, oryzalin had a highly negatively-charged sulphonamide group and trifluralin had a mildly negatively charged tri-fluoro group.

The exposed oxygen atom on the APM may be partially responsible for reducing the binding affinity of APM for tubulin relative to the dinitroanilines although further examination would be required to confirm this result. Therefore, replacement of this group or even the attachment of long alkyl chains to hide its charge may serve to improve the affinity of APM derivatives to the tubulin. The para sulphonamide group of oryzalin is unique as the para position for trifluralin and APM is fitted with either a tri-fluoro moiety ($-CF_3$) or a methyl group respectively. The tri-

fluoro moiety is weakly negatively charged as opposed to the sulphonamide group which is very negatively charged. Nonetheless, trifluralin is a more potent inhibitor of cultured parasites than oryzalin, although, due to its extreme hydrophobicity, it was not possible to measure its *in vitro* affinity for recombinant tubulin. The methyl group on APM confers a slightly positive charge. Therefore, it is not known whether these are important for binding to tubulin. However, the most active compound produced, C70, differed from APM primarily in the position of the nitro and groups (they were the opposite on either compound). The nitro group was strongly negative. This may indicate that a negatively charged group at the para position on the benzene ring is favourable. Although, C70 is at least one log more lipophilic than APM which could affect its transport into the cell.

It was not conclusive from comparing the IC_{50} of analogous sulphur-containing compounds to oxygen-containing ones that the difference was significant. This was due to the sample size. Therefore, to investigate this issue further, APM was aligned with a similar compound (C32) that had oxygen in place of sulphur. A second difference was that C32 had a ethyl chain attached to a different oxygen residue where APM had a methyl chain. Since, the difference was quite small and on the opposite side of the compound, it was thought that its effect would be minimal. The comparison of APM to C32 highlighted that these compounds were similar overall suggesting that the oxygen and ethyl versus the methyl chain differences were not significant in causing a major conformational change to the molecule. Examination of the compounds determined that the sulphur is very hydrophobic whereas the oxygen was as least partially hydrophilic (Fig. 4.7 C). Both residues were strongly electronegative (data not shown). Therefore, if the binding pocket on tubulin for this head group is hydrophobic, a hydrophilic oxygen atom is likely to reduce the affinity for the compound to tubulin. However, it is plausible that a hydrophilic oxygen atom could be buried by a hydrophobic alkyl chain. This would explain the results from several compounds with different alkyl chain lengths. C42 has an oxygen atom instead of sulphur and a long alkyl chain (5 carbon), yet is still active against cultured parasites (31 μM). The analogous sulphur containing compound, C71, is only ~7-fold more active than C42 after 72 h. Conversely, APM is ~35 times more active than C32 which has an ethyl chain (IC_{50} of 2.3 μM and 80 μM respectively after 72 h). Lipophilicity alone would not explain this result considering APM has a one order of

magnitude lower cLogP than C71 and both compounds have comparable IC_{50}. However, more *in vitro* binding data is required to substantiate these predictions.

This modelling was also used to explain how compounds that structurally appeared to be closely related could have very different affinities for tubulin and activities against cultured parasites. In particular, C2 and C5 were studied in more detail. C2 had an ortho nitro and a meta methyl while C5 had a meta nitro and an ortho methyl. These compounds were otherwise identical. However, alignment with APM and examination of the resulting structures highlighted several interesting features. Due to constraints imposed on the compounds by the linkage of the nitrogen-oxygen moieties by a carbon chain, the compounds could not align well with APM (Fig. 4.8). In fact, the most favourable conformation for C2, is to place the meta methyl group where the nitro group of APM resides and the nitro group in the vicinity of the APM methyl. Therefore, C2 had a hydrophobic and partially positively- charged group where APM had a polar, strongly negative group. A similar situation exists for the meta and para substituents on either compound. This seems to be the key reason why C2 was not active. This was further supported by the intrinsic fluorescence quenching assay which predicted only a weak affinity for tubulin for this compound (Fig. 4.4). The opposite was true for C5 which managed to adopt a similar conformation to APM. Since this methyl/nitro group swap of C2 abolished its affinity for tubulin, this raises an interesting point; was it the lack of the nitro group in C2 that was responsible for this effect or was it due to the insertion of a methyl group which has different properties to the nitro that was important? Considering that the nitro group can be lost without comprising activity (C69 and C71 in particular), the intolerance of the methyl groups seems more reasonable. To verify this theory, it would be interesting to generate a derivative that is identical to APM with a methyl group on either ortho position to determine if this was tolerated. One curious result that was highlighted while examining these compounds was the fact that an oxygen atom that is common to all three compounds was exposed in C2 and C5 but not APM. Since an oxygen atom was apparently responsible for the loss of activity for C32, it is difficult to explain how C5 can still be active in culture and maintain a comparable affinity for tubulin to that of APM. In C32, the oxygen atom was partially hydrophilic, presumably induced by the surrounding atoms. However, in C2 and C5, the oxygen is neutral if not very slightly hydrophobic. Therefore, the exposure of this residue is not thought to be an issue. Examination of the electrostatics of these

compounds revealed that the oxygen provided an extra negative charge not seen in APM. However, this extra negative charge provided by this exposed oxygen beside a much stronger negatively charged sulphur, so this difference is unlikely to be important.

Further analysis was done on two compounds (C1 and C6) which showed them to have only weak affinity for the recombinant tubulin by the intrinsic tryptophan quenching assay (see Fig. 4.4). It was difficult to determine the exact reason for the lack of activity for these two compounds except that the several groups appear rearranged on the electrostatic map. For C1, the sulphur ended up facing in the opposite direction to its orientation in APM. Although the molecule could be rotated so that the sulphur points in the same direction as in APM, that would mean the molecule as a whole would be less similar to APM. Therefore, it is possible that the conformation of C1 can not match that of APM correctly or more importantly cannot fit into the binding site in tubulin. Explaining the difference between APM and C6 was not as straightfoward. APM had a nitro group that is missing on C6, but as discussed earlier, this may not be critical. The other noticeable difference is the shape of the head group between the two compounds. A methyl group beside the sulphur is slightly positively charged on APM. This is absent on C6 and may be an important residue. However, the difference could also just be small conformational restraints due to the structure of C6 which may inhibit correct binding to the tubulin.

By examining all of the results, several conclusions can be drawn about the APM molecule and related compounds. Based on structure and charge, APM is very similar to the dinitroanilines and could probably be inserted into a related if not identical binding site. These molecules can be split into two sections, the head group which is generally consists of hydrophobic alkyl chains and the body which has the benzene ring, nitro and methyl moieties. The benzene ring appears to be the most tolerant to substitution of various residues with some exceptions occurring at the ortho position. Replacement of the sulphur atom with an oxygen atom significantly reduces the effectiveness of the compound, presumably due to the hydrophilic nature of the latter moiety. However, it may be possible to reduce the impact of the oxygen atom by compensating with hydrophobic alkyl chains which could add extra hydrophobicity to the area or even partially shield the hydrophilic nature of the oxygen atom. Finally, lipophilicity appears to be an important factor for an increased activity against the parasites. Extended alkyl chains in the head group or para

substitutions to the benzene ring were well tolerated. Although a negative charge in the para position of the benzene seemed to be favourable it was not essential. Overall, it seems reasonable to speculate that APM interacts with a hydrophobic pocket through a mixture of hydrophobic bonds and electrostatic charges. However, more detailed *in vitro* binding studies which were not feasible in this project would provide invaluable information to support these predictions.

Chapter 5

Investigation into the Molecular Basis of Herbicide Binding and the Unusual Electrophoretic Migration of *P. falciparum* Tubulins

5.1 INTRODUCTION

Development of more potent compounds based on the structure of the phosphorothioamidates and the dinitroanilines has been hampered by the fact that their binding site on tubulin is unknown. It was, therefore, of interest to gain an insight into the difference between tubulin from organisms sensitive and resistant to the herbicides.

It was observed that lower eukaryotes often had "inverted" tubulin i.e. the migration of β-tubulin was slower than that of α-tubulin on denaturing SDS-polyacrylamide gels, even though it is smaller (see Table 5.1). This unusual feature was not seen in the higher eukaryotes and may represent a unique difference between tubulins from different organisms (see Table 5.1). Furthermore, this reversed mobility was demonstrated not to be related to post-translational modifications as the effects were found to occur in both native and recombinant tubulins, including those produced in *E. coli,* which is unlikely to carry the relevant machinery for these modifications (Shah *et al.,* 2001 and Fennell, 2005). As a result, it seemed likely that the reason for this unusual feature was contained within the amino acid (AA) sequences of the proteins. Since tubulin AA sequence identities from different organisms generally exceed 65% (Bell, 1998), detecting the relevant conserved differences based on analysing the protein sequences seemed a realistic goal. Therefore, this investigation aimed to identify the molecular basis behind the tubulin inversion. It was also plausible that this work may shed light on the herbicide-tubulin interactions by identifying unique features associated with tubulin from herbicide-sensitive organisms.

Tubulin mutations have been discovered which have increased the resistance of several different organisms to the herbicide compounds (Table 5.1). However, these mutations are frequently associated with super-sensitivity to other anti-mitotic inhibitors, particularly taxol. Therefore, it is questionable whether these alterations are just affecting the stability of the MT's or if they were directly targeting the binding site of these ligands. This is particularly evident for the Leu350Glu mutation in β-tubulin of *Chlamydomonas reinhardtii,* which confers resistance to the unrelated compounds (i.e. dinitroanilines and colchicine) but super-sensitivity to taxol (see Table 5.2). Nonetheless, at least three distinct putative herbicide-binding sites have been proposed based on information related to these mutations which confer herbicide

"Normal" tubulin	Electrophoretic migration reference	Herbicide sensitivity reference
Homo sapiens	Fourest-Lieuvin *et al.*, 2006	Werbovetz *et al.*, 2003
Bos taurus	Suprenant *et al.*, 1985	Werbovetz et al., 2002
Ovis aries	Clayton *et al.*, 1980	Rawlings *et al.*, 1998
Ascardia galli	Dawson *et al.*, 1982	unconfirmed
Drosophila melanogaster	Piperno *et al.*, 1985	Kaya *et al.*, 2004
Strongylocentratus droebachiensis	Stephen *et al.*, 1998	unconfirmed
Spisula solidissima	Little *et al.*, 1983	unconfirmed
Sus scrofa	Cleveland *et al.*, 1976	unconfirmed
Echinosphaerium nucloefilum	Little *et al.*, 1983	unconfirmed
"Inverted" tubulin		
Plasmodium falciparum	Fennell, 2005	Fennell *et al.*, 2006
Nicotiona plumbaginifolia	Blume *et al.*, 1998	Yemets *et al.*, 2008
Oryza sativa	Bon-Sung *et al.*, 2009	Brewer *et al.*, 1982
Zea mays	Giani *et al.*, 2002	Hugdahl *et al.*, 1993
Chlamydomonas reinhardtii	Hugdahl *et al.* 1993	James *et al.*, 1993
Tetrahymena thermophila	Wloga *et al.*, 2008	Stargell *et al.*, 1992
Vigna angularis	Mizuno *et al.*, 1985	Soltani *et al.*, 2005
Daucus carota	Mizuno *et al.*, 1985	Deyle *et al.*, 2004
Phaseolus vulgaris	Hussey *et al.*, 1984	Struckmeyer *et al.*, 1976
Naegleria gruberi	Shea *et al.*, 1987	Wang *et al.*, 1995
Paramecium polycephalum	Adoutte *et al.*, 1984	Lignowski *et al.*, 1972
Toxoplasma gondii	Plessmann *et al.*, 2004	Stokkermanns *et al.*, 1996
Trypanosoma brucei	Schneider *et al.*, 1997	Giles *et al.*, 2008
Solanum tuberosum	Bon-Sung *et al.*, 2009	unconfirmed
Reticulomyxa filosa	Linder *et al.*, 1997	unconfirmed
Crithidia fasiculata	Russell *et al.*, 1984	unconfirmed
Euplotes eurystomus	Delgado *et al.*, 1991	unconfirmed
Oxytricha nova	Delgado *et al.*, 1991	unconfirmed
Tetrahymena pyrimformis	Barahona *et al.*, 1988	unconfirmed

Table 5.1. List of the known tubulins that display "normal" (α-tubulin above β-tubulin) or "inverted" (β-tubulin above α-tubulin) migration patterns by SDS-PAGE. It was not possible to determine if all the tubulins were sensitive or resistant to the herbicide compounds as they may not have been tested.

Organism	Mutation		Organism sensitivity to inhibitor				Comment	Reference
	α-tubulin	β-tubulin	Dinitroaniline	Phosphorothioamidate	Colchicine	Taxol		
Chlamydomonas reinhardtii	T24H		R	R	S	SS		James *et al.* 1993
		L350E	R	R	R	SS		Schibler *et al.* 1991 and Lee *et al.* 1990
		L350M	R	R	R	SS		Schibler *et al.* 1991 and Lee *et al.* 1990
Setaria viridis L. Beauv	L136P		R				Carbamate (S)	211 Delye *et al.* 2004
	T239I		R				Carbamate (S)	211 Delye *et al.* 2004
Eluecine Indica	T239I		R			S		Yamamoto *et al.* 1998 and Cronin *et al.* 1993
	M268T		R			S		Yamamoto *et al.* 1998 and Cronin *et al.* 1993
Zea mays	T239I		R				Proamide (S)	Anthony *et al.* 1999 and Anthony *et al.* 1998
	M239I		R					Anthony *et al.* 1999
Toxoplasma gondii	L136P		R				Fitness cost	Ma *et al.* 2007
	T239I		R				Fitness cost	Ma *et al.* 2007
	R243S		R				Fitness cost	Ma *et al.* 2007
	V252L		R				Fitness cost	Ma *et al.* 2007
	M301T		R					Morrissette *et al.* 2004

Table 5.2. List of the mutations associated with dinitroaniline or phosphorothioamidate resistance. R, resistant; S sensitive; SS super-supersensitive. Only the most resistant mutations are shown for *Toxoplasma gondii*. There was also a fitness cost associated with some of the mutations in *T. gondii*.

resistance (Blume *et al.*, 2003, Délye *et al.*, 2004 and 94 Morrissette *et al.*, 2004). These sites were elucidated using molecular homology models based on the crystal structure from mammalian brain tubulin. Both Blume *et al.*, and Délye *et al.*, concur that the binding site is located on the intra-dimer interface (Blume *et al.*, 2003 and Délye *et al.*, 2004). This contrasts with the putative Morrissette site and the later refined version which was developed by Mitra and Sept, who proposed a site just beneath the H1/S2-loop on α-tubulin (Morrissette *et al.*, 2004 and Mitra and Sept, 2006). The Morrissette site was further supported by mutational studies using live parasites (Morrissette *et al.*, 2004 and Ma *et al.*, 2007). Nonetheless, an underlying problem associated with these molecular models is the fact that they are based on bovine brain tubulin, which is resistant to the herbicide compounds. Furthermore, as mentioned already, these mutations may confer resistance in a non-specific manner i.e. increasing the stability of the tubulin. This fact could explain the results that Ma *et al.*, (2007) obtained from the mutated parasites. Therefore, despite the above work, it is still vital to substantiate these predictions using *in vitro* techniques that are specific for measuring the tubulin-ligand interactions.

In this chapter, an investigation was conducted to identify and explain some of the more salient differences between tubulin from the lower and higher eukaryotes. The "inversion" phenomenon was examined by identifying key features, on an AA level, associated with the tubulin from herbicide-sensitive and -resistant organisms. These predictions made were subsequently verified using purified tubulin. In order to validate the putative herbicide binding sites, altered tubulins were generated using site-directed mutagenesis on the αI-tubulin gene. These alterations were specifically chosen based on the aforementioned putative binding sites (Blume *et al.*, 2003, Délye *et al.*, 2004 and Mitra and Sept, 2006). Recombinant MBP-tubulin fusions with these alterations were expressed and purified. The binding constants (K_d) were then determined for these proteins using APM and a dinitroaniline representative, oryzalin, with the intrinsic tryptophan quenching assay.

5.2 RESULTS

5.2.1 Investigation of the electrophoretic inversion phenomenon of α/β-tubulin

To identify differences between tubulin from herbicide-sensitive and -resistant organisms, alignments of α- and β-tubulins were compared. The α-tubulin was previously identified to have the most variable migration on SDS-PAGE (Cyr *et al.*, 1987). Only organisms, with the "inverted" tubulin, that were conclusively determined to be sensitive to herbicides were used in the alignments. Since only higher eukaryotes were identified with the "normal" tubulin an assumption was made that they were resistant to the dinitroanilines and phosphorothioamidates. This assumption was based on the fact that these compounds are herbicides and widely used. Furthermore, there have been numerous reports confirming that these compounds are relatively inactive against tubulin from higher eukaryotes (Dow *et al.*, 2002, Fennell *et al.*, 2006, Stokkermans *et al.*, 1996, Bhattachatya *et al.*, 2003, Bell, 1998, Kaya *et al.*, 2004 and Werbovetz *et al.*, 2003). These alignments were analysed by several different methods in order to elucidate the conserved differences. To further support the *in silico* predictions, the recombinant *P. falciparum* tubulin protein was modified in an attempt to "flip" the "inverted" tubulins so that the α-tubulin would migrate slower than the β-tubulin.

5.2.1.1 Alignment of the "inverted" and "normal" tubulin proteins

The α- and β-tubulins were identified and aligned as described in section 2.7.2. Although numerous isotypes exist for some of the tubulins (e.g. 8 for the *Z. mays* β-tubulin), only one isotype was used, with the exception of *Plasmodium*. This was done due to the fact that the tubulin isotype was generally not known or described in the literature and using all of the isotypes may weight the alignments towards a particular sequence of AA's. Both isotypes of *Plasmodium* were used since further recombinant work was conducted using both proteins. The AA's were colour-coded according to their individual properties (see Fig. 5.1). Regions where there was a conserved difference between the "normal" versus the "inverted" tubulin were highlighted (see Fig. 5.1 and 5.2). The total list of changes was also compiled (see Table 5.3). There were only a few consensus changes in β-tubulin that were specific

A

Position	Normal Tubulin	Inverted Tubulin
4	Cysteine	Valine, Isoleucine, Alanine, Cysteine
48	Serine	Alanine
94	Threonine	Serine, Threonine
103	Tyrosine	Phenylalanine, Tyrosine
118	Valine	Cysteine, Alanine, Serine
128	Glutamate	Asparagine
139	Histidine	Serine, Asparagine, Histidine
140	Serine	Alanine, Serine
141	Phenylalanine	Valine
149	Phenylalanine	Leucine
150	Threonine	Glycine
168	Glutamic acid	Asparagine, Glycine
174	Alanine	Serine
190	Threonine	Serine
194	Threonine	Leucine
198	Serine	Threonine
200	Cysteine	Valine
202	Phenylalanine	Isoleucine, Valine, Alanine
204	Valine	Leucine
235	Valine	Isoleucine, Valine
238	Isoleucine	Leucine
252	Leucine	Valine, Isoleucine, Leucine
268	Proline	Methionine, Valine
271	Threonine	Serine
295	Cysteine	Alanine, Valine
300	Asparagine	Serine, Asparagine
301	Glutamine	Methionine
303	Valine	Alanine, Threonine
318	Leucine	Methionine
332	Isoleucine	Valine, Isoleucine
353	Valine	Cysteine, Valine
378	Leucine	Isoleucine
381	Threonine	Serine, Asparagine
387	Alanine	Valine, Isoleucine
388	Tryptophan	Phenylalanine
389	Alanine	Serine, Alanine
438	Aspartic acid	Glutamic acid

B

Position	Normal Tubulin	Inverted Tubulin
67	Valine	Methionine, Isoleucine
114	Valine	Isoleucine
166	Asparagine	Glutamic acid, Leucine, Methionine
233	Threonine	Threonine, Alanine, Valine
249	Alanine	Alanine, Serine
258	Methionine	Leucine
259	Valine	Isoleucine, Valine
268	Proline	Isoleucine, Valine, Methionine
314	Valine	Alanine
315	Alanine	Cysteine, Serine
353	Alanine	Serine, Threonine, Alanine
360	Arginine	Lysine, Isoleucine, Histidine, Arginine
378	Leucine	Methionine

Table 5.3. List of the AA changes between the "normal" and "inverted" α- (A) and β-tubulins (B). Only AA's which were all identical for the "normal" tubulins were used to identify differences found in the "inverted" tubulin. AA's where there was no variation in either the "normal" group or the "inverted" group are highlighted.

A

Tubulin Alteration	APM Kd (μM)	F_{max} R^2 value	P value	Oryzalin Kd (μM)	F_{max} R^2 value	P value
Val4Cys	106.47 +/- 17.9	0.9621	0.099			
Val4Cys/β-tubulin	34.89+/- 7.79	0.7457	0.1182	25.26 +/- 5.33	0.9995	0.004
Phe24His	104.43 +/- 29.5	0.8244	0.2417			
Phe24His/β-tubulin	47.28 +/- 9.88	0.9295	0.5555	15.31 +/- 4.36	0.8261	0.9313
Cys65Ala	96.11+/- 20.76	0.9586	0.4236			
Cys65Ala/β-tubulin	57.27 +/- 8.10	0.9709	0.0106	13.75 +/- 1.96	0.9955	0.2819
Leu136Phe	89.47 +/- 14.57	0.8612	0.8481			
Leu136Phe/β-tubulin	46.52 +/- 17.54	0.9869	0.7665	24.56+/- 7.54	0.9581	0.0239
Thr239Ile	75.86 +/- 8.14	0.9862	0.6677			
Thr239Ile/β-tubulin	57.95 +/- 6.01	0.9203	0.0076	N.D.	N.D.	N.D.
Arg243Ser	60.86 +/- 16.24	0.8531	0.0552			
Arg243Ser/β-tubulin	32.49 +/- 12.36	0.925	0.0676	17.64 +/- 4.51	0.9345	0.372

B

Protein Sample	Conc. (μM)	Compound	F_{max} R^2 Value
Bovine Tubulin	0.15	*Vinblastine* 0.91 μM ± 0.29	0.8797
MBP-αI/β-tubulin	0.15	*Oryzalin* 15.51 μM ± 3.55	0.9453
	0.15	*APM* 44.14 μM ± 7.15	0.9712

Table 5.4 List of the binding affinities (K_d) for APM and oryzalin for the altered MBP-tubulin fusions (A) and the wild type (B). **A**. The alterations in the MBP-αI-tubulin were just written as the AA change for simplicity. "β-tubulin" indicates the mixture of the altered αI-tubulin with wild-type β-tubulin. **F_{max} R^2 value**, the correlation co-efficient of the line measuring the F_{max} (F_{max} = maximum possible quench if the ligand the ligand occupies all of its binding sites on tubulin). The p **values** shown are for the comparison with the wild type tubulin(s). **N.D.**, not determined. Cys65Ala/β-tubulin and Thr239Ile/β-tubulin had a statistically-significant, slightly lower affinity for APM than that of MBP-αI/β-tubulin. Val4Cys/β-tubulin and Leu136Phe/β-tubulin had a statistically-significant, slightly lower affinity for oryzalin than that of MBP-αI/β-tubulin. **B**. The wild type values are shown only for comparison and were discussed in section 3.2.3.2.

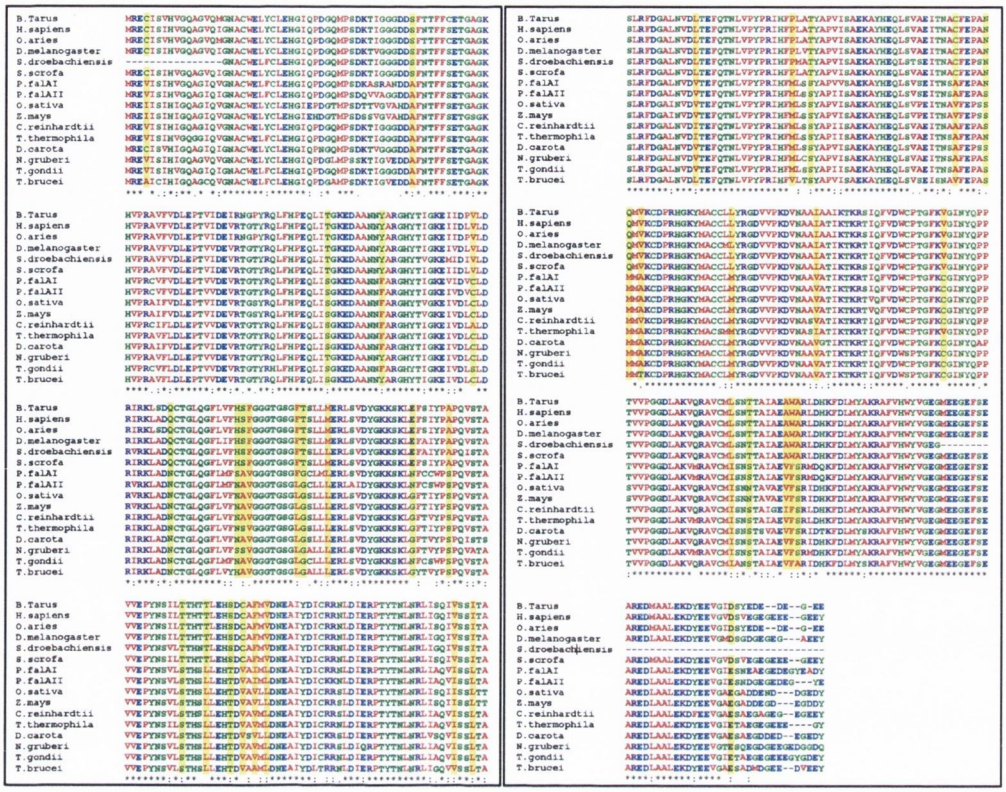

AVFPMILW	RED	Small (small+ hydrophobic (incl.aromatic -Y))
DE	BLUE	Acidic
RHK	MAGENTA	Basic
STYHCNGQ	GREEN	Hydroxyl + Amine + Basic - Q

Fig. 5.1. Alignment of the "normal" and "inverted" α-tubulins from different organisms. AA 1–240 (left) and 241– ~450 (right). *S. droebachiensis* has not been completely sequenced to date so some AA are missing from the alignment. Conserved sequences for the "normal" proteins that were different to the "inverted" proteins were highlighted in yellow. The table shows an AA map that describes the colour coding scheme (reproduced from www.ebi.ac.uk/Tools/es/cgi-bin/tcoffee). "*" means conserved sequence. ":" means conserved according to the type of change i.e. an acidic AA for a different acidic AA. "." means semi-conserved. Semi-conserved means that most of the AA's are similar in type or identical but at least one is completely different.

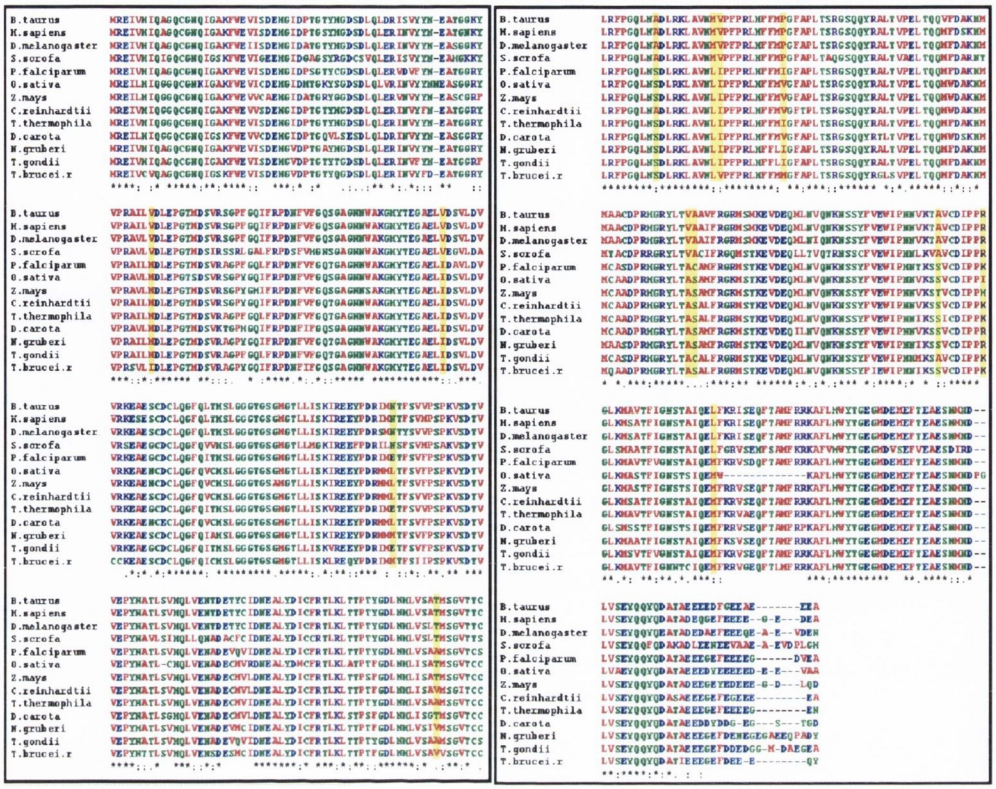

AVFPMILW	RED	Small (small+ hydrophobic (incl.aromatic -Y))
DE	BLUE	Acidic
RHK	MAGENTA	Basic
STYHCNGQ	GREEN	Hydroxyl + Amine + Basic - Q

Fig. 5.2. Alignment of the "normal" and "inverted" β-tubulins from different organisms. AA 1–240 (left) and 241– ~450 (right). Conserved sequences for the "normal" proteins that were different from the "inverted" proteins are highlighted in yellow. The table shows an AA map that describes the colour coding scheme (reproduced from www.ebi.ac.uk/Tools/es/cgi-bin/tcoffee). "*" means conserved sequence. ":" means conserved according to the type of change i.e. an acidic AA for a different acidic AA. "." means semi-conserved. Semi-conserved means that most of the AA's are similar in type or identical but at least one is completely different.

for the "normal" and "inverted" tubulins. Therefore, most of the work focused on α-tubulin. From the examination of the changes in α-tubulin, it became apparent that a region between the 128th and 204th AA had the greatest conserved difference. This region from the "normal" and "inverted" tubulins was aligned separately. The "normal" tubulins were greater than 99% identical as opposed to the "inverted" tubulins which were only 83% identical (data not shown). This difference was likely due to the fact that more diverse organisms were used in the sequence alignment studies for the "inverted" tubulin than the "normal" tubulin. To determine the impact these changes had on the proteins, a hydropathy plot was employed to measure the hydrophobicity and hydrophilicity of the AA's based on the Kyle-Doolittle and Hopp-Woods scales (see Fig. 5.3) (Kyte *et al.,* 1982 and Hopp *et al.,* 1981). The difference between these plots was relatively small, which was not surprising considering that most of the mutations were similar in nature i.e. a hydrophobic AA for another hydrophobic AA. A hydropathy plot was conducted for the full length protein for all of the aligned proteins, but no obvious differences were noted (data not shown). Therefore, hydrophobicity was considered not to be a major determinant of the unusual protein migration.

5.2.1.2 Examination of the molecular basis of inversion in recombinant *Plasmodium* tubulins

It was previously established that the a high pH and low quality SDS could be used to "flip" the migration of plant tubulin subunits so that α-tubulin migrates slower on a denaturing polyacrylamide gel than β-tubulin (Cyr *et al.,* 1986). However, this result was not repeated for recombinant *Plasmodium* tubulins although they did migrate closer to each other under these conditions (Fennell, 2005). Therefore, these experiments were aimed at further analysing the potential cause of this phenomenon and substantiating the *in silico* predictions. Untagged tubulin were used for all these experiments (see section 2.5.2). These proteins were insoluble but this was not a problem because only apparent molecular weight by SDS–PAGE was being examined. Furthermore, even soluble *Plasmodium* tubulins (i.e. the MBP-tubulin fusions) have the same migration pattern.

We postulated that a possible cause for the tubulin inversion was the formation of disulphide bonds within the tubulin during electrophoresis as previous reports

indicated that alkylating these proteins can affect the migration pattern (Perry *et al.*, 1982). Although a reducing agent (2-mercaptoethanol) was always added to the sample buffer, it could be possible that the reducing agent dissipates during electrophoresis, permitting the formation of disulphide bonds and affecting the electrophoretic migration. To eliminate disulphide bond formation as a possible explanation for the inversion, the tubulin were exposed to iodoacetic acid to irreversibly block these residues from reacting. However, this did not affect the inversion pattern of these proteins, indicating that disulphide bonds are probably not responsible for this phenomenon (data not shown).

In order to investigate further the inversion of *Plasmodium* tubulin, site–directed mutagenesis was employed to alter the tubulin genes. Untagged tubulin was again used in these experiments even though it was completely insoluble and formed inclusion bodies. The major source of variability among tubulin sequences is the C-terminal tail (Figs. 5.1 and 5.2). Although no consensus could be distinguished from the sequence alignment studies, it was thought likely that the C-terminus may hold the key to inversion. (Miss Deirdre O' Flynn assisted in the generation of specific mutations in the tubulin genes for these experiments under my supervision as part of her 4th year BA (Mod) project at Trinity College.) A non-native stop codon was inserted into the αI-, αII- and β-tubulin genes to induce premature translation termination as described in section 2.3.8.3. Care was taken to ensure that the molecular weights of the AA's that were being removed affected the molecular weight of the α- and β-tubulins equally. In total, these altered tubulins had 14 fewer AA's than wild–type controls, with predicted reductions in molecular weight of 1.82 kDa for αI- or αII-tubulin and 1.83 kDa for β-tubulin. This modification did not affect the inversion of these proteins, although the altered tubulins did migrate marginally faster on the gel as expected (see Fig. 5.4).

Since the C-terminal tail was ruled out as the source of the AA's conferring inversion, it seemed reasonable that the AA 128 – 204 on α-tubulin might be responsible for this unusual migration effect. However, most of the changes in this region appeared to be insignificant because they constituted minor changes to charge and size. One exception, the asparagine at position 168 that was conserved on the "normal" tubulin, was specifically changed to a glutamic acid (N168E) (see section 2.3.8.3). Asparagine was not found to be conversed for the "inverted" tubulins as it was commonly found as a glycine. However, the asparagine and glycine are slightly

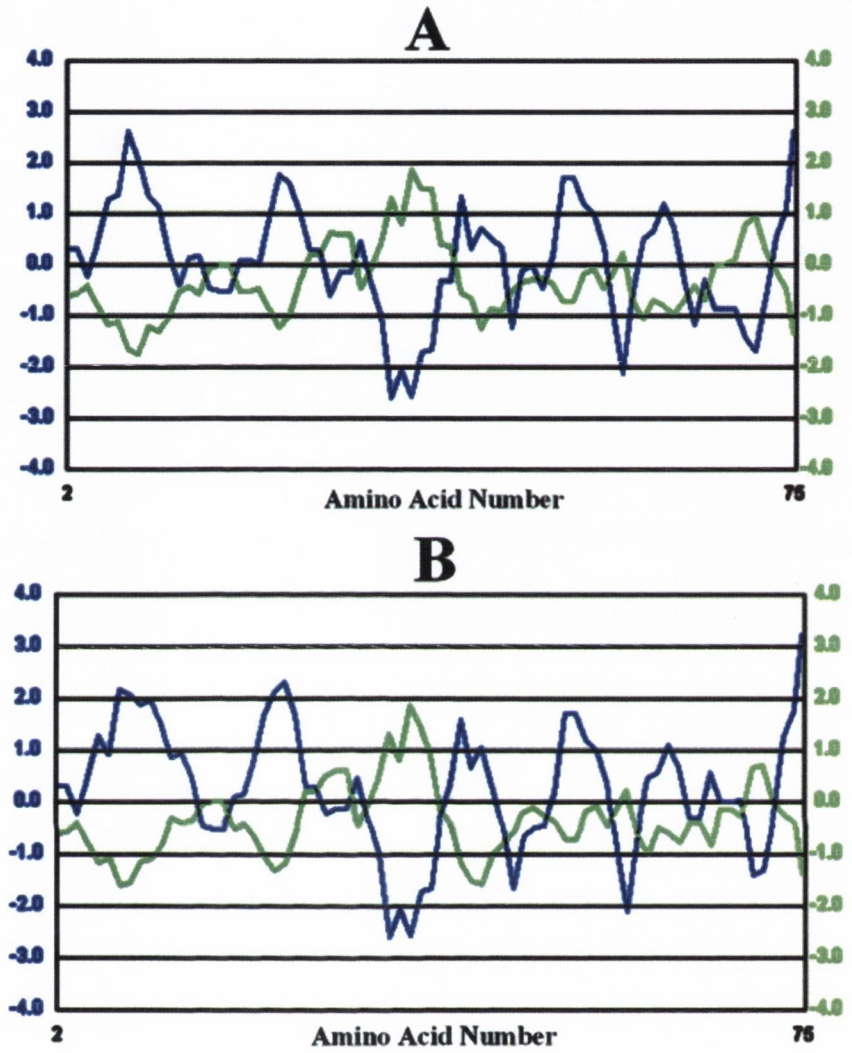

Fig. 5.3. Hydropathy plot for the AA's 128 – 204 of α-tubulin for *B. taurus* and *P. falciparum* (αI-tubulin). The **blue** line represents the Kyle-Doolittle hydrophobic scale for the AA's while the **green** line represents the Hopp-Woods scale for hydrophilicity for AA's. **A.** *B. taurus*. **B.** *P. falciparum*. Although there are some differences between the α-tubulins from the two organisms, they are small.

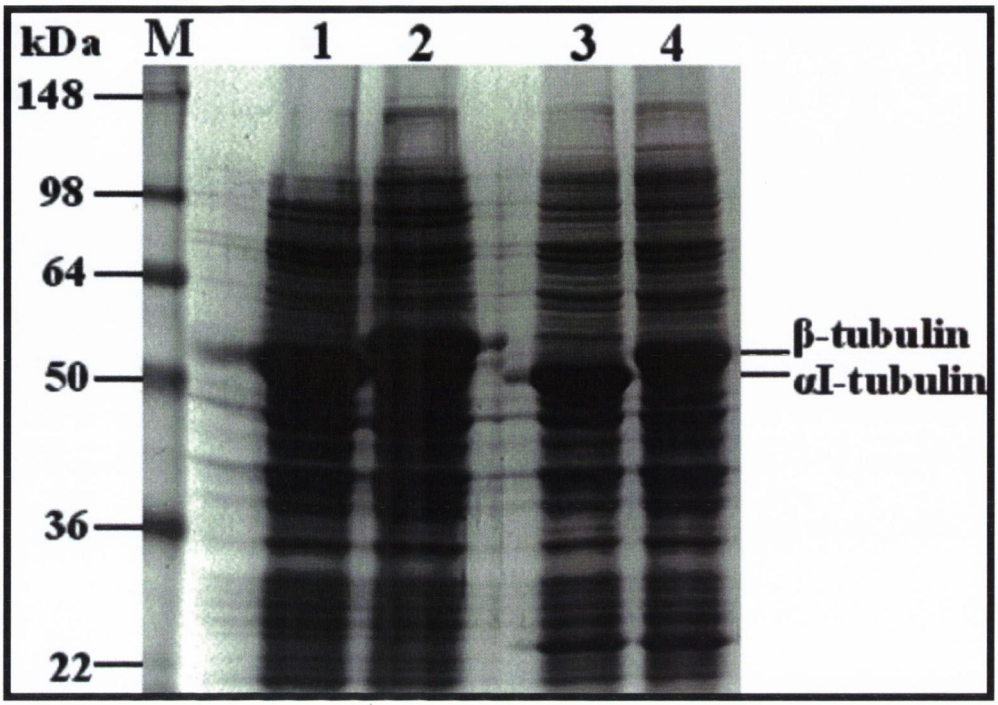

Fig. 5.4 Resolution of wild type and truncated αI- and β-tubulin by SDS 10%-PAGE. **M**, molecular weight marker (Invitrogen). **1)** αI-tubulin, **2)** β-tubulin, **3)** α-tubulin Δ-C-terminal tail and **4)** β-tubulin Δ-C-terminal tail. The unaltered αI-tubulin migrated faster than β-tubulin (Lanes **1** and **2**). Insertion of stop codons to induce premature translation of both of the tubulin genes did not affect their relative migration pattern and both ran further as expected. This was solely due to the loss of several AA's from the C-terminus.

basic or neutral compared to the acidic glutamic acid. Nonetheless, this alteration did not affect the inversion of the recombinant *Plasmodium* tubulins (data not shown).

Overall, it was not possible to "flip" the migration of the *Plasmodium* α- and β-tubulins with the experiments described here. However, some insights were gained from this examination, particularly the identification of a possible region on α-tubulin that may be important for this effect.

5.2.2 Investigation of the herbicide-binding site on *P. falciparum* tubulin

To gain an insight into the preferential binding of the herbicide compounds to tubulin, an investigation of the three putative binding sites was undertaken (Blume *et al.*, 2003, Délye *et al.*, 2004 and Morrissette *et al.*, 2004). The strategy entailed generating alterations in the tubulin-fusion proteins that would disrupt or occlude the putative sites, so as to verify their presence on *Plasmodium* tubulin. The tubulin-ligand interactions were measured using the intrinsic tryptophan quenching assay as outlined in chapter 3.

5.2.2.1 Selection and generation of the tubulin alterations for the determination of the phosphorothioamidate and dinitroaniline binding site

Selection of the AA alterations was based on several factors so as to confirm definitely the existence of these binding sites on *Plasmodium* tubulin. Since further evidence supporting the Morrissette site in *Toxoplasma* has emerged since its inception, there was more emphasis placed on verifying this site than those of Blume or Délye, for which there was essentially no experimental evidence in any organism (Mitra and Sept, 2006, Ma *et al.*, 2007 and Ma *et al.*, 2008). Therefore, changes in AA that were found on more than one of putative binding sites, or in AA found to be in herbicide resistant tubulins (i.e. Val4Cys alteration is found in bovine brain tubulin) or in AA that were likely significantly to affect the tubulin-ligand interaction according to Ma *et al.*, (2007) were selected. Six alterations for the αI-tubulin protein were chosen: Val4Cys, His24Phe, Cys65Ala, Leu136Phe, Thr239Ile and Arg243Ser. To ensure that these changes would be significant, the residues which comprise the Morrissette site were isolated on molecular models and the specific alterations were then highlighted to ensure that their location and presence was significant (see Fig.

5.5). From the molecular models, the alterations were centrally located and they were predicted to drastically affect the structure of the putative binding site.

Site directed mutagenesis was employed specifically to change the *Plasmodium* αI-tubulin gene, generating six independent alterations in the protein as described in section 2.3.8.1 These proteins, all fused to MBP at the N-termini, were purified to near homogeneity using the same approach as described in chapter 3 (section 3.2.1.2) (Fig. 5.6 A). A western blot was used to determine that all of the altered tubulins were fully translated and relatively pure (Fig. 5.6 B). Since the tubulins were relatively pure and equal in concentration, they were subsequently used for ligand-binding studies.

5.2.2.2 Investigation into the interactions of APM and oryzalin with the altered tubulins

Tubulin-ligand interactions were measured using the intrinsic fluorescence quenching assay that was described in section 3.2.3.2. The interaction with APM of the altered αI-tubulins were assayed with and without the MBP-β-tubulin fusions. For oryzalin, only the MBP-α/β-tubulin mixture was used, as the main focus of this study was to verify if the putative binding sites were relevant for the phosphorothioamidate compounds. This assay permitted the elucidation of K_d's for APM and oryzalin to all of the altered tubulins (see table 5.4 A). For comparison, the K_d from the unaltered tubulins are reproduced again (see table 5.4 B).

A K_d value was generated for all the altered tubulins, as monomers for APM and as a mixture for APM and oryzalin. These alterations in α-tubulin did not induce any obvious changes in the tubulin binding-affinity for either APM or oryzalin (see section 3.2.3.2). However, some of the alterations were later confirmed to be statistically significant with a 95% confidence for either APM or oryzalin, as judged by a Student t-test. This effect was only seen in the αI-β-mixture but not in the corresponding altered αI-tubulin monomer.

Two different alterations caused a slight decrease in affinity for both APM and oryzalin (see Table 5.4). Cys65Ala/β-tubulin and Thr239Ile/β-tubulin had statistically lower affinity for APM than that of MBP-αI/β-tubulin while Val4Cys/β-tubulin and Leu136Phe/β-tubulin had statistically lower affinity for oryzalin than that of MBP-αI/β-tubulin. However, the change in affinity was not as dramatic as expected.

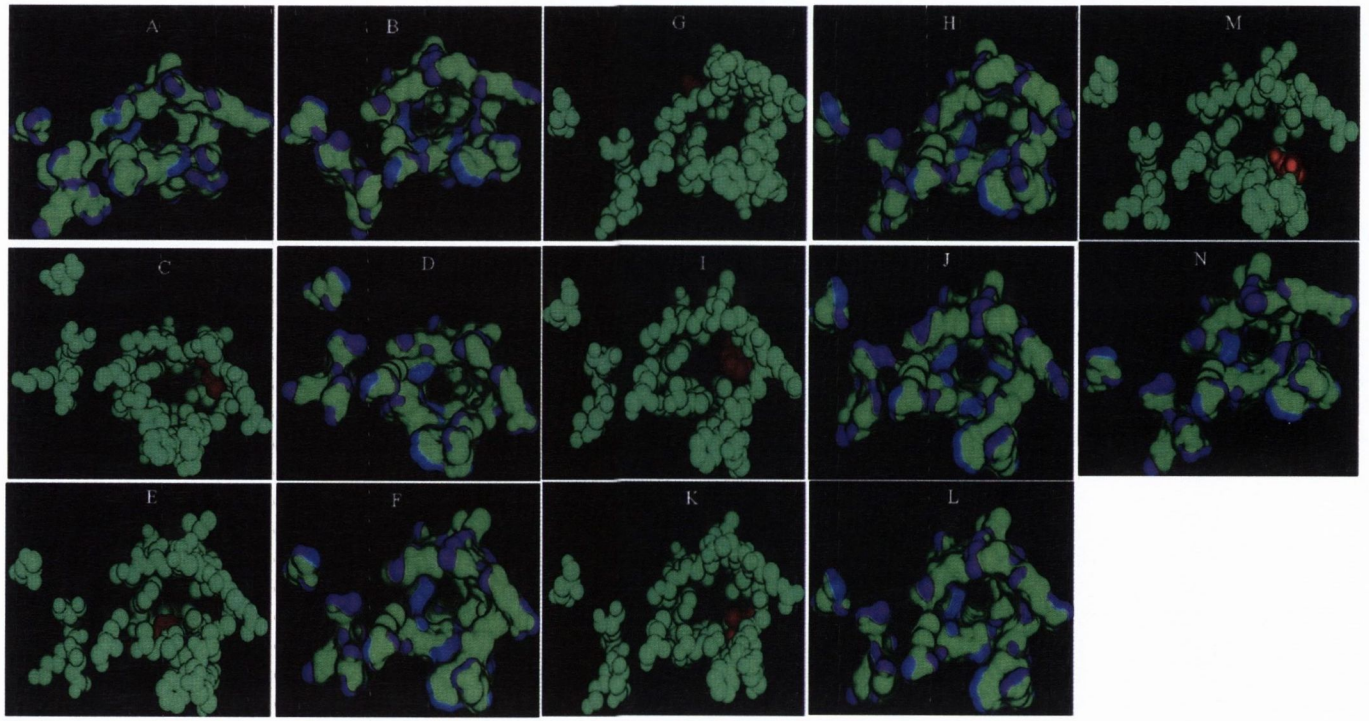

Fig. 5.5 Models constructed using MOE of the residues which comprise the putative Morrissette binding site on *P. falciparum* αI-tubulin. Only Morrissette site is highlighted. The models were displayed using either a surface molecular map (Connolly analytic) (**A**, **B**, **D**, **F**, **H**, **J**, **L** and **N**) or space-filled AA's (**C**, **E**, **G**, **I**, **K** and **M**). The surface molecular map highlighted predicted hydrophobic (**green**), polar (**blue**) and hydrogen-bonding (**purple**) regions. The space-filled models highlighted the Morrissette site residues (**aqua**) or the specific alteration (**red**) **A.** *B. taurus* α-tubulin. **B.** Homology model of the *P. falciparum* αI-tubulin WT, **C** and **D** Val4Cys alteration, **E and F** Phe24His alteration, **G** and **H** Cys65Ala alteration, **I** and **J** Leu136Phe alteration, **K and L** Thr239Ile alteration, **M** and **N** Arg243Ser alteration.

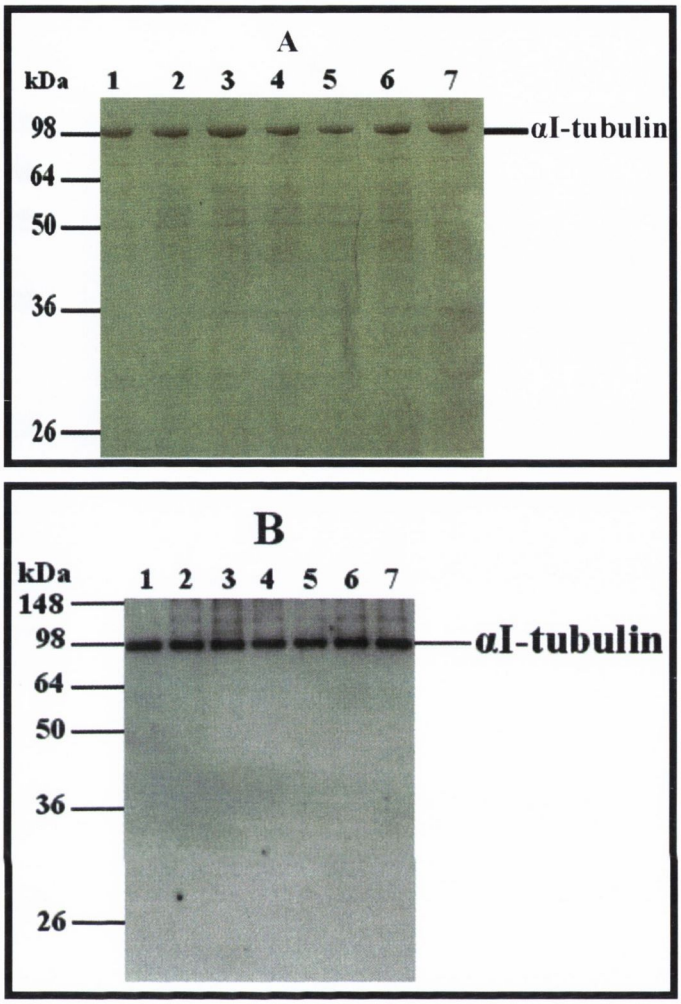

Fig. 5.6 Resolution of the wild type and altered MBP-αI-tubulin by SDS 10%–PAGE and western blotting. All the samples represent 3 μg of MBP-αI-tubulin with or without AA alterations. **A.** SDS 10%–PAGE. **B.** Western blot of a similar gel probed with an anti-α-tubulin serum. **1.** Wild type tubulin. **2.** Val4Cys. **3.** Phe24His. **4.** Cys65Ala. **5.** Leu136Phe. **6.** Thr239Ile. **7.** Arg243Ser. All of the α-tubulins were relatively pure and were equally loaded (3 μg). No obvious breakdown was observed on either the polyacrylamide gel or the western blot.

Therefore, these alterations may be having an allosteric effect on the tubulin instead of directly affecting the binding site(s). These results do not completely exclude the possibility of the Morrissette site existing on *Plasmodium* tubulin as some of the alterations were significant, but it is difficult to explain the reason for very small changes in affinity and the other alterations being ineffective.

Overall, it appeared that this data did not support the putative Morrissette or Blume binding sites. Although some of the alterations reduced the affinity of the herbicide compounds to tubulin, this reduction was not as drastic as expected particularly since the AA's that were changed were considered crucial to these binding sites. Furthermore, some alterations had no affect at all. Therefore, this data does not support the existence of these putative binding sites *Plasmodium* tubulin. For putative Délye site, altering the Asp251 and/or Asn 253 would verify this site definitely.

5.3 DISCUSSION

The primary aim of this chapter was to appreciate the preferential affinity for the herbicide compounds for different tubulins. It was previously observed that tubulin from lower eukaryotes tended to be more sensitive to the herbicide compounds than higher eukaryotes. Furthermore, tubulin from lower eukaryotes were often observed to have tubulin with inverted migration on denaturing polyacrylamide gels. This was not seen in tubulin from higher eukaryotes. Therefore, even if this "inversion" phenomenon is not related to the sensitivity of the tubulin to the herbicides, it still merited investigation as it represented a difference between the herbicide-sensitive and -resistant tubulin.

Specifically, an exclusive herbicide binding site was predicted to exist only on tubulin from lower eukaryotes. So far, at least three putative sites have been suggested by other researchers (Blume *et al.*, 2003, Délye *et al.*, 2004 and Morrissette *et al.*, 2004). These sites were chosen based on mutations within the tubulin genes that caused previously sensitive organisms to acquire resistance to the herbicide compounds. As a result, these sites were proximal to each other and even shared some critical residues. Therefore, generating altered tubulins and measuring the binding affinity of the herbicides to the altered tubulin should determine the validity of these putative binding sites in relation to *P. falciparum* tubulin.

An extensive search was conducted to identify as many organisms with "normal" and "inverted" electrophoretic migration of tubulin as possible so as to conduct an investigative analysis of their tubulin AA sequences. However, this search was hindered by a number of factors. **1)** The method used to separate the tubulin proteins, either that of Studier (1973) or Laemmli (1970) could reverse the migration of the "inverted" tubulins. This was eloquently demonstrated by Cyr *et al.,* for *D. carota,* and contrasted with previously published reports for this organism (Cyr *et al.,* 1986 and Morejohn *et al.,* 1983). **2)** The predominant tubulin isotypes were often not identified, which meant that choosing which gene to use for the sequence alignment studies was exceedingly difficult. In some cases, it was possible to predict which gene was relevant due to the fact that there was only one isotype. Alternatively, in *B. taurus*, some isotypes are more highly expressed than others in particular tissues so they were considered more likely to be isolated as the tubulin purification method was concentration-dependent (Renthal *et al.,* 1993). However, this was not always possible so an assumption had to be made that all of the isotypes from one organism were either "normal" or "inverted" but not both. This was demonstrated to be true for several organisms with either "normal" or "inverted" tubulin, although the isoelectric points of these isotypes were frequently different (Hussey *et al.,* 1984, Piperno *et al.,* 1985, Banerjee *et al.,* 1992, Suprenant *et al.,* 1985, Blume *et al.,* 1998 and James *et al.,* 1993). It was originally planned to use all of the tubulin isotypes from an organism when applicable, although it was thought that this may skew the results by highlighting patterns that are specific for that organism. This was considered particularly true if there were numerous isotypes such as in *Z. mays*, which has eight β-tubulins. **3)** The identities of the tubulins were not always confirmed by a specific experiment such as western blotting, or even run on the same gel, so a size comparison could not always be made. **4)** Only organisms that demonstrated sensitivity to the dinitroanilines or the phosphorothioamidates were used to ensure that the critical residues were present in the AA sequence. An exception was made for the higher eukaryotes as they are considered to be resistant to these herbicides (Dow *et al.,* 2002, Fennell *et al.,* 2006, Stokkermans *et al.,* 1996, Bhattachatya *et al.,* 2003, Bell, 1998 and Werbovetz *et al.,* 2003). **5)** Finally, it was not always possible to obtain the tubulin AA sequence as not all of them have been reported to date.

Nonetheless, a selection of sequences was compiled and analysed to identify particular trends. Specifically, AA's that were conserved in the tubulin from

herbicide sensitive or resistant organisms but different to each other i.e. glutamate 128 on "normal" tubulin but asparagine 128 on "inverted" tubulin, were highlighted as being potentially interesting. Using this approach, it was noted that the α-tubulin had significantly more conserved changes than β-tubulin, 37 and 13 respectively (see Table 5.3). Furthermore, of these conserved changes, there were 18 on α-tubulin and only 4 on β-tubulin that were absolutely conserved without any variation. This was not surprising since it was previously noted that the α-tubulin was often "responsible" for the inversion pattern by migrating faster than the β-tubulin, which mostly co-migrates with the "normal" β-tubulins (Hussey *et al.*, 1984, Cyr *et al.*, 1986 and Suprenant *et al.*, 1985). In some organisms the opposite was true (Little *et al.*, 1983). However for *Plasmodium*, the apparent molecular weight of both αI- and αII-tubulin was ~53 kDa and that of β-tubulin ~57 kDa, compared to the predicted molecular weight of ~50 kDa for all three. Since the both tubulin subunits in *Plasmodium* had unusual apparent molecular weights, it was considered likely that the inversion "mechanism" applies to both subunits. It was reported previously that the type of SDS used in the denaturing polyacrylamide gels can affect the migration patterns of tubulin (Best *et al.*, 1981). It was later demonstrated that the impurities (longer-chain alkyl sulphates) in the SDS preparation were crucial to the mobility of these proteins (Stephens, 1998). However, SDS containing these impurities had only a limited impact on the migration of *P. falciparum* tubulins (Fennell, 2005). Nonetheless, differential binding of SDS to the proteins is still the likely reason for the inversion phenomenon, particularly since it was responsible for aberrant migration for other proteins (Matagne *et al.*, 1991 and Rath *et al.*, 2009). Typically, very hydrophobic or hydrophilic regions on a protein tend to bind more or less SDS respectively (Rath *et al.*, 2009). Examination of these alignments revealed a specific region on α-tubulin (AA 128-204) that had numerous amino acid changes that were specific to either herbicide-sensitive or -resistant tubulin. A hydropathy plot measuring the hydrophobicity and hydrophilicity of the AA in this region did not detect any obvious change between the herbicide-sensitive and -resistant tubulins. However, Rath *et al.* did show that single amino acid substitutions were sufficient to drastically change protein migration patterns (Rath *et al.*, 2009). Despite a number of totally conserved AA's which could be replaced in this region, a more variable substitution was chosen, N168E. This was done because these amino acids are quite differerent, the asparagine is basic while glutamic acid is acidic, so this change would have a noticeable effect.

Unfortunately, this change did not appear to affect the migration pattern. However, it may be necessary to change a number of residues in the same protein in order to convert the migration to "normal". Several other possible explanations were examined. The cysteine residues were blocked using iodoacetic acid, so disulphide bonds could not form. This made no difference, indicating that this reaction was not significant. Removal of the C-terminal tail was also done, as this is one of the most variable regions on the proteins. This made no difference either.

In conclusion, it was not possible conclusively to identify the specific region that causes the inversion. However, the highly variable region, AA 128-204 appears to be promising. It may be worth expressing this region from the higher and lower eukaryotes to see if it has an aberrant migration on a denaturing gel. This would prevent the more laborious task of generating multiple mutations in the *Plasmodium* tubulin. Furthermore, introducing a premature stop codon into tubulin so that only half or three-quarters of the protein is expressed may yield information regarding the location of the source of this phenomenon.

Since at least three independent binding sites have been proposed for the herbicide compounds, an investigation into their relevance to *Plasmodium* was merited (Blume *et al.*, 2003 and Délye *et al.*, 2004 and Morrissette *et al.*, 2004). This was conducted by generating recombinant tubulin-fusions which had several residues altered. These residues were predicted to disrupt the putative Morrissette binding site and as a result decrease the binding affinity of the dinitroanilines and phosphorothioamidates to the tubulins. This tubulin-ligand interaction was measured using the fluorescence quenching assay which was first described in chapter 3 (see section 3.2.3.2).

All three binding sites were proposed to exist in a similar area on α-tubulin where specific mutations that confer resistance to the herbicides frequently occurred. The Morrissette site was later refined by Mitra and Sept and was further supported by more mutational studies (Mitra and Sept 2006, Ma *et al.*, 2007 and Ma *et al.*, 2008). Therefore, with this increased evidence, specific focus was placed on confirming this site in particular. However, mutations were generated in residues over-lapping the other two putative sites. One significant problem with introducing new AA's into any protein is the risk that they may induce partial mis-folding. In the case of tubulin, this could non-specifically reduce the affinity of herbicide ligands to the protein giving a false-positive result. Therefore, alterations were generated which were shown to be

tolerated previously, i.e. the Val4Cys change exists in bovine tubulin. Also, Ma *et al.*, mentioned that replication defects in *Toxoplasma* are most likely to occur from mutations that hyper-stabilise the tubulin but mutations that increase these defects the least are more likely to be associated with the dinitroaniline binding site (Ma *et al.*, 2007). Therefore, this was another reason that Val4Cys, among others, was chosen as it increased the replication defects the least in *Toxoplasma* (Ma *et al.*, 2007). Furthermore, several mutations were reported to cause significant increases in resistance to the herbicide compounds, most notably Thr239Ile and Arg243Ser. Nonetheless, to ensure that selected alterations were significant, a homology model of the *Plasmodium* αI-tubulin with or without the AA changes was constructed using the crystal structure of bovine brain tubulin as a template. This permitted visualisation of the location of each of the planned alterations. Furthermore, it was possible to predict that their effect would be significant by using a surface molecular map to highlight changes in hydrophobicity. These models were not detailed enough for ligand docking studies so this was not attempted. Mis-sense overlapping primers were used to introduce the specific changes into the αI-tubulin sequence. The expression and purification of these proteins was done as described in chapter 3. The protein integrity and concentration was determined to be satisfactory by a denaturing polyacrylamide gel electrophoresis and western blotting.

The tryptophan fluorescence quenching assay was used to generate binding data for all of the altered tubulins. Both monomers of αI-tubulin and a mixture were used with APM to determine if there was a difference in the results. Since the mixture consistently produced a lower K_d and was likely to be more physiologically relevant, the MBP-αI-tubulin fusions alone were not used for oryzalin.

Overall, there were no dramatic changes in binding affinity of either APM or oryzalin to the altered tubulins. However, some of the alterations were considered statistically significant by using a Student t-test with a 95% confidence interval. Even still, the data presented here did not appear to support the Morrissette site in *Plasmodium* because all of these alterations should have made an obvious impact on affinity of the herbicides to tubulin. The results do not appear to agree with the Blume site either. However, since the alterations made during this project were not essential for the putative Délye site, so it is not possible to completely rule it out.

For the monomers, a larger deviation in results was observed compared to that of the mixture (Table 5.4). The reason for this was that an increased concentration of

ligand was required to detect a change in the fluorescence. However, the more ligand present, the greater the non-specific quenching that occurred. Correction of this data had an unavoidable intrinsic error which was exacerbated at higher ligand concentrations (Table 5.4). Therefore, this data was not conclusive so the MBP-α/β-tubulin mixture was used for the subsequent binding experiments. Nonetheless, no major changes in K_d were found. This contradicts the results of the altered tubulin mixtures, Cys65Ala/β-tubulin and Thr239Ile/β-tubulin for APM. However, this could be explained by the increased error associated with the monomer samples which could mask any significant differences or it could be linked to the improper presentation/formation of the herbicide binding site in the absence of β-tubulin.

Two different alterations were demonstrated to marginally decrease the affinity of either APM or oryzalin to tubulin. For APM these alterations were Cys65Ala and Thr239Ile. For oryzalin the important alterations were Val4Cys and Leu136Phe. This result could represent a different binding site for these ligands, although that is considered very unlikely as there is indirect evidence to support a similar if not identical binding site (Ellis *et al.,* 1994 and Murthy *et al.,* 1994). Furthermore, the decrease in binding affinity is not large. Instead, it is likely that either peripheral AAs to the herbicide binding site were changed or that these results represent an allosteric effect.

It seems unlikely that the Morrissette site applies to *Plasmodium* based on the inconsistent effects of the alterations on APM and oryzalin. Secondly, the actual decrease in ligand affinity for tubulin was only slight, contrary to the dramatic resistance caused by this change in live parasites (Ma *et al.,* 2007). These results did not concur with the existence of the Blume site either as changes to critical AA's, Leu136, Thr239 and Arg243, again did not make a hugely significant difference if any at all.

It was possible that the assay was not accurate enough to detect the subtle differences caused by the alterations in the α-tubulin subunit. Leu136Phe/β-tubulin had the largest error margin for all the mixture samples (46.52 μM +/- 17.54), although the majority of the samples had an acceptable error. Tryptophan fluorescence is very sensitive to even small perturbations in its environment which in this assay can have a significant effect. This was further exacerbated by the presence of the MBP tag which adds eight tryptophans to the protein. Therefore, a significant increase in background fluorescence was added to all the samples which did not help

detect the tubulin-ligand interaction. This fluorescence could be non-specifically quenched by the presence of the ligands, particularly at high concentrations. Although, this non-specific effect was accounted for by using free tryptophans, small over- or under-corrections could add an extra error. As a result, this made accurate determinations of weak-binding ligands very difficult. However, these alterations were specifically and carefully chosen as they dramatically improved the resistance of cultured parasites and plants to dinitroanilines and phosphorothioamidates (Morrissette *et al.*, 2004, Ma *et al.*, 2007, Délye *et al.*, 2004, James *et al.*, 1993 and Yamamoto 1998). Therefore, if these mutations were affecting the actual binding site of these compounds, it was anticipated that an equally dramatic result would occur for the *in vitro* experiments so that the unavoidable error would not matter. No dramatic change in binding was observed for any of the α-tubulin alterations so the error associated with this assay was not deemed to be a major factor. Nonetheless, it may be worthwhile in the future to generate multiple alterations in the same tubulin subunit in case individual subtle changes in the ligand-tubulin affinity can in fact add up to give a significant effect.

As mentioned previously, the binding of APM and oryzalin to the tubulins could be influenced by non-physiologically-relevant factors. The presence of the MBP tag or the possibility that the tubulins are not forming "normal" dimers could affect the conformation of the protein and more importantly the binding site. The fact that the recombinant tubulin has probably aged (see section 3.3) could also affect the tubulin-ligand interaction. Unfortunately, there was no way to characterise the possible influence that these factors may have on the ligand binding studies. However, as mentioned previously, the binding affinity of oryzalin to *Leishmania* tubulin (17 +/- 8 μM) was similar to the affinity of oryzalin to the recombinant tubulin here (15.51 +/- 3.55 μM) (Werbovetz *et al.*, 2003).

Alternatively, the putative Morrissette binding sites may not be applicable to *P. falciparum* or may not be relevant at all for the dinitroanilines and phosphorothioamidates. Mitra and Sept recently refined the Morrissette site and claimed that it also existed in *P. falciparum* and *Leishmania* spp. (Mitra and Sept, 2006). This work was done using molecular models but with no further experimental data to support the existence of this site in *Plasmodium*. Also, the *Plasmodium* tubulin was modelled on a model, that of the *Toxoplasma* tubulin, which seems likely to exacerbate errors generated in the first structure (Mitra and Sept, 2006). The

molecular models that were used by Morrissette *et al.,* and Mitra and Sept were both homology models based on the better-defined crystal structure of *B. taurus* brain tubulin (Lowe *et al.,* 2001, Morrissette *et al.,* 2004 and Mitra and Sept, 2006). This crystal structure did not resolve a large portion of the N-terminal loop (AA's 35-60) due to the fact that it was too flexible (Lowe *et al.,* 2001). Since this missing loop formed an integral part of the Morrissette site, a homology model was made using the β-subunit as a template. Furthermore, using these homology models, an assumption has to be made that the dinitroaniline binding site is actually present, which it may not be as bovine tubulin is resistant to the herbicide compounds. The putative Morrissette site also has a number of AA residues present on resistant organisms e.g. *B. taurus* tubulin. However, it was argued that allosteric effects from other AA's disrupt the binding site on tubulin from vertebrate organisms (Morrissette *et al.,* 2004). A computationally predicted binding affinity for oryzalin to the Morrissette site on α-tubulin was predicted to be 23 nM, which is almost 1000 times lower than the K_d determined here for *Plasmodium* tubulin or for *Leishmania* tubulin (Morrissette *et al.,* 2004 and Werbovetz *et al.,* 2003). Furthermore, the Morrissette site was predicted to exist solely on α-tubulin, but the results here concur with those of other researchers that the binding can occur on both tubulin subunits, albeit to a lesser extent on the β-monomer (Fennell *et al.,* 2006 and Giles *et al.,* 2009). Similar problems also apply to the putative Délye and Blume dinitroaniline sites (Blume *et al.,* 2003 and Délye *et al.,* 2004).

The mutational work supporting the Morrissette site also has inherent problems. All of the mutations that were generated caused a fitness cost to the *Toxoplasma* parasite which was sometimes associated with hyper-stable tubulin (Ma *et al.,* 2007). In fact, some these mutations were predicted to counter-balance the effect of oryzalin rather than reducing its ability to bind to the tubulin protein (Ma *et al.,* 2007). This was also independently demonstrated for the specific mutation Phe24His which conferred an increased resistance to the dinitroanilines and phosphorothioamidates but also super-sensitivity to taxol (James *et al.,* 1993). Also, in *Toxoxplasma*, secondary mutations were spontaneously acquired that reduced the stability of the MT's in the absence of oryzalin (Ma *et al.,* 2008). Therefore, confirming whether these mutations are just affecting the stability of the tubulin or the actual binding may not be possible using cultured parasites.

Taken together, the results here implied that in all likelihood the Morrissette site is not applicable to *Plasmodium* tubulin. Furthermore, although there is evidence to support this site, particularly in *Toxoplasma*, it may still not be relevant in any organism. These results also imply that the putative Blume site is unlikely to exist in *Plasmoidium*. The Délye site is still potentially relevant as the alterations were not absolutely critical for this site.

Overall in this chapter, an investigation was made into discovering the nature behind the differential affinity the herbicide compounds have for the lower eukaryotic tubulin. Examining the tubulin sequences from organisms sensitive and resistant to the herbicides was conducted initially. Significant focus was placed on identifying the mechanism which causes tubulin inversion as this phenomenon appears to be restricted to tubulin from lower eukaryotes. A region on α-tubulin (AA128-204) was found to contain numerous conserved AA's on either the herbicide sensitive or resistant tubulin. Therefore, since AA in this region may influence the inversion effect, a residue was changed but it made no difference, possibly because several must be changed at once. Additional work was also done to rule out any other obvious causes such as the variability of the C-terminal tail or the formation of dissuphide bonds. However, it was not possible to "flip" the migration of the inverted *Plasmodium* tubulins though a particular region was identified which could be relevant.

Since at least three putative binding sites had been proposed for different organisms, an investigation into their relevance to *Plasmodium* was merited. Alterations in α-tubulin were made so that these binding sites, particularly the Morrissette site, would be disrupted. However, the binding affinities generated by the intrinsic tryptophan assay did not highlight any obvious decrease in the ligand-tubulin interactions, though some of alterations were significant. Careful analysis of the results does appear to suggest that the Morrissette or Blume site appear not to be relevant to *Plasmodium*. However, the Délye site was not excluded.

Chapter 6

General Discussion

6.1 MICROTUBULE INHIBITORS AS POTENTIAL ANTIMALARIAL AGENTS

Microtubules play several critically important roles throughout the entire parasite life cycle. Most notably, they form the mitotic spindle during cell division. Even a slight disruption of the MT dynamics has a severe impact on the viability of the parasites. In fact, MT inhibitors have been widely used for a treatment of number of afflictions, particularly cancer. Although most of the MT inhibitors studied to date are equally effective at poisoning parasite and human cells, two distinct classes of common herbicides, the dinitroanilines and the phosphorothioamidates, are potentially selective (Dow *et al.*, 2002, Fennell *et al.*, 2006, Morrissette *et al.*, 2004, Werbovetz *et al.*, 2003 and Giles *et al.*, 2009). It was later established using *in vitro* experiments with purified tubulin that this was likely due to the existence of a unique binding site for the dinitroanilines and phosphorothioamidates on the tubulin of lower eukaryotes including *Plasmodium falciparum* (Werbovetz *et al.*, 2003, Traub-Cseko *et al.*, 2001, Fennell *et al.*, 2006 and Koo *et al.*, 2009). Therefore, a real target exists on the parasite MT's that may be exploited for the development of future drugs.

6.2 *P. FALCIPARUM* TUBULIN: ANALYSIS OF THE RECOMBINANT PROTEINS

6.2.1 Investigation into the optimal strategy for generating recombinant tubulin

The original isolation of tubulin was achieved by Weisenberg *et al.* over four decades ago by a temperature-dependent differential centrifugation approach. This method has since been modified to include an extra affinity chromatography step but the essential principle remains the same. However, a major limitation with this strategy is the prerequisite that a high starting concentration of tubulin is present in the sample. For organisms such as *Leishmania spp.*, this can be greater than 10% of the overall cellular protein content (Fong *et al.*, 1981). However, in *Plasmodium,* it has been estimated that the tubulin content is ~0.25%, which is likely to result in cell extracts containing tubulin well below the required critical concentration for assembly (Fennell *et al.*, 2008). Furthermore, over-expression of tubulin in *S. cerevisiae* was

toxic and this would be likely to be case in *Plasmodium* as well (Burke *et al.*, 1989). Even now, genetic manipulation of the parasites still remains a very challenging task. Therefore, recombinant production of the *Plasmodium* tubulin was the only available option for conducting biochemical interaction experiments *in vitro*.

Previously, the *Plasmodium* tubulins were generated as MBP-fusion proteins. Although these recombinant proteins were able to bind trifluralin (Fennell *et al.*, 2006) they could not polymerise and form MT's (Fennell, 2005). However, MBP-αI-tubulin was capable of co-assembly with bovine brain tubulin (Fennell, 2005). The inability of the MBP-tubulin fusions to polymerise prevented the development of a number of well-established assays for function and ligand binding, most notably the turbidimetric and GTPase assays. Also, polymerising tubulin would permit the examination of the polymers using electron microscopy. Therefore, a significant effort was made to improve the recombinant protein to make it assembly-competent. This was attempted using several different approaches. The MBP tag was considered a possible reason for the inability of the tubulin-fusion proteins to polymerise, and maybe even dimerise, perhaps due to steric hindrance. This result would then explain why MBP-αI-tubulin was able to be incorporated into bovine brain microtubules. However, removal of this tag by specific endoprotease cleavage was problematic. The original enzyme used, factor Xa, could non-specifically digest both recombinant tubulins. This was surprising as there was no consensus recognition site on either of the tubulin subunits and MacDonald *et al.* had previously achieved success with this enzyme, albeit with tubulin from a different organism (MacDonald *et al.*, 2003). A subsequent effort to remove this tag required the re-cloning of the tubulin genes into a related vector (pMAL-c2G), which had an enzyme recognition site for genenase I. Despite the fact that this enzyme did not cleave the tubulins themselves, it was highly inefficient at cutting the MBP tag from the recombinant tubulins despite an exhaustive search for the optimal conditions. However, it was interesting to note that the separated tubulin was still soluble after the link to the MBP tag was cut. It is possible that these proteins have affinity for each other and even when there is no covalent bond, they will still remain attached. Nonetheless, removal of the MBP tag from the tubulin fusions may be still be a viable approach by using different enzyme, possibly the tobacco etch virus (TEV) protease which was reported to be highly specific and efficient (Fox *et al.*, 2003).

Generally, the recombinant production of the tubulin subunits was done in isolation. Therefore, since these proteins naturally form dimers, it seemed logical to attempt to co-express them in the same cell as this might prevent inclusion body formation. The proteins were produced without any tag to maximise the chance that they may display native-like qualities. Furthermore, it was hoped that these proteins could be isolated in similar fashion to that described by Weisenberg *et al.* (1968). However, these tubulins were mostly insoluble even when kept cold. Therefore, it is unlikely that this co-expression made a significant difference. It may be worthwhile to add a small tag, e.g. a hexa-histidine tag, to one of the proteins. Therefore, the formation of tubulin heterodimers could be unequivocally established by metal-chelate affinity chromatography which also would aid in their isolation.

One of the most common problems with expressing tubulin in the bacterial cells is the formation of insoluble inclusion bodies. In the past, two approaches have been taken to renature such proteins, a chemical approach and a biological approach.

The chemical refolding method relies on the intrinsic ability of tubulin to refold into its proper conformation once it has been completely denatured. This has been successfully achieved by several different groups, although each group developed their own unique protocol. This is not surprising as this strategy often requires extensive optimisation for each protein. The protocols outlined by Lubega *et al.* (1993) and Oxberry *et al.* (2001) were previously attempted without success in our lab (Fennell, 2005). However, a novel strategy to refold the tubulin while it was still attached to an affinity column was reported (Jang *et al.*, 2008). Although this strategy did not produce functional tubulins as determined by the turbidimetric and sedimentation assays, they were at least soluble in the absence of urea. Therefore, this procedure may still work if it is further optimised.

The biological approach essentially consists of using the native chaperones present in the RRL to refold the tubulins which have been completely denatured (usually by urea) (Shah *et al.*, 2001). This strategy was attempted here and appeared to be successful. However, it was very labour intensive and only small quantities of functional tubulin (<<1 μg) were eventually produced. Nonetheless, if this method can be scaled up to produce tens of micrograms of functional tubulin, then this would be sufficient for surface plasmon resonance experiments to measure ligand binding. Another limitation of using the RRL was the fact that a specific concentration of tubulin had to be added to the samples. This was due to the presence of urea in the

tubulin samples. Therefore, adding in too much tubulin caused other proteins in the RRL to be denatured. Conversely, adding in too little tubulin, meant that the urea became too diluted so the tubulins would form inclusion bodies. However, it may be possible to increase the efficiency of this method by using the soluble, chemically refolded tubulins. These proteins would have a tag attached but Jang *et al.* (2008) previously described a strategy to remove these tags. Despite an intensive examination of several different recombinant strategies for generating soluble tag-free tubulin, the MBP-tubulin fusions were found to be the best method for generating large quantities tubulin for biochemical studies. Therefore, all the subsequent ligand-binding assays were developed using the MBP-tubulin fusions.

6.2.2 Functional analysis of the MBP-tubulin fusions

A deeper analysis of the MBP-tubulin fusion proteins was conducted. Initial efforts focused on trying to determine if these proteins were capable of forming dimers. However, it was difficult to conclusively confirm whether or not the tubulins could form dimers especially since there have been reports of α-tubulin and β-tubulin homodimers (Jang *et al.*, 2008 and Oxberry *et al.*, 2001). However, if tubulins could form polymers, even in low amounts, this would lend some support to the idea that these proteins are capable of forming some dimers. Although the tubulin fusions had no effect in the turbidimetric assay (Fennell, 2005) this could be due to the fact that this method is relatively insensitive. Therefore, the tubulin fusions were examined for their ability to assemble in a temperature dependent way by differential centrifugation. This experiment did not achieve an absolute answer, as some of the recombinant tubulin appeared to become irreversibly insoluble after prolonged exposure to 37°C. The same was true for the positive control, bovine brain tubulin. This suggested that tubulin aging may be responsible. This was further supported by the lower reactivity of the recombinant tubulins for the DTNB reagent compared to bovine tubulin, despite the former having more cysteine residues. Therefore, the steric hindrance caused by the MBP in conjunction with the phenomenon of tubulin aging may be responsible for the inability of these tubulins to polymerise. It may be worthwhile in the future to try to induce the expression of the tubulin fusions for a shorter period of time to determine if the aging effect occurs during their expression in the bacteria.

A critical aspect of this project was to develop a rapid, reliable and robust assay that was capable of detecting interactions between small ligands and tubulin. As mentioned earlier, two of the most common assays were not applicable to tubulin that was unable to polymerise. Nonetheless, a sulphydryl based assay and an intrinsic tryptophan fluorescence assay were studied in detail. The sulphydryl assay was not useful in reporting tubulin-ligand interactions, possibly due to the tubulin being aged. However, the tryptophan fluorescence assay was further developed and generated useful ligand binding data for representative compounds from both the dinitroaniline and the phosphorothioamidate classes. This assay is highly sensitive which is advantageous as it can report the interaction of these small ligands. A very high precision is required to generate accurate results but this also means the work becomes very time consuming. Therefore, this assay is only useful for measuring a small number of ligands. Nonetheless, this was the first time the K_d of either APM or oryzalin were determined for *Plasmodium* tubulin. This method may now be part of a strategy that permits the development of ligands with an increased tubulin affinity.

6.3 ANALYSIS OF THE NEWLY SYNTHESIZED APM-RELATED COMPOUNDS

The phosphorothioamidates, as mentioned previously, were demonstrated to be significantly more active toward the cultured parasites (IC_{50} ~3.5 μM) than human cells (IC_{50} >64 μM) (Fennell *et al.*, 2006). This selectivity provided a therapeutic window that might be exploited for novel treatments. APM was also considered to have a greater aqueous solubility than the dinitroanilines but also retained a comparable IC_{50} (Murthy *et al.*, 1994 and Fennell *et al.*, 2006). Furthermore, problems with *in vivo* metabolism had been demonstrated with the dinitroanilines. Taken together, APM was seen as the obvious choice of starting compound for generating more potent derivatives. To achieve this goal, a medicinal chemist, Mrs. Christine Mara, generated a relatively large library of APM derivatives and other related compounds.

A particular strategy was taken to evaluate these compounds. Cultured parasites were initially incubated with the APM analogues in order to determine their IC_{50}. To further investigate these results a simplified version of the fluorescence quenching assay was used to generate the relative binding affinities of these

compounds for tubulin compared with APM. Since the aqueous solubility of these compounds was likely to vary, a spectrophotometric assay was developed to identify compounds with which this could be a problem. Several compounds were identified as having low aqueous solubility and were therefore not applicable to the fluorescence quenching assay. Furthermore, due to the sheer number of compounds and the length of time associated with conducting the fluorescence quenching assay, only a selection was examined. Finally, molecular models of the all compounds were developed and some were overlapped with APM. Using this data in conjunction with that from the cultured parasites and the *in vitro* binding assay, it was possible to elaborate on the potentially important regions of these compounds and explain why some compounds were more active than others. Specifically, the replacement of the sulphur with oxygen reduced the activity of the compound against cultured parasites. Using molecular modelling, it was possible to propose that the difference was caused by the oxygen atom being a hydrophilic source in a hydrophobic domain. Overall, an increase in lipophilicity seemed to correlate with an increase in activity against cultured parasites. However, some exceptions were identified and this was thought to be due to differential binding affinity to tubulin. The nitro groups were demonstrated not to be essential. Their optimum position on the benzene ring varied, depending upon the family of APM-related compounds. Finally, it appeared that a negatively charged group on the para position of the benzene ring was favourable.

In future, this strategy may be used to identify new compounds that are generated and possibly expand on the *in vitro* data, particularly by elucidating the binding affinity of these compounds for tubulin so as to confirm any new predictions. This would be best achieved by the development of a high-throughput assay but until that time, using the fluorescence based assay to determine a relative quench should be satisfactory.

6.4 INVESTIGATION INTO THE NATURE OF "HERBICIDE-SENSITIVE" TUBULIN

Tubulin from lower eukaryotes were observed to have two major distinguishing features from that of higher eukaryotes, an inverted α- and β-tubulin migration on denaturing polyacrylamide gels and a preferential affinity for the herbicide compounds, dinitroanilines and phosphorothioamidates. This inversion

phenomenon was thought to be related to the amino acid sequence of the tubulins rather than post-translational modifications. The reason for this was that recombinant and native tubulin have the same migration pattern (Fennell, 2005 and Shah *et al.*, 2001). Therefore, it should be possible to elucidate the mechanism behind the cause for this phenomenon by a thorough examination of the amino acid sequence. It was not certain if the inversion was linked to these tubulins being sensitive to the herbicides, although an investigation was merited due to the interesting nature of this feature alone but also the fact that it represents another difference between the lower and higher eukaryotic tubulins.

To investigate the inversion phenomenon, a list was compiled of the organisms known to have either non-inverted or inverted tubulin. A sequence alignment study picked out one region on α-tubulin (AA 128-204) which had numerous conserved differences between the "normal" and "inverted" tubulins. To test this region, the most significant amino change between the non-inverted and inverted tubulins was made. Although this made no difference, it may be the case that several amino acids need to be changed for the tubulins to swap the migration patterns. The only other highly variable region was the C-terminal tail and this was ruled out by generating altered α- and β-tubulins which did not have this region. Therefore, a further examination of this region is justified.

To date, at least three putative binding sites for dinitroanilines have been proposed to exist only on tubulin from the lower eukaryotes over that of the higher eukaryotes. These binding sites were largely based on molecular models and some mutations that could generate resistance to the herbicide compounds. However, as previously described, these models were certainly not conclusive. In fact, only the Morrissette site was supported by subsequent mutational work. Even if one was correct, it was not clear whether it was present on *Plasmodium* as well or whether it accommodated phosphorothioamidates as well as dinitroanilines. Therefore, an initial study was undertaken to try to substantiate which of the putative binding sites, if any were relevant to *Plasmodium*.

To specifically investigate the affinity of the herbicides to the lower eukaryotic tubulin, the three putative binding sites were studied in more detail. The Morrissette site (Morrissette *et al.*, 2004) appeared to have greater experimental support than those published by Blume *et al.* (2003) or Délye *et al.* (2004). Therefore, specific alterations in αI-tubulin were made that should significantly affect

the binding of APM and/or oryzalin if this site was present on *Plasmodium*. None of the changes drastically affected the affinity for either APM or oryzalin.

In the tubulin mixture (αI/β-tubulin), slight decreases in affinity for APM were observed by two different alterations in the MBP-αI-tubulin. Slight decreases in affinity for oryzalin by two alterations different from those that affected affinity for APM were also observed. No firm conclusion could be drawn from the monomers samples (αI-tubulin alone), particularly due to the error margin associated with these experiments. Overall, the effect these alterations made on the affinity for either APM or oryzalin for tubulin did not confirm the presence of either the Morrissette site or the Blume site. Therefore, these putative sites are not applicable for *P. falciparum*. They may exist on other organisms explaining the contrast in results here with that of Blume *et al.* (2003) and Morrissette *et al.* (2004). Although Mitra and Sept (2006) proposed that the Morrissette site does exist on *P. falciparum*, there was no experimental work other than homology molecular modelling to support this claim. As previously mentioned, this modelling work needs to be supported by *in vitro* data as it can problematic, particularly in the absence of a relevant tubulin crystal structure. The Délye site was not ruled out by these experiments. Therefore, further work would need to be done to verify the relevance of this site to *Plasmodium*. In the absence of generating assembly-competent tubulin, a secondary assay to confirm these results would be very useful. Surface plasmon resonance or isothermal calibration could be possible alternatives.

6.5 FUTURE DIRECTIONS

One of the key goals of this project was to establish a system whereby novel tubulin inhibitors could be rapidly evaluated for their antimalarial potential. Although this was not achieved in full, some significant progress was made. Perhaps the most challenging aspect of this study was contending with the limitations surrounding the recombinant tubulin protein. The inability of our tubulin to self-assemble and the requirement of a large molecular tag hindered the development of multiple important experiments and assays. This issue likely arises due the inability of prokaryotic systems to accurately fold or process eukaryotic proteins. Therefore, it would be worthwhile to try and establish a new system to generate *Plasmodium* tubulin. Unfortunately, the most obvious options may not improve the situation due to the

occurrence of different obstacles. For example, it was previously calculated that ~20 l of parasite culture would be required to attain 1 mg of tubulin. Using a eukaryotic system such as yeast cells instead of *E. coli* has the main advantage of guaranteeing correct post-translational processing but is also problematic due to the presence of intrinsic tubulin contamination and the fact that over-expression of the protein is lethal. However, these issues may be over-come if the yeast tubulin can be substituted for that of *Plasmodium*. Furthermore, protein yields may be sufficient even if the cells die. Another approach would be to use an *in vitro* translation system which is cell free. Unfortunately, this technique is expensive and the protein returns are low (~ 50 μg/ml). Finally, it was already shown in this project that a rabbit reticulocyte lysate could refold completely denatured tubulin that has already been produced in *E. coli*. This procedure worked in principle, therefore, it may be worthwhile investigating the plausibility of purifying the tubulin chaperone machinery specifically from an animal source as described by Ferreyra and Frydman (2000).

Despite the significant number of APM derivatives that were synthesized, the vast majority were almost completely ineffective in the parasite assay. Although initially discouraging, these compounds were useful for determining the potential pharmacophore regions on the APM molecule. As a result, more potent compounds were steadily produced, culminating in the only compound which was more effective than the parent, c70. Although, the improvement was not hugely significant, important insights have been gained based on this library of inhibitors. Furthermore, it was possible to generate some compounds that retained decent antimalarial activity in the absence of the potentially carcinogenic nitro group. Future work should possibly examine the *in vitro* binding of these compounds to the tubulin protein as some of these ligands had a low lipophilicity and potentially low permeability through the cell membrane. Also, c70 should be examined for its ability to bind mammalian tubulin to determine if it is still selective.

The herbicide binding site still remains elusive despite the examination of three potential sites. Molecular modelling, despite being very useful, can be limited particularly when large protein complexes are being interrogated by small hydrophobic ligands. In reality, it is likely that the crystal structure of *Plasmodium* tubulin will need to be solved before the herbicide binding site can be confirmed.

Unfortunately, this usually requires milligram amounts of correctly folded protein to generate these structures, which to date, is not achievable.

Overall, tubulin remains a remarkable drug target and with the sustained interest in these herbicide compounds, a novel, effective antimalarial is within reach.

Appendix

APPENDIX

Compounds 1-72 that were generated during the course of the study (with the exception of APM) are displayed below:

APM

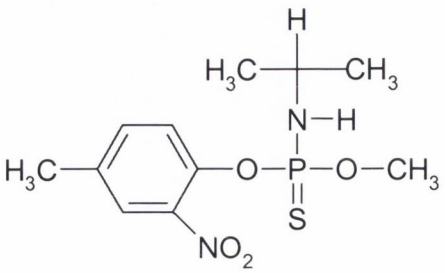

C1

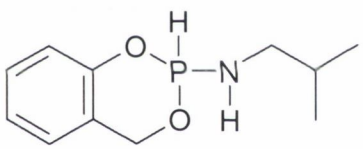

C2

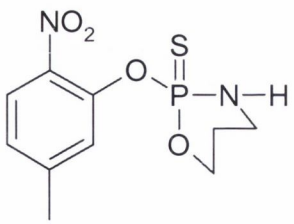

C3

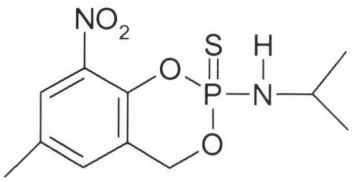

C4

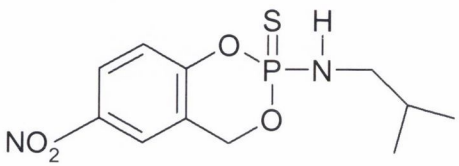

C5

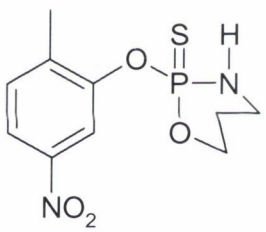

C6

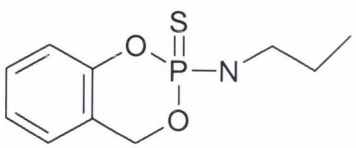

C7

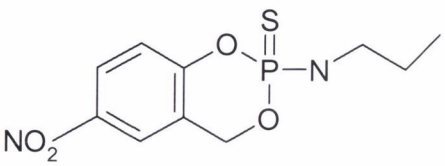

C8

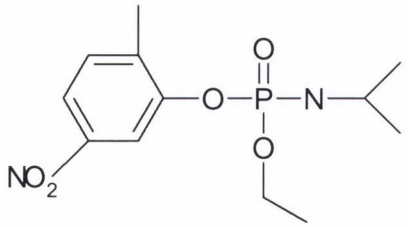

C9

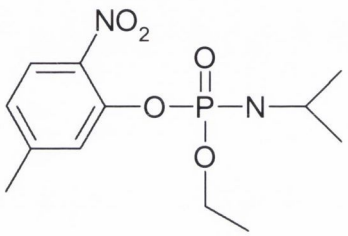

C10

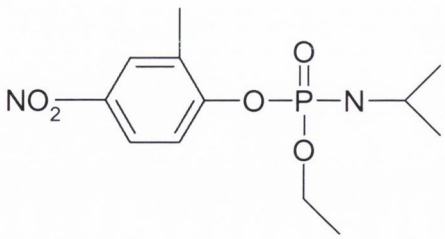

C11

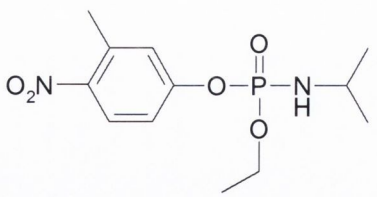

C12

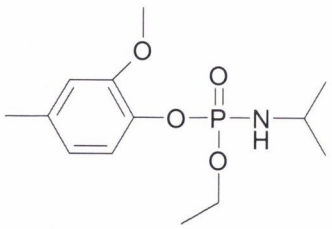

C13

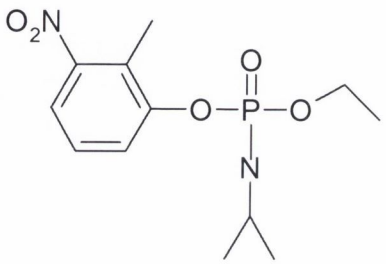

C14

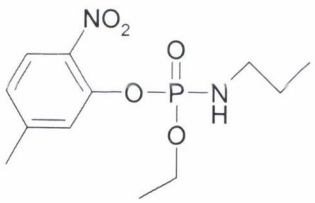

C15

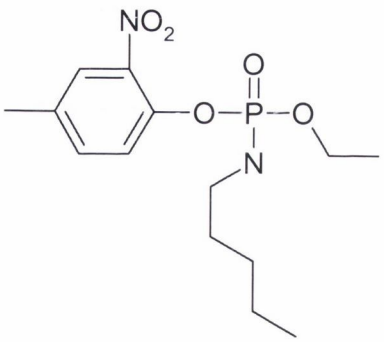

C16

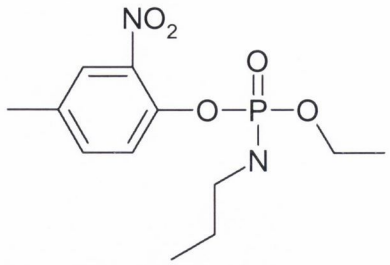

C17

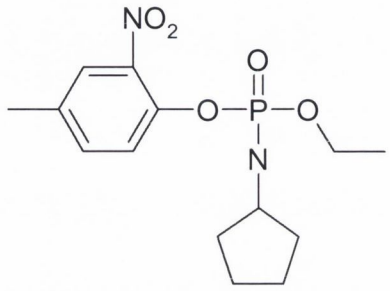

C18

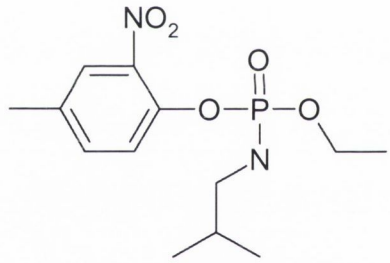

C19

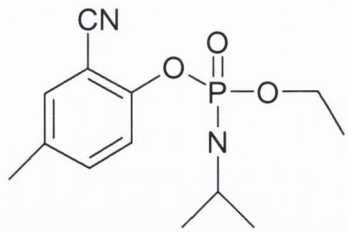

C20

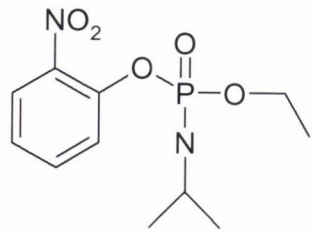

C21

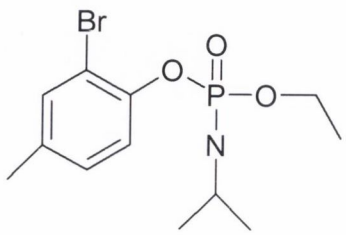

C22

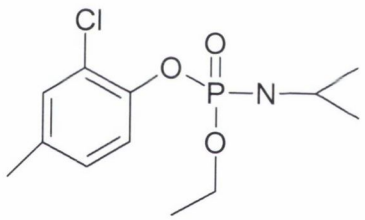

C23

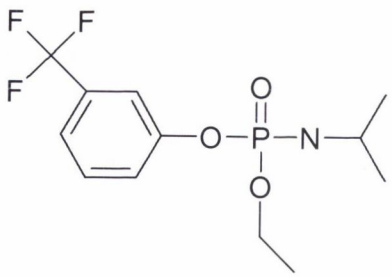

C24

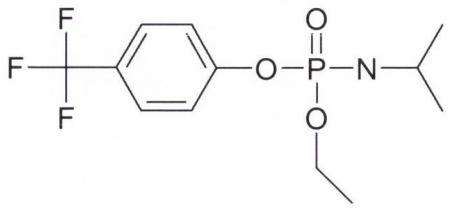

C25

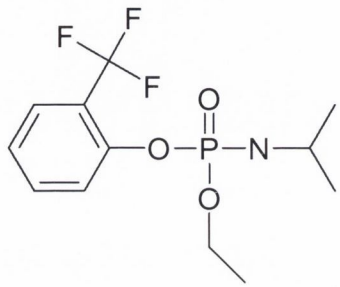

C26

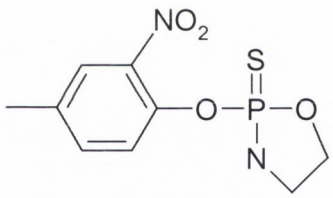

C27

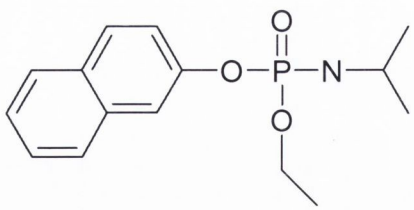

C28

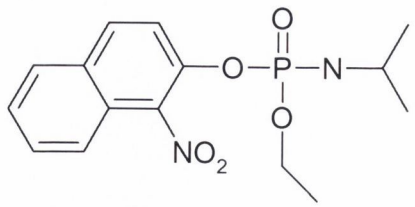

C29

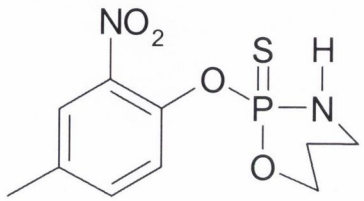

C30

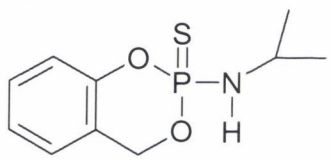

C31

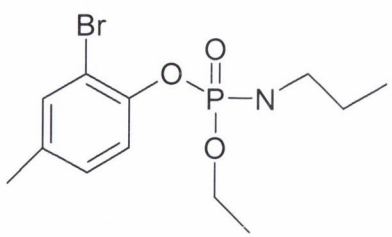

C32

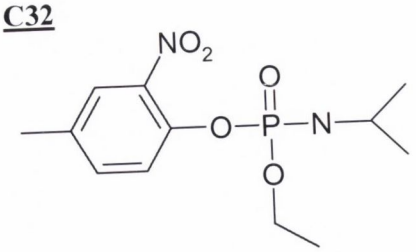

C33

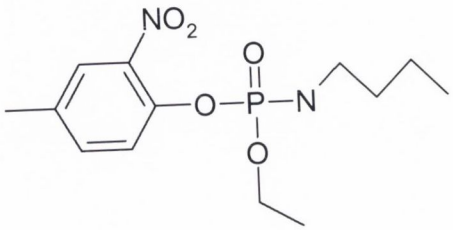

C34

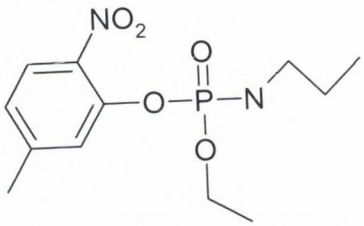

C35

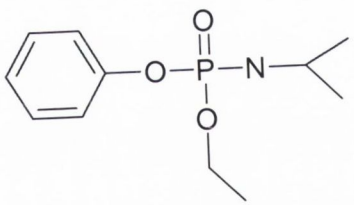

C36

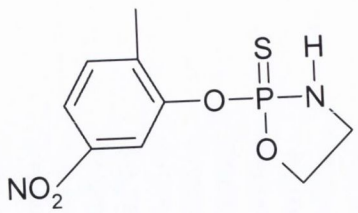

c37

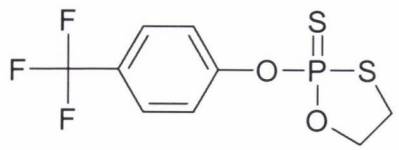

c38

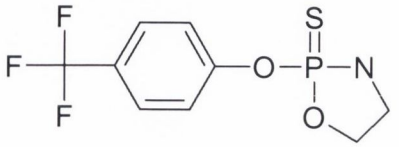

c39

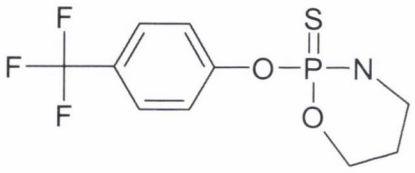

c40

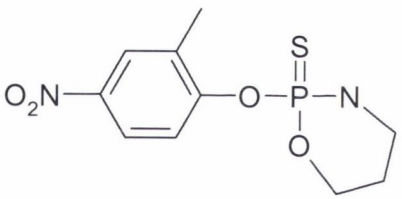

c41

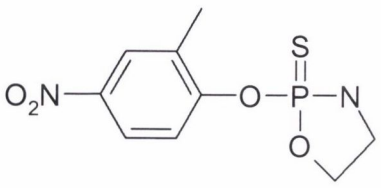

c42

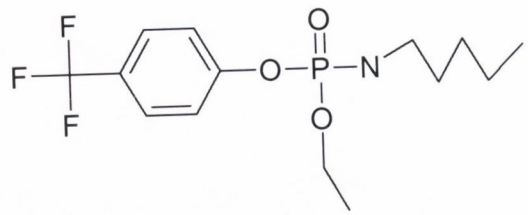

c43

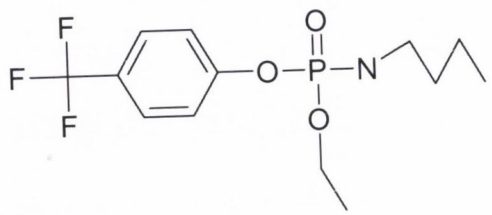

c44

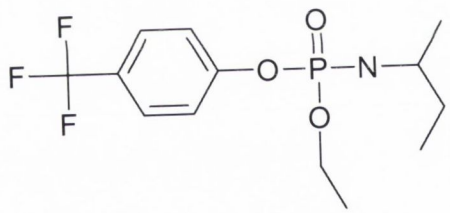

c45

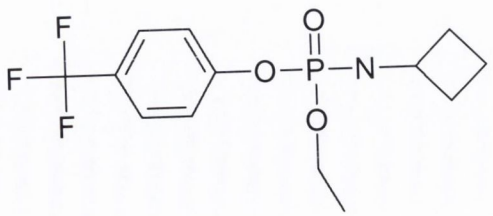

c46

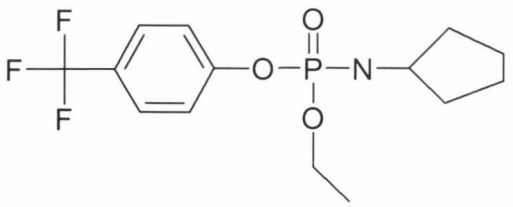

c47

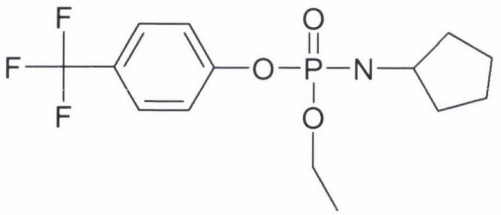

c48

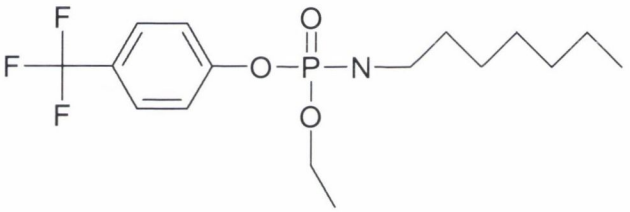

c49

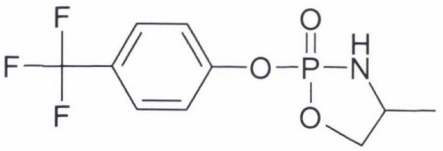

c50

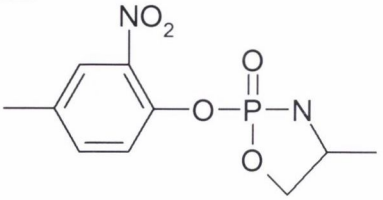

c51

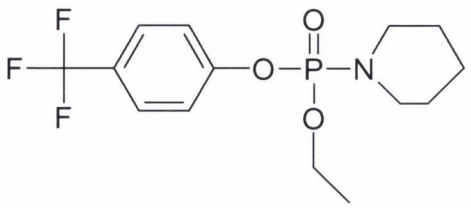

c52

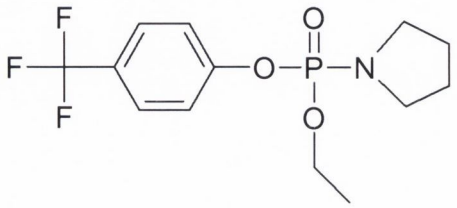

c53

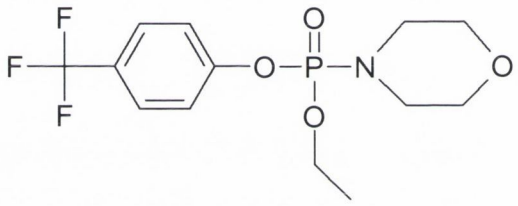

c54

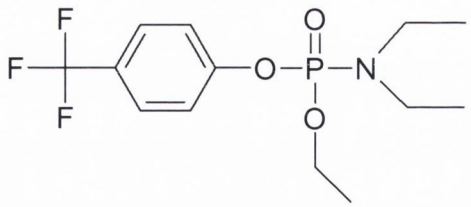

c55

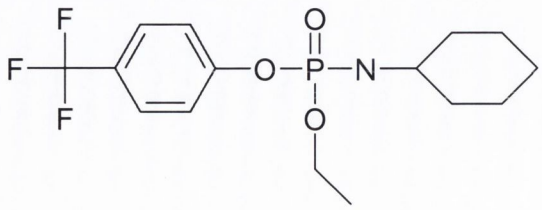

c56

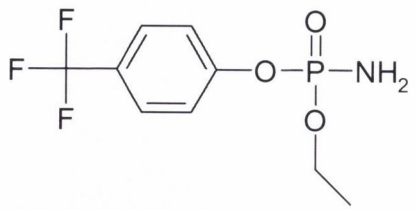

c57

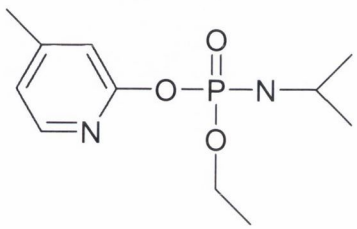

c58

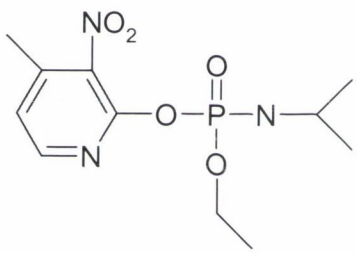

c59

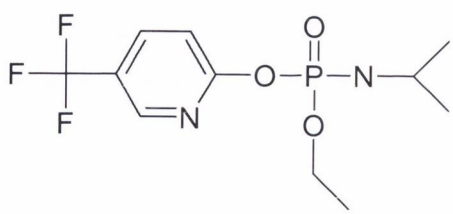

c61

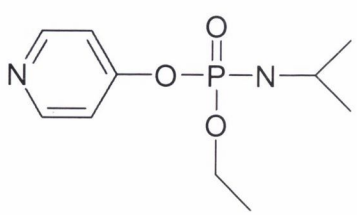

c62

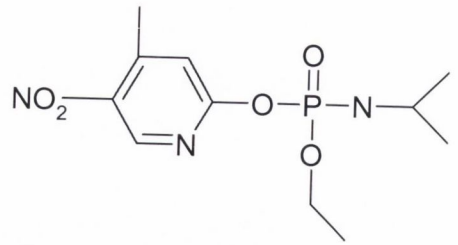

c63

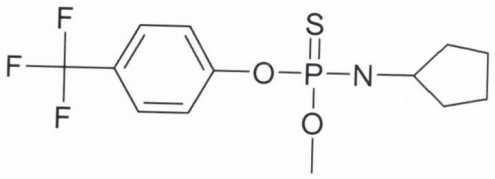

c64

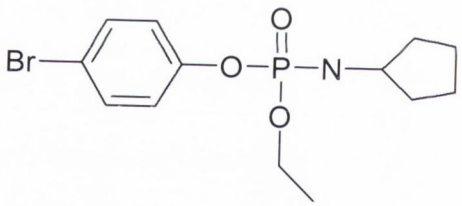

c65

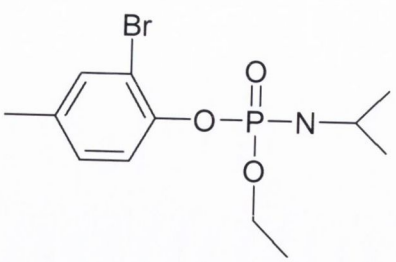

c66

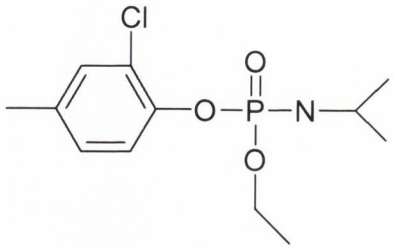

c67

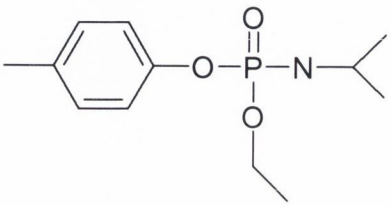

c68

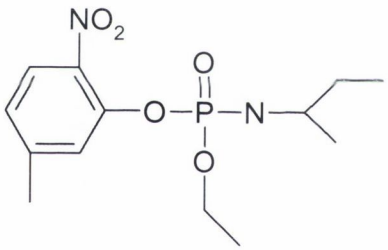

c69

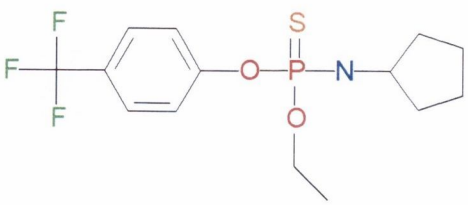

c70

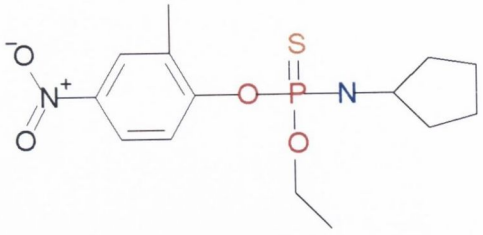

c71

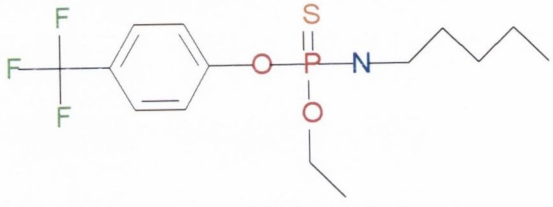

c72

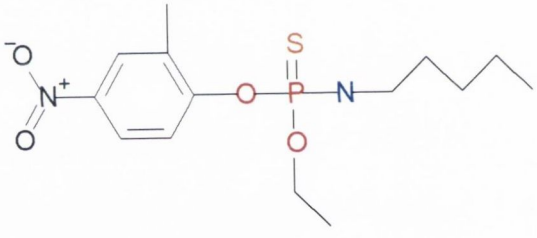

References

REFERENCES

1. **Acharya, B. R., B. Bhattacharyya, and G. Chakrabarti.** 2008. The natural naphthoquinone plumbagin exhibits antiproliferative activity and disrupts the microtubule network through tubulin binding. Biochemistry **47:**7838-45.
2. **Adoutte, A., M. Claisse, and J. Cance.** 1984. Tubulin evolution: an electrophoretic and immunological analysis. Orig Life **13:**177-82.
3. **Akhmanova, A., and M. O. Steinmetz.** 2008. Tracking the ends: a dynamic protein network controls the fate of microtubule tips. Nat Rev Mol Cell Biol **9:**309-22.
4. **Amos, L. A., and D. Schlieper.** 2005. Microtubules and maps. Adv Protein Chem **71:**257-98.
5. **Anthony, R. G., and P. J. Hussey.** 1999. Dinitroaniline herbicide resistance and the microtubule cytoskeleton. Trends Plant Sci **4:**112-116.
6. **Anthony, R. G., and P. J. Hussey.** 1999. Double mutation in eleusine indica alpha-tubulin increases the resistance of transgenic maize calli to dinitroaniline and phosphorothioamidate herbicides. Plant J **18:**669-74.
7. **Anthony, R. G., T. R. Waldin, J. A. Ray, S. W. Bright, and P. J. Hussey.** 1998. Herbicide resistance caused by spontaneous mutation of the cytoskeletal protein tubulin. Nature **393:**260-3.
8. **Armson, A., S. W. Kamau, F. Grimm, J. A. Reynoldson, W. M. Best, L. M. MacDonald, and R. C. Thompson.** 1999. A comparison of the effects of a benzimidazole and the dinitroanilines against Leishmania infantum. Acta Trop **73:**303-11.
9. **Avila, J.** 1990. Microtubule Proteins. CRC Press:1-270.
10. **Bai, R. L., G. R. Pettit, and E. Hamel.** 1990. Binding of dolastatin 10 to tubulin at a distinct site for peptide antimitotic agents near the exchangeable nucleotide and vinca alkaloid sites. J Biol Chem **265:**17141-9.
11. **Banerjee, A., M. C. Roach, P. Trcka, and R. F. Luduena.** 1992. Preparation of a monoclonal antibody specific for the class IV isotype of beta-tubulin. Purification and assembly of alpha beta II, alpha beta III, and alpha beta IV tubulin dimers from bovine brain. J Biol Chem **267:**5625-30.
12. **Bannister, L. H., J. M. Hopkins, R. E. Fowler, S. Krishna, and G. H. Mitchell.** 2000. A brief illustrated guide to the ultrastructure of Plasmodium falciparum asexual blood stages. Parasitol Today **16:**427-33.
13. **Barahona, I., H. Soares, L. Cyrne, D. Penque, P. Denoulet, and C. Rodrigues-Pousada.** 1988. Sequence of one alpha- and two beta-tubulin genes of Tetrahymena pyriformis. Structural and functional relationships with other eukaryotic tubulin genes. J Mol Biol **202:**365-82.
14. **Barron, D. M., S. K. Chatterjee, R. Ravindra, R. Roof, E. Baloglu, D. G. Kingston, and S. Bane.** 2003. A fluorescence-based high-throughput assay for antimicrotubule drugs. Anal Biochem **315:**49-56.
15. **Beier, J. C., F. K. Onyango, J. K. Koros, M. Ramadhan, R. Ogwang, R. A. Wirtz, D. K. Koech, and C. R. Roberts.** 1991. Quantitation of malaria sporozoites transmitted in vitro during salivation by wild Afrotropical Anopheles. Med Vet Entomol **5:**71-9.
16. **Bell, A.** 1998. Microtubule inhibitors as potential antimalarial agents. Parasitol Today **14:**234-40.
17. **Bell, A., B. Wernli, and R. M. Franklin.** 1995. Expression and secretion of malarial parasite beta-tubulin in Bacillus brevis. Biochimie **77:**256-61.

18. **Berman, J. D.** 1994. Structure-function analysis of antimicrotubule dinitroanilines against promastigotes of the parasitic protozoan Leishmania mexicana. Antimicrob Agents Chemother **38:**1692-3.
19. **Best, D., P. J. Warr, and K. Gull.** 1981. Influence of the composition of commercial sodium dodecyl sulfate preparations on the separation of alpha- and beta-tubulin during polyacrylamide gel electrophoresis. Anal Biochem **114:**281-4.
20. **Bhattacharya, A., B. Bhattacharyya, and S. Roy.** 1994. Magnesium-induced structural changes in tubulin. J Biol Chem **269:**28655-61.
21. **Bhattacharya, G., J. Herman, D. Delfin, M. M. Salem, T. Barszcz, M. Mollet, G. Riccio, R. Brun, and K. A. Werbovetz.** 2004. Synthesis and antitubulin activity of N1- and N4-substituted 3,5-dinitro sulfanilamides against African trypanosomes and Leishmania. J Med Chem **47:**1823-32.
22. **Bhattacharya, G., M. M. Salem, and K. A. Werbovetz.** 2002. Antileishmanial dinitroaniline sulfonamides with activity against parasite tubulin. Bioorg Med Chem Lett **12:**2395-8.
23. **Bhattacharyya, B., D. Panda, S. Gupta, and M. Banerjee.** 2008. Anti-mitotic activity of colchicine and the structural basis for its interaction with tubulin. Med Res Rev **28:**155-83.
24. **Bhattacharyya, B., and J. Wolff.** 1976. Tubulin aggregation and disaggregation: mediation by two distinct vinblastine-binding sites. Proc Natl Acad Sci U S A **73:**2375-8.
25. **Blume, Y. B., A. Y. Nyporko, A. I. Yemets, and W. V. Baird.** 2003. Structural modeling of the interaction of plant alpha-tubulin with dinitroaniline and phosphoroamidate herbicides. Cell Biol Int **27:**171-4.
26. **Brewer, F., T. Lavy, and R. Talbert.** 1982. Effects of flooding on dinitroaniline persistance in soybean (glycine max) - rice (*oryza sativa*) rotations. Weed Sci. **30:**531-539.
27. **Britto, P. J., L. Knipling, P. McPhie, and J. Wolff.** 2005. Thiol-disulphide interchange in tubulin: kinetics and the effect on polymerization. Biochem J **389:**549-58.
28. **Britto, P. J., L. Knipling, and J. Wolff.** 2002. The local electrostatic environment determines cysteine reactivity of tubulin. J Biol Chem **277:**29018-27.
29. **Buckling, A. G., L. H. Taylor, J. M. Carlton, and A. F. Read.** 1997. Adaptive changes in Plasmodium transmission strategies following chloroquine chemotherapy. Proc Biol Sci **264:**553-9.
30. **Burke, D., P. Gasdaska, and L. Hartwell.** 1989. Dominant effects of tubulin overexpression in Saccharomyces cerevisiae. Mol Cell Biol **9:**1049-59.
31. **Callahan, H. L., C. Kelley, T. Pereira, and M. Grogl.** 1996. Microtubule inhibitors: structure-activity analyses suggest rational models to identify potentially active compounds. Antimicrob Agents Chemother **40:**947-52.
32. **Caplow, M., and J. Shanks.** 1996. Evidence that a single monolayer tubulin-GTP cap is both necessary and sufficient to stabilize microtubules. Mol Biol Cell **7:**663-75.
33. **Carter, R., and K. N. Mendis.** 2002. Evolutionary and historical aspects of the burden of malaria. Clin Microbiol Rev **15:**564-94.
34. **Chakrabarti, G., S. Sengupta, and B. Bhattacharyya.** 1996. Thermodynamics of colchicinoid-tubulin interactions. Rrol of B-ring and C-7 substituent. J Biol Chem **271:**2897-901.

35. **Chan, M. M., and D. Fong.** 1994. Structure-function analysis of antimicrotubule dinitroanilines against promastigotes of the parasitic protozaon *Leishmania mexicana*. Antimicrob Agents Chemother **38:**1692-1693.
36. **Chan, M. M., J. Tzeng, T. J. Emge, C. T. Ho, and D. Fong.** 1993. Structure-function analysis of antimicrotubule dinitroanilines against promastigotes of the parasitic protozoan Leishmania mexicana. Antimicrob Agents Chemother **37:**1909-13.
37. **Chaudhuri, A. R., I. A. Khan, and R. F. Luduena.** 2001. Detection of disulfide bonds in bovine brain tubulin and their role in protein folding and microtubule assembly in vitro: a novel disulfide detection approach. Biochemistry **40:**8834-41.
38. **Chaudhuri, A. R., and R. F. Luduena.** 1996. Griseofulvin: a novel interaction with bovine brain tubulin. Biochem Pharmacol **51:**903-9.
39. **Clayton, L., R. A. Quinlan, A. Roobol, C. I. Pogson, and K. Gull.** 1980. A comparison of tubulins from mammalian brain and Physarum polycephalum using SDS-polyacrylamide gel electrophorsis and peptide mapping. FEBS Lett **115:**301-5.
40. **Clement, M. J., K. Rathinasamy, E. Adjadj, F. Toma, P. A. Curmi, and D. Panda.** 2008. Benomyl and colchicine synergistically inhibit cell proliferation and mitosis: evidence of distinct binding sites for these agents in tubulin. Biochemistry **47:**13016-25.
41. **Cleveland, D. W., S. G. Fischer, M. W. Kirschner, and U. K. Laemmli.** 1977. Peptide mapping by limited proteolysis in sodium dodecyl sulfate and analysis by gel electrophoresis. J Biol Chem **252:**1102-6.
42. **Cooper, J. R., and L. Wordeman.** 2009. The diffusive interaction of microtubule binding proteins. Curr Opin Cell Biol **21:**68-73.
43. **Cormier, A., M. Marchand, R. B. Ravelli, M. Knossow, and B. Gigant.** 2008. Structural insight into the inhibition of tubulin by vinca domain peptide ligands. EMBO Rep **9:**1101-6.
44. **Correia, J. J., L. D. Lipscomb, and S. Lobert.** 1993. Nondisulfide crosslinking and chemical cleavage of tubulin subunits: pH and temperature dependence. Arch Biochem Biophys **300:**105-14.
45. **Correia, J. J., and S. Lobert.** 2001. Physiochemical aspects of tubulin-interacting antimitotic drugs. Curr Pharm Des **7:**1213-28.
46. **Correia, J. J., and R. C. Williams, Jr.** 1983. Mechanisms of assembly and disassembly of microtubules. Annu Rev Biophys Bioeng **12:**211-35.
47. **Cronin, K. E., P. J. Hussey, J. A. Ray, and T. R. Waldin.** 1993. Herbicide resistance plants. World Intellectual Property Organisation International Publication No. WO 93/24637.
48. **Cyr, R. J., M. Sotak, M. M. Bustos, and M. J. Guiltinan.** 1987. Changes in the relative electrophoretic mobility of higher plant tubulin subunits in SDS-polyacrylamide gels. Biochimica et Biophysica Acta **914:**28-34.
49. **Dawson, P. J., W. E. Gutteridge, and K. Gull.** 1983. Purification and characterisation of tubulin from the parasitic nematode, Ascaridia galli. Mol Biochem Parasitol **7:**267-77.
50. **Delgado, P., M. R. Romero, and A. Torres.** 1991. Alpha/beta inversion of the Euplotes and Oxytricha tubulins. Cytobios **66:**87-91.
51. **Delves, C. J., R. G. Ridley, M. Goman, S. P. Holloway, J. E. Hyde, and J. G. Scaife.** 1989. Cloning of a beta-tubulin gene from Plasmodium falciparum.

Mol Microbiol **3:**1511-9.

52. **Delye, C., Y. Menchari, S. Michel, and H. Darmency.** 2004. Molecular bases for sensitivity to tubulin-binding herbicides in green foxtail. Plant Physiol **136:**3920-32.
53. **Dieckmann-Schuppert, A., and R. M. Franklin.** 1989. Compounds binding to cytoskeletal proteins are active against Plasmodium falciparum in vitro. Cell Biol Int Rep **13:**207-14.
54. **Dieckmann-Schuppert, A., and R. M. Franklin.** 1990. Mode of action of tubulozoles against Plasmodium falciparum in vitro. Antimicrob Agents Chemother **34:**1529-34.
55. **Dimitrov, A., M. Quesnoit, S. Moutel, I. Cantaloube, C. Pous, and F. Perez.** 2008. Detection of GTP-tubulin conformation in vivo reveals a role for GTP remnants in microtubule rescues. Science **322:**1353-6.
56. **Dow, G. S., A. Armson, M. R. Boddy, T. Itenge, D. McCarthy, J. E. Parkin, R. C. Thompson, and J. A. Reynoldson.** 2002. Plasmodium: assessment of the antimalarial potential of trifluralin and related compounds using a rat model of malaria, Rattus norvegicus. Exp Parasitol **100:**155-60.
57. **Downing, K. H., and H. Sui.** 2007. Structural insights into microtubule doublet interactions in axonemes. Curr Opin Struct Biol **17:**253-9.
58. **Elie-Caille, C., F. Severin, J. Helenius, J. Howard, D. J. Muller, and A. A. Hyman.** 2007. Straight GDP-tubulin protofilaments form in the presence of taxol. Curr Biol **17:**1765-70.
59. **Ellis, J. R., R. Taylor, and P. J. Hussey.** 1994. Molecular Modeling Indicates that Two Chemically Distinct Classes of Anti-Mitotic Herbicide Bind to the Same Receptor Site(s). Plant Physiol **105:**15-18.
60. **Fennell, B. J.** 2005. Investigation of Micotubule Inhibitors as Potential Antimalarial Agents. PhD Thesis.
61. **Fennell, B. J., Z. A. Al-shatr, and A. Bell.** 2008. Isotype expression, post-translational modification and stage-dependent production of tubulins in erythrocytic Plasmodium falciparum. Int J Parasitol **38:**527-39.
62. **Fennell, B. J., S. Carolan, G. R. Pettit, and A. Bell.** 2003. Effects of the antimitotic natural product dolastatin 10, and related peptides, on the human malarial parasite Plasmodium falciparum. J Antimicrob Chemother **51:**833-41.
63. **Fennell, B. J., J. A. Naughton, E. Dempsey, and A. Bell.** 2006. Cellular and molecular actions of dinitroaniline and phosphorothioamidate herbicides on Plasmodium falciparum: tubulin as a specific antimalarial target. Mol Biochem Parasitol **145:**226-38.
64. **Ferreyra, R. G., and J. Frydman.** 2000. Purification of the cytosolic chaperonin TRiC from bovine testis. Methods Mol Biol **140:**153-60.
65. **Fisher, D. K., and T. J. Higgins.** 1994. A sensitive, high-volume, colorimetric assay for protein phosphatases. Pharm Res **11:**759-63.
66. **Fong, D., and K. P. Chang.** 1981. Tubulin biosynthesis in the developmental cycle of a parasitic protozoan, Leishmania mexicana: changes during differentiation of motile and nonmotile stages. Proc Natl Acad Sci U S A **78:**7624-8.
67. **Foss, M., B. W. Wilcox, G. B. Alsop, and D. Zhang.** 2008. Taxol crystals can masquerade as stabilized microtubules. PLoS One **3:**e1476.
68. **Fourest-Lieuvin, A.** 2006. Purification of tubulin from limited volumes of cultured cells. Protein Expr Purif **45:**183-90.
69. **Fowler, R. E., R. E. Fookes, F. Lavin, L. H. Bannister, and G. H. Mitchell.**

1998. Microtubules in Plasmodium falciparum merozoites and their importance for invasion of erythrocytes. Parasitology **117 (Pt 5):**425-33.

70. **Fox, J. D., and D. S. Waugh.** 2003. Maltose-binding protein as a solubility enhancer. Methods Mol Biol **205:**99-117.
71. **Fox, J. D. a. W., D. S.** 2002. Maltose-Binding Protein as a Solubility Enhancer. Methods in Mol. Biol. **205:**99-115.
72. **Freedman, H., J. T. Huzil, T. Luchko, R. F. Luduena, and J. A. Tuszynski.** 2009. Identification and characterization of an intermediate taxol binding site within microtubule nanopores and a mechanism for tubulin isotype binding selectivity. J Chem Inf Model **49:**424-36.
73. **Frevert, U.** 2004. Sneaking in through the back entrance: the biology of malaria liver stages. Trends Parasitol **20:**417-24.
74. **Garland, D. L.** 1978. Kinetics and mechanism of colchicine binding to tubulin: evidence for ligand-induced conformational change. Biochemistry **17:**4266-72.
75. **George, T. G., M. M. Endeshaw, R. E. Morgan, K. V. Mahasenan, D. A. Delfin, M. S. Mukherjee, A. J. Yakovich, J. Fotie, C. Li, and K. A. Werbovetz.** 2007. Synthesis, biological evaluation, and molecular modeling of 3,5-substituted-N1-phenyl-N4,N4-di-n-butylsulfanilamides as antikinetoplastid antimicrotubule agents. Bioorg Med Chem **15:**6071-9.
76. **Gestaut, D. R., B. Graczyk, J. Cooper, P. O. Widlund, A. Zelter, L. Wordeman, C. L. Asbury, and T. N. Davis.** 2008. Phosphoregulation and depolymerization-driven movement of the Dam1 complex do not require ring formation. Nat Cell Biol **10:**407-14.
77. **Geuens, G. M., R. M. Nuydens, R. E. Willebrords, R. M. Van de Veire, F. Goossens, C. H. Dragonetti, M. M. Mareel, and M. J. De Brabander.** 1985. Effects of tubulozole on the microtubule system of cells in culture and in vivo. Cancer Res **45:**733-42.
78. **Giani, S., P. Campanoni, and D. Breviario.** 2002. A dual effect on protein synthesis and degradation modulates the tubulin level in rice cells treated with oryzalin. Planta **214:**837-47.
79. **Gigant, B., C. Wang, R. B. Ravelli, F. Roussi, M. O. Steinmetz, P. A. Curmi, A. Sobel, and M. Knossow.** 2005. Structural basis for the regulation of tubulin by vinblastine. Nature **435:**519-22.
80. **Giles, N. L., A. Armson, and S. A. Reid.** 2009. Characterization of trifluralin binding with recombinant tubulin from Trypanosoma brucei. Parasitol Res **104:**893-903.
81. **Guha, S., and B. Bhattacharyya.** 1997. Refolding of urea-denatured tubulin: recovery of nativelike structure and colchicine binding activity from partly unfolded states. Biochemistry **36:**13208-13.
82. **Guinovart, C., J. J. Aponte, J. Sacarlal, P. Aide, A. Leach, Q. Bassat, E. Macete, C. Dobano, M. Lievens, C. Loucq, W. R. Ballou, J. Cohen, and P. L. Alonso.** 2009. Insights into long-lasting protection induced by RTS,S/AS02A malaria vaccine: further results from a phase IIb trial in Mozambican children. PLoS One **4:**e5165.
83. **Gupta, K., and D. Panda.** 2002. Perturbation of microtubule polymerization by quercetin through tubulin binding: a novel mechanism of its antiproliferative activity. Biochemistry **41:**13029-38.
84. **Hamel, E., B. W. Day, J. H. Miller, M. K. Jung, P. T. Northcote, A. K. Ghosh, D. P. Curran, M. Cushman, K. C. Nicolaou, I. Paterson, and E. J.**

Sorensen. 2006. Synergistic effects of peloruside A and laulimalide with taxoid site drugs, but not with each other, on tubulin assembly. Mol Pharmacol **70:**1555-64.

85. **Hammond, J. W., D. Cai, and K. J. Verhey.** 2008. Tubulin modifications and their cellular functions. Curr Opin Cell Biol **20:**71-6.
86. **Hari, M., Y. Wang, S. Veeraraghavan, and F. Cabral.** 2003. Mutations in alpha- and beta-tubulin that stabilize microtubules and confer resistance to colcemid and vinblastine. Mol Cancer Ther **2:**597-605.
87. **Hollomon, D. W., J. A. Butters, H. Barker, and L. Hall.** 1998. Fungal beta-tubulin, expressed as a fusion protein, binds benzimidazole and phenylcarbamate fungicides. Antimicrob Agents Chemother **42:**2171-3.
88. **Holloway, S. P., M. Gerousis, C. J. Delves, P. F. Sims, J. G. Scaife, and J. E. Hyde.** 1990. The tubulin genes of the human malaria parasite Plasmodium falciparum, their chromosomal location and sequence analysis of the alpha-tubulin II gene. Mol Biochem Parasitol **43:**257-70.
89. **Holloway, S. P., P. F. Sims, C. J. Delves, J. G. Scaife, and J. E. Hyde.** 1989. Isolation of alpha-tubulin genes from the human malaria parasite, Plasmodium falciparum: sequence analysis of alpha-tubulin. Mol Microbiol **3:**1501-10.
90. **Hopp, T. P., and K. R. Woods.** 1981. Prediction of protein antigenic determinants from amino acid sequences. Proc Natl Acad Sci U S A **78:**3824-8.
91. **Hugdahl, J. D., and L. C. Morejohn.** 1993. Rapid and Reversible High-Affinity Binding of the Dinitroaniline Herbicide Oryzalin to Tubulin from Zea mays L. Plant Physiol **102:**725-740.
92. **Hussey, J. P., and G. K.** 1985. Multiple isotypes of alpha- and beta-tubulin in the plant *Phaseolus vulgaris*. FEBS Lett **181:**113-118.
93. **Ito, J., A. Ghosh, L. A. Moreira, E. A. Wimmer, and M. Jacobs-Lorena.** 2002. Transgenic anopheline mosquitoes impaired in transmission of a malaria parasite. Nature **417:**452-5.
94. **James, S. W., C. D. Silflow, P. Stroom, and P. A. Lefebvre.** 1993. A mutation in the alpha 1-tubulin gene of Chlamydomonas reinhardtii confers resistance to anti-microtubule herbicides. J Cell Sci **106 (Pt 1):**209-18.
95. **Jameson, L., and M. Caplow.** 1980. Effect of guanosine diphosphate on microtubule assembly and stability. J Biol Chem **255:**2284-92.
96. **Jang, M. H., J. Kim, S. Kalme, J. W. Han, H. S. Yoo, J. Kim, B. S. Koo, S. K. Kim, and M. Y. Yoon.** 2008. Cloning, purification, and polymerization of Capsicum annuum recombinant alpha and beta tubulin. Biosci Biotechnol Biochem **72:**1048-55.
97. **Jang, M. H., J. Kim, S. Kalme, J. W. Han, H. S. Yoo, B. S. Koo, S. K. Kim, and M. Y. Yoon.** 2008. Cloning, purification, and polymerization of Capsicum annuum recombinant alpha and beta tubulin. Biosci Biotechnol Biochem **72:**1048-55.
98. **Kaya, B., R. Marcos, A. Yanikoglu, and A. Creus.** 2004. Evaluation of the genotoxicity of four herbicides in the wing spot test of Drosophila melanogaster using two different strains. Mutat Res **557:**53-62.
99. **Kelling, J., K. Sullivan, L. Wilson, and M. A. Jordan.** 2003. Suppression of centromere dynamics by Taxol in living osteosarcoma cells. Cancer Res **63:**2794-801.
100. **Kerssemakers, J. W., E. L. Munteanu, L. Laan, T. L. Noetzel, M. E.**

Janson, and M. Dogterom. 2006. Assembly dynamics of microtubules at molecular resolution. Nature **442:**709-12.

101. **Koo, B. S., S. Kalme, S. H. Yeo, S. J. Lee, and M. Y. Yoon.** 2009. Molecular cloning and biochemical characterization of alpha- and beta-tubulin from potato plants (Solanum tuberosum L.). Plant Physiol Biochem **47:**761-8.
102. **Koo, B. S., H. Park, S. Kalme, H. Y. Park, J. W. Han, Y. S. Yeo, S. H. Yoon, S. J. Kim, C. M. Lee, and M. Y. Yoon.** 2009. Alpha- and beta-tubulin from Phytophthora capsici KACC 40483: molecular cloning, biochemical characterization, and antimicrotubule screening. Appl Microbiol Biotechnol **82:**513-24.
103. **Kooij, T. W., B. Franke-Fayard, J. Renz, H. Kroeze, M. W. van Dooren, J. Ramesar, K. D. Augustijn, C. J. Janse, and A. P. Waters.** 2005. Plasmodium berghei alpha-tubulin II: a role in both male gamete formation and asexual blood stages. Mol Biochem Parasitol **144:**16-26.
104. **Kumar, N.** 1981. Taxol-induced polymerization of purified tubulin. Mechanism of action. J Biol Chem **256:**10435-41.
105. **Kyte, J., and R. F. Doolittle.** 1982. A simple method for displaying the hydropathic character of a protein. J Mol Biol **157:**105-32.
106. **Lacey, E.** 1988. The role of the cytoskeletal protein, tubulin, in the mode of action and mechanism of drug resistance to benzimidazoles. Int J Parasitol **18:**885-936.
107. **Laemmli, U. K.** 1970. Cleavage of structural proteins during the assembly of the head of bacteriophage T4. Nature **227:**680-5.
108. **Lakowicz, J. R.** 1999. Principles in Fluoresence Spectroscopy. Kluwer Academic/Plenum Publishers, New York **2nd ed.**
109. **Lalloo, D. G., D. Shingadia, G. Pasvol, P. L. Chiodini, C. J. Whitty, N. J. Beeching, D. R. Hill, D. A. Warrell, and B. A. Bannister.** 2007. UK malaria treatment guidelines. J Infect **54:**111-21.
110. **Langhans, M., S. Niemes, P. Pimpl, and D. G. Robinson.** 2009. Oryzalin bodies: in addition to its anti-microtubule properties, the dinitroaniline herbicide oryzalin causes nodulation of the endoplasmic reticulum. Protoplasma **236:**73-84.
111. **Laufer, M. K., and C. V. Plowe.** 2004. Withdrawing antimalarial drugs: impact on parasite resistance and implications for malaria treatment policies. Drug Resist Updat **7:**279-88.
112. **Lee, J. C., D. J. Field, and L. L. Lee.** 1980. Effects of nocodazole on structures of calf brain tubulin. Biochemistry **19:**6209-15.
113. **Lee, J. C., D. Harrison, and S. N. Timasheff.** 1975. Interaction of Vinblastine with Calf Brain Microtubule protein. J Biol Chem **250:**9276-82.
114. **Lee, V. D., and B. Huang.** 1990. Missense mutations at lysine 350 in beta 2-tubulin confer altered sensitivity to microtubule inhibitors in Chlamydomonas. Plant Cell **2:**1051-7.
115. **Lewis, S. A., G. Tian, and N. J. Cowan.** 1997. The alpha- and beta-tubulin folding pathways. Trends Cell Biol **7:**479-84.
116. **Li, C., J. W. Schwabe, E. Banayo, and R. M. Evans.** 1997. Coexpression of nuclear receptor partners increases their solubility and biological activities. Proc Natl Acad Sci U S A **94:**2278-83.
117. **Lignowski, E. M., and E. G. Scott.** 1972. Effects of trifluralin on mitosis. Weed Sci. **20:**267-270.
118. **Linder, S., M. Schliwa, and E. Kube-Granderath.** 1998. Expression of

Reticulomyxa filosa alpha- and beta-tubulins in Escherichia coli yields soluble and partially correctly folded material. Gene **212:**87-94.

119. **Linder, S., M. Schliwa, and E. Kube-Granderath.** 1997. Sequence analysis and immunofluorescence study of alpha- and beta-tubulins in Reticulomyxa filosa: implications of the high degree of beta2-tubulin divergence. Cell Motil Cytoskeleton **36:**164-78.
120. **Little, M., R. A. Quinlan, E. J. Hoffman, and R. F. Luduena.** 1983. Identification and characterization of axopodial tubulins from Echinosphaerium nucleofilum. Eur J Cell Biol **31:**55-61.
121. **Llorca, O., J. Martin-Benito, M. Ritco-Vonsovici, J. Grantham, G. M. Hynes, K. R. Willison, J. L. Carrascosa, and J. M. Valpuesta.** 2000. Eukaryotic chaperonin CCT stabilizes actin and tubulin folding intermediates in open quasi-native conformations. EMBO J **19:**5971-9.
122. **Lowe, J., H. Li, K. H. Downing, and E. Nogales.** 2001. Refined structure of alpha beta-tubulin at 3.5 A resolution. J Mol Biol **313:**1045-57.
123. **Lubega, G. W., T. G. Geary, R. D. Klein, and R. K. Prichard.** 1993. Expression of cloned beta-tubulin genes of Haemonchus contortus in Escherichia coli: interaction of recombinant beta-tubulin with native tubulin and mebendazole. Mol Biochem Parasitol **62:**281-92.
124. **Luduena, R. F.** 1998. Multiple forms of tubulin: different gene products and covalent modifications. Int Rev Cytol **178:**207-75.
125. **Ma, C., C. Li, L. Ganesan, J. Oak, S. Tsai, D. Sept, and N. S. Morrissette.** 2007. Mutations in alpha-tubulin confer dinitroaniline resistance at a cost to microtubule function. Mol Biol Cell **18:**4711-20.
126. **Ma, C., J. Tran, C. Li, L. Ganesan, D. Wood, and N. Morrissette.** 2008. Secondary mutations correct fitness defects in Toxoplasma gondii with dinitroaniline resistance mutations. Genetics **180:**845-56.
127. **MacDonald, L. M., A. Armson, A. R. Thompson, and J. A. Reynoldson.** 2004. Characterisation of benzimidazole binding with recombinant tubulin from Giardia duodenalis, Encephalitozoon intestinalis, and Cryptosporidium parvum. Mol Biochem Parasitol **138:**89-96.
128. **MacDonald, L. M., A. Armson, R. C. Thompson, and J. A. Reynoldson.** 2003. Characterization of factors favoring the expression of soluble protozoan tubulin proteins in Escherichia coli. Protein Expr Purif **29:**117-22.
129. **Matagne, A., B. Joris, and J. M. Frere.** 1991. Anomalous behaviour of a protein during SDS/PAGE corrected by chemical modification of carboxylic groups. Biochem J **280 (Pt 2):**553-6.
130. **McKean, P. G., S. Vaughan, and K. Gull.** 2001. The extended tubulin superfamily. J Cell Sci **114:**2723-33.
131. **Mitra, A., and D. Sept.** 2006. Binding and interaction of dinitroanilines with apicomplexan and kinetoplastid alpha-tubulin. J Med Chem **49:**5226-31.
132. **Mitra, A., and D. Sept.** 2008. Taxol allosterically alters the dynamics of the tubulin dimer and increases the flexibility of microtubules. Biophys J **95:**3252-8.
133. **Mizuno, K., J. Perkin, F. Sek, and B. Gunning.** 1985. Some biochemical properties of higher plant tubulins. Cell Biol Int Rep **9:**5-12.
134. **Molineaux, L.** 1997. Nature's experiment: what implications for malaria prevention? Lancet **349:**1636-7.
135. **Molinski, T. F., D. S. Dalisay, S. L. Lievens, and J. P. Saludes.** 2009. Drug development from marine natural products. Nat Rev Drug Discov **8:**69-85.

136. **Morejohn, L. C., T. E. Bureau, L. P. Tocchi, and D. E. Fosket.** 1984. Tubulins from different higher plant species are immunologically nonidentical and bind colchicine differentially. Proc Natl Acad Sci U S A **81:**1440-1444.
137. **Morris, P. G., and M. N. Fornier.** 2008. Microtubule active agents: beyond the taxane frontier. Clin Cancer Res **14:**7167-72.
138. **Morrissette, N. S., A. Mitra, D. Sept, and L. D. Sibley.** 2004. Dinitroanilines bind alpha-tubulin to disrupt microtubules. Mol Biol Cell **15:**1960-8.
139. **Murthy, J. V., H. H. Kim, V. R. Hanesworth, J. D. Hugdahl, and L. C. Morejohn.** 1994. Competitive Inhibition of High-Affinity Oryzalin Binding to Plant Tubulin by the Phosphoric Amide Herbicide Amiprophos-Methyl. Plant Physiol **105:**309-320.
140. **Naughton, J. A.** 2007. The cell biology of microtubule inhibition in Plasmodium falciparum. PhD Thesis.
141. **Naughton, J. A., R. Hughes, P. Bray, and A. Bell.** 2008. Accumulation of the antimalarial microtubule inhibitors trifluralin and vinblastine by Plasmodium falciparum. Biochem Pharmacol **75:**1580-7.
142. **Nogales, E.** 2000. Structural insights into microtubule function. Annu Rev Biochem **69:**277-302.
143. **Nogales, E., and H. W. Wang.** 2006. Structural mechanisms underlying nucleotide-dependent self-assembly of tubulin and its relatives. Curr Opin Struct Biol **16:**221-9.
144. **Nogales, E., H. W. Wang, and H. Niederstrasser.** 2003. Tubulin rings: which way do they curve? Curr Opin Struct Biol **13:**256-61.
145. **Nogales, E., S. G. Wolf, and K. H. Downing.** 1998. Structure of the alpha beta tubulin dimer by electron crystallography. Nature **391:**199-203.
146. **O'Brien, E. T., E. D. Salmon, and H. P. Erickson.** 1997. How calcium causes microtubule depolymerization. Cell Motil Cytoskeleton **36:**125-35.
147. **Ogawa, T., R. Nitta, Y. Okada, and N. Hirokawa.** 2004. A common mechanism for microtubule destabilizers-M type kinesins stabilize curling of the protofilament using the class-specific neck and loops. Cell **116:**591-602.
148. **Okouneva, T., B. T. Hill, L. Wilson, and M. A. Jordan.** 2003. The effects of vinflunine, vinorelbine, and vinblastine on centromere dynamics. Mol Cancer Ther **2:**427-36.
149. **Olliaro, P., and T. N. Wells.** 2009. The global portfolio of new antimalarial medicines under development. Clin Pharmacol Ther **85:**584-95.
150. **Oxberry, M. E., T. G. Gear, and R. K. Prichard.** 2001. Assessment of benzimidazole binding to individual recombinant tubulin isotypes from Haemonchus contortus. Parasitology **122:**683-7.
151. **Oxberry, M. E., T. G. Geary, C. A. Winterrowd, and R. K. Prichard.** 2001. Individual expression of recombinant alpha- and beta-tubulin from Haemonchus contortus: polymerization and drug effects. Protein Expr Purif **21:**30-9.
152. **Pain, R.** 2004. Determining the Fluoresence Spectrum of a Protein. Current protocols in Protein Science **7:**1-15.
153. **Panda, D., V. Ananthnarayan, G. Larson, C. Shih, M. A. Jordan, and L. Wilson.** 2000. Interaction of the antitumor compound cryptophycin-52 with tubulin. Biochemistry **39:**14121-7.
154. **Patz, J. A., and S. H. Olson.** 2006. Malaria risk and temperature: influences from global climate change and local land use practices. Proc Natl Acad Sci U

S A **103:**5635-6.
155. **Perry, G. W., and D. L. Wilson.** 1982. On the identification of alpha- and beta-tubulin subunits. J Neurochem **38:**1155-9.
156. **Phadtare, S., M. T. Fisher, and L. R. Yarbrough.** 1994. Refolding and release of tubulins by a functional immobilized groEL column. Biochim Biophys Acta **1208:**189-92.
157. **Piperno, G., and M. T. Fuller.** 1985. Monoclonal antibodies specific for an acetylated form of alpha-tubulin recognize the antigen in cilia and flagella from a variety of organisms. J Cell Biol **101:**2085-94.
158. **Plessmann, U., I. Reiter-Owona, and K. F. Lechtreck.** 2004. Posttranslational modifications of alpha-tubulin of Toxoplasma gondii. Parasitol Res **94:**386-9.
159. **Prudencio, M., and M. M. Mota.** 2007. To migrate or to invade: those are the options. Cell Host Microbe **2:**286-8.
160. **Qiang, L., W. Yu, A. Andreadis, M. Luo, and P. W. Baas.** 2006. Tau protects microtubules in the axon from severing by katanin. J Neurosci **26:**3120-9.
161. **Rath, A., M. Glibowicka, V. G. Nadeau, G. Chen, and C. M. Deber.** 2009. Detergent binding explains anomalous SDS-PAGE migration of membrane proteins. Proc Natl Acad Sci U S A **106:**1760-5.
162. **Rawlings, N. C., S. J. Cook, and D. Waldbillig.** 1998. Effects of the pesticides carbofuran, chlorpyrifos, dimethoate, lindane, triallate, trifluralin, 2,4-D, and pentachlorophenol on the metabolic endocrine and reproductive endocrine system in ewes. J Toxicol Environ Health A **54:**21-36.
163. **Raynaud-Messina, B., and A. Merdes.** 2007. Gamma-tubulin complexes and microtubule organization. Curr Opin Cell Biol **19:**24-30.
164. **Read, M., T. Sherwin, S. P. Holloway, K. Gull, and J. E. Hyde.** 1993. Microtubular organization visualized by immunofluorescence microscopy during erythrocytic schizogony in Plasmodium falciparum and investigation of post-translational modifications of parasite tubulin. Parasitology **106 (Pt 3):**223-32.
165. **Reiter, P.** 2008. Global warming and malaria: knowing the horse before hitching the cart. Malar J **7 Suppl 1:**S3.
166. **Reitera, P., C. J. Thomas, P. M. Atkinson, S. I. Hay, S. E. Randolph, D. J. Rogers, G. D. Shanks, R. W. Snow, and A. Spielman.** 2004. Global warming and malaria: a call for accuracy. Lancet Infect Dis **4:**323-4.
167. **Renthal, R., B. G. Schneider, M. M. Miller, and R. F. Luduena.** 1993. Beta IV is the major beta-tubulin isotype in bovine cilia. Cell Motil Cytoskeleton **25:**19-29.
168. **Risinger, A. L., F. J. Giles, and S. L. Mooberry.** 2009. Microtubule dynamics as a target in oncology. Cancer Treat Rev **35:**255-61.
169. **Robinson, M. W., N. McFerran, A. Trudgett, L. Hoey, and I. Fairweather.** 2004. A possible model of benzimidazole binding to beta-tubulin disclosed by invoking an inter-domain movement. J Mol Graph Model **23:**275-84.
170. **Roychowdhury, M., N. Sarkar, T. Manna, S. Bhattacharyya, T. Sarkar, P. Basusarkar, S. Roy, and B. Bhattacharyya.** 2000. Sulfhydryls of tubulin. A probe to detect conformational changes of tubulin. Eur J Biochem **267:**3469-76.
171. **Russell, D. G., D. Miller, and K. Gull.** 1984. Tubulin heterogeneity in the trypanosome Crithidia fasciculata. Mol Cell Biol **4:**779-90.

172. **Sacarlal, J., P. Aide, J. J. Aponte, M. Renom, A. Leach, I. Mandomando, M. Lievens, Q. Bassat, S. Lafuente, E. Macete, J. Vekemans, C. Guinovart, B. Sigauque, M. Sillman, J. Milman, M. C. Dubois, M. A. Demoitie, J. Thonnard, C. Menendez, W. R. Ballou, J. Cohen, and P. L. Alonso.** 2009. Long-Term Safety and Efficacy of the RTS,S/AS02A Malaria Vaccine in Mozambican Children. J Infect Dis **200:**329-336.

173. **Sackett, D. L.** 1995. Vinca site agents induce structural changes in tubulin different from and antagonistic to changes induced by colchicine site agents. Biochemistry **34:**7010-9.

174. **Sardar, P. S., S. S. Maity, L. Das, and S. Ghosh.** 2007. Luminescence studies of perturbation of tryptophan residues of tubulin in the complexes of tubulin with colchicine and colchicine analogues. Biochemistry **46:**14544-56.

175. **Schek, H. T., 3rd, M. K. Gardner, J. Cheng, D. J. Odde, and A. J. Hunt.** 2007. Microtubule assembly dynamics at the nanoscale. Curr Biol **17:**1445-55.

176. **Schibler, M. J., and B. Huang.** 1991. The colR4 and colR15 beta-tubulin mutations in Chlamydomonas reinhardtii confer altered sensitivities to microtubule inhibitors and herbicides by enhancing microtubule stability. J Cell Biol **113:**605-14.

177. **Schneider, A., U. Plessmann, and K. Weber.** 1997. Subpellicular and flagellar microtubules of Trypanosoma brucei are extensively glutamylated. J Cell Sci **110 (Pt 4):**431-7.

178. **Schrevel, J., V. Sinou, P. Grellier, F. Frappier, D. Guenard, and P. Potier.** 1994. Interactions between docetaxel (Taxotere) and Plasmodium falciparum-infected erythrocytes. Proc Natl Acad Sci U S A **91:**8472-6.

179. **Shah, C., C. Z. Xu, J. Vickers, and R. Williams.** 2001. Properties of microtubules assembled from mammalian tubulin synthesized in Escherichia coli. Biochemistry **40:**4844-52.

180. **Sharma, S., T. Ganesh, D. G. Kingston, and S. Bane.** 2007. Promotion of tubulin assembly by poorly soluble taxol analogs. Anal Biochem **360:**56-62.

181. **Shea, D. K., and C. J. Walsh.** 1987. mRNAs for alpha- and beta-tubulin and flagellar calmodulin are among those coordinately regulated when Naegleria gruberi amebae differentiate into flagellates. J Cell Biol **105:**1303-9.

182. **Snyder, J. P., J. H. Nettles, B. Cornett, K. H. Downing, and E. Nogales.** 2001. The binding conformation of Taxol in beta-tubulin: a model based on electron crystallographic density. Proc Natl Acad Sci U S A **98:**5312-6.

183. **Soltani, N., C. Shropshire, D. E. Robinson, and P. H. Sikkema.** 2005. Sensitivity of adzuki bean (*vigna angularis*) to preplant-incorporated herbicides Weed Tech. **19:**897-901.

184. **Stargell, L. A., D. P. Heruth, J. Gaertig, and M. A. Gorovsky.** 1992. Drugs affecting microtubule dynamics increase alpha-tubulin mRNA accumulation via transcription in Tetrahymena thermophila. Mol Cell Biol **12:**1443-50.

185. **Steinmetz, M. O., R. A. Kammerer, W. Jahnke, K. N. Goldie, A. Lustig, and J. van Oostrum.** 2000. Op18/stathmin caps a kinked protofilament-like tubulin tetramer. EMBO J **19:**572-80.

186. **Stephens, R. E.** 1998. Electrophoretic resolution of tubulin and tektin subunits by differential interaction with long-chain alkyl sulfates. Anal Biochem **265:**356-60.

187. **Stokkermans, T. J., J. D. Schwartzman, K. Keenan, N. S. Morrissette, L. G. Tilney, and D. S. Roos.** 1996. Inhibition of Toxoplasma gondii replication by dinitroaniline herbicides. Exp Parasitol **84:**355-70.

188. **Struckmeyer, E. B., L. K. Binning, and R. G. Harvey.** 1976. Effect of dinitroaniline herbicides in a soil medium on snap bean and soybean. Weed Sci. **24:**366-369.
189. **Studier, F. W.** 1973. Analysis of bacteriophage T7 early RNAs and proteins on slab gels. J Mol Biol **79:**237-48.
190. **Sulimenko, V., T. Sulimenko, S. Poznanovic, V. Nechiporuk-Zloy, K. J. Bohm, L. Macurek, E. Unger, and P. Draber.** 2002. Association of brain gamma-tubulins with alpha beta-tubulin dimers. Biochem J **365:**889-95.
191. **Suprenant, K. A., E. Hays, E. LeCluyse, and W. L. Dentler.** 1985. Multiple forms of tubulin in the cilia and cytoplasm of Tetrahymena thermophila. Proc Natl Acad Sci U S A **82:**6908-12.
192. **Tan, D., W. J. Rice, and H. Sosa.** 2008. Structure of the kinesin13-microtubule ring complex. Structure **16:**1732-9.
193. **Teklehaimanot, A., and P. Mejia.** 2008. Malaria and poverty. Ann N Y Acad Sci **1136:**32-7.
194. **Thomas, N., Y. Imafuku, T. Kamiya, and K. Tawada.** 2002. Kinesin: a molecular motor with a spring in its step. Proc Biol Sci **269:**2363-71.
195. **Tilney, L. G., and M. S. Tilney.** 1996. The cytoskeleton of protozoan parasites. Curr Opin Cell Biol **8:**43-8.
196. **Trape, J. F., G. Pison, A. Spiegel, C. Enel, and C. Rogier.** 2002. Combating malaria in Africa. Trends Parasitol **18:**224-30.
197. **Traub-Cseko, Y. M., J. M. Ramalho-Ortigao, A. P. Dantas, S. L. de Castro, H. S. Barbosa, and K. H. Downing.** 2001. Dinitroaniline herbicides against protozoan parasites: the case of Trypanosoma cruzi. Trends Parasitol **17:**136-41.
198. **Turner, D., C. Chang, K. Fang, P. Cuomo, and D. Murphy.** 1996. Kinesin movement on glutaraldehyde-fixed microtubules. Anal Biochem **242:**20-5.
199. **Vaughn, K. C., M. D. Marks, and D. P. Weeks.** 1987. A Dinitroaniline-Resistant Mutant of Eleusine indica Exhibits Cross-Resistance and Supersensitivity to Antimicrotubule Herbicides and Drugs. Plant Physiol **83:**956-964.
200. **Verdier-Pinard, P., N. Sitachitta, J. V. Rossi, D. L. Sackett, W. H. Gerwick, and E. Hamel.** 1999. Biosynthesis of radiolabeled curacin A and its rapid and apparently irreversible binding to the colchicine site of tubulin. Arch Biochem Biophys **370:**51-8.
201. **Vlachou, D., T. Schlegelmilch, E. Runn, A. Mendes, and F. C. Kafatos.** 2006. The developmental migration of Plasmodium in mosquitoes. Curr Opin Genet Dev **16:**384-91.
202. **Walliker, D., P. Hunt, and H. Babiker.** 2005. Fitness of drug-resistant malaria parasites. Acta Trop **94:**251-9.
203. **Wampande, E. M., J. Richard McIntosh, and G. W. Lubega.** 2007. Classical ligands interact with native and recombinant tubulin from Onchocerca volvulus with similar rank order of magnitude. Protein Expr Purif **55:**236-45.
204. **Wang, A., and W. Kopachik.** 1995. Effects of trifluralin on growth and differentiation of the amoebo-flagellate *Naegleria*. FEMS microbioloy letters **127:**99-103.
205. **Weisenberg, R. C., G. G. Borisy, and E. W. Taylor.** 1968. The colchicine-binding protein of mammalian brain and its relation to microtubules. Biochemistry **7:**4466-79.

206. **Werbovetz, K. A.** 2002. Tubulin as an antiprotozoal drug target. Mini Rev Med Chem **2:**519-29.
207. **Werbovetz, K. A., J. J. Brendle, and D. L. Sackett.** 1999. Purification, characterization, and drug susceptibility of tubulin from Leishmania. Mol Biochem Parasitol **98:**53-65.
208. **Werbovetz, K. A., D. L. Sackett, D. Delfin, G. Bhattacharya, M. Salem, T. Obrzut, D. Rattendi, and C. Bacchi.** 2003. Selective antimicrotubule activity of N1-phenyl-3,5-dinitro-N4,N4-di-n-propylsulfanilamide (GB-II-5) against kinetoplastid parasites. Mol Pharmacol **64:**1325-33.
209. **Westermann, S., and K. Weber.** 2003. Post-translational modifications regulate microtubule function. Nat Rev Mol Cell Biol **4:**938-47.
210. **White, N. J.** 2008. The role of anti-malarial drugs in eliminating malaria. Malar J **7 Suppl 1:**S8.
211. **WHO.** 2006. Guidelines For The Treatment Of Malaria.
212. **Wiese, C., and Y. Zheng.** 2006. Microtubule nucleation: gamma-tubulin and beyond. J Cell Sci **119:**4143-53.
213. **Williams, R. C., Jr., J. J. Correia, and A. L. DeVries.** 1985. Formation of microtubules at low temperature by tubulin from antarctic fish. Biochemistry **24:**2790-8.
214. **Wloga, D., K. Rogowski, N. Sharma, J. Van Dijk, C. Janke, B. Edde, M. H. Bre, N. Levilliers, V. Redeker, J. Duan, M. A. Gorovsky, M. Jerka-Dziadosz, and J. Gaertig.** 2008. Glutamylation on alpha-tubulin is not essential but affects the assembly and functions of a subset of microtubules in Tetrahymena thermophila. Eukaryot Cell **7:**1362-72.
215. **Wu, D., T. G. George, E. Hurh, K. A. Werbovetz, and J. T. Dalton.** 2006. Pre-systemic metabolism prevents in vivo antikinetoplastid activity of N1,N4-substituted 3,5-dinitro sulfanilamide, GB-II-150. Life Sci **79:**1081-93.
216. **Xiao, H., P. Verdier-Pinard, N. Fernandez-Fuentes, B. Burd, R. Angeletti, A. Fiser, S. B. Horwitz, and G. A. Orr.** 2006. Insights into the mechanism of microtubule stabilization by Taxol. Proc Natl Acad Sci U S A **103:**10166-73.
217. **Yaffe, M. B., B. S. Levison, J. Szasz, and H. Sternlicht.** 1988. Expression of a human alpha-tubulin: properties of the isolated subunit. Biochemistry **27:**1869-80.
218. **Yakovich, A. J., F. L. Ragone, J. D. Alfonzo, D. L. Sackett, and K. A. Werbovetz.** 2006. Leishmania tarentolae: purification and characterization of tubulin and its suitability for antileishmanial drug screening. Exp Parasitol **114:**289-96.
219. **Yamamoto, E., L. Zeng, and W. V. Baird.** 1998. Alpha-tubulin missense mutations correlate with antimicrotubule drug resistance in Eleusine indica. Plant Cell **10:**297-308.
220. **Yang, Y., A. A. Alcaraz, and J. P. Snyder.** 2009. The Tubulin-Bound Conformation of Paclitaxel: T-Taxol vs "PTX-NY" (dagger). J Nat Prod **72:**422-9.
221. **Yemets, A., V. Radchuk, O. Bayer, G. Bayer, A. Pakhomov, W. Vance Baird, and Y. B. Blume.** 2008. Development of transformation vectors based upon a modified plant alpha-tubulin gene as the selectable marker. Cell Biol Int **32:**566-70.
222. **Zhu, H., K. Fang, and G. Fang.** 2009. Mechanism, function and regulation of microtubule-dependent microtubule amplification in mitosis. Mol Cells **27:**1-3.